MIR-10a REGULATION OF DRUG RESPONSE AND CANCER STEM CELL POPULATIONS IN NON-SMALL CELL LUNG CARCINOMAS

APPROVED BY SUPERVISORY COMMITTEE

Alexander Pertsemlidis, Ph.D. (Mentor)

John D. Minna, M.D. (Mentor)

Diego H. Castrillon M.D., Ph.D. (Chairman)

Jerry W. Shay, Ph.D.

Pier Paolo Scaglioni, M.D.

Dedicated to:
My wife Digvi K. DeSevo

miR-10a REGULATION OF PACLITAXEL RESPONSE AND CANCER STEM CELL POPULATIONS IN NON-SMALL CELL LUNG CARCINOMAS

By

CHRISTOPHER GERARD DESEVO

Presented to the Faculty of the Graduate School of Biomedical Sciences

The University of Texas Southwestern Medical Center at Dallas

In Partial Fulfillment of the Requirements

For the Degree of

DOCTOR OF PHILOSOPHY
The University of Texas Southwestern Medical Center at Dallas

Dallas, Texas

December 2013

AKNOWLEDGMENTS

I would like to thank Dr. Alexander Pertsemlidis for taking a chance with me and giving me the independence I needed to grow as a scientist and reminding me that I am not as smart as I think. I sincerely thank Dr. Liqin Du for all the training and support she provided when I first started and for laying the ground for my entire dissertation and Dr. Minna for giving me the resources I needed to finish my degree, valuable insights that took each project to the next level and for welcoming me into one of the best research laboratories in the country.

I would like to thank all the members of the Minna lab for their guidance and support, in particular Dr. Larsen and Dr. Shao for help with mouse work and experimental design, Dr. Kenneth Huffman for all the cell lines and all the early-morning political rants, Ryan for providing transfection conditions on the entire panel of cell lines, and Dr. Girard for all the computational and database management help. And the rest of the Minna lab: Dr. Peyton, Dr. Gao, Dr. Das, Patrick, Suzie, Dhurba, Robin, Rebecca, Paul, and Maithili for all the friendship, advice, and counseling they each provided during my time in the Minna lab. I also thank Dr. Brenda Timmons for all the support and lab management help that expedited my graduation and the entire office staff for all their support to keep the lab running smoothly and efficiently.

I would like to thank Dr. Shay, who in addition to being a valued member of my thesis committee, helped guide me during my transition me from each of my three labs to the next and encouraged me not to give up. Dr. Castrillon and Dr. Scaglioni I thank for the support during my transition and experimental design suggestions that were not only insightful, but also added to my dissertation and publications.

I thank my parents for understanding it is okay to be in school until the age of thirty. Mark, Peter and Blake for not only supporting my move to Dallas but also for taking care of Dig while she finished her Master's degree.

The reason for my success is my loving and understanding wife, who supported me while I pursued my dreams and helped keep me sane and our home in order. Finally my "kids" Harley, Bailey, and Prince always helped melt the stress and provided many great memories.

miR-10a REGULATION OF DRUG RESPONSE AND CANCER STEM CELL IN NON-SMALL CELL LUNG CARCINOMAS

Publication No._____

CHRISTOPHER GERARD DESEVO

DOCTOR OF PHILOSOPHY

The University of Texas Southwestern Medical Center at Dallas, 2013

Supervising Professors: Dr. Alexander Pertsemlidis and Dr. John D. Minna

Phosphatidylinositol 3-kinases (PI3Ks) are enzymes involved in diverse cellular functions including cell growth, proliferation, differentiation, motility, survival and apoptosis. Many of these functions relate to class I PI3Ks, heterodimers composed of regulatory and catalytic subunits that convert extracellular cues to intracellular responses upon activation. Overall, this signaling pathway is under tight regulation and even slight perturbations can lead to aberrant pathway activation. In NSCLC cell lines, we found that manipulation of miR-10a results in significant changes to both mRNA and protein levels of PI3K. In the context of cellular response to front-line chemotherapeutic agents used to treat NSCLC, I uncovered that miR-10a mimic decreases cell viability10-fold in the presence of paclitaxel relative to

drug alone, while inhibiting miR-10a results in a 10-fold increase, suggesting that high levels of miR-10a may be predictive of response to such agents. To assess its prognostic value, we interrogated miR-10a expression in NSCLC tumors and found that high miR-10a levels correlate with longer overall patient survival. miRNAs can target hundreds of genes, meaning that miR-10a may regulate PIK3CA expression both directly and indirectly. We identified the transcription factor GATA6 as both a target of miR-10a with a predicted miR-10a target site in its 3'UTR and a regulator of PI3K expression, with several conserved binding sites in the promoter of PIK3CA. These findings demonstrate that miR-10a regulates the PI3K pathway at two distinct levels.

Microarray expression profiling of NSCLC cells treated with miR-10a mimic had significant down regulation of ALDH1A3, a marker of cancer stem cells. This relationship was confirmed through functional validation of ALDH activity. Multiple miRNA target prediction algorithms showed that ALDH1A3 is not a direct target of miR-10a. To uncover the direct target of miR-10a we used a targeted siRNA screen containing genes implicated in stem cell maintenance to reveal that the WNT and Notch pathway are important for cell survival. Both pathways are down-regulated when cells are treated with a miR-10a mimic. Bioinformatic analysis identified DVL3 as a miR-10a target gene. Manipulation of miR-10a levels resulted in significant changes in both mRNA and protein levels of DVL3. Finally, loss of DVL3 expression significantly decreased ALDH1A3 protein levels and the population of ALDH+ cells.

Collectively, my work has uncovered miR-10a as mediator of the potent PI3K oncogenic pathway through both direct and indirect mechanisms, a modulator of cellular response to paclitaxel and finally its identification in NSCLC stem cell maintenance through regulation of the WNT and NOTCH pathways.

Table of contents

PRIOR PUBLICATIONS

DeSevo C, Du L, Borkowski R, Behrens C, Wistuba II, Minna JD, Pertsemlidis A. (2013). miR-10a regulation of the PI3K pathway through direct and indirect mechanism in non-small cell lung cancer. (In preparation)

DeSevo C, Shao C, Larsen J, Minna JD, Pertsemlidis A. (2013). miR-10a regulation of cancer stem cells through modulation of the WNT pathway in non-small cell lung cancer. (In preparation)

Caudy AA, Guan Y, Jia Y, Hansen C, **Desevo C**, Hayes AP, Agee J, Alvarez-Dominguez JR, Arellano H, Barrett D, Bauerle C,Bisaria N, Bradley PH, Breunig JS, Bush EC, Cappel DA, Capra E, Chen W, Clore J, Combs PA, Doucette C, Demuren O,Fellowes P, Freeman S, Frenkel E, Gadala-Maria D, Gawande R, Glass D, Grossberg S, Gupta A, Hammonds-Odie L,Hoisos A, Hsi J, Hsu YH, Inukai S, Karczewski KJ, Ke X, Kojima M, Leachman S, Lieber D, Liebowitz A, Liu J, Liu Y, Martin T,Mena J, Mendoza R, Myhrvold C, Millian C, Pfau S, Raj S, Rich M, Rokicki J, Rounds W, Salazar M, Salesi M, Sharma R,Silverman SJ, Singer C, Sinha S, Staller M, Stern P, Tang H, Weeks S, Weidmann M, Wolf A, Young C, Yuan J, Crutchfield C,McClean MN, Murphy CT, Llinás M, Botstein D, Troyanskaya OG, Dunham MJ. *Saccharomyces bayanus*, a new system for comparative functional genomics. Genetics113(1): e152918

Du L, Subauste MC, **DeSevo C**, Zhao Z, Baker M, Borkowski R, Schageman J, Greer R, Yang C, Suraokar M, Wistuba I, Gazdar A, Minna J, Pertsemlidis A. (2012) miR-337-3p and Its Targets *STAT3* and *RAP1A* Modulate Taxane Sensitivity in Non-Small Cell Lung Cancers. *PLoS ONE* 7(6): e39167 .

Calahan D, Dunham M, **DeSevo C**, Koshland D. (2011) Genetic Analysis of Desiccation Tolerance in *Saccharomyces cerevisiae.* Genetics 180(2):507-519
some titles are sentence case, others in title case

Martin O, **DeSevo C**, Guo B, Koshland D, Dunham M, Zheng Y. (2009) Telomere behavior in a hybrid yeast. *Cell Research* 19(7):910-2.

Gresham D, Desai M, Tucker C, Jenq H, Pai D, Ward A, **DeSevo C**, Botstein D, Dunham M. (2008) The repertoire and dynamics of evolutionary adaptations to controlled nutrient-limited environments in yeast. *PLoS Genet*. 4(12):e1000303.

LIST OF FIGURES

Chapter 1

Chapter 2

Chapter 3

Chapter 4

Chapter 5

CHAPTER 6

LIST OF TABLES

LIST OF ABBREVIATIONS

Argonaute	AGO
Aldehyde Dehydrogenase	ALDH
Acute Lymphoblastic Leukemia	ALL
All-Trans Retinoic Acid	ATRA
Cycle Dependent Kinases	CDK
Chronic Lymphocytic Leukemia	CLL
Cancer Stem Cells	CSC
Connective Tissue Growth Factor	CTGF
Dishevelled	DVL
Extra Cellular Matrix	ECM
Epidermal Growth Factor Receptor	EGFR
Eukaryotic Translation Initiation Factor 4E	eIF4E
Echinoderm Microtubule-Associated Protein-like 4 to Anaplastic Lymphoma Kinase	EML4-ALK
Epithelial-Mesenchymal Transition	EMT
Fibroblast Growth Factor Receptor 3	FGFR3
Frizzled	Fz
Glutaminase	GLS
Glycogen Synthase Kinase 3 beta,	GSK3Beta
Histone Deacetylases 4	HDAC4
Homology-Dependent Repair	HDR

Human Epidermal Growth Factor Receptor 2	HER2
Hypoxia-Inducible Factor 1	HIF
Lethal-7	Let-7
Lock Nucleic Acids	LNA
Murine Embryonic Fibroblast	MEF
Mismatch Repair	MMR
Mammalian Target of Rapamycin	mTOR
Normal Adjacent Tissues	NAT
Nuclear co-repressor 2	NcoR2
Nucleotide Excision Repair	NER
National Institutes of Health	NIH
Natural-killer group 2, member D	NKG2D
Non-Small Cell Lung Cancer	NSCLC
Nucleotide	NT
Open Reading Frame	ORF
Phosphoinostide-Dependent Kinase	PDK1
Pleckstrin Homology	PH
Phosphatidylinositide 3-kinases	PI3K
Phoshatidyinositol 4,5-bisphosphate	PIP2
Phoshatidyinositol 3,4,5-triphosphate	PIP3
Phosphatase and Tensin homolog	PTEN
Retinoblastoma	RB

RNA-induced Silencing Complex	RISC
RNA interference	RNAi
Reactive Oxygen Species	ROS
Receptor Tyrosine Kinase	RTK
Small Cell Lung Cancer	SCLC
Small Hairpin RNA	shRNA
Smad-Interacting Protein 1	SIP1
Small Interfering RNA	siRNA
Suppressor of Cytokine Signaling 1	SOCS1
TriCarboxylic Acid	TCA
The Cancer Genome Atlas	TCGA
Transforming Growth Factor beta	TFGB1
Tumor protein 53	TP53
Thrombospondin-1	TSP1
United States	US
Upstream Stimulatory Factor 2	USF2
Untanslated Region	UTR
Vascular Cell Adhesion Molecule-1	VCAM1
Vascular Endothelial Growth Factor-A	VEGF-A

LIST OF APPENDICES

CHAPTER ONE miRNA regulation of the Hallmarks of Cancer

1.1 miRNAs: Small Non-Coding RNAs That Control Gene Evolution

miRNAs are short hairpin structures that are typically 20-24 nucleotides long. They post-transcriptionally repress the expression of target gene transcripts through interaction with the 3'untranslated region (UTR). MiRNA expression is vital for normal development, as several knockout studies have shown that loss of any critical part of the miRNA biogenesis pathway leads to embryonic lethality (Bernstein, Kim et al. 2003, Imielinski, Berger et al. 2012). In worms, flies and mammals, miRNAs as a class, make up less than 1% of the genes. However their regulatory potential is vast, they are predicted to regulate 60% of protein coding genes (Garzon, Calin et al. 2009, Kota, Chivukula et al. 2009).

Their regulatory strength is so great that they have influenced how genes evolve. Essential housekeeping genes have evolved to have short UTRs that are devoid of miRNA binding sites (Stark, Brennecke et al. 2005), in contrast to developmental and tissue specific genes, which tend to have a greater density of target sites. Intriguingly, miRNAs tend to target genes expressed in neighboring tissues in order to prevent unwanted expression of target transcripts. Finally, genes that contain miRNAs in their introns do not contain target sites of the co-transcribed miRNA (Stark, Brennecke et al. 2005). Taken together, these findings indicate that miRNAs represent a new level of regulation in the genome.

1.1.2 An Almost Missed Opportunity

miRNAs were first identified in 1993 in the laboratory of Victor Ambros, who noticed that lin-4, an essential gene for the normal development of *C. elegans*, did not encode a protein. He was able to identify lin-4s mature product was 22nt. Additionally, his group determined the precursor (61nt), was predicted to fold back on itself to form a stem-loop structure. Finally, his laboratory also reported that LIN-14, a gene important in larval development that caused a phenotype opposite to the loss of lin-4, contains sequences complementary to lin-4 in its UTR (Lee, Feinbaum et al. 1993). At the same time, work from the Ruvkun lab, which also identified complementarity between lin-4 and sites in the lin-14 3'UTR, showed that lin-4 was able to dramatically reduce LIN-14 protein with little effect on lin-14 mRNA (Wightman, Ha et al. 1993). Taken together, these findings support lin-4 as encoding a small RNA that, unlike most other RNAs, does not produce a protein, but is capable of regulating LIN-14 protein through potential interaction with the lin-14 3'UTR (Lee, Feinbaum et al. 1993) (Wightman, Ha et al. 1993).

This work was relatively unnoticed for almost a decade, before it was recognized that lin-4 was the founding member of a whole new class of small non-coding RNAs that are highly conserved and have vast regularity potential (Lau, Lim et al. 2001, Lee 2001, Lee and Ambros 2001).

1.1.3 MiRNA Biogenesis

miRNAs are RNA polymerase II-dependent transcripts. They are either intergeneic, where they are co-transcribed with their host gene, or under control of their own promoter. Once transcribed the precursor miRNA or pri-miRNA is bound by Pasha, an RNA binding protein which acts as a scaffold for Drosha, a class III RNase, and then this miRNA processing complex produces a hairpin structure that is ~70 nucleotides in length. The hairpin structure is then exported from the nucleus through a RAN-GTP dependent nuclear transporter, Exportin 5 (Krol, Loedige et al. 2010).

Once in the cytosol, the stem-loop structure is further processed by another class III RNAase, Dicer, which binds and removes the loop. Since the duplex RNA is not perfectly complementary, the resulting duplex RNA contains two mature miRNAs – called either miR and miR* or miR-5p and miR-3p, either of which can be loaded into the RNA-induced silencing complex, or RISC, depending on the degree of complementarity at the two ends of the duplex. One protein member of the RISC complex is the Argonaute, or AGO, family of proteins, which contains two distinct RNA binding domains, facilitating the interaction of miRNAs with their target genes (Bartel 2009) (Figure 1).

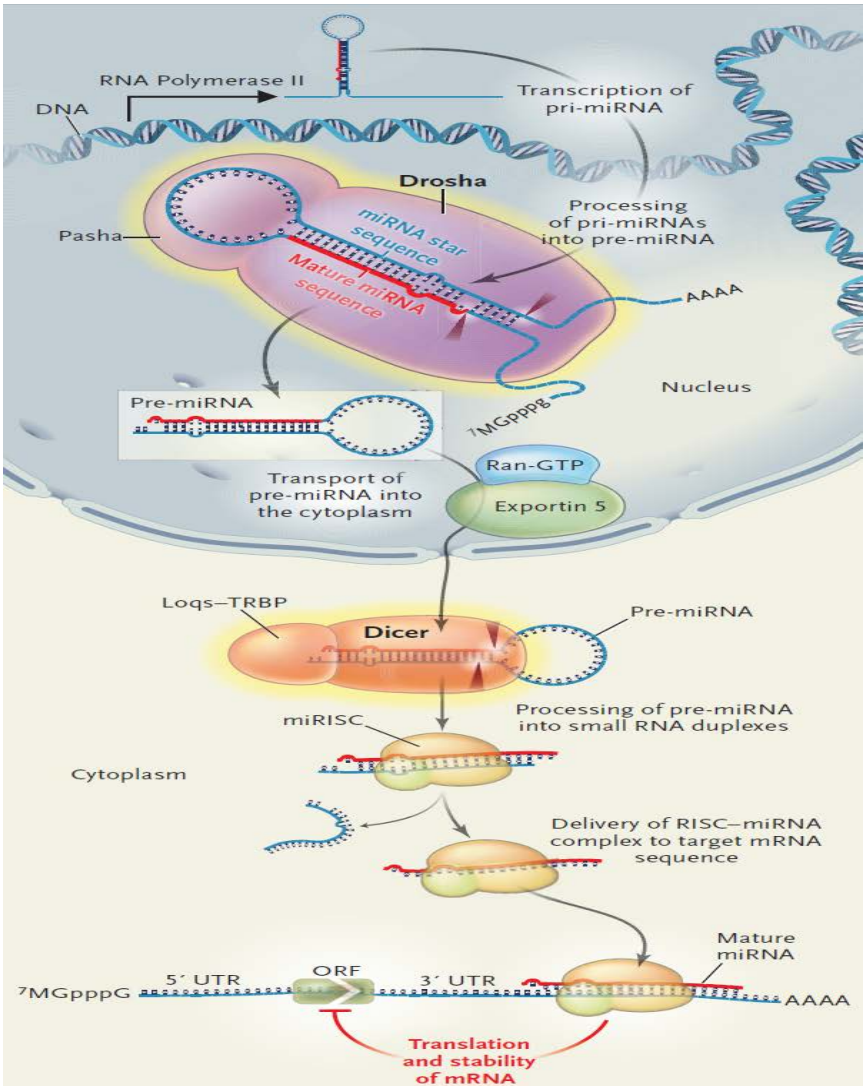

Figure 1.1 miRNA Biogenesis. Summary of the process creating a mature miRNA and all known enzymes involved. While this only shows miRNA interaction with the 3'UTR recent work has uncovered that this only accounts for a little more then half of all miRNA:mRNA interactions. F. Slack. N Engl J Med 359;25

1.1.4 Mechanisms of miRNA Gene Silencing

miRNA-mediated silencing occurs through one of several mechanisms (Eulalio, Huntzinger et al. 2008). If there is perfect complementarity between the miRNA and the target mRNA, the mRNA is degraded. This is not typically observed in mammals, as the only reported example is miR-196 regulation of HOXB8 mRNA (Yekta, Shih et al. 2004). However, perfect complementarity is a common feature in plants and RNA interference (RNAi) (Zamore, Tuschl et al. 2000, Llave, Xie et al. 2002).

The canonical mechanism that operates in mammals is partial complementarity, which inhibits gene translation in several ways. Prior to the elongation step, AGO, part of RSIC, directly interacts with eIF4E (eukaryotic translation initiation factor 4E) and the large subunit of the ribosome to inhibit cap-dependent translation initiation (Chendrimada, Finn et al. 2007). It has also been shown that miRNA:mRNA interactions are associated with the polysomes in sucrose sedimentation gradients, indicating that these interactions occur while the amino acid chain is forming. However, the ribosome falls off in the presence of the miRNA:mRNA duplex resulting in premature termination of protein synthesis (Petersen, Bordeleau et al. 2006). Finally, miRNAs induce accelerated deadenylation, causing decay of mRNAs by directing them to the general mRNA degradation machinery (Giraldez, Mishima et al. 2006). The exact mechanism of degradation appears to be a feature of the target mRNA and not the miRNA, as it has been determined that the same miRNA can affect different target genes in different ways (Eulalio, Rehwinkel et al. 2007). Some of the important variable accounting for these differential effects

include the number of miRNA target sites, the distance separating them, and there location within the UTR (Grimson, Farh et al. 2007).

1.1.5 MiRNA Target Recognitions

As alluded to above, the key to miRNA regulation is sequence complementarity between the miRNA and its target gene's UTR, as was the case with lin-14 and lin-4. Detailed analysis of miRNA:mRNA interaction uncovered that a mammalian miRNA conserved among vertebrates has, on average, 300 target mRNAs (Friedman, Farh et al. 2009). Several rules have been developed to determine true miRNA target sites. First, the observation of the miRNA "seed" sequence, which is defined as Watson-Crick base pairing of nucleotides 2-8 of the 5' end of the miRNA with the target transcript (Lewis, Burge et al. 2005). Additional sequence context is used to identify high confidence binding sites: an A at position 1 and Watson-Crick pairing at position 9, while not required, do decrease false positives in target prediction (Bartel 2009). A key advancement in target prediction was understanding that portions of the UTR which are "real" miRNA regulatory sites are likely to be conserved relative to other segments of the UTR that are not under selective pressure (Lewis, Shih et al. 2003). Currently there are close to a dozen prediction tools – most of these computer programs are freely available and the advantages and disadvantages of each have been reviewed (Bartel 2009).

Given the high level of conservation of the entire miRNA it is likely that there are supplemental interaction between the 3' portion of the miRNA and the 3'UTR. While this

possibility was suggested fairly early (Doench and Sharp 2004, Brennecke, Stark et al. 2005), recent work in our lab and other labs have begun to support this claim. It has been shown that nucleotides 13-16 of the miRNA that bind three to four contiguous Watson-Crick pairs, uninterrupted by bulges or mismatches, of the target 3'UTR compensate for any bulges, mismatches or wobbles that might be present in the seed sequence (Grimson, Farh et al. 2007). Supplemental binding events add to the specificity of miRNA within families, which have the same seed sequence but differ in the remaining sequence composition (Brennecke, Stark et al. 2005).

Finally, the context of the target site within the 3'UTR must be considered. The first 20-50 base pairs of the 3'UTR are less likely to be accessible to the miRNA and the RISC complex due to shielding caused by the ribosome (Grimson, Farh et al. 2007). Additionally, the middle regions of long 3'UTRs tend to be devoid of conserved miRNA binding sites due to abundant secondary structure and sites recognized by RNA binding proteins. Thus, the majority of miRNA target sites are near the ends of 3'UTRs (Pasquinelli 2012). Only in rare circumstances have miRNA binding sites been found outside of the 3'UTR, and these sites were not considered effective (Grimson, Farh et al. 2007, Orom, Nielsen et al. 2008). Recently it has been suggested that target prediction is not that simple: large scale non-canonical miRNA binding throughout the mRNA was uncovered (Helwak, Kudla et al. 2013). Helwak, et al. were able to directly interrogate miRNA:mRNA interaction through crosslinking and pull down of AGO protein(s), followed by sequencing the resulting RNA. It was reported that over 60% of the identified

miRNA interactions were non-canonical - with 18% containing bulges or mismatched nucleotides in the seed region and seed base-pairing often accompanied by non-seed interactions. They also found that almost 50% of miRNA:mRNA interactions occurred outside the 3'UTR in the ORF or 5'UTR (Helwak, Kudla et al. 2013). By historical standards, this field is still evolving.

1.1.6 Biological Functions of miRNAs

Since the discovery of lin-4 regulation of lin-14 in the larval development of C.elegans, miRNAs have been found to regulate a plethora of biological functions. Given that more than half of all genetic loci are thought to be under miRNA regulation, it is not surprising that a wide range of biological processes and functions have been shown to be influenced by miRNA regulation (Volinia, Calin et al. 2006). miRNAs typically only have modest effects on mRNA levels and have only been found to act as binary switches in a few circumstances (Li, Wang et al. 2006). It is much more common to observe one or a family of miRNAs regulating a biological process at multiple points, where no single change affects the phenotype, but as a whole they have a dramatic phenotypic response. This has been experimentally proven with the well-studied miR-17~92 family that controls growth (Mendell 2008).

miRNAs can also be thought of as a failsafe to distinguish biological signals from background noise. They can prevent a transcript from producing functional protein until a

threshold is met, at which point most signaling pathways have a positive feed-forward loop effectively overwhelming the miRNA (Stark, Brennecke et al. 2005). It is this feature of miRNAs that allows them to maintain cellular homeostasis by setting up boundaries of transcripts.

Stress can be defined as a state when a cell deviates from homeostasis due to extrinsic factors, such as growth and differentiation signals or carcinogens, or intrinsic changes such as mutation, damage to organelle or macromolecules, or changes in the oxidative state. As such, the cell must adapt and alter gene expression to cope with the stress and restore homeostasis. If stress is too severe and the damage caused too great--the cell will eventually undergo cell death. One of the most prevalent and deadly diseases in the modern world—cancer—is defined by constant cellular stress, and the subversion of the normal intracellular pathways that control cell death in the setting of such stress.

1.2 Cancer, Broadly Defined

Cancer is a broad term given to uncontrolled cellular growth, migration and invasion. Worldwide, cancer is the number two cause of death and responsible for one in eight deaths, surpassed only by cardiovascular disease. In the developed world, however, it is the number one cause of death(Siegel, Naishadham et al. 2013). In developing and developed countries around the world, the burden of cancer is increasing due to industrialization, physical inactivity(Mathers, Fat et al. 2008), smoking, diets high in fats and animal proteins, and general aging of the global

population. Cancer is intrinsically heterogeneous, and is composed of hundreds of distinct diseases with wide ranging risk factors, survival and treatment options.

According to the most recent figures from the NIH, in 2007 there were 1.44 million cancer cases diagnosed in the U.S with a total economic cost of 230 billion dollars. The average cost to the U.S economy for each cancer diagnosis is just under $160,000. Costs directly associated with treatment are $86,111 to treat each cancer patient. These figures clearly show that improvements in the detection and treatment could have an enormous impact not only on the lives of individual patients, but may also have substantial economic benefits.

Decades of research have contributed to our understanding that cancer is a multi-step process that arises from genomic alterations. Genomic alterations acquired by cells can be classified into six core and several emerging hallmarks and characteristics of cancer (Hanahan and Weinberg 2011). At the core of the hallmarks are sustaining proliferative signaling, evading growth suppressors, resisting cell death, enabling replicative immortality, inducing angiogenesis, and activating invasion and metastasis(Hanahan and Weinberg 2000) .

1.2.2 Hallmarks of Cancer

1.2.2.1 Sustaining Proliferative Signaling

One of the most fundamental traits of cancer cells is their ability to sustain proliferative signaling, essentially becoming masters of their own destiny. Growth signals coming from the outside environment bind to receptors on the cell surface. These receptors then become activated, internalize the signal and transmit it down signaling transduction pathways. Normal cells carefully control proliferative signals with multiple checkpoints throughout the process. Cancer cells on the other hand dysregulate this process at multiple steps. For example, cancers cells can produce the growth ligand, stimulate nearby cells to do so, or mutate the receptor such that it is consistently in the active state (Di Cristofano and Pandolfi 2000, Yardena Samuels1 2004) (Sharma, Bell et al. 2007).

1.2.2.2 Evading Growth Suppressors

A cancer cell must overcome powerful regulatory signals that normally restrain growth and proliferation. Such is the case with PTEN, a potent tumor suppressor, which lies directly downstream of the RTK, Ras, and PI3K inhibiting their downstream effects. In order to evade growth suppressors, a cancer cell must deactivate tumors suppressors or induce their degradation. Some of the most widely studied tumors suppressors that are frequently inactivated are TP53, RB1 and PTEN (Charles J Sherr1 2002, Sherr and McCormick 2002).

1.2.2.3 Resisting Cell Death

The avoidance of apoptosis can occur through a variety of strategies. The most common is loss of the tumor suppressors which function in genome surveillance. Other mechanism takes advantage of the apoptotic machinery itself, which is composed of both upstream regulators and downstream effectors. The set of proteins that bridge these two signals are composed of both anti-apoptotic members of the BCL-2 family, which bind to and inhibit their counterparts, the pro-apoptotic proteins Bax and Bak, which are embedded in the mitochondrial outer membrane (Adams and Cory 2007). When relieved of inhibition, Bax and Bak disrupt the integrity of the mitochondrial outer wall, causing the release of cytochrome c, which in turn activates a cascade of caspases, the effectors of apoptosis (Scott W. Lowe1 2004). Cancer takes advantage of this pathway by overexpression of the anti-apoptotic proteins, decreasing expression of the pro-apoptotic proteins, or by short-circuiting the signaling from the receptors to the effectors (Scott W. Lowe1 2004).

1.2.2.4 Enabling Replicative Immortality

Normal cells have limited replicative capacity and consequently undergo either senescence, a state where they are still viable but no longer proliferate, or cell death, which can occur through a variety of mechanisms depending on the cell type. Activation of telomerase is

central to this bypass as shown in the varied response of NSCLC cell lines to telomere inhibition (Wright1 2000). The telomerase catalytic subunit (TERT) is currently being investigated as a drug target in several ongoing clinical trials.

1.2.2.5 Angiogenesis

Tumors require sources of energy, nutrients and oxygen, as well as removal of metabolic wastes and carbon dioxide. Due to their fast and largely unstructured growth, they usurp processes that are used especially during embryogenesis and are relatively inactive in adult tissues. Surprisingly, early in tumor progression tumors turn on angiogenic pathways, indicating that this is an early event that must occur for tumor formation and potential therapeutic opportunity (Raica, Cimpean et al. 2009). Two well-studied proteins, vascular endothelial growth factor-A (VEGF-A) and thrombospondin-1 (TSP1), are both expressed by the tumor cells and work antagonistically against one another, producing a disordered, leaky, and underdeveloped vascular system (Nagy, Chang et al. 2010). This creates microenvironments within a tumor that have different access to oxygen and nutrients, resulting in oxygen and pH gradients. This intratumor heterogeneity can produce chemotherapies resistance as the drug cannot access the core of the tumor as well as radiotherapy resistance, which requires radical oxygen species to cause genotoxic stress. The innate immune system unwittingly collaborates with this process by promoting an inflammatory response that induces angiogenesis (Ferrara 2010).

1.2.2.6 Invasion and Metastasis

The final hallmark of cancer is invasion and metastasis, which occurs in two phases. First, the cells acquire the ability to disseminate from the primary tumor. Second, the cell then needs the ability to attach to a distant site and adapt to the foreign microenvironment. It is well appreciated that tumors that have invaded and metastasized are as a group histologically different (i.e. usually poorly differentiated). Alterations occur on a genetic basis resulting in changes to proteins that influence cellular shape, attachment and interactions with neighboring cells. For example, loss of E-cadherin, a surface protein that binds epithelial cells through interactions with the extra cellular matrix (ECM) and maintains a state of quiescence, is frequently observed (Berx and van Roy 2009). Genes involved in embryogenesis, cell migration and inflammation are up-regulated, orchestrated by a set of well-studied transcription factors: Snail, Slug, Twist, and Zeb1/2 (Klymkowsky and Savagner 2009). This genetic reprograming, known as epithelial-mesenchymal transition (EMT), gives the tumor cells the ability to invade, resist apoptosis, disseminate and become resistant to chemotherapies (Polyak and Weinberg 2009).

1.2.3 Emerging Hallmarks and Enabling Characteristics of Cancer

Two enabling characteristics that produce an environment conducive for the acquisition of the hallmarks are genomic instability and mutation, and promoting inflammation (Hanahan and Weinberg 2011). Mutation rates in cancer are highly variable, ranging from under a dozen to thousands of insertions, deletions or nonsynonymous polymorphism (Pleasance, Cheetham et al. 2010)(Haas and Sakr 1997, Uematsu, Kanazawa et al. 2003, Pleasance, Cheetham et al. 2010).

Lung adenocarcinoma mutation rates range from as low as 0.04 to over 117.4 mutations per megabase in more advanced invasive carcinomas (Imielinski, Berger et al. 2012). In pancreatic cancer, clonal populations of cells in the primary tumor which give rise to distant metastases have more mutations than the parental population and represent a more evolved population; notably, mutation occur at a faster rate as the cancer progresses (Salk, Fox et al. 2010, Yachida, Jones et al. 2010, Imielinski, Berger et al. 2012). This positive feed-forward system of mutation rate is attributed to the loss of the surveillance system (TP53, RB) that would normally force DNA damaged cells to undergo apoptosis (Jackson and Bartek 2009). Finally, the loss of telomeres produces large scale genomic reengagements in efforts to try and stabilize chromosomes producing large scale aneuploidy contributing to cancer progression (Artandi and DePinho 2010).

In an effort to arrest tumor growth, the innate immune system is recruited to the area around the tumor, resulting in inflammation, which has the untended effect of promoting tumor growth. Inflammation supplies the tumor with growth factors, pro-angiogenic factors, ECM-modifying enzymes that support or further promote angiogenesis and can even induce metastasis (Grivennikov, Greten et al. 2010). Cells of the immune system that have infiltrated the tumor microenvironment can further promote mutations and genomic instability by producing reactive oxygen species (ROS), which act as a mutagenic agent (Grivennikov, Greten et al. 2010).

Two emerging features that are only just starting to be understood are the deregulation of cellular metabolism and avoiding immune destruction. Cancer cells have an insatiable appetite for growth. To feed this appetite, they require the basic building blocks of all macromolecules. To meet this demand cancer cells usually undergo anaerobic glycolysis, even if there is enough oxygen present for the end product of glycolysis to enter the tricarboxylic acid (TCA) cycle. This phenomenon was first observed by Dr. Otto Warburg and since been referred to as the Warburg effect (Warburg 1956). Here is instance of the interdependence of the hallmarks of cancer: the poor access to oxygen in parts of the tumor induces a hypoxic response, which in turn up-regulates many glucose transporters and metabolic enzymes in the glycolytic pathway (Warburg 1956). Relying solely on glycolysis for energy frees up all the biological intermediates produced in the TCA cycle for the biosynthesis of macromolecules and organelle needed for cellular division (Warburg 1956).

The final emerging hallmark is evading the immune response, which has been illustrated by the increase of tumors in immunocompromised humans or following organ transplant(Vajdic and van Leeuwen 2009). This has been confirmed experimentally using several methods. It was observed that human melanoma cells injected into NOD/SCID immunocompromised mice were less capable of generating tumors than in mice that were interleukin-2 receptor gamma chain null, a more highly immunocompromised mouse model (Quintana, Shackleton et al. 2008). It has also been shown that tumors that arise in immunodeficient mice will not engraft in

immunocompetent mice, while tumors that form in immunocompetent mice will engraft in immunodeficient mice (Kim, Emi et al. 2007).

1.3 MiRNAs: An Overlooked Hallmark of Cancer

1.3.1 General Observations on miRNAs in Cancer

miRNAs work by repressing gene translation and can act as oncogenes or tumor suppressors. This role can change for individual miRNAs depending on the mutational status of the cell and tissue of origin. The first study linking miRNAs to cancer was in patients with chronic lymphocytic leukemia, CLL. It was observed that most patients had large deletions in chromosome 13q14, which was determined to contain two miRNAs, miR-15 and miR-16 (Calin, Dumitru et al. 2002). Further genomic profiling of human cancers discovered that of the 186 miRNAs known at the time, 98 were located in cancer-associated genomic regions. These regions are frequently located at fragile sites and susceptible to heterozygous loss and translocations (Calin 2004). Array based approaches of miRNAs in cancer showed that miRNA expression profiles are more informative than mRNA expression at classifying poorly-differentiated tumors. Additionally, miRNA expression could classify human cancers to developmental lineages and distinct mechanism of transformation. Finally, a general downregulation of miRNAs in tumors compared to normal tissue was observed (Lu, Getz et al. 2005) (Figure 2A).

There can be several explanations for the global down-regulation of miRNAs in tumors, one of which was mentioned above: miRNAs are located in regions of genome that tend to be

lost or disrupted in cancer. Another is an epigenetic silencing mechanism, which appears to be a tissue-specific. More frequently observed are abnormalities of the miRNA biogenesis pathway. It was first reported in non-small lung cancer patients that lower Dicer expression correlated with reduced post-surgery survival (Karube, Tanaka et al. 2005). Both in cell culture and genetically engineered mouse models of lung cancer, loss of various components of the miRNA biogenesis pathway promoted tumor growth and invasiveness (Kumar, Lu et al. 2007) (Figure 2B). It should be noted that homozygous deletions of such components have not been observed in tumors. Recent knockout experiments have shown that cells deficient for these components produce viable cells that were able to form tumors in mice (Ravi, Gurtan et al. 2012). However, these cells had a much slower doubling time and delayed tumor onset in mice and it appeared that miRNA levels were maintained in the tumor from interaction with the microenvironment, further supporting Dicer as a haploinsufficient tumor suppressor (Ravi, Gurtan et al. 2012). To further complicate Dicer's role in cancer, human prostate cell lines loss of Dicer was shown to suppress tumor growth, but it also enhanced migration in some cell lines, illustrating Dicers pleotropic role in cancer (Zhang, Chen et al. 2013). In addition to selective loss of miRNA, it has been reported that genes will swap or shorten 3'UTRs to avoid miRNA regulation. This was first observed with let-7 regulation of the oncogene Hmga2, where a chromosomal translocation disrupted the repression of let-7 resulting in oncogenic transformation (Mayr, Hemann et al. 2007). The Bartel lab further found that compared to proliferating non-transformed cell lines, cancer cells often had shorter 3'UTRs and that the shorter UTRs resulted in increased mRNA stability and loss of miRNA-mediated repression (Mayr and Bartel 2009).

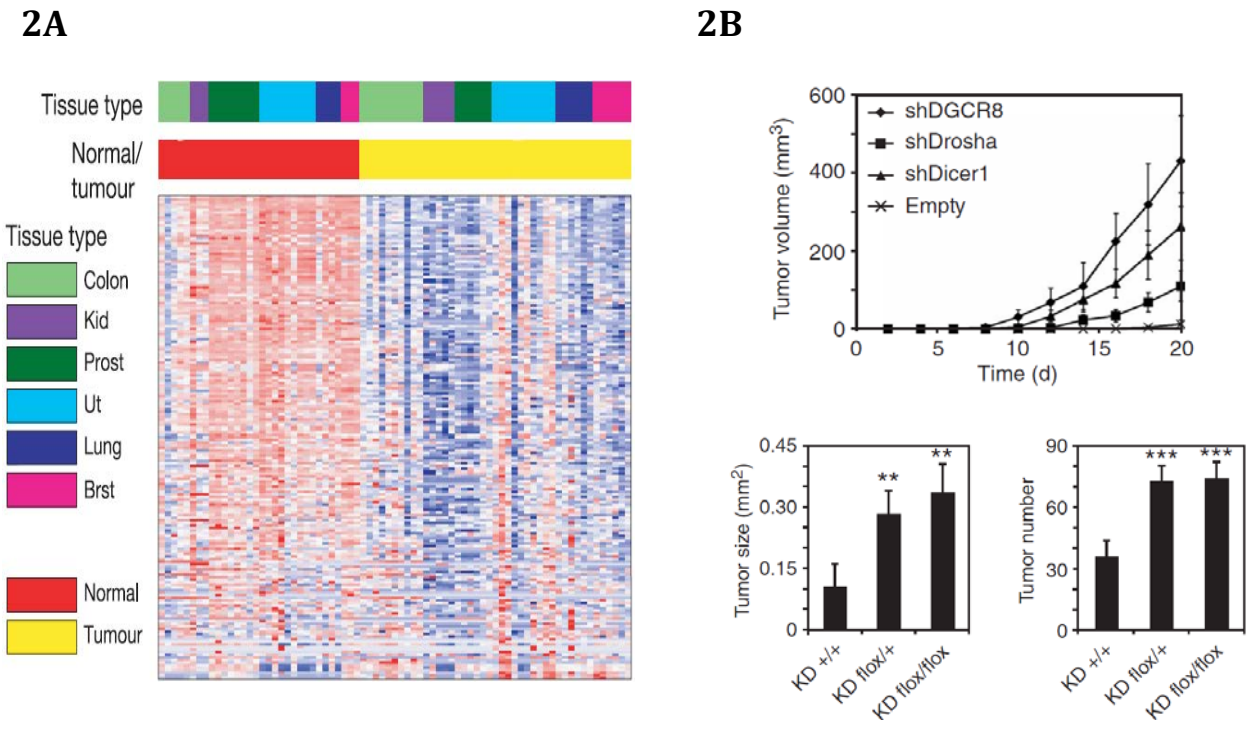

Figure 1.2: Emerging Hallmark of cancer. A. Genome wide profiling of miRNA expression across several tumor and normal adjacent tissue samples. Results show that miRNA expression profiles can be used to classify tumor based on tissue type and that in general miRNA expression is lost in tumor samples. Golub, T et al. Nature 2005. **B.** Stable cell lines were produced using shRNA targeting several key components of the miRNA biogenesis pathway. This resulted in a significant increase in tumor growth rate. Genetically engineered mice in the background of Kras G12D mutant animals further supported the previous finding. Animals with impaired miRNA biogenesis resulted in increased tumor size and burden. Jacks, T. et al. Nature genetics 2007

1.3.2 MiRNA Regulation of the Hallmarks of Cancer

1.3.2.1 Sustaining Proliferative Signaling

Lethal-7 (let-7), a founding member of the miRNA field, like lin-4 is required for timing of cell fate determination in *C.elegans* (Reinhart, Slack et al. 2000) . Regulation of vulval development, a process that requires RAS/MAP kinase signaling, is carried out through let-7 family regulation of KRAS (Johnson, Grosshans et al. 2005). Furthermore, let-7 is poorly expressed in lung tumors, which have one of the highest incidents of K-RAS mutation (Reinhart, Slack et al. 2000). The reduction of let-7 expression is associated with significant shorter overall survival in lung cancers patients(Takamizawa, Konishi et al. 2004) . Finally, ectopic expression of let-7 in KRAS-driven NSCLC cell lines inhibited growth in vitro and overexpression of let-7 in the KRAS G12D mouse model reduced tumor formation(Takamizawa, Konishi et al. 2004) .

A second example of a miRNA regulating proliferative signals is the observation that loss of chromosome 3p21.3, an early and frequent event in lung carcinogenesis, contains miR-128b, which is predicted to regulate EGFR. Patients who had deletion of chromosome 3p21.3 and were treated with gefitinib had increased survival relative to patients who did not have this deletion

and were also treated with gefitinib (Weiss, Bemis et al. 2008). Indicating that patients with chromosome 3p21.3 deletion and loss of miR-128b are more “addicted” to EGFR signaling and subsequently more sensitive to gefitinib treatment.

1.3.2.2 Evading Growth Suppressors

The tumor suppressor p53 is a central regulator of DNA damage, cellular stress and improper mitogenic signals. It surveys the cell and integrates these signals and promotes growth arrest, inhibits angiogenesis, initiates DNA repair or induces apoptosis if the damage is too severe (Levine, Hu et al. 2006). Given its importance in preventing tumor formation, it is no surprise that it is mutated in nearly all cancers at rates higher than 50% (Olivier, Hollstein et al. 2010). While p53 was discovered over five decades ago, its role as a tumor suppressor is still being explored (Levine AJ 1991).

Recently, p53 was shown to regulate miRNA expression; in particular it had profound effects on the miR-34 family, by directly binding to their promoter and inducing transcription in the presences of oncogenic stress or DNA damage (He, He et al. 2007). When ectopically expressed, miR-34 induced cell cycle arrest, cellular senescence and apoptosis and inhibited tumor growth in vivo (Hermeking 2010). When determining miR-34 target genes it was (perhaps unsurprisingly) noticed that genes involved in cell cycle progression and DNA damage response were overrepresented. (He, He et al. 2007). Several of the more notable genes experimentally shown to be directly regulated by miR-34 were cell cycle dependent kinases (CDKs) 4 and 6,

Cyclin E2, MET and Bcl-2, all of which have been documented to promote cellular growth or inhibit apoptosis (He, He et al. 2007)

1.3.2.3 Resisting Cell Death

BCL-2 is a central player in cell survival that acts by inhibiting cell death. BCL-2 is overexpressed in various human cancers, is associated with resistance to many chemotherapies, and is currently being investigated as a druggable target by several large pharmaceutical companies (Vogler, Dinsdale et al. 2008). Upon receiving a death signal, Bax and Bak, also members of the BCL-2 family, form oligomers on the outer wall of the mitochondria, leading to its permeabilization and subsequent release of cytochrome C and caspase activation, BCL-2 acts by blocking the formation of oligomers (Cory and Adams 2002). BCL2 is overexpressed in 70% of B-cell CCL, however in only 5% of the cases could its overexpression be explained. Another characteristic of B-cell CCL is loss of chromosome 13q14.3, which is also lost in several other cancer types, suggesting it harbors a tumor suppressor. After sequencing the entire region two miRNAs, miR-15 and miR-16 were identified, it was noted that their loss is reported in 70% of CCL, which is proportional to the number of cases with BCL-2 overexpression (Cory and Adams 2002). Finally, it was experimentally proven that miR-15 and miR-16 do in fact directly regulate BCL-2 and their ectopic expression induce apoptosis in a verity of cancers (Aqeilan, Calin et al. 2010).

1.3.2.4 Angiogenesis

The first hints of the importance of miRNAs in the regulation of vasculature arose from mouse models of homozygous deletion of Dicer. These mice were deficient for angiogenesis and died at between days 12.5 and 14.5 of gestation (Yang, Yang et al. 2005). To further elucidate miRNAs role in vascular development, dicer was selective deleted in endothelial cells. The knockout mice were viable and normal compared to littermates. Interestingly, the endothelial cells had diminished response to VEGF-A, increased expression of several pro-angiogenic factors, and reduced microvessel formation (Suarez, Fernandez-Hernando et al. 2008). However, none of the data points to the direct regulation of angiogenesis by a specific miRNA. Several candidate miRNAs (miR-296, -130a and 132) were selected based on their upregulation in tumor cells, their responsiveness to VEGF-A and ability to stimulate tumor growth, survival and angiogenesis (Chen and Gorski 2008).

Another potent oncogene frequently overexpressed, MYC, is associated with robust neovascularization and tumors rich in red blood cells (Dews, Homayouni et al. 2006). MYC is known to up regulate the first identified oncogenic miRNAs described in mammals, the miR-17-92 family (Mendell 2008). This family of miRNA is directly responsible for the MYC-driven angiogenesis by their regulation of Tsp1, which antagonizes the pro-angiogenic VEGF-A signaling and connective tissue growth factor, CTGF, a modulator of the ECM allowing for infiltration of nascent blood vessels (Dews, Homayouni et al. 2006).

1.3.2.5 Invasion and Metastasis

The miR-200 family is perhaps the most widely studied miRNA family, with over four thousand papers published since they first came to light as regulators of EMT (Gregory, Bert et al. 2008). The family is composed of five members in two clusters, miR-200a/b and 429 reside on chromosome 1 and miR-200c and 141 on chromosome 12. In a screen to identify miRNAs that respond to EMT, only miR-200 family expression was significantly affected with a complete loss of the entire family (Gregory, Bert et al. 2008). Forced expression of a polycistron was sufficient to inhibit EMT, demonstrating that the miR-200 family downregulation was a critical step in EMT. Additionally, was shown that over-expression of the miR-200 family was able to reverse the mesenchymal characteristics of the highly invasive breast carcinoma cell line 4T07 (Korpal, Lee et al. 2008).

The miR-200 family mediated its anti-tumorigenic effect through its regulation of E-cadherin transcriptional repressors ZEB1 and SIP1, Smad-interacting protein 1, also called ZEB2 (Korpal, Lee et al. 2008). These transcription factors lie at the core of the machinery responsible for EMT by repressing E-cadherin and promoting cancer cell migration and invasion (Vandewalle 2005). Finally, in attempting to understand how the miR-200 family expression was lost, it was observed that ZEB1/2 e-box sites were located in close proximity to each polycistron and in fact ectopic expression of ZEB1/2 led to down regulation of the miR-200 family (Bracken, Gregory et al. 2008). Collectively, these findings established a double-negative feedback loop between miR-200 and ZEB1/2 during EMT and tumorigenesis.

1.3.2.5.2 MiRNAs Found in Exosomes and Potential Regulation of EMT

It has been observed that miRNAs expressed in dicer null cells were attributed to miRNA secreted from surrounding cells (Ravi, Gurtan et al. 2012). This is in support of the observation made by the Lotvall group, they were able to isolate exosomes and found that they contained both mRNA and miRNAs (Valadi, Ekstrom et al. 2007). Exosomes are small (50-90nm) membrane vesicles and have been shown to be important for signaling (Raposo and Geuze 1996). Valadi et al. determined that exosomes contain miRNAs and mRNA that can be internalized by a cell and that these miRNAs can regulate target mRNAs, thereby exerting an effect on the production of functional proteins. This claim has further been supported by the notion that miRNAs from plants can and have been absorbed in sufficient quantity to influence gene expression in human livers (Zhang, Hou et al. 2012). It appears that the exosome protected its content from not only the pH of the stomach but also various RNAases that naked RNAs would normally encounter. Finally, this same group and others have shown that miRNAs that are found in exosomes can be used as biomarkers in the detections of cancers of various origins (Chen, Ba et al. 2008).

My first experiments focused on exosome isolation and the potential that they might have on priming a distant site for tumor metastasis, a possibility that was further substantiated by the

finding that trypsinization reduces the expression of the miR-200 family that regulates ZEB and EMT (Gregory, Bert et al. 2008). However, further analysis suggested that this was due to a bias in the RNA prep chosen by the group and the paper was retracted (Kim, Yeo et al. 2012). Additionally, exosomes are extremely small and might only contain several hundred total miRNAs whereas a cell will contain thousands of copies of a single miRNA. It has been postulated that tumors secrete more exosomes than non-malignant cells; however, this has not been experimentally tested. But the sheer number of exosomes that a cell would have to absorb to have a meaningful effect on gene expression does (in retrospect) raise doubts about the plausibility of the physiologic significance of exosomes and miRNAs in tumor metastasis.

1.3.2.6 Enabling Replicative Immortality

As of this writing there are no miRNAs implicated in this process. The enzyme responsible for telomere maintenance, Telomerase, consists of two principal components, reverse transcriptase (hTERT) and an RNA template (hTR) (Wright1 2000). The RNA template is a repeated hexamer and too short for conical miRNA regulation; furthermore, the UTR of hTERT is poorly conserved and devoid of high confidence miRNA seed matches. This could reflect the important nature of telomere maintenance in stem cell maintenance and that the gene evolved to contain no function miRNA target sites.

1.3.3 Emerging Hallmarks and Enabling Characteristics of Cancer

1.3.3.1 Enabling Characteristics of Cancer

miRNAs also have significant roles in establishing the tumor microenvironment. The tumor microenvironment tends to have a low pH and be hypoxic, conditions which promote genomic instability by affecting DNA repair trough the downregulation of genes involved in mismatch repair (MMR), homology-dependent repair (HDR), and nucleotide excision repair (NER) (Bindra and Glazer 2007). It was determined that under hypoxic conditions MYC and MAX were displaced from the promoter of MLH1, a gene involved in MMR, but this was in hypoxia-inducible factor 1alpha (HIF1α) independent manner (Bindra and Glazer 2007). This was surprising as HIF-1α is thought to be a master regulator of the hypoxic genetic switch. To explore the effects that HIF-1α on genomic stability in a miRNA dependent manor, HeLa cells were cultured in hypoxia conditions and RNA was extracted for miRNA profiling. It was determined that several miRNA were upregulated, the most significant of which were miR-373 and the previously reported miR-210 (Camps, Buffa et al. 2008, Crosby, Kulshreshtha et al. 2009). After bioinformatic analysis it was determined that these miRNAs regulated RAD52 and RAD23B, genes involved in HDR and NER, respectively. Inhibiting these miRNAs led to the restoration of these target genes under hypoxic conditions (Crosby, Kulshreshtha et al. 2009).

Exploring miRNA regulation of the second enabling characteristic, tumor promoting inflammation, we again find a miRNA that is able to produce a genetic landscape that promotes tumor progression. miR-155 has been reported to be upregulated in breast cancer and promote pancreatic tumor development. Additionally, its transgenic overexpression in B-cells caused Acute Lymphoblastic Leukemia (ALL) (Costinean, Sandhu et al. 2009). While miR-155's role

and targets have been determined in other cancer types, its role in breast cancer tumorigenesis has not been defined. It was determined that several inflammatory signals, IFN-gamma, IL-6 and LPS induce miR-155 expression (Jiang, Zhang et al. 2010). Following miR-155 induction it was noticed that STAT3, a mediator of the inflammatory response, was activated (Jiang, Zhang et al. 2010). miR-155's effect in promoting inflammation was dependent on its regulation of suppressor of cytokine signaling 1 (SOCS1), a tumor suppressor that functions as a negative regulator of the JAK/STAT pathway. Interestingly, it was observed that in two tumor samples SOCS1 had mutations in its UTR, which abolished the effect of miR-155. This suggests that early events in tumor formation require down regulation of the JAK/STAT pathway indicating a potential dichotomous role (Jiang, Zhang et al. 2010).

1.3.3.2 Emerging Hallmarks of Cancer

1.3.3.3 Reprogramming of Energy Metabolism

One of the central regulators of aberrant cellular metabolism is MYC, which directly regulates glucose metabolic enzymes and genes involved in mitochondrial biogenesis (Eilers and Eisenman 2008). In an effort to understand MYC effect on the mitochondrial proteome (Gao, Tchernyshyov et al. 2009) uncovered that glutaminase, GLS, expression was upregulated upon induction of MYC expression. GLS converts glutamine to glutamate for further catabolism by the TCA cycle for the production of ATP and glutathione. Cancer cells that are "addicted" to MYC expression are sensitive to glutamine deprivation (Yuneva, Zamboni et al. 2007). The miR-23 family was identified as candidate miRNAs, as GLS contains conserved binding sites and miR-23 has been documented to be down-regulated in response to MYC driven oncogensis

in prostate cancer (Porkka, Pfeiffer et al. 2007). Experimental validation proved that MYC binds to the promoter of the miR-24 family, reducing their expression and increasing GLS production, which, in part, facilities the Warburg affect.

1.3.3.4 Avoiding Immune destruction

miRNAs are involved in every facet of immune development. They are also involved in both the innate and adaptive immune response, modulate inflammation, and regulate development of T and B-cells. Finally, they can induce differentiation and restrict lineage plasticity (Lindsay 2008). Natural-killer group 2, member D (NKG2D) is a receptor found on natural killer cells and T cells. NKG2D allows immune cells to respond to cells under stress through the recognition of stress molecules upregulated on pre-neoplastic cell surface facilitating their destruction (Trowsdale 2007). Two ligands for the NKG2D receptor--MICA and MICB--are induced following several types of stressors (Stephan Gasser 2006). Previous work has shown that human cytomegalovirus produces a miRNA that specifically down-regulates MICB, thereby avoiding immune detection (Stern-Ginossar, Elefant et al. 2007). It was determined that several endogenous miRNA set a threshold that limit the amount of protein produce and only a "real" stress signal produce enough mRNA to elicit a response, as the level of miRNAs did not change under stress conditions (Stern-Ginossar, Gur et al. 2008). All of these miRNAs are overexpressed in various tumor types and their forced expression protected tumor cells that were injected into BALB/C mice from natural killer cells (Stern-Ginossar, Gur et al. 2008).

Thus in summary, miRNAs regulate five out of the six core hallmarks of cancer and both the enabling characteristics and emerging hallmarks, as summarized in Figure 3.

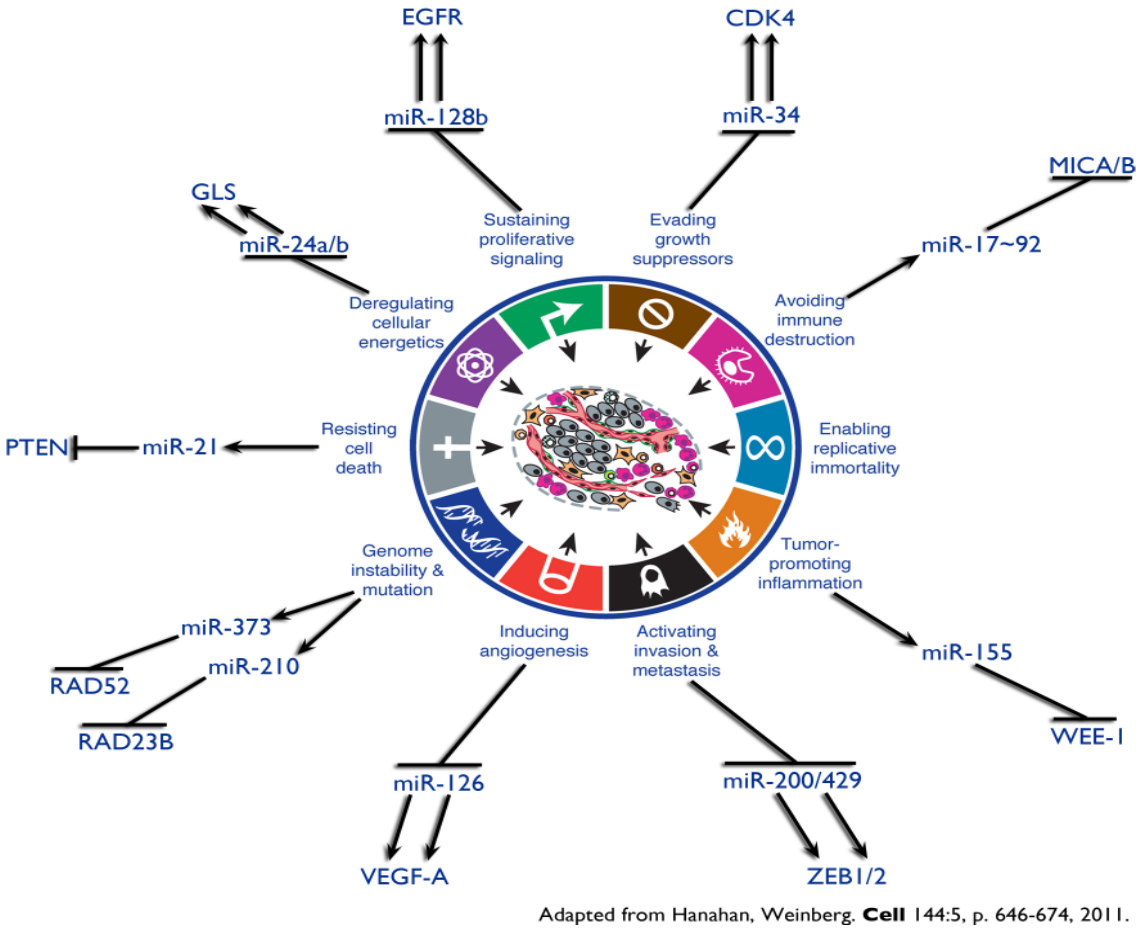

Figure 1.3 MiRNAs Regulate the Hallmarks of Cancer. Five of the six core hallmarks, both emerging hallmarks and enabling characteristics are regulated by miRNAs.

1.4 Lung Cancer

1.4.1 Statistics

Lung cancer comprised over 1.5 million new cases and was responsible for 1.4 million deaths worldwide in 2008, more than breast, colon, prostate, and pancreatic cancers combined (Figure 4A). Unsurprisingly, smoking causes 85% of lung cancer and smokers have a 10 to 20-fold increased risk of developing the disease than never smokers (Brownson, Alavanja et al. 1998). While lung cancer death rates are decreasing among males, a reflection of the changes in smoking habits, it is increasing in women, likely a result of the adoption of smoking by women later in the 20th century (Escobedo and Peddicord 1996). Currently more than 50% of newly-diagnosed lung cancers are former smokers, illustrating that the damage caused by smoking over a person's lifetime is permanent.

The overall 5-year survival is a dismal 16% and only 4% if metastatic disease is present at the time of diagnosis (Larsen, Cascone et al. 2011) (Figure 4B). This reflects in large part the lack of effective screening programs for lung cancer. Only 15% of lung cancers are diagnosed at early stages, typically serendipitously due to chest imaging for unrelated reasons (Raz 20007) . In contrast, effective population based screening is available for breast, colon, and prostate cancer, as well as melanoma, and other superficial (and hence more readily-palpable and visualized) cancers. This early detection leads to better treatment response and overall survival.

A

Estimated Cancer Related Deaths in 2011

Males			Females		
Lung & bronchus	85,600	28%	Lung & bronchus	71,340	26%
Prostate	33,720	11%	Breast	39,520	15%
Colon & rectum	25,250	8%	Colon & rectum	24,130	9%
Pancreas	19,360	6%	Pancreas	18,300	7%
Liver & intrahepatic bile duct	13,260	4%	Ovary	15,460	6%
Leukemia	12,740	4%	Non-Hodgkin lymphoma	9,570	4%
Esophagus	11,910	4%	Leukemia	9,040	3%
Urinary bladder	10,670	4%	Uterine Corpus	8,120	3%
Non-Hodgkin lymphoma	9,750	3%	Liver & intrahepatic bile duct	6,330	2%
Kidney & renal pelvis	8,270	3%	Brain & other nervous system	5,670	2%
All Sites	**300,430**	**100%**	**All Sites**	**271,520**	**100%**

B

Five-year Relative Survival Rates* (%) by Stage at Diagnosis, 2001-2007

	All Stages	Local	Regional	Distant		All Stages	Local	Regional	Distar
Breast (female)	89	99	84	23	Ovary	44	92	72	27
Colon & rectum	64	90	69	12	Pancreas	6	22	9	2
Esophagus	17	37	18	3	Prostate	99	100	100	29
Kidney†	70	91	63	11	Stomach	26	62	28	4
Larynx	61	77	42	33	Testis	95	99	96	73
Liver‡	14	27	9	4	Thyroid	97	100	97	56
Lung & bronchus	16	52	24	4	Urinary bladder§	78	71	35	5
Melanoma of the skin	91	98	61	15	Uterine cervix	69	91	57	19
Oral cavity & pharynx	61	82	56	34	Uterine corpus	82	96	67	16

American Cancer Society, Surveillance Research 2012

Figure 1.4 Lung Cancer: Leading Cause of Cancer Related Deaths World Wide. A. In 2011 there were 156,940 total reported deaths caused by lung cancer comprising 27% of all cancer related deaths. Adapted from Jemal A, et al. Cancer Statistics, 2011. **B.** While improvements in survival have been made in other types of cancer, lung cancer remains at a dismal overall 5-year survival rate of 16%. Only liver and pancreatic cancer have worse 5-year survival, yet represent a small fraction of new cancer diagnosis. American Cancer Society, Surveillance Research 2012.

1.4.2 Molecular Epidemiology

Lung cancer is a heterogeneous disease, molecularly, biologically and histologically. Two main types of lung cancer are non-small cell lung cancer (NSCLC) and small cell lung cancer (SCLC), which represent 85% and 15% of new cases respectively. NSCLC can further be classified into adenocarcinoma, squamous carcinoma, large-cell carcinoma, and mixed histologic subtypes. SCLC occurs with higher incidence in smokers, and typically originates in the central airways. These different classifications are not based only on histology and gene expression signatures, but also in the mutations that lie at the core of disease initiation.

Never-smokers can be classified as a distinct subclass of lung cancer, as it is molecularly and clinically different. Forty-five percent of never smokers have mutations in the EGFR, another 10% have mutation in human epidermal growth factor receptor 2 (HER2), or a chromosomal translocation resulting in the fusion of the echinoderm microtubule-associated protein-like 4 (EML4) gene with the anaplastic lymphoma kinase gene (ALK), producing the EML4-ALK fusion protein (Rudin, Avila-Tang et al. 2009). Cells that contain mutations in these receptors are addicted to the signaling pathways and responsive to “targeted” treatments (Rudin, Avila-Tang et al. 2009). This is in stark contrast to lung cancers arising in smokers which are characterized by mutation in KRAS in 50% of cases, PIK3CA in 8% of cases and inactivation of tumor suppressors including p53 with mutation rates approaching 50% (Pao and Hutchinson 2012). The sheer number of mutation in lung cancers associated with smokers and lack of treatments targeting driving oncogenic mutations have left many patients with potentially suboptimal treatment options such as cytotoxic cancer therapy.

1.4.2 Treatment

Treatment of oncogene addicted cancers by targeted therapies has been very successful (Larsen and Minna 2011). However, targeted therapies are only available for a small number of lung cancers and relapse is commonly observed. The recurrent tumor is typically refractory to targeted treatment (Kosaka, Yatabe et al. 2006). Treatment, while moving towards targeted therapies, is still largely based on the stage of the tumor, which is determined by confinement of the tumor and if/where the tumor has metastasized to. In any case, surgery is the first choice with adjuvant chemotherapy for stage I/II. For stage III (the tumor has metastases to the lymph nodes), the standard treatment is chemotherapy with focused radiation on the metastatic site. Stage IV is incurable and treatment is chemotherapy, radiation and palliative care (Gadgeel, Ramalingam et al. 2012). Front line chemotherapy is four cycles of a two drug regiment, one of which is platinum based (cisplatin or carboplatin) plus a third-generation chemotherapeutic agent such as paclitaxel, docetaxel, vinorelbine, gemcitabine, or pemetrexed, with paclitaxel used most often (Gadgeel, Ramalingam et al. 2012). The five-year survival for stage 1 lung cancer with only local disease is 27%. For stage II the five-year survival rate is only 12% due in large part to resistance and or recurrence which typically occurs within 4 to 6 months of disease remission. Stage III and IV are generally incurable (Gadgeel, Ramalingam et al. 2012).

Anyone of the hallmarks of cancer could be responsible for drug resistance, and, given that all the hallmarks have been experimentally proven to be regulated by miRNAs, it is no surprise that miRNAs have been shown to participate in the phenomenon of drug resistance

(Dong, Boyd et al. 2001, Siddik and Mehta 2009, Sarkar, Li et al. 2010, Zheng, Wang et al. 2010).

We sought to better understand the role that miRNAs play in lung cancer and drug responses. We made several profound discoveries of novel miRNAs involved in well-established oncogenic pathways encompassing every hallmark of cancer.

CHAPTER TWO MATERIALS AND METHODS

2.1 Cell Lines

All human lung cancer cell lines used in this study were established in the John D. Minna and Adi F. Gazdar laboratories. Cells were maintained in RPMI 1640 (Life Technologies Inc) with 5% fetal calf serum (FBS) and grown in humidified incubators at 37°C at 5% CO_2 and 95% air. Cell passage was kept and all experiments were performed on cell lines, which had fewer than 25 passages. Normal human bronchial epithelial cells (HBECs) were immortalized with ectopic overexpression of CDK4 and hTERT and were maintained in KSFM with supplied supplements (Invitrogen). All cell lines were fingerprinted using the PowerPlex 1.2 kit (Promega) and confirmed to be the same as the DNA fingerprint library maintained either by ATCC or the Minna and Gazdar labs. Additionally cells were mycoplasma tested (Bulldog Bio) prior to use and at various time points throughout their time in culture. Cell lines beginning with "H" were established National Cancer Institute and cell lines beginning with "HCC" were established at The University of Texas Southwestern Medical Center Hamon Center for Therapeutic Oncology Research while colon and pancreatic cell lines were kind gifts from Shay and Brekken Lab on campus. For experimental studies in charcoal striped media, cells were given two weeks to adjust to new media conditions, charcoal striped media and serum were supplied from Invitrogen. All other cell lines used in this study were obtained from collaborators and maintained in RPMI 1640 with 5% FBS.

2.2 Bacterial Work

All bacterial cell lines were selected in ampicillin at 10ug/ml from a 1000x stock. Transformations were as follows: 100ng of plasmid incubated in 50ul of XL1-Gold chemically competent cells (Aglient) for 30 minutes on ice followed by a 45 second heat shock at 42^{o}C. Bacterial cells were then allowed to recover on ice for 5 minutes and 500 ul of SOC media was added and cells were incubated at 37^{o}C shaking for 1 to 3 hours. Cells were then plated at various dilutions and spread using glass beads for even distribution and grown over night at 37^{o}C.

Single colonies (usually 10) were then picked and grown up overnight in 5ml of LB with ampicillin. 1,200ul of overnight culture was then spun down and plasmids were purified following directions of Qiagen mini prep kits, with the exception that elution was done in water, not TE, as most samples were sent for sequence verification. All plasmids were sequence verified using primers recommended by the manufacturer (Appendix C). Bacterial overnight cultures were frozen down using a 50/50 mixture of overnight culture and 80% glycerol as the cryogenic agent. Following sequence verification, only one or two samples were kept at -80°C for long-term storage (Appendix A).

Following sequence verification, starter cultures volumes of 5ml were prepared and allowed to grow for eight to twelve hours before inoculation of 200-300ml LB for overnight cultures to be used for Qiagen midi preps. Cells were spun down in a Sorvall RC5B using a GS-3

rotor for 30min at 4500rpm. Several modifications to the protocol were made to the protocol to increase yield: 1) Instead of 6ml of P1, P2 and N3 solutions, 12ml of each were used, 2) During the five minute incubation with P2, the 50ml conical tube was repeatedly inverted, 3) Once N3 was added, the solution sat in the 50ml conical for 10 minutes at a time of the liquid phase at the bottom was added to the filter cartage to prevent overflow and clogging the cartridge. DNA was quantified using a NanoDrop 2000. Yields were in the range of 200ng/ul to 500ng/ul when elution volume was 1ml. Plasmids then were sequenced to ensure no point mutation had occurred.

2.3 Transient Transfections

Lung cancer cell lines were optimized for transfection conditions in both 6 well and 96 well formats by varying lipid volume and cell number, and measuring the proliferative difference between scrambled control (Qiagen) and toxic control (Qiagen). For 6 well experiments, 3-6ul of RNAiMAX (Invitrogen) was added to 100ul of serum free RPMI-1640, SFM, and incubated at room temperature for 5 minutes. Ranges of siRNA and miR-10a mimic were from 5nM-50nM and are listed in Appendix B. Standard procedure, however was to use 20nM unless otherwise stated. 20nM of oligo was also incubated in 100ul SFM for 5 minutes at room temperature. The content of each tube was then mixed and allowed to incubate at room temperature for 20 minutes for lipid-oligo complex to form. Cells were seeded at varying densities based on growth rate and effects of oligo on cell viability; ranges from $1x10^5$ to $4x10^5$ were used. For 96 well assays 0.3ul of RNAiMAX was used and complex with olio in 50ul SFM and added to cells suspension of

100ul media with serum. Cells were seeded in ranges of 1,000 to 30,000 cells per well. Cells were quantified using a Beckman coulter counter 2000 or a hemocytometer.

2.4 Quantitative RT-PCR

RNA was harvested from cells using the mirVana miRNA isolation kit (Invitrogen). Cells were first washed with cold PBS; 300ul of lysis solution was then added to each plate or well of a six well dish. Cells were scraped off and not spun down to ensure no stress response genes were up regulated. Kit directions were then followed with the following exception; I used 100ul RNAase free water for elution. Quality was then determined using a NanoDrop 2000 and diluted to 40ng/ul. Both stock and diluted RNA was stored at -80^{o}C and cataloged (see Appendix B)

cDNA was produced using the iScript cDNA synthesis kit (BioRad) in 20ul reactions. We diluted enzyme 4-fold and were still able to obtain the same amount of cDNA, thus the limiting reagent was the 5x reaction buffer. cDNA was then diluted to 200ul final volume. Target gene TaqMan probes (Applied Biosystems, Table 2.1) were used for quantification and internally normalized to GAPDH for large RNAs or RNU19 for miRNAs. RT-PCR reactions were performed in an ABI-7900 Real-time PCR System. All reactions were repeated in triplicates and Prism GraphPad 5 or 6 was used to normalize and plot all data. qPCR primers are listed in Table 2.1.

GENE NAME	ASSAY ID
ALDH1A1	Hs00946916_m1
ALDH1A3	Hs00167476_m1
AXIN2	Hs00610344_m1
CDK6	Hs01026371_m1
DVL2	Hs00182901_m1
DVL3	Hs00610263_m1
GATA6	Hs00232018_m1
GLI2	Hs01119974_m1
HES1	Hs00172878_m1
HEY1	Hs01114113_m1
HOXB3	Hs01587922_m1
HOXD10	Hs00157974_m1
hsa-miR-101*	MIMAT0004513
hsa-miR-10b*	MIMAT0004556
hsa-miR-15a*	MIMAT0004488
miR-101-3p	MIMAT0000099
miR-10a-5p	MIMAT0000253
miR-10a*	MIMAT0004555
miR-10b	MIMAT0000254
miR-15a	MIMAT0000068
miR-337-3p	MIMAT0000754
NCOR2	Hs00196955_m1
PIK3CA	Hs00907957_m1
PIK3R1	Hs00933163_m1
PTCH1	Hs00181117_m1
PTEN	Hs02621230_s1
RNU19	X94290
U6 snRNA	NR_004394

Table 2.1: TaqMan Probes and Assay IDs for qPCR Analysis.

2.4 Microarray Analysis

Transcript expression data for all lung cancer cell lines was generated in the Minna Lab using the Illumina (WG6-V2 and V3 BeadChip) array platforms. Tumor cell RNA was isolated using Qiagen RNeasy kit and total RNA quality was confirmed by formaldehyde gel and/or capillary electrophoresis on the Experion System (Bio-Rad). Total RNA was labeled, amplified and re-analyzed for quality prior to hybridization by the UTSW Simmons Comprehensive Cancer Center Genomics Core.

RNA isolated from the mirVana kit was submitted to core facilities for expression profiling on Illumina HumanHT-12 V4 BeadArrays. Data was pre-processed using R package mbcb for probe summarization and background correction (Ding, Xie et al. 2008). Following pre-processing data was log-transformed after quartile-normalization. Finally MATRIX (MicroArray Transformation in Microsoft Excel) software version 1.41 was used to import and analyze microarray expression data. Using MATRIX, transcript expression was normalized across samples by the median value, and then normalized expression signals were $\log_2$-transformed and color-coded. Correlations in expression, were determined by Pearson's correlation coefficient. For comparison between sample classes (such as miR-10a and control mimic transfections), the ratio of log2- transformed signals from sample classes were generated and two-sample t-tests were performed in MATRIX to filter out non-significant differences in expression ($P = 0.05$).

2.5 NSCLC Tissue Microarray

Archived, formalin-fixed, paraffin-embedded tissues from surgically resected lung cancer specimens (lobectomies and pneumonectomies) containing tumor and adjacent normal epithelium tissues were obtained from the Lung Cancer Specialized Program of Research Excellence (SPORE) Tissue Bank at The University of Texas M. D. Anderson Cancer Center (Houston, TX). The tissue specimens were histologically examined and classified using the 2004 World Health Organization classification system and 282 NSCLC samples (177 adenocarcinomas and 105 squamous cell carcinomas) were selected for our tissue microarray (TMA). TMAs were constructed using triplicate 1-mm diameter cores per tumor; each core included central, intermediate, and peripheral tumor tissue. Detailed clinical and pathologic information, including patient demographics, smoking history, smoking status, clinical and pathologic TNM stage, overall survival duration, and mutation status of KRAS and EGFR, was available for most cases. The local institutional review board approved the study.

2.5 Protein Expression

Cell lysates were obtained using M-PER mammalian protein Extraction reagent (Thermo) supplemented with protease and phosphatase inhibitor (Roche). For miRNA mimic and transient transfections using siRNAs, cells were seeded at 200-300 thousand per well and five wells were pooled. All other treatments were in 10 cm plates and protein lysates were collected when cells were at 70-90% confluence. All samples have been cataloged (Appendix D). Protein lysates were

then quantified using a Bradford assay (Promega) and boiled in water, not a heat block, for even denaturation. Samples were then loaded at a concentration of either 30 or 40ug per well and then separated using 10% precast SDS/polyacrylamide gels (BioRad) followed by transfer to nitrocellulose membrane (Millipore). Membranes were then blocked for one hour at room temperature (RT) then incubated at 4°C overnight in primary antibody (see appendix B for overnight directions), followed by HARP conjugated secondary (Cell Signaling) for 1-4 hours at RT. Detection of proteins was obtained by enhanced chemiluminescences (Thermo Scientific). Primary antibodies are listed in Table 2.2.

Antibody	Cat No	Company	Dilution	
GATA6	SC9500	Santa Cruz	1 to 1000	5% BSA
Dvl3	3218	Cell signaling	1 to 2000	5% BSA
PI3K	4249	Cell signaling	1 to 3000	5% BSA
pATK Thr308	4056	Cell signaling	1 to 1000	5% BSA
pATK Ser473	9271	Cell signaling	1 to 1000	5% BSA
ATK	9297	Cell signaling	1 to 4000	5% blocking
pmTOR SER2448	5536	Cell signaling	1 to 1000	5% BSA
ALDH1A3	AP7847a	ABGENT	1 to 1000	5% blocking
GAPDH	2118	Cell signaling	1 to 30000	5% blocking
HSP90	4877	Cell signaling	1 to 3000	5% blocking
Cleaved PARP	9541	Cell signaling	1 to 1000	5% BSA

Table 2.2 Antibodies used along with catalog number, company purchased from, working concentration and blocking in overnight.

2.6 Aldefluor Assay

The Aldefluor kit (Stem Cell Technologies) was used to profile ALDH activity. Briefly, cells were counted and aliquoted at 1 million per tube and then spun down and resuspended in

100ul assay buffer containing BAAA, the assay substrate BODIPY-aminoacetaldehyde (BAAA) is catalyzed to a fluorescent product BODIPY-aminoacetate (BAA). This was then split into 500ul aliquots, with DEAB, an inhibitor of ALDH added to one aliquot. These samples were then incubated for 45min at 37°C for 45 minutes in the dark. Before the samples were taken to the core facility, 1ul of propidium iodine was added. Gating for ALDH+ cells is determined by inhibiting ALDH activity using diethylamino-benzaldehyde (DEAB). The assay was performed on a FACScan flow cytometer (BD Biosciences) while sorting was performed on either a MoFlow (Cytomation) or BD Aria (BD Biosciences). Purity of isolated cells was confirmed by post-sorting analyses.

2.7 Colony Formation and Growth Assay

For colony formation assays, stably transfected cell lines were plated and allowed to grow for two to three weeks at which point they were stained with 0.5% crystal violet and quantified. Transiently transfected cell lines were first reverse transfected with 20nm of miR-10a mimic, siDVL3, siPIK3CA, siGATA6 or miR-10a inhibitor and appropriate control, allowed to recover for 48 hours and then plated into six well dishes. Cells were plates at various concentrations ranging from 100 to 1,000 cells per well and allowed to grow until colonies were observed in the control wells. To measure growth rates, cells were plated into 96 well assay plates following reverse transfection and relative cell number was quantified using Cell Titer Glo (Promega) over 5 days. Cell numbers were optimized prior to transfection such that the control

cells were at 90% confluence when data was collected for end point assays; otherwise data points were collected at stated time points and normalized to controls. Cellular growth was also measured kinetically in 6 well dishes using an Essen Biosciences IncuCyte, with measurements intervals of four hours over several days for 96 time points. Plots were made in software packages provided by Essen Biosciences.

2.8 MiRNA Target Validation

A one kilobase segment of the DVL3 and GATA6 3'UTRs and the entire PIK3CA 3'UTR were cloned into pmirGLO Dual-Luciferase miRNA Target Expression Vector (Promega). H11155 cells were seeded at 20,000 cells per well in a 96 well dish and were transfected concurrently with the 100ng plasmid and 20nM either miR-10a mimic or control mimic. After 96 hours luciferase levels were quantified and normalized to the internal control using a luminometer (LUMIstar OPTIMA). The GGG in the miR-10a target site was changed to TTT using the QuikChange Site Directed Mutagenesis kit (Agilent), with the above protocol used to quantify luciferase levels. Primers used are in listed in Appendix C. All measurements were made in quadruplicate and raw data was analyzed in Prism GraphPad 5 or 6.

2.9 shRNA and miR-10a Over-Expression

Validated shRNAs targeting DVL3, GATA6 and PI3KCA and a non-targeting control were purchased from the Sigma TRC library (DVL3, cat. no. TRCN0000033344; PIK3CA, cat

no. TRCN0000196582; GATA6, cat. no. TRCN0000005392; non-targeting control, cat no. SHC002). Several shRNAs targeting the three genes were used from the pGIPZ library (), but the results were inconsistent and knock-down was always less than 50%. The difference in performance was likely due to differences in backbone construction: the Sigma TRC shRNA construct is driven by the U6 promoter with is RNA polymerase III dependent, while the pGIPZ shRNA construct from OpenBiosystems is CMV driven and processed using the miRNA machinery in the context of miR-30 (Figure 5). The use of pGIPZ makes several assumptions: 1) the cell line expresses miR-30 and can process the shRNA to produce a mature product, and 2) CMV promoter efficiency is consistent across all cell lines. This has been documented to be case and could be the reason for the inconsistent data generated from the pGIPZ shRNAs (Robert Jan Lebbink, Maggie Lowe et al. 2011) (Figure 6 A-D). miR-10a over expression construct and control were purchased from System Biosciences (miR-10a, cat. no. PMIRH10aPA-1; control, cat. no. PMIRH000PA-1).

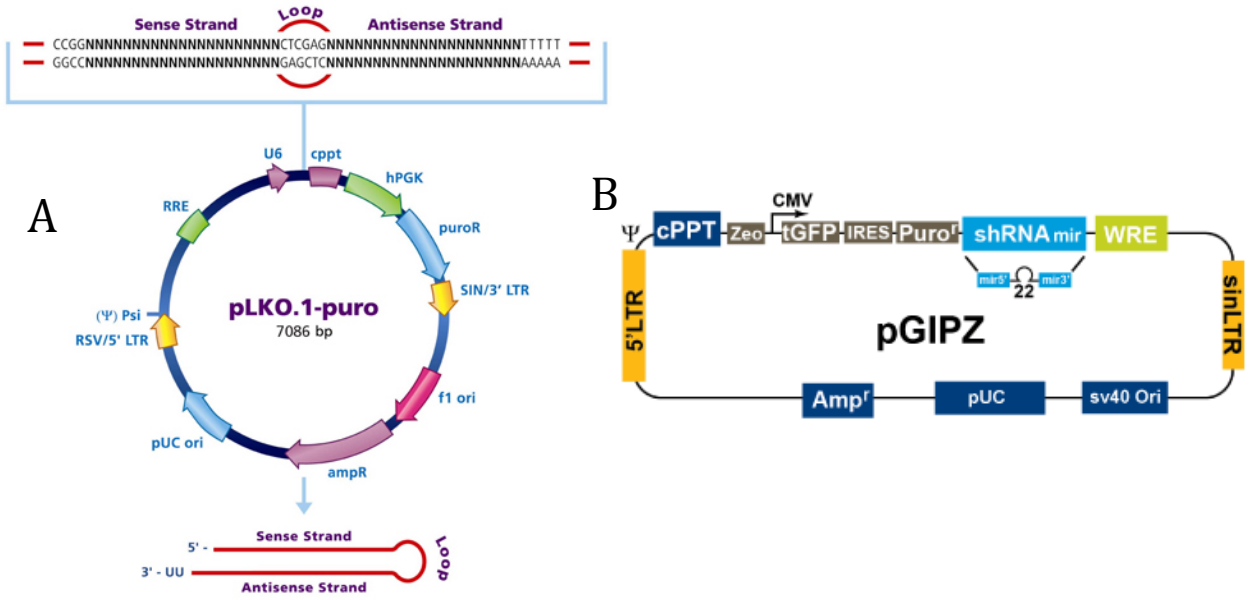

Figure 2.1. RNA Polymerase II Vs. III in Gene Silencing A. Backbone of Sigma's TRC vector, selection marker is on a pol-II dependent promoter while the shRNA is driven by pol-III. **B.** Vector map of the pGIPZ, which has two selection markers and the shRNA under control of one pol-II dependent promoter.

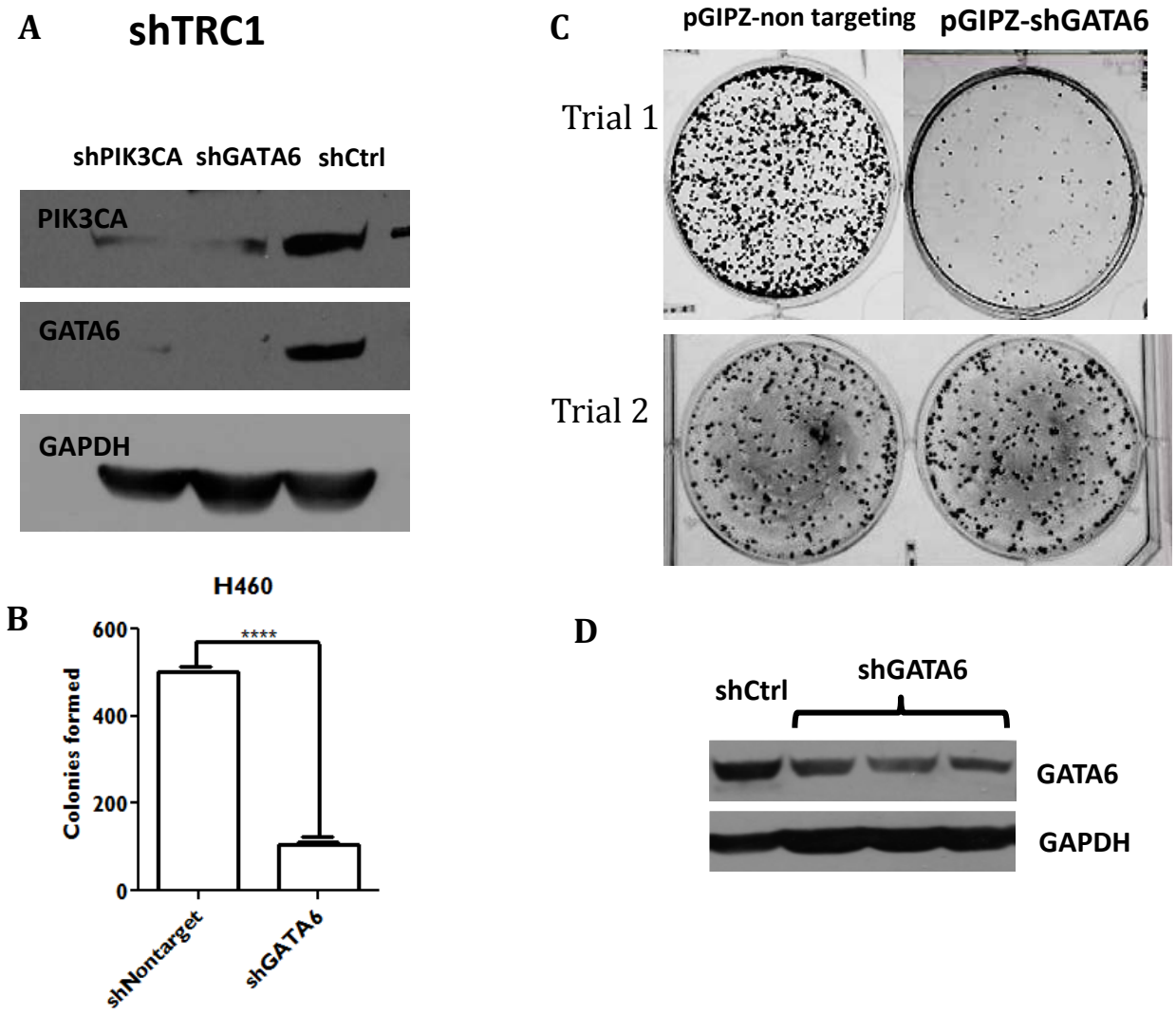

Figure 2.2 Gene Silencing is More Efficient From Polymerase III Promoters.
A. shRNAs targeting PI3K or GAT6 resulted in complete and consistent loss of protein levels following selection. **B.** Several cells lines were tested and transduced multiple times consistently leading to same phenotype. **** $P \leq 0.0001$ two tailed T-test. **C.** shGIPZ results were inconsistent over multiple cell lines and transduction. **D.** shRNAs only resulted in slight reduction of target genes even after selection dual selection, puromycin selection and then GFP sorting.

2.10 Lentiviral Production

Lentivirus was generated using lentiviral plasmids pGIPZ and Sigma's TRC using 293T-packaging cells. Lentiviral plasmid DNA is co-transfected with pMD2-VSVG (envelope plasmid) and either pCMV-deltaR8.91 or psPAX2 (gag/pol and rev expressing packaging plasmids with HIV backbone). psPAX2 reportedly has better efficiency, but both work very well.

Requirements:

293T cells at 50-70% confluence (maintain in RPMI 1640 R5 + G418 (0.5 mg/mL)

Don't use cells that have been in culture for > 1 month

Lentiviral plasmid DNA (in dH_2O or 1X TE pH8.0) (midiprep purified)

pCMV-deltaR8.91 or psPAX2 (gag/pol and rev expressing with HIV backbone)

pMD2-VSV-G (envelope expressing with HIV backbone)

FuGENE6 (Roche, #11 815 091 001, or 11 814 443 001)

Serum-free media (SFM) e.g. Opti-MEM (Invitrogen, #51985) (pre-warmed to 37°C)

Day 1:

The day before, seed 293T cells in R5 (no G418) to obtain 50-70% confluence

60mm: $4.0\text{-}5.0\times10^5$ cells

100mm: $1.3\text{-}1.5\times10^6$ cells

On the day of the transfection (in the afternoon):

Dilute FuGENE6 in SFM – adding FuGENE directly to media and not touching the tube (use table below). Flick to mix.

In a separate tube, dilute lentiviral plasmid and packaging/envelope plasmids in SFM (use table below). Flick to mix.

Incubate tubes at RT for 5min.

Use a 3:1 (µL:µg) FuGene6 to DNA ratio (total DNA from all plasmids)

Add entire plasmid mix to FuGENE6 mix, tap the tube or vortex for one second to mix the contents. Incubate complex for 20-30 min at RT.

Continued incubation for up to 45 minutes (for some cell lines up to two hours) will not affect transfection efficiency.

1. During incubation, aspirate media off 293T cells and replace with appropriate volume of R5 (no G418) (60mm:3.5mL, 100mm: 9.0mL)
    - 293T cells detach easily, add media slowly against the side of the plate
2. Gently add the DNA:FuGENE6 complex (60mm:100-200µL, 100mm: 200-400µL) to cells in a drop-wise manner (hold tip close to media surface). Mix by gently moving plate in ↕ and ↔ directions.
3. Incubate plates overnight in 37°C 5% CO_2 incubator**

** Media will begin to accumulate infectious virus so take appropriate precautions

		pGIPZ		pLKO	
		60mm	**100mm**	**60mm**	**100mm**
FuGENE Mix	FuGENE6	21µL	63µL	6µL	18µL
	SFM	129µL	237µL	74µL	142µL
Plasmid Mix	Lentiviral plasmid	3.0µg	9.0µg	1.0µg	3.0µg
	pCMV-dR8.91 or psPAX2	3.0µg	9.0µg	0.75µg	2.25µg
	pMD2-VSV-G	1.0µg	3.0µg	0.25µg	0.75µg
	Total volume (in SFM)	50µL	100µL	20µL	40µL
	Total transfection volume	200µL	400µL	100µL	200µL
Plating volume	R5	3.5mL	8.0mL	3.5mL	8.0mL

Day 2:

The next day (in morning), remove medium containing DNA-FuGENE6 complexes and replace with 4 mL R5 (no G418). Incubate plates in 37°C 5% CO_2 incubator overnight**

Can replace with R2 (RPMI 1640 with 2% FBS) instead of R5 to produce low serum containing virus (for example if using virus to transduce HBECs)

Media will contain infectious virus. Dispose of virus-containing media and plasticware appropriately

Day 3, 4, 5:

Media will contain infectious virus. Dispose of virus-containing media and plasticware appropriately

4. Virus can be harvested from days 3-5 (can harvest every 12-24 hrs). Harvest virus-containing supernatants by removing medium into a 15 mL tube.
    - If several harvests are being made, virus can be pooled and stored at 4^{o}C until harvesting finished, then continue with steps 10-12
    - Minimal differences in viral titer are observed between collection at 48-120hr
5. (Optional) Centrifuge supernatant at 3,000 rpm for 15 min at 4°C to pellet debris
    - Skipping this step avoids potential contamination of centrifuge with viral supernatant.
6. Filter viral supernatant through 0.45 μm filter (may require more than one filter)
7. Pipette supernatants into cryovials in 1-2 mL aliquots. Store at -80°C.
8. (Optional) If collecting sequential harvests, add fresh R5 to transfected 293T cells and incubate at 37°C for 12-24hr before harvesting.

2.10 In vivo Xenograft Growth

The NOD/SCID mouse xenograft model was used to characterize the tumorigenicity of prospective human lung cancer stem cell populations. All in vivo experiments were performed in female NOD/SCID mice, bred and purchased from the UTSW Mouse Breeding Core. The care and treatment of experimental animals were in accordance with institutional guidelines, and this project was approved by the UTSW animal care committee (IACUC).

Induction of subcutaneous tumors using shDVL, shCTRl, pCDH miR-10a and pCDH ctrl were carried out through injection of 1 million cells in 100ul of PBS. To minimize leakage at the injection site, 27 1⁄2 or 30 1⁄2 gauge needles were used and the subcutaneous region was made

accessible for injection by lifting the skin at the site of injection to alleviate pressure on the injected volume. Prior to subcutaneous injection, fur on the right flanks of mice was shaved off using an electric razor to improve detection of xenograft formation. Tumor volume was measured by caliper biweekly for up to ten weeks. Tumor volumes were calculated as follows: $V_{tumor} = (\pi/6)(d_{large})(d_{small})^2$.

2.11 Dose Response Curves

hsa-miR-337

H1155 cells were reverse transfected with 50nM of miR-337 mimic or control non-targeting mimic complex with 0.6ul Dharmafect (Invitrogen) and seeded at a density of 6,000 cells per well in a 96 well assay plates. Following 72 hrs. of pretreatment the appropriate drug was added and following incubation with drug for 72 hrs. cell viability was determined using Celltiter 96 AQueous One Solution Cell Proliferation Assay (MTS) (Promega).

For combinatorial studies, siRAP1A and siSATA3 oligos were purchased from Thermo Scientific, and used at a concentration of 25nM; the control non-targeting oligo was delivered at 50nM. The above protocol was followed.

miR-10a and miR-15a Mimic

H1155 and H460 cells were seeded at 6,000 cells per well and reverse transfected with 20nM of miR-10a mimic or control mimic #2 using 0.3ul RNAiMAX. Following 72 hrs. of pre-

treatment, the appropriate drug was added; following incubation with drug for 72 hrs., cell viability was determined using Celltiter 96 (Promega).

miR-10a Inhibitor

H1155 and H460 cells were seeded at 2,000 cells per well and reverse transfected with 20nM of miR-10a mimic or control mimic #2 using 0.3ul RNAiMAX. Following 72 hrs. of pretreatment the appropriate drug was added; following incubation with drug for 72 hrs., cell viability was determined using Celltiter 96 (Promega).

2.12 Drug Dilutions and Resuspension

Vinorelbine (FW: 778.932 g/mol)

From stock of 10 mg/ml (12.8 mM) remove 5 microliters and add to 25 ml of R5 to give a starting stock of 2560 nM. Add 100 microliters to the first well, when diluted this will give a final concentration of 1024 nM. 1 to 4 dilutions can be preformed all the way down to 0.0039 nM.

Vincristine (FW: 824.958 g/mol)

From stock of 1 mg/ml (1 mM) remove 64 microliters and add to 25 ml of R5 to give a starting stock of 2560 nM. Add 100 microliters to the first well, when diluted this will give a final concentration of 1024 nM. 1 to 4 dilutions all the way down to 0.0039 nM.

Vinblastine (FW: 810.974 g/mol)

From stock of 1 mg/ml (1.23 mM) remove 52 microliters and add to 25 ml of R5 to give a starting stock of 2560 nM. Add 100 microliters to the first well, when diluted this will give a final concentration of 1024 nM. 1 to 4 dilutions were done all the way down to 0.0039nM.

Gemcitabine (FW: 263.198 g/mol)

From stock of 38 mg/ml (141 mM) needs a 1 to 10 dilution first done in Milli-Q water. From the 1 to 10 dilution, remove 4.539 microliters into 25 ml of R5 (this will give a starting stock of 2560 nM). Add 100 microliters to the first well, when diluted this will give a final concentration of 1024 nM. 1 to 4 dilutions can be preformed all the way down to 0.0039 nM.

Cisplatin (FW: 300.05 g/mol)

From stock 1 mg/ml (3.3 mM), remove 2.1 ml and add to 7.9 ml R5 to give a starting stock of 693 μM. Add 100 microliters to the first well, when diluted this will give a final concentration of 262 μM. 1 to 4 dilutions can be preformed all the way down to 4 nM.

BEZ-235 (FW: 418.477g/mol)

BEZ-235was resuspended in DMSO to give a stock of concentration of 2 mM. From this stock remove 16 μL into 12.5 ml R5 for a working stock of 2560 nM.

ATRA Resuspension (**FW: 300.44 g/mol**)

50 mg (0.00016 moles) ATRA was obtained from Sigma (cat. no. R2625). This was dissolved in 16ml of DMSO for a 10mM stock from which a 1 to 10 dilution was done to make a 1 mM or 1000 μM working stock. Keep protected from light.

9-Cis Resuspension (FW: 300.44g/mol)

1 mg 9-cis retinoic acid (3.328 μmoles) was obtained from Sigma (cat. no. R4643) and dissolved in 332 μL of DMSO for a stock concentration of 10mM, from which a 1 to 10 dilution were performed to make a working stock of 1000 μM.

2.13 Statistical Methods

Correlations between expression of different genes the panel of NSCLC lines was done by simple linear regression. Differences in RT-PCR, proliferation, tumor growth and colony formation assays were assessed by analysis of variance and Student's *t*-test using GraphPad Prism 5 or 6 software(Marcato, Dean et al.). Difference between control and experimental groups were considered statistically significant when $P<0.05$. Drug sensitivity assays were graphed using nonlinear-fit baseline-corrected dose response curves in GraphPad Prism 5 or 6; significance was determined using sum-of-squares F test.

2.14 Apoptosis Assay

H460 cells were reverse transfected with 20 nM of miR-10a mimic or control oligo and plated into 96 well plates and incubated with DEVD-NucView (Essen Bioscience), which is a florescence reporter for Caspase-3/7 activation. Overall cell number is determined by staining all cells with a nuclear staining dye 72 hrs. post transfection. Differences in florescence before the endpoint determine the percent of cells undergoing apoptosis. For H2009 cells, we used Promega Caspase-glo 3/7 72 hrs. post transfection with miR-10a mimic and control mimic.

2.15 GATA6 ChiP

As described in (Verzi, Shin et al. 2010), the antibody and kit were used as directed by the manufacturer. Cells were plated and allowed to grow to 60-80% confluence in 10 cm dishes and cross-linked using 37% formaldehyde. The reaction was quenched using glycine, and samples were lysed using 10% SDS. Genomic DNA was purified using the EZ-ChiP Chromatin Immunoprecipitation kit (Millipore, cat no. 17-371). Samples were sonicated to generate a 1 Kb smear and then incubated with the GATA6 antibody listed in Table 2.2. Following purification, DNA was amplified using primers listed in Appendix C. PCR products were run on a 1% agarose gel.

2.16 miRNA Inhibitor Screen and Validation

A miRNA inhibitor library containing inhibitors for 747 human miRNAs was purchased from Exiqon. H1155 cells were seeded at 10,000 cells per well, suspended in 100 ul R5 and transfected with 0.6ul Dharmafect in 25ul of SFM and 50nM of the miRNA inhibitor in 25ul SFM. After 72 h incubation with the miRNA inhibitor, cells were treated with paclitaxel at the EC20 (in this case 10 nM) or media only for 72 hrs., at which point viability was determined using CellTiter-Glo (Promega). Perimeter wells contained media only. Each measurement was made in triplicate. Hits were determined by an FDR of less than 0.05. All data graphed are z-scores (Figure 4.1A). All called hits were validated using the same experimental design.

CHAPTER THREE miR-337 and Cellular Response to Paclitaxel

3.1 Introduction

Paclitaxel is a mitotic inhibitor isolated in the 1960s from the Pacific yew tree. It first showed anti-tumor activity in a mouse model of leukemia. However, it was not until ten years later that it was shown to be effective in xenograft tumors of breast, endometrium, ovary, brain, lung and tongue tumors(Riondel, Jacrot et al. 1986) . Paclitaxel-treated mice showed as much as a 91-day growth delay compared to mice in the control group. Currently, it is still used to treat lung, ovarian, breast and head and neck cancers.

Paclitaxel acts by binding to the beta-subunit of tubulin, an interaction that stabilizes microtubules. Microtubules are dynamic structures that rapidly polymerize and depolymerize and are key components of the cytoskeleton and are essential in all eukaryotic cells. They are made up of tubulin heterodimers composed of alpha and beta tubulin monomers, each with a molecular mass of 50kD. The tubulin subunits form the microtubule structures, which are hollow tubes approximately 25nm in diameter and radiate from centrosomes. These dynamic structures are involved in many cellular processes, including but not limited to cellular movement, intracellular transportation and cell division. The biological functions of microtubules are determined and regulated by polymerization dynamics (Storer and Salmon 1997).

Compounds that target microtubules can be grouped as either microtubule stabilizing such as taxanes or microtubule-destabilizing. Each class suppresses microtubule dynamics, which blocks cell cycle progression and causes cell death via apoptosis. However there is wide

variation of response among our panel of NSCLC cell lines (Figure 3.1). Understanding biological causes of these variations has been studied intensely.

There are several genes that encode different isotypes of both the alpha and beta tubulin, which are not only encoded on different chromosomes but are also expressed in different tissues. Tubulin is highly conserved with exception of the C-terminus, which can be post-transcriptionally modified. Changes in expression patterns of these isoforms and thus modifications to the C-terminal can prevent the movement of paclitaxel to the lumen of microtubules (Hammond, Cai et al. 2008). Additionally, microtubules provide binding sites for many proteins, one of which is BIM, a pro-apoptotic protein. Cell lines that have high levels of BIM were more susceptible to paclitaxel treatment (Li, Moudgil et al. 2005). Finally, a genome-wide synthetic lethal screen revealed dozens of pathways that can affect cellular response to paclitaxel (Whitehurst, Bodemann et al. 2007). Upon starting my thesis work I honed in on miR-337 as a modulator of paclitaxel response in NSCLC. Of the three miRNAs that had an anti-correlation with paclitaxel response only manipulation in miR-337 had an effect on cellular response to paclitaxel. miR-337 is conserved among mammals and no SNPs have been reported in the pri-miR-337 structure. We observed a fourfold sensitization of H1155 to paclitaxel with pre-treatment of miR-337 mimic (Figure 3.2 A&B). Testing this finding in several other cell lines revealed a consistent effect (Du, Subauste et al. 2012). We were then interested whether miR-337 would have similar effects on other microtubule targeting agents and if its validated targets, RAP1A and STAT3, might affect cellular response to paclitaxel (Du, Subauste et al. 2012).

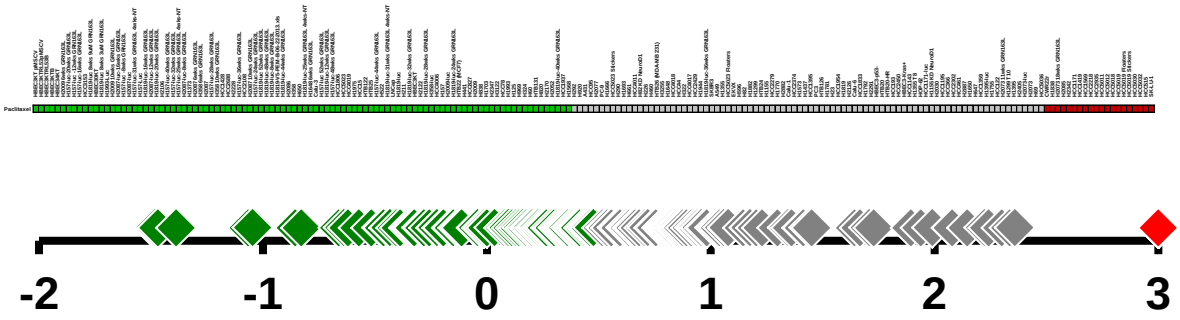

Figure 3.1 Variations in Paclitaxel Response Across NSCLC. Range of the EC50 of paclitaxel across our panel of NSCLC. Scale is log10. Assays were preformed on 189 cell lines, most repeated N=4 some were N=1 others were N=14, resulted in an average EC50 of 119.01nM (SD of 303.4). Normal Human HBEC lines cluster together.

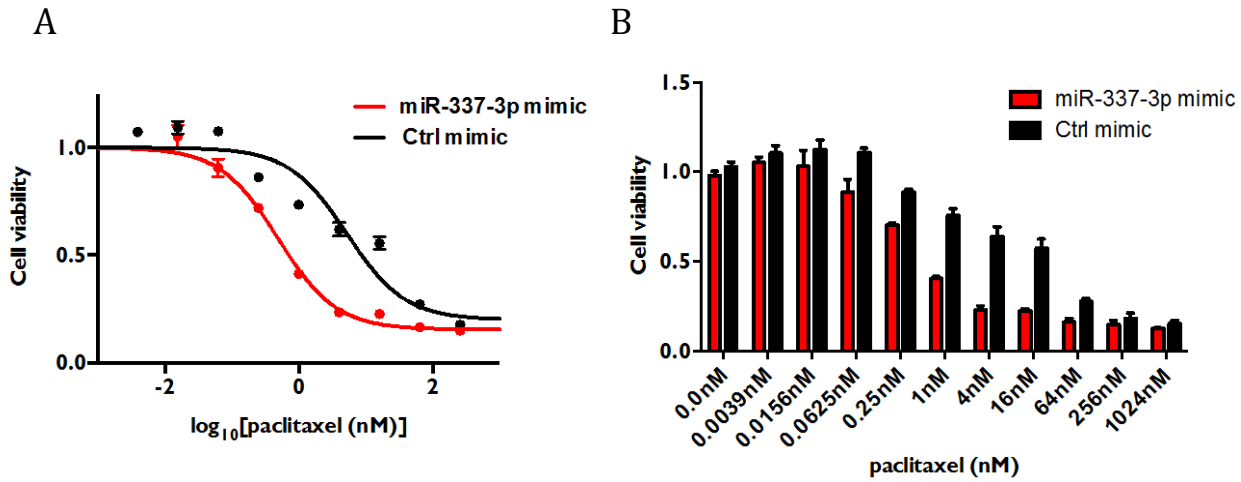

Figure 3.2 miR-337 Sensitizes H1155 to Paclitaxel Treatment. A. H1155 cells pretreated with miR-337 for 72hrs followed by paclitaxel treatment. EC-50 control mimic cells was 5.199nM, miR-337 mimic treated cells was 0.4898nM. $P \leq 0.0001$, each data point is an N=3. **B.** Bar graph representation of raw data collected.

3.2 Results

3.2.1 miR-337 Modulation of Drug Response is Specific to Microtubule Targeting Agents

Docetaxel is a semi-synthetic analogue of paclitaxel and differs at only two positions in its chemical structure. These structural differences make it more water-soluble than paclitaxel. Docetaxel is considered for treatment only after initial response to standard therapy fails and it demonstrates modest improvements in overall survival. Following 72hrs of miR-337 mimic treatment we exposed H1155 cells to various doses of docetaxel and observed an EC_{50} of 2.43nM when cells were pretreated with miR-337 and EC_{50} of 14.66nM when treated with the scramble control (Figure 3.3 A&B).

Since paclitaxel and docetaxel are in the same family of microtubule stabilizers and across the panel of cell lines there is a strong correlation of cellular response, we evaluated several microtubule destabilizing compounds: vinorelbine, vincristine, and vinblastine. These drugs make up the vinca alkaloids subset of microtubule-targeting agents and are derived from the Madagascar periwinkle plant. They were discovered in the 1950s for the treatment of diabetes and serendipitously found to have anti-tumor effects. Unlike paclitaxel, which binds to and stabilizes microtubules, this class of drugs binds to the tubulin monomers preventing their polymerization. These drugs bind directly to microtubules and cause their rapid depolymerization (Tiburi and andrade 2002).

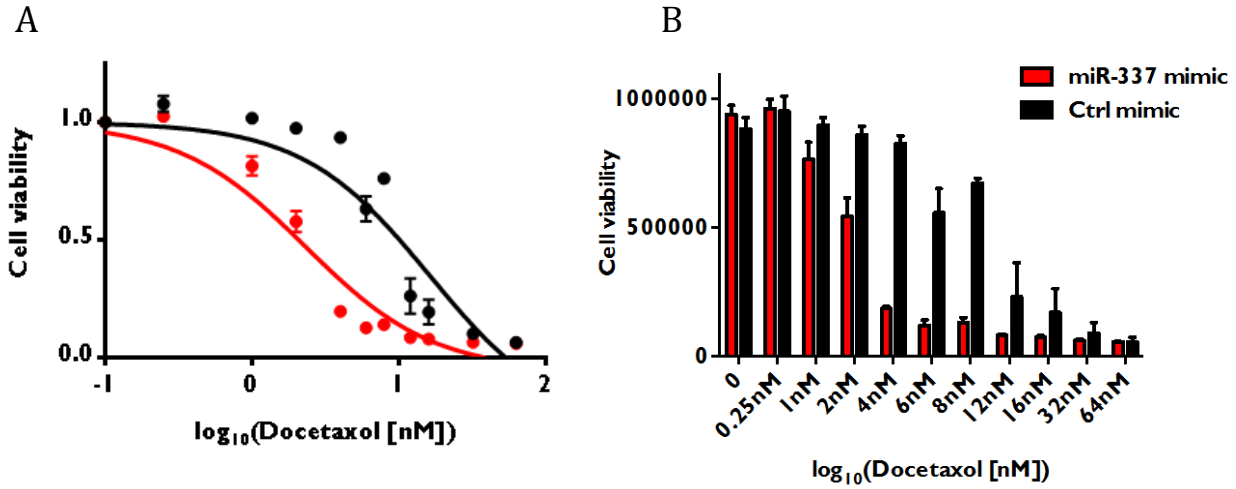

Figure 3.3 miR-337 Sensitizes H1155 to Docetaxel Treatment A. Following 72 hours of miR-337 mimic treatment we exposed H1155 cells to various concentrations of docetaxel and observed an EC_{50} of 2.434nM when cells were pretreated with miR-337 and EC_{50} of 14.66nM for the scramble control, each data point is N=4 $P \leq 0.0001$. **B.** Bar graph representation of the raw data.

Vincristine and vinblastine are naturally occurring and vinorelbine is semi-synthetic analog. Vinblastine, vinorelbine and vincristine all bind to the beta subunit of the tubulin dimers at distinct region called the vinca binding domain and each has higher affinity for free tubulin then that bound in microtubules (Bai, Pettit et al. 1990). When we treated H1155 with the Vinca alkaloids we observed similar phenotypes that were observed with paclitaxel and docetaxel when miR-337 mimic was present (Figure 3.4 A-C, Table 3.1).

Finally, in order to examine whether other types of chemotherapies would be affected by miR-337 we tested the effect of miR-337 on the DNA crosslinking agents Cisplatin, a platinum based chemotherapy, and Gemcitabine, a nucleoside analog. Both of these drugs cause growth arrest by disrupting normal DNA replication and repair. However, miR-337 was unable to sensitize the cells to these therapies indicating the specificity of miR-337 to microtubule targeting agents (Figure 3.5 A&B, Table3.1).

Drug	EC_{50}miR-337 (nM)	EC_{50} ctrl mimic (nM)
Paclitaxel	0.4898	5.199
Docetaxol	2.331	16.3
Vincristine	0.5345	4.669
Vinblastine	0.002807	0.2033
Vinorelbine	0.03038	1.87
Gemcitabine	10.61	11.68
Cisplatin	5980	2993

TABLE 3.1 miR-337 Effect on H1155 Treated With Various Chemotherapies

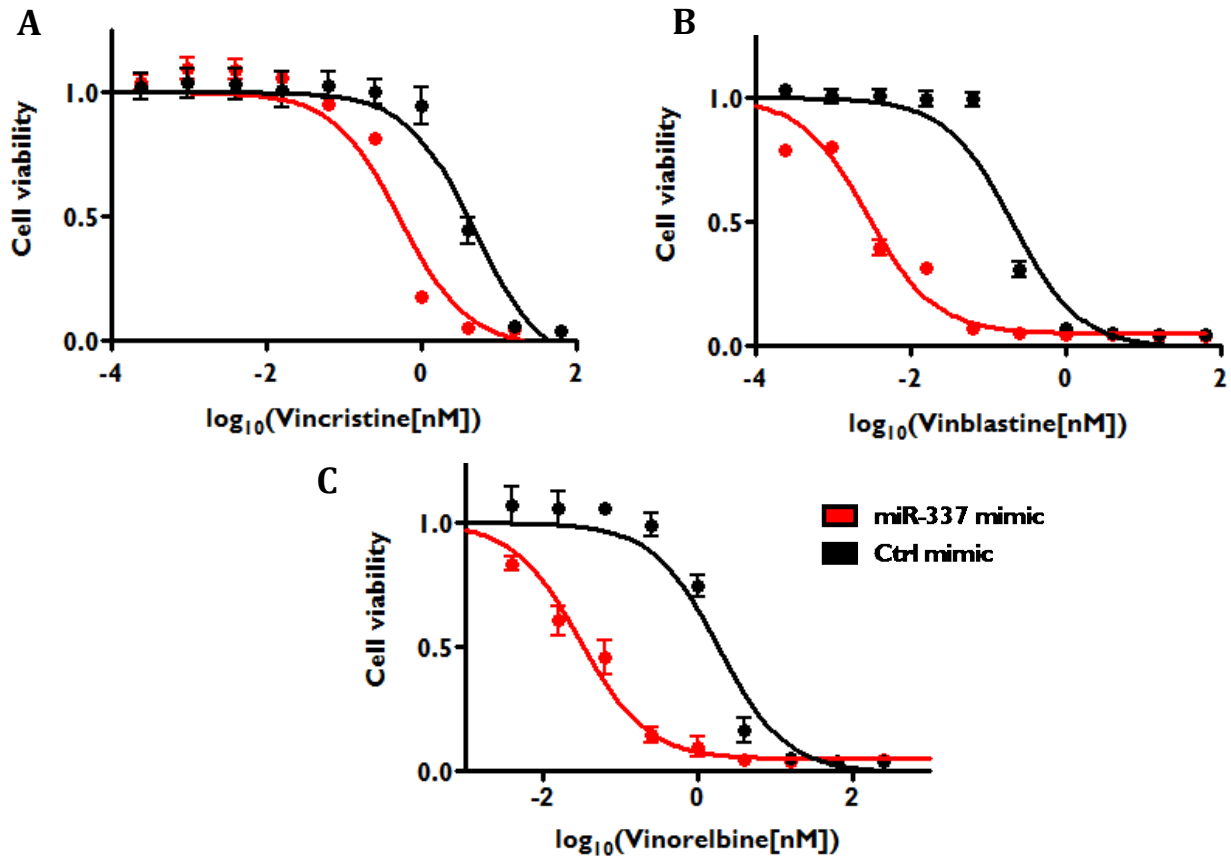

Figure 3.4 miR-337 Sensitizes H1155 to Vinca Alkaloids. **A.** Cells treated with control mimic had an EC_{50} of 4.66nM while miR-337 treated cells had an EC_{50} of 0.53nM. $P \leq 0.0001$ N=3. **B.** Cells treated with control mimic had an EC_{50} of 0.20nM while miR-337 treated cells had an EC_{50} of 0.0028nM. $P \leq 0.0001$ N=3. C. Cells treated with control mimic had an EC_{50} of 1.870nM while miR-337 treated cells had an EC_{50} of 0.03038nM. $P \leq 0.0001$ N=3.

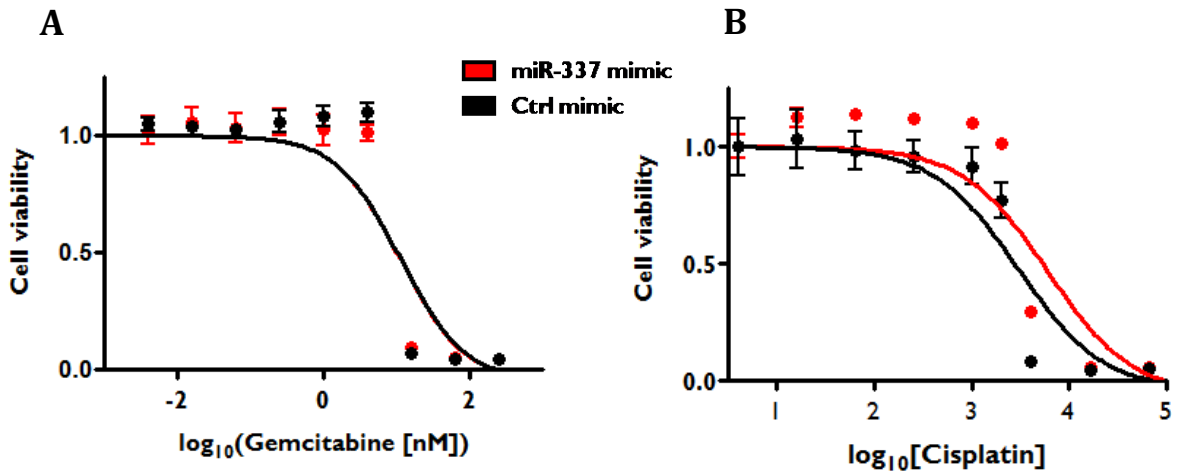

Figure 3.5 miR-337 does not Affect Cellular response to Gemcitabine or Cisplatin
A. H1155 cell pretreated with miR-337 had no effect on Gemcitabine treatment: Ctrl mimic EC_{50} 11.68nM, miR-337 mimic 10.61nM. **B.** Similar observations when H1155 cells were treated with cisplatin: Ctrl mimic EC_{50} 2993nM, miR-337 mimic EC-50 5980nM. N=3 for each data point on both graphs.

3.2.2 RAP1A and STAT3 Are Responsible for miR-337's Effect on Cellular Response to Microtubule Targeting Agents.

To understand which of miR-337 target genes were sensitizing cells to microtubule targeting agents we performed a microarray 72hrs post transfection with miR-337 mimic to determine which genes decreased in expression and contained miR-337 target sites. Following bioinformatic analysis and biological target validation, it was determined that miR-337 regulated both RAP1A and STAT3 (Du, Subauste et al. 2012). STAT3 is a transcription factor involved in the inflammation response and has been demonstrated to be hyperactive in a variety of tumor types and contribute to oncogenesis by promoting cell survival and proliferation, invasion, angiogenesis and also drug resistance (Sara Pensa, Gabriella Regis et al. 200). RAP1A is a ubiquitously expressed member of the Ras GTPase subfamily and has two isoforms, RAP1A and RAP1B, which share 95% sequence identity. RAP1A is an important mediator of integrin inside-out signaling. Integrins are transmembrane receptors that mediate the attachment between a cell and its surroundings, such as other cells or the ECM. They are also involved in cell signaling, shape, motility and even cell cycle control (Kinashi and Katagiri 2004, Shen, Delaney et al. 2012).

Loss of STAT3 or RAP1A expression following siRNA-mediated knockdown had no effect on paclitaxel response alone (Figure 3.6 A&B). However, when we took a combinatorial approach we observed similar sensitization to paclitaxel that was observed with miR-337 (Figure 3.2 A).

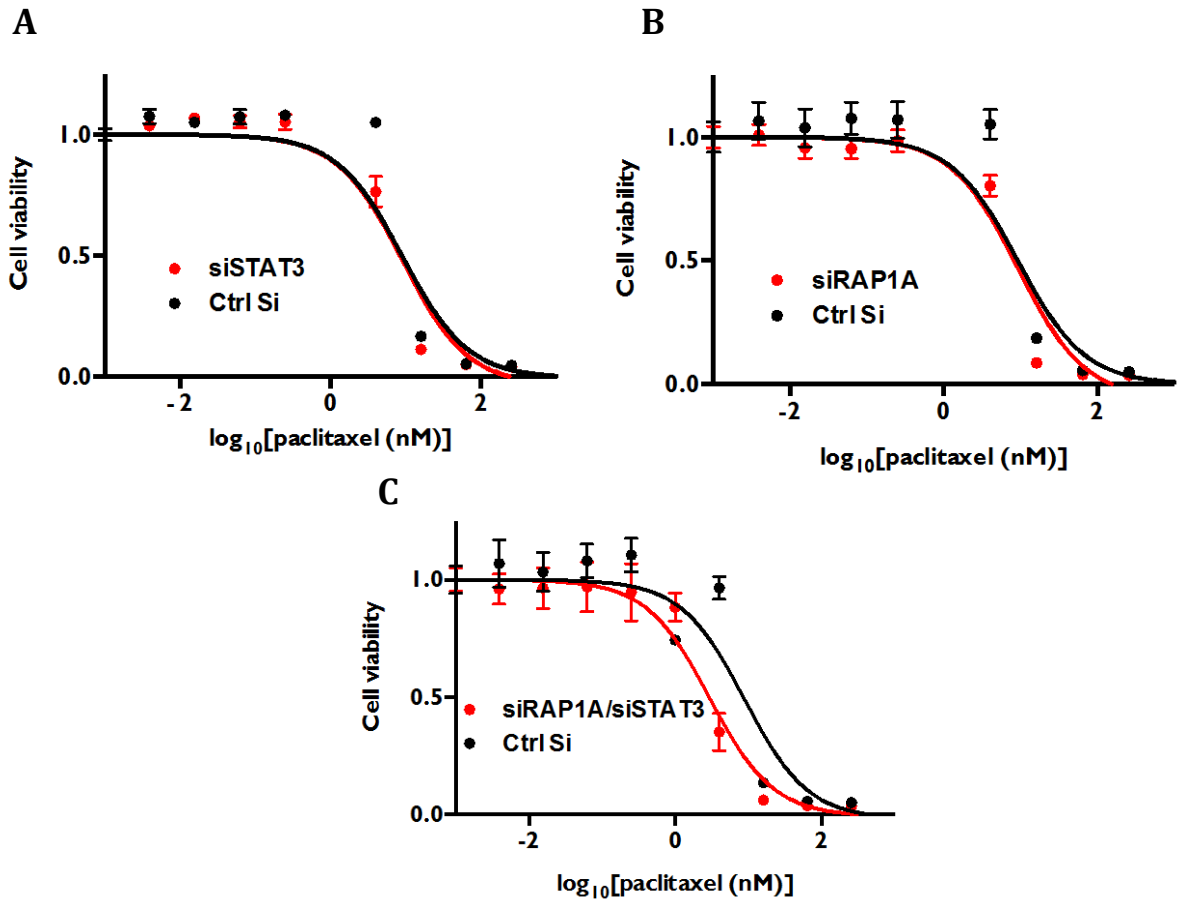

Figure 3.6 Combination of RAP1A and STAT3 Affect H1155 response to Paclitaxel. **A.** H1155 cells treated with 25nM siSTAT3 for 72 hours prior to paclitaxel addition had no effect on EC_{50}, each data point is N=4 **B.** H1155 cells treated with 25nM of siRAP1A for 72 hours before paclitaxel was added had no effect on EC_{50}, each data point is N=4. **C.** H1155 cells treated with 12.5nM of each siSTAT3 and siRAP1A and 25nM of ctrl SI. EC_{50} ctrl SI = 11.89nM while the combination of siRAP1A/siSTAT3 = 3.94nM, p-value =0.0026. Each data point is N=4.

3.4 Discussion

In summary, we identified miR-337 as a modulator of microtubule targeting agent responses in NSCLC cell lines and uncovered a novel regulator network that involves STAT3 and RAP1A. We first discovered that miR-337 expression was anti-correlated with paclitaxel response in our panel of NSCLC cell lines. Following overexpression we observed a four-fold sensitization to paclitaxel. Expanding on this finding we evaluated other microtubule targeting agents (Table 3.1). We first explored miR-337's effect on docetaxel, as we predicted miR-337 modulated cellular response to treatment. We observed an almost ten-fold sensitization, which could be due to docetaxel's ability to enter the cell at higher concentrations than paclitaxel. We then tested whether miR-337 would sensitize cells to other chemotherapies. miR-337 was able to sensitize cells to vinorelbine, vincristine, and vinblastine. In the case of vinorelbine and vinblastine the sensitization was over 100-fold. It is interesting that miR-337 had a larger effect on vinblastine and vinorelbine treated cells, which act in a similar manor than that of vincristine. This could be due to the fact that only vinblastine and vinorelbine bind to the plus end of microtubules (the growing end) and reduces microtubule treadmilling (the process of microtubule growth) (bai, Pettit et al. 1990). However, miR-337 had no effect on the cellular response to cisplatin or gemcitabine, suggesting that the specificity of the effect we observed was based on the ability of miR-337 to regulate microtubules.

Following unbiased genome-wide microarray analyses we uncovered and validated RAP1A and STAT3 as miR-337 targets, and following a combinatorial approach, we were able

to phenocopy miR-337 overexpression. Activation of STAT3 has been shown to up-regulate Survivin via direct binding to the promoter in breast cancer, which conferred resistance to paclitaxel treatment (Gritsko, Williams et al. 2006). Survivin is a fetal gene typically turned off in adult tissue. It is a member of the IAP family of anti-apoptotic proteins and is overexpressed in breast and gastric cancers and lymphomas (Gritsko, Williams et al. 2006). Additionally, it is possible that STAT3 is conferring resistance through other mechanism such as directly interacting with the microtubules antagonizing the effects of the microtubule targeting agents. This has been shown in murine embryonic fibroblast (MEF) cells where pSTAT3 interacts with the microtubules through its interaction with Stathmin, a small ubiquitous phosphoprotein that binds to microtubules and facilitates their depolymerization(Ng, Lin et al. 2006) .

RAP1A is an important mediator of integrin inside-out signaling. Integrins are transmembrane receptors that mediate the attachment of a cell and to its surroundings. There is strong evidence suggesting that the ECM influences intercellular microtubule dynamics and thus paclitaxel sensitivity. It was recently shown that transforming growth factor beta (TFGB1) modulated a component of the ECM to influence microtubule polymerization and stabilization and affect cellular response to paclitaxel (Ahmed, Mills et al. 2007). TFGB1 has been shown to mediate adhesion in an integrin-dependent manner (Jeong and Kim 2004). Taken together RAP1A could potentially be inhibiting integrin signaling and destabilizing microtubules reducing the effectiveness of paclitaxel.

We are the first to report on miR-337's ability to modulate cellular response specifically to microtubule targeting agents and elicit a response in NSCLC. Additionally, we are the first to report the regulation of STAT3 and RAP1A by miR-337 and their ability to mediate cellular response to paclitaxel (all drug sensitivity assays EC-50 can be found in table 3.1)

3.5 Future Directions

Given the observed sensitization of miR-337-3 to vinorelbine and vinblastine, we should further explore RAP1A and STAT3 interaction with the plus end the microtubules, to determine if there is preferential interaction with this end. Additionally, we should explore if loss of RAP1A and STAT3 will affect cellular response to the other drugs that were tested, to determine if this response will be specific to microtubule targeting agents and not DNA cross linkers. It should be noted that miR-337, siSTAT3 or siRAP1A did not have any effect on cell viability (Figure 3.2B & data not shown). This finding is particular interesting with regard to STAT3, given its importance in tumor maintenance and progression. Currently vast resources are being invested in the development of novel small molecules inhibitor of STAT3 that could be employed in a combinatorial treatment with paclitaxel against NSCLC.

CHAPTER FOUR Synthetic Lethal Screen to Identify miRNA Inhibitors That Sensitize NSCLC to Paclitaxel Treatment

4.1 Introduction

Synthetic lethality in the context of cancer research is becoming a popular term to define the susceptibility of the oncogenic process that can be exploited to understand basic biological function or for drug discovery. This approach has been experimentally proven in NSCLC to identify gene targets that will sensitize cells to front line chemotherapy (Whitehurst, Bodemann et al. 2007). It was shown that modulation of 87 genes in various pathways demonstrated the ability to sensitize H1155 cells to paclitaxel treatment. We however were interested in the role that miRNAs might play in the synthetic lethal process to sensitize cell to paclitaxel, as our work with miR-337 has already experimentally proven this possible.

The importance of miRNA in cancer is proven by the observation that most miRNAs are located in fragile regions. Not only are they globally downregulated but global shorting of UTRs in rapidly dividing cells is observed, loss of key enzymes in the biogenesis process promote tumor formation, and finally their role in all the hall marks of cancer (Calin, Dumitru et al. 2002, Mayr, Hemann et al. 2007, Mayr and Bartel 2009, Ravi, Gurtan et al. 2012) (Figure 1.3). To further explore the impact of miRNA expression on drug resistance we built on the literature and employed a miRNA inhibitor screen using lock nucleic acids (LNAs). LNAs are chemically

stable inhibitor that bind to miRNAs and inhibit their function by sequestering them away from their target genes (Orom, Kauppinen et al. 2006).

Our screen results showed that only a select few miRNA modulates cellular response to paclitaxel treatment. We uncovered some widely studied miRNAs such as miR-101, miR-15 and let-7 families, but we also uncovered several novel miRNAs that are involved in modulation of paclitaxel response.

4.2 Results

4.2.1 miRNA Inhibitor Screen Results

An inhibitor library screen composed of 748 miRNAs inhibitors revealed that most miRNAs have no effect on paclitaxel response (Figure 4.1B). We did find 20 miRNAs, which sensitized H1155 cells to a sub-lethal dose of paclitaxel, and 17 miRNA inhibitors that increased cellular resistance to paclitaxel. miR-337 was used as a positive control to sensation to paclitaxel treatment, as were many transfection controls. siPLK is shown as a positive transfection control (Figure 4.2 A& B). Of particular interest were miRNAs that when lost would desensitize cells to paclitaxel. We selected several miRNA for further investigation, which included the miR-15/16 family and miR-10a as each had several family members or star strands that also validated out of the initial screen.

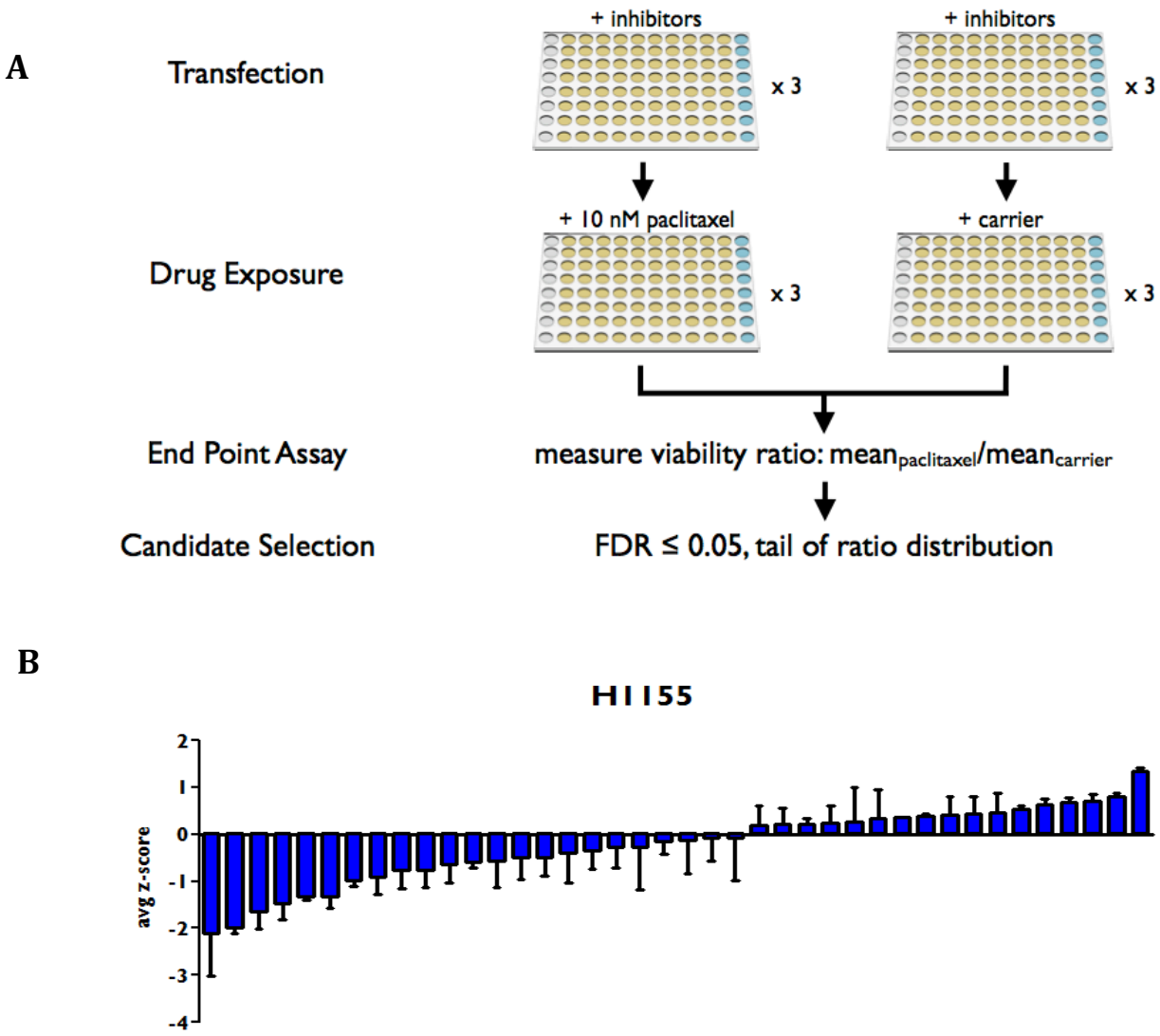

Figure 4.1 Genome Wide MiRNA inhibitor Screen. A. Screen layout. H1155 were reverse transfected with LNA library from Exiqon for 72hrs before EC50 of paclitaxel was added. Cell viability was measured 72hrs after drug was administered and the ratio of mean paclitaxel divided by mean carrier. **B.** Screen validation. Plotted are Z-scores of validated hits from the screen. Screen validation resulted in 20 miRNA inhibitors that decreased viability in the presence of paclitaxel, 709 that had no effect and 17 that increased viability in the presence of paclitaxel.

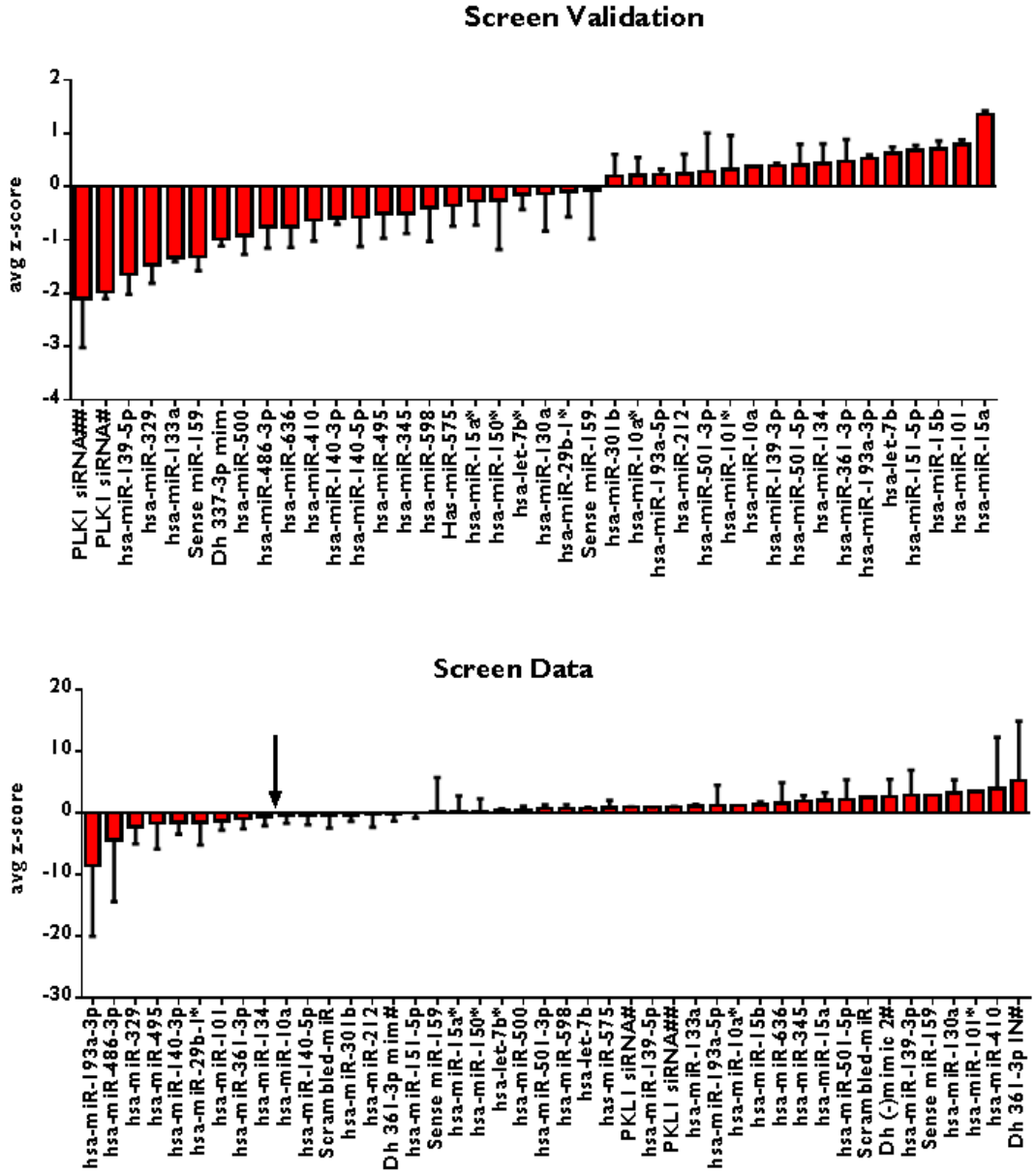

Figure 4.2 Discordance of Screen Hits Following Validation. A. Screen validation. Transfection controls had the greatest effect on cellular viability and positive control miR-337 sensitized H1155 cells to paclitaxel **B.** Processed data from the inhibitor screen. Several hits switch from one arm to the other following validation. Notable ones: miR-101, miR-10a, miR-139-5p and miR-575.

4.2.2 miR-15/16 Family

The miR-15/16 family was first identified in chronic lymphocytic leukemia (CLL) and due to their location on chromosome 13q14, a region that is deleted in ~70% of CLL cases, their expression is frequently down-regulated (Calin, Dumitru et al. 2002). Deletion of this region has also been reported in multiple myeloma, mantle cell lymphoma and prostate carcinoma. The miR-15/16 family has been shown to function as important tumor suppressors in both ovarian and non-small cell lung cancer (Bandi, Zbinden et al. 2009, Bhattacharya, Nicoloso et al. 2009) (Dong and Frierson 2001). Taken together this data suggest that this miRNA cluster is important as a broad tumor suppressor. Using bioinformatics tools it was discovered that the miR-15/16 family regulates BCL2, which is overexpressed in 65-70% of CLL and blocks programmed cell death (Cimmino, Calin et al. 2005) (Hockenbery, Nuñez et al. 1990). Given the amount of literature on miR-15/16 we pursued it as are candidate miRNA.

4.2.3 miR-15 Results

Expanding on our screen data over a range of paclitaxel concentrations we observed a four-fold increase in the EC_{50} of paclitaxel response when H1155 were pretreated with miR-15a inhibitor, in line with our inhibitor screen results (Figure 4.3A). When then asked if we were to overexpress miR-15a could be then shift the curve in the other direction, making the cell more sensitive to paclitaxel treatment. When H1155 cells were treated with miR-15a mimic we were able to shift the curve in the opposite direction and observed a four-fold sensitization to

paclitaxel (Figure 4.3B). To determine how low of a concentration of miR-15a we needed, we did a serial dilution down to 12.5 nM -- one quarter of what was used in the screen -- and were still able to observe the phenotype (Figure 4.3C). Finally, we quantified miR-15a levels we were able to achieve, following either transfection with a miR-15a inhibitor or a mimic in H1155 (Figure 4.3D). Collectively, these results suggest that miR-15a is an important mediator of cellular response to paclitaxel.

4.2.4 Introduction miR-10a/b

miR-10a is located on chromosome 17 in the HOXB cluster of genes between HOXB4 and HOXB5. Its expression was first identified in *D. melanogaster* and later confirmed in both mouse and human cells (Lagos-Quintana, Rauhut et al. 2001, Lagos-Quintana 2003). During development, each member of the miR-10 family expression parallels that of the HOX cluster that it resides in, suggesting similar regulatory mechanisms (Mansfield, Harfe et al. 2004). Using expression data on our panel of lung cancer cells lines we did not observe a correlation of miR-10a with either HOXB4 or HOXB5 (data not shown). However, it should be noted that transcriptional regulation of HOXB4 is complex, with experimentally validated regulatory pressures during transcription, post-transcription and translation of the HOXB4 gene (Brend 2003). Interestingly, appropriate pattering of HOXB4 is dependent on an intact UTR (Brend 2003). Any one of these factors could explain the lack of concordance between expression of HOXB4 and miR-10a in our panel of cell lines.

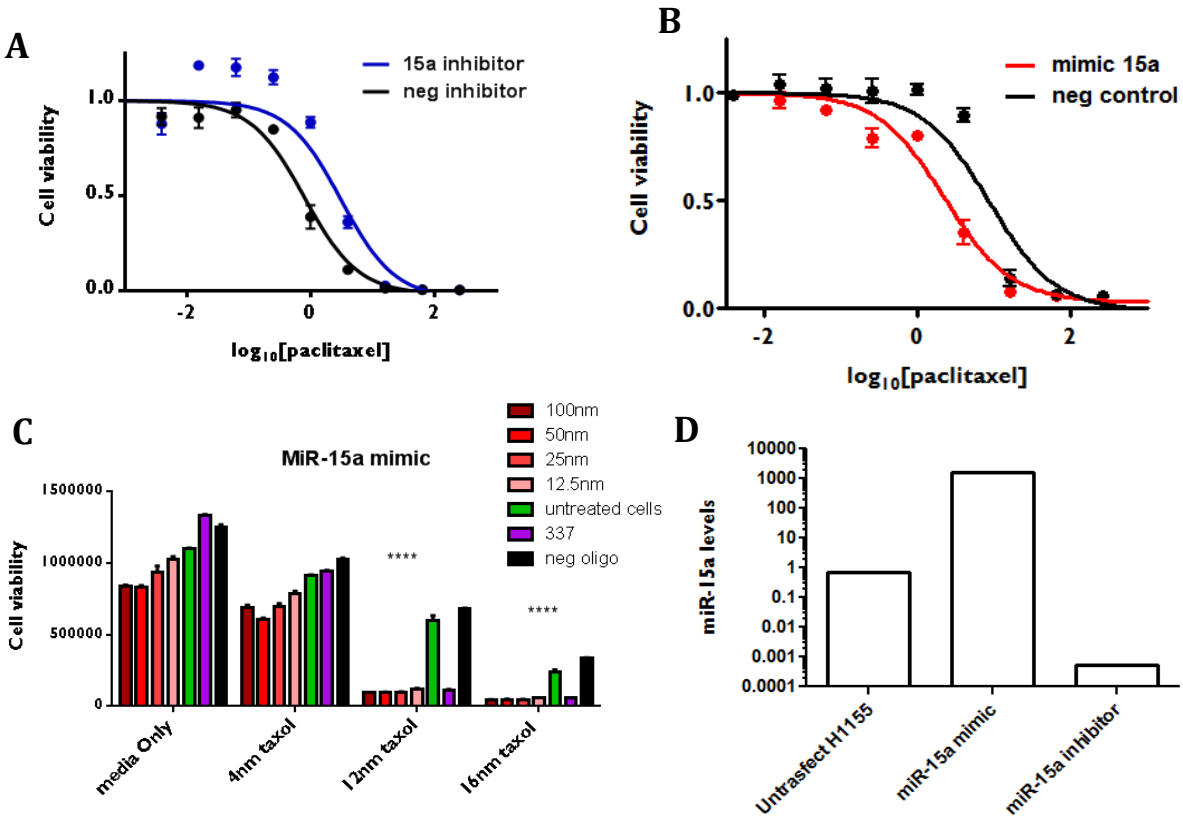

FIGURE 4.3 miR-15a Regulates Paclitaxel Response. **A.** H1155 treated with miR-15a inhibitor desensitized cells to paclitaxel. Treatment with miR-15a inhibitor increased EC_{50} from 0.79nM for the control inhibitor to 3.09nM for miR-15a inhibitor. $P \leq 0.0001$ each data point is N=4. **B.** miR-15a mimic was able to sensitize H1155 to paclitaxel treatment. H1155 treated with ctrl mimic had an EC_{50} of 8.50nM while miR-15a mimic EC_{50} was 2.19nM $p \leq 0.0001$ each data point is N=4. **C.** Titration of miR-15a mimic shows that 12.5nM is sufficient to sensitize H1155 to paclitaxel. **** $P \leq 0.0001$. **D.** Range of miR-15a we were able to achieve following transfections. Data was first normalized to appropriate control**.**

miR-10a role in the context of cancer is ill-defined. It was discovered that miR-10a expression is increased during the early stages of urothelial carcinomas when the carcinoma is confined to the inner lining of the bladder wall. During later stages of cancer progression no difference in miR-10a levels were observed (Veerla, Lindgren et al. 2009). In chronic myeloid leukemia (CML), however, it was observed that miR-10a is down-regulated in 70% of patient samples. In CML miR-10a was found to directly regulate upstream stimulatory factor 2 (USF2). In 60% patient samples, which had up regulation of USF2, loss of miR-10a expression was observed (Agirre, Jimenez-Velasco et al. 2008). This finding supports data from The Cancer Genome Atlas, TCGA, which shows miR-10a is down-regulated in tumors of the breast and head and neck (Figure 4.4A&B). Finally, we mined TCGA data and found a slight increase in miR-10a expression in lung tumor samples relative to normal adjacent tissues (NAT) (Figure 4.4C).

Some of the first work on miR-10a explored its contributions to ATRA-induced smooth muscle cell differentiation (Huang, Xie et al. 2010). It was discovered that treating human ES cells with ATRA for just 24 hours increased miR-10a levels 24-fold and pretreatment of ES cells with a miR-10a inhibitor impaired differentiation. The observed effect of miR-10a was a result of its regulation of histone deacetylase 4 (HDAC4), a known inhibitor of differentiation (Göttlicher, Minucci et al. 2001). However, there was no observed change in miR-10b, indicating that the effects observed were specific to miR-10a and they each have different means of induction in muscle tissues.

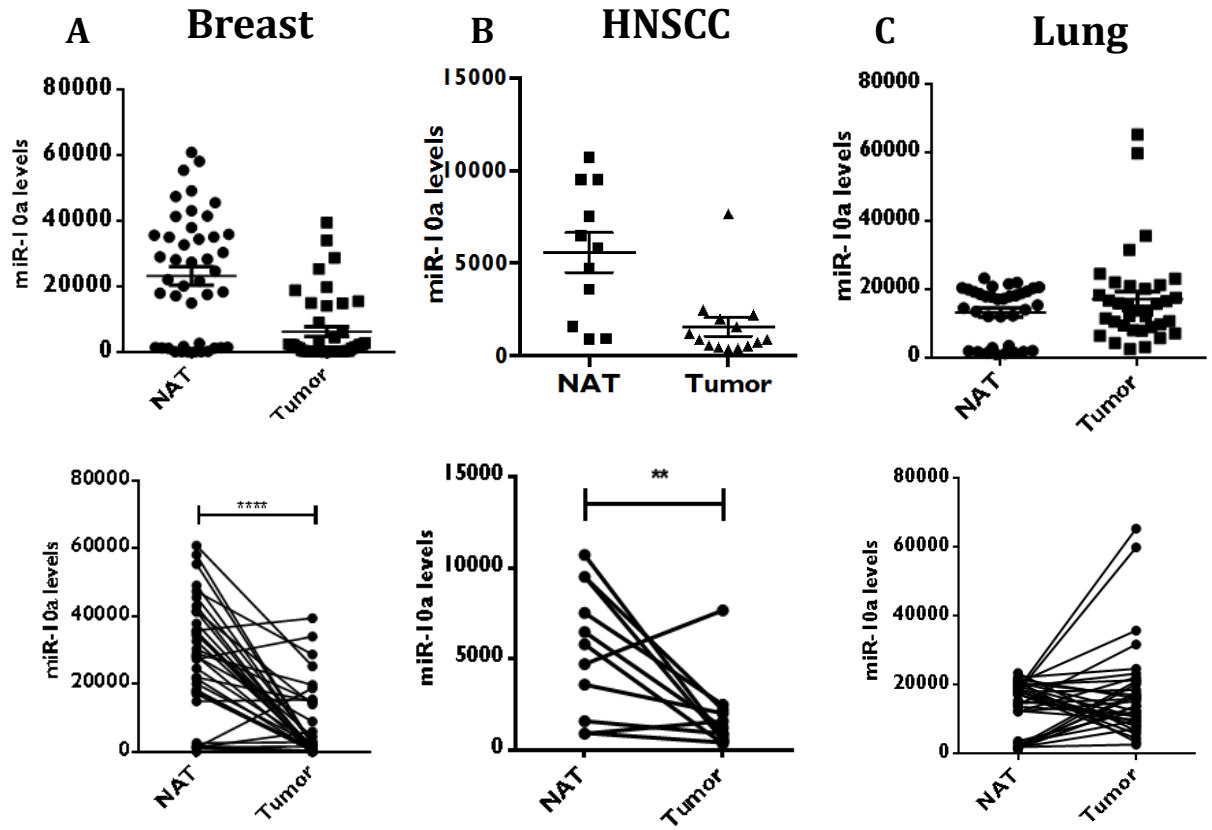

Figure 4.4 miR-10a Expression in Tumor and Normal Adjacent Tissue. A. 45 paired samples from TCGA. NAT had a mean expression of 23135 while tumor samples had a mean expression of 6185. Plotted data are sequence reads mapped to miR-10a loci. Data was processed and normalized by TCGA. **** $P \leq 0.0001$. **B.** Head and Neck Squamous Cell Carcinoma sample data provided to us by Dr. Michael Story. 11 paired samples, mean expression of miR-10a in Tumor 1577 and 5572 in NAT. Data plotted are sequence reads mapped to miR-10a loci. ** $P = 0.0014$.**C.** 35 paired samples from TCGA mean expression from tumor samples is 17284 and in NAT 13460. Data plotted are sequence reads mapped to miR-10a loci.

The up regulation of miR-10a upon ATRA treatment was of particular interest to the neuroblastoma field, as ATRA treatment causes neural cell differentiation and is used to study the biochemical process of differentiation. It was found that after ATRA treatment, both miR-10a and -10b levels increased and ectopic expression of each increased neurite outgrowth, a proxy for differentiation (Foley, Bray et al. 2011). Bioinformatics analysis of down regulated genes containing miR-10 target sites and known to be important in neurite outgrowth uncovered nuclear co-repressor 2 (NcoR2) as a direct target of miR-10 regulation. NcoR2 functions as a transcriptional repressor through the recruitment of histone deacetylases (1-4) to target genes and inhibiting their transcription. It was also shown that loss of miR-10a is associated with poor clinical outcome in patients with chromosome 11q deletions or MYCN amplification (Foley, Bray et al. 2011). However, miR-10b expression levels in tumors and patient survival were not significant. Finally it was observed that while miR-10a is located on chromosome 17q that is amplified in 90% of neuroblastomas, and the expression of other genes in the amplicon are concordantly increased, miR-10a expression is decreased by an unknown mechanism.

miR-10a differs from miR-10b at a single nucleotide outside the seed sequence and are thus expected to have the same target genes. They do however differ dramatically in expression, which could be a result of their location relative to neighboring HOX genes (Landgraf, Rusu et al. 2007). miR-10a is not located within any HOXB gene and thus has its own promoter while miR-10b is located within the last intron of HOXD4 suggesting that its expression is more likely tied to that of HOXD4.

The seminal paper on the miR-10 family was from the Weinberg lab, which reported that miR-10b is over-expressed in breast cancer cell lines that are capable of metastasizing (Ma, Teruya-Feldstein et al. 2007). Ectopic expression of miR-10b promoted invasion and metastasis in breast cancer cell lines both in vitro and in vivo through regulation of HOXD10. Ma, et al. also discovered that miR-10b expression is induced by TWIST, a potent EMT inducer, while patients whose tumors had high miR-10b levels had reduced overall survival (Ma, Teruya-Feldstein et al. 2007). They then went on to show that systemic delivery of a miR-10b antagomir, a chemically modified miRNA inhibitor, suppressed breast cancer invasion in vivo but had no effect on tumor growth (Ma, Reinhardt et al. 2010). However, this work is not conclusive, as no correlation of miR-10b levels and patient survival or metastatic potential was observed in larger cohort of patients (Gee, Camps et al. 2008).

Other groups working on parsing miRNA targets of individual family members explored the miR-34 family, which is composed of miR-34a on chromosome 1 and miR-34b/c on chromosome 11. It was observed that most of the miRNA targets are conserved among the family (He, He et al. 2007) with a notable exception: miR-34b/c have a higher affinity to MYC than miR-34a, which can only be explained by binding events outside of the seed match (Hermeking 2010). Finally, when we compare the literature of miR-10a to other miRNAs such as the miR-200 family, let-7, and miR-15/16 family, relatively little is known about miR-10a and its role in cancer and drug response in NSCLC, providing additional rationale for its study.

4.2.5 miR-10a Results

4.2.5.1 miR-10a Regulates Cellular Response to Paclitaxel

To further validate the screen results we used a paclitaxel dose-response curve with the highest concentration of 1024nM followed by four-fold dilution to the lowest concentration of 0.003nM. Following pretreatment with miR-10a inhibitor we observed a shift in the EC_{50} from 0.22nM for the negative control inhibitor to an EC_{50} of 2.63 when miR-10a inhibitor was transfected into H1155 cells (Figure 4.5A&B). To determine if miR-10a could shift the EC_{50} in the other direction and sensitize H1155 paclitaxel we transiently transfected H1155 cells with miR-10a mimic and the EC_{50} decreased to 1.73nM with miR-10a mimic from an EC_{50} of 11.69nM for the negative control (Figure 4.5C&D). As we observed with miR-337 mimic, which was able to sensitize cells to both paclitaxel and docetaxel, miR-10a had the same effect. The negative control mimic had an EC_{50} of 0.74nM while miR-10a was able to lower it to 0.028nM (Figure 4.6A&B).

We then tested other cell lines to ensure this effect was not limited to H1155. In order not to arbitrarily select a cell line we explored miR-10a expression across our panel of cell lines where we observed a 60-fold range in expression across the cell line panel (Figure 4.7). We selected H460, as expression of miR-10a fell in the middle of the distribution. After pretreatment with either control inhibitor or mimic the EC_{50} were 1.91nM and 1.63nM respectively (Figure 4.8A). However, modulation of miR-10a was able to shift the curve in either direction, when we removed miR-10a form the system the EC_{50} increased to 6.15nM and when we added miR-10a to

H460 the EC_{50} dropped to 0.25nM (Figure 4.8A). We then measured the effectiveness of the inhibitor on miR-10a, which was able to completely remove miR-10a from each cell line (Figure 4.9A). While miR-10a mimic was able to increase miR-10a expression over 1000 fold in each cell line (Figure 4.9B).

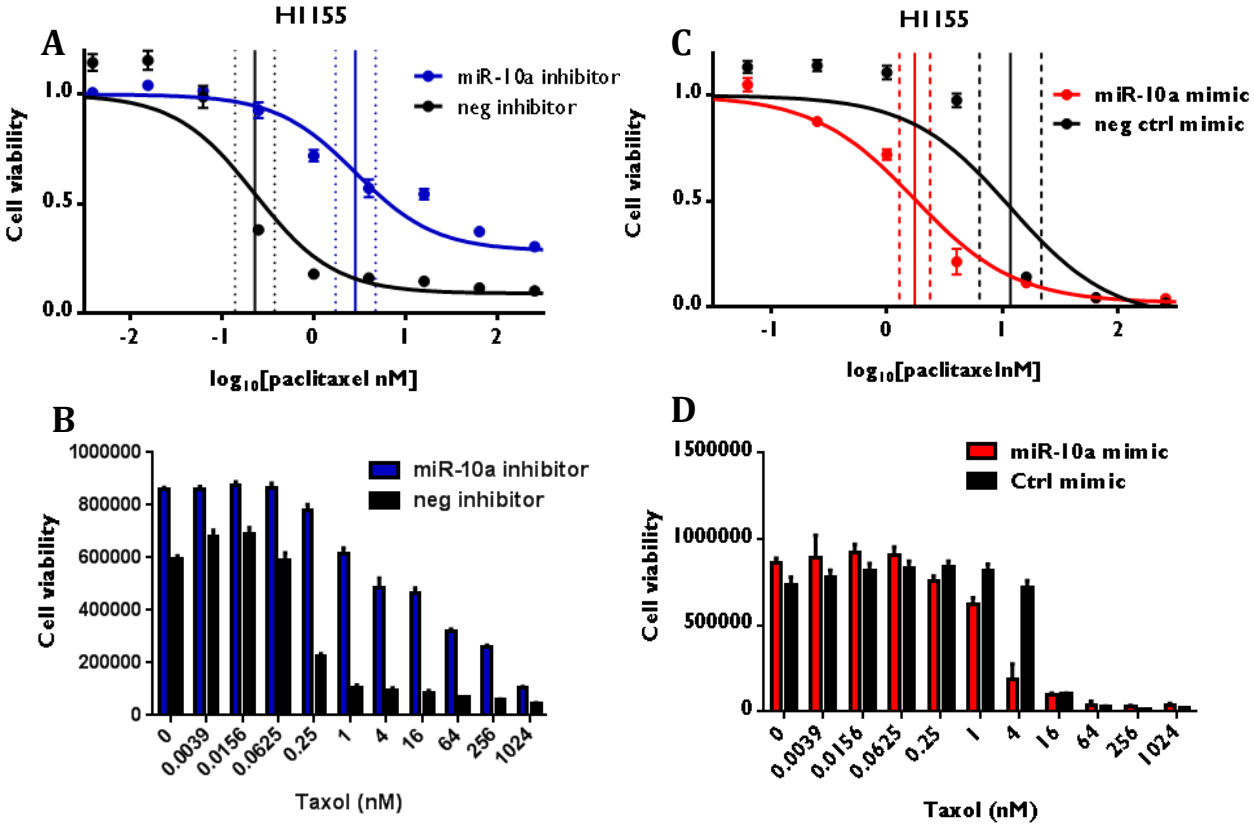

FIGURE 4.5 miR-10a is Capable of Modulating Paclitaxel Response in H1155. A. H1155 cells pretreated with 50nM miR-10a inhibitor for 72hrs before paclitaxel was added. Cell viability was measured post 72hrs of drug treatment. Inhibiting miR-10a resulted in an EC_{50} of 2.630nM while control treated cells EC_{50} = 0.2292nM. N=4 $p \leq 0.0001$. **B.** Bar graph is representation of raw dose response data. **C.** H1155 pretreated with 20nM miR-10a mimic sensitized cell to paclitaxel. EC_{50} shifted from 11.69nM for control treated cells to 1.739nM in cells treated with miR-10a mimic. N=4, $p \leq 0.0001$. **D.** Bar graph is representation of raw dose response data. Vertical solid lines indicate EC_{50}s; dashed lines are the 95% confidence interval.

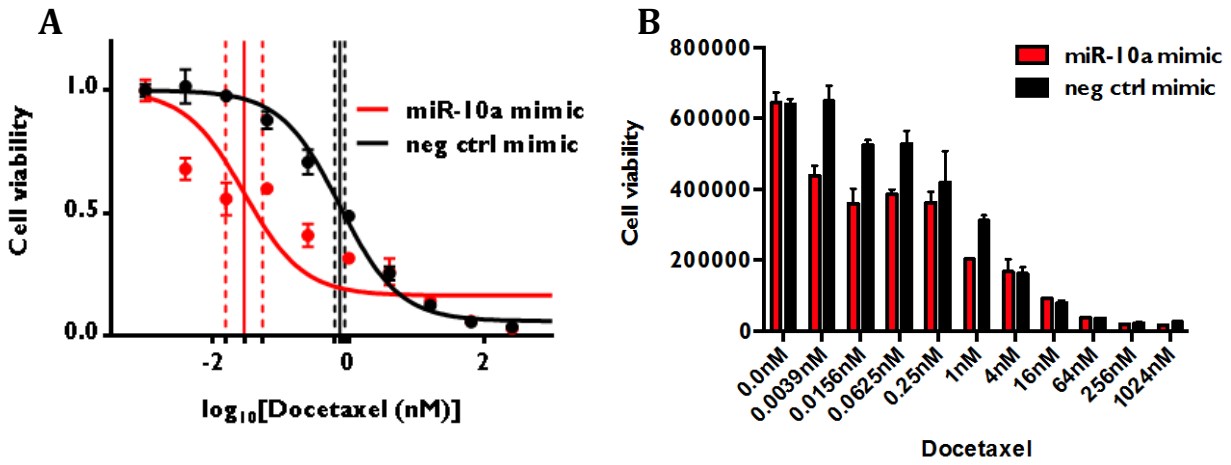

Figure 4.6 miR-10a Affects H1155 Cellular Response to Docetaxel. A. H1155 cells pretreated with 20nM miR-10a mimic for 72hrs before docetaxel was added. Cell viability was measured post 72hrs of drug treatment. miR-10a mimic resulted in an EC_{50} of 0.02868nM while control treated cells was 0.7404nM. N=4 $p \leq 0.0001$. Vertical solid lines indicate EC_{50}s; dashed lines are the 95% confidence interval. **B.** Bar graph is representation of raw dose response data.

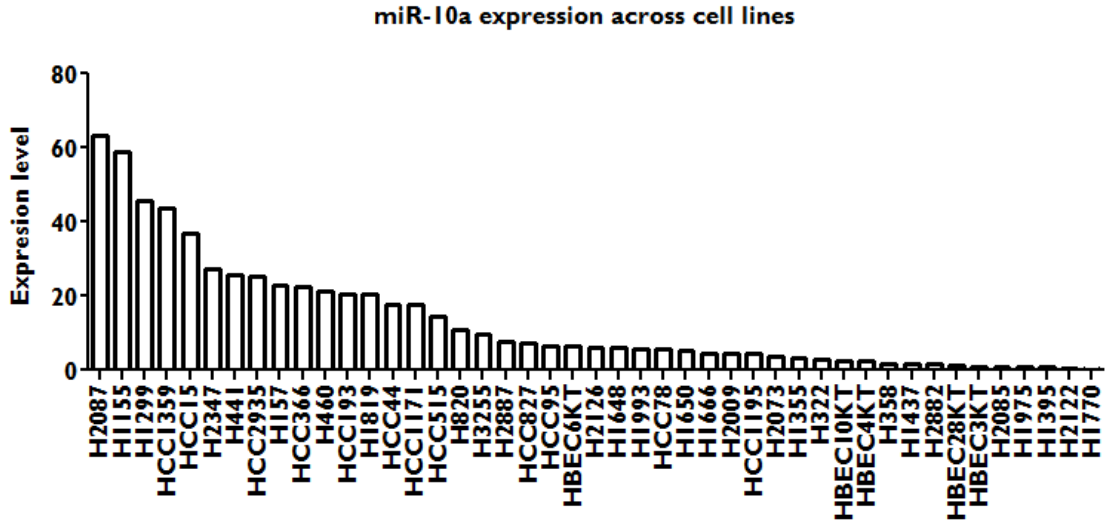

FIGURE 4.7 miR-10a Expression Across NSCLC Panel of Cell Lines. miRNA expression arrays profiling miR-10a levels across our NSCLC panel normalized to HBEC3KT as “1”.

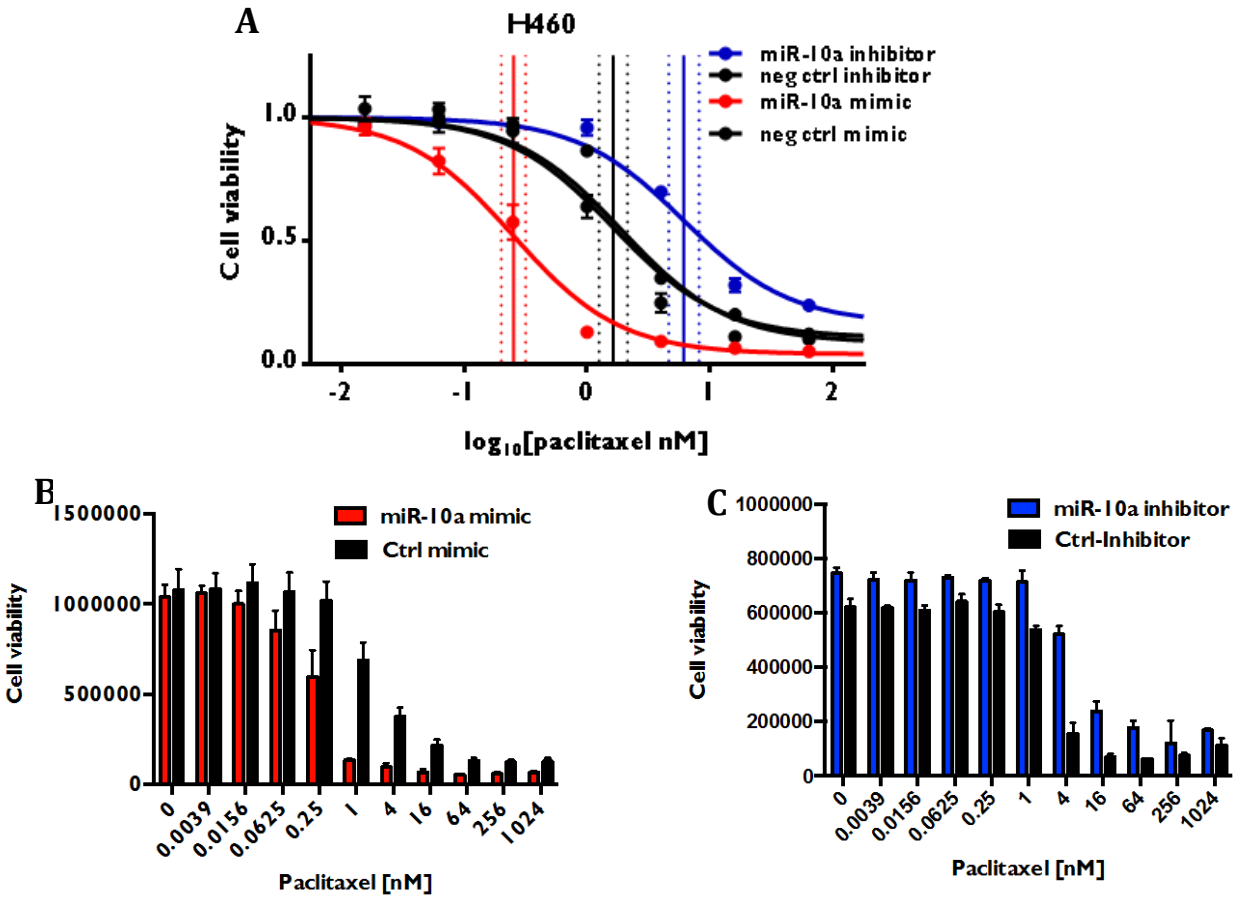

FIGURE 4.8 Modulation of Paclitaxel Response is not Specific to H1155 A. H460 cells treated with either miR-10a mimic or inhibitor. Both controls had an EC_{50} of 1.75nM. Transfection of miR-10a mimic resulted in a 5-fold reduction of the EC_{50}; transfection of miR-10a inhibitor increased the EC_{50} 3-fold. N=3 for each data point shown. All EC_{50} P values were ≤ 0.0001. Vertical solid lines indicate EC_{50}s; dashed lines are the 95% confidence interval. **B&C** Bar graphs of raw data.

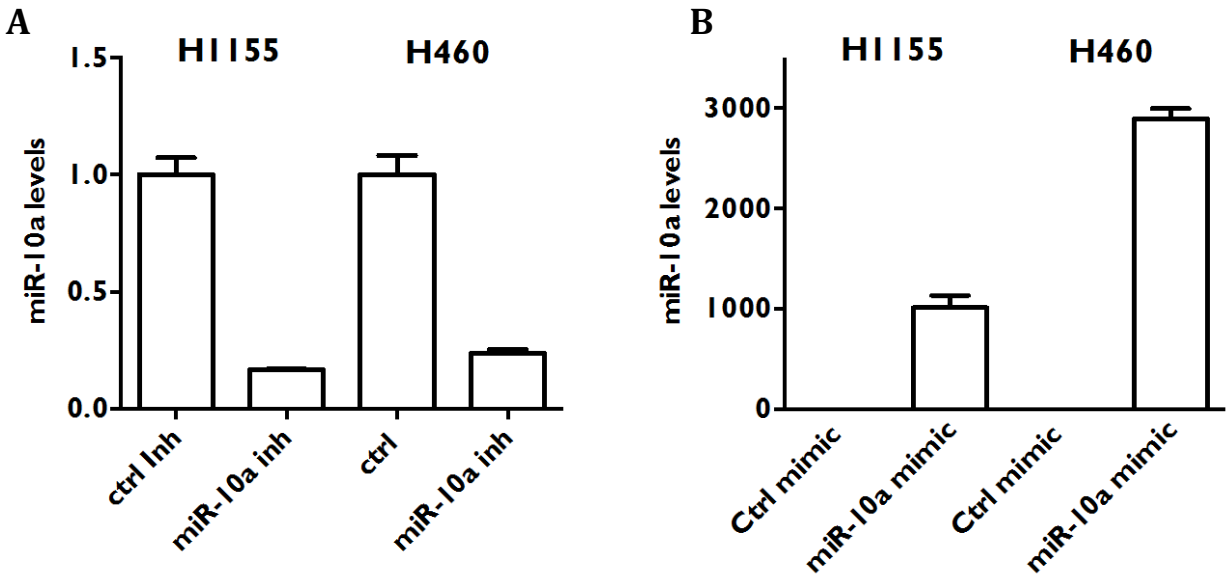

FIGURE 4.9 Dynamic Range Achieved in Manipulation of miR-10a Levels. A. miR-10a levels quantified by qPCR following inhibition-using Exiqon LNA, in each cell line miR-10a expression inhibition is > 90%. **B.** miR-10a levels following transfection with miR-10a mimic, H1155 resulted in a 1000 fold increase and in H460 3200 fold increase. qPCR reads were first internally normalized to RNU-19 and then the control sample before fold change was calculated. Each is an N=3.

4.2.5.2 Parsing miR-10a from miR-10b

As mentioned above, miR-10a is part of the miR-10 family, which includes miR-10b. As stated earlier, the difference is a single base change outside of the seed sequence (Figure 4.10C). miR-10b was not a hit on the original screen, and this was not due to its lack of expression in H1155, as this cell line exhibited the highest level of miR-10b among the panel of cell lines (Figure 4.10A). To ensure that miR-10b was not missed as a hit due to poor inhibitor quality we transfected H1155 with miR-10b inhibitors (Figure 4.11A). The miR-10b inhibitor was effective and removed miR-10b, but cross reaction was observed as inhibitors for both miR-10b and miR-10a were affecting the other family member's levels, thereby confounding the previous experimental results. To address this issued we used the Dharmacon inhibitor, which uses a hairpin design. While it was more specific then the Exiqon design it was not as effective, only reducing miR-10a level by 85% (Figure 4.11B).To determine the specificity of the Taqman qPCR probes we transfected H1975, which has undetectable endogenous miR-10a/b levels, with both miR-10a and 10b mimic. Following transfection we observed cross detection of the qPCR probes (Figure 4.11C).

Now that we have established that the miR-10b inhibitor is functional we then wanted to test if it would modulate cellular response to paclitaxel in H1155. We did not observe any effect on cellular response to paclitaxel treatment in H1155 with miR-10b inhibitor (Figure 4.12A). Since we observed inhibitor cross reaction using the Exiqon design, to completely rule out miR-10b as a cause of the sensitization, we used the Dharmacon design. Inhibiting miR-10a with the

Dharmacon inhibitor desensitized H1155 cells to paclitaxel by two fold, shifting the EC_{50} from 0.46nM to 0.90nM (Figure 4.12B). Taken together this data suggest that miR-10a and not miR-10b is responsible for the modulation of cellular response paclitaxel.

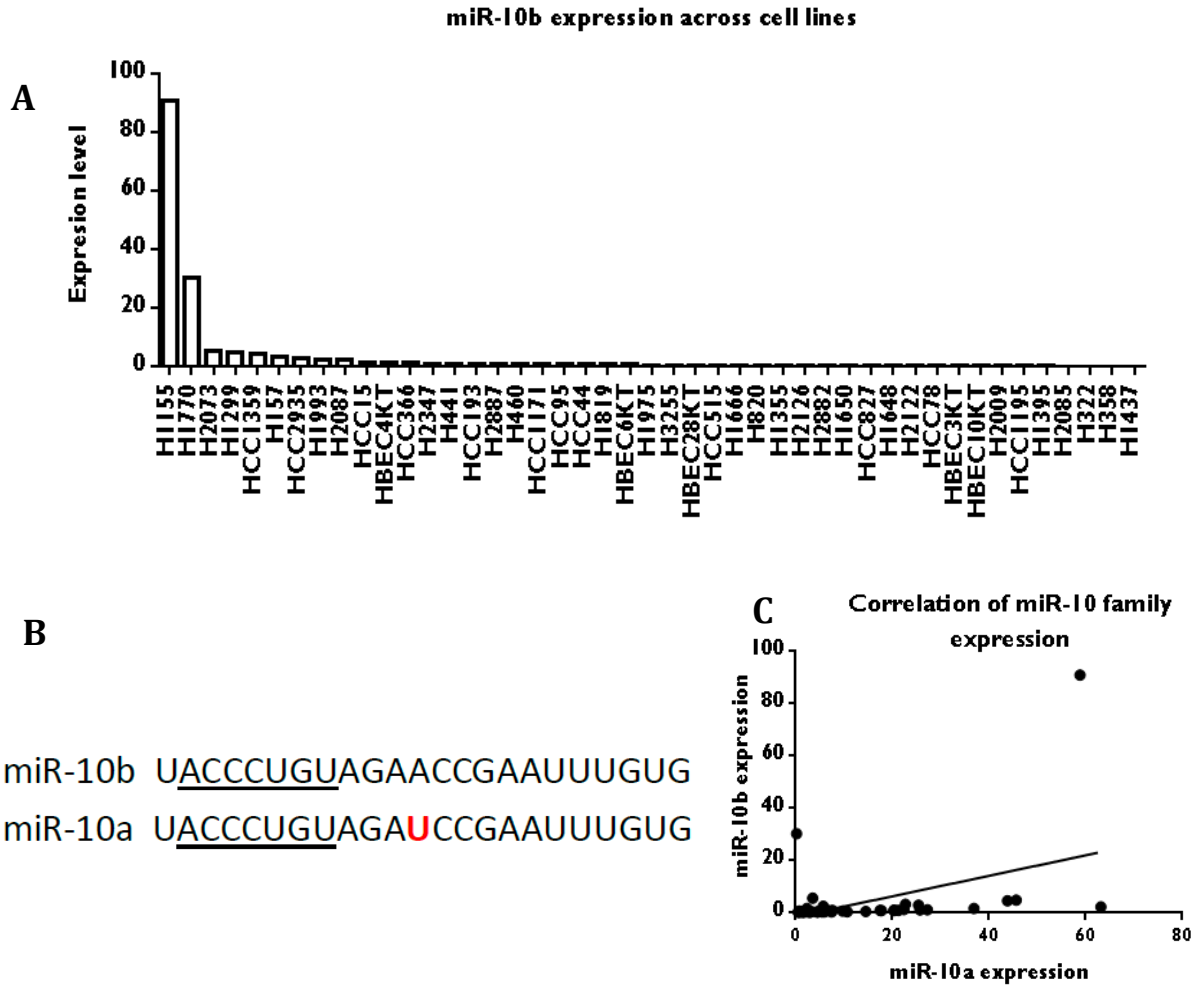

Figure 4.10 miR-10b Expression is Not Correlated with miR-10a Across NSCLC. A. miR-10b expression measured by miRNA array. **B.** Sequence comparison of miR-10a and 10b, U in red denotes only base difference in mature miRNA, underlined is the seed sequence. **C.** Correlation of miR-10a and 10b in NSCLC. Expression levels were quantified by miRNA array.

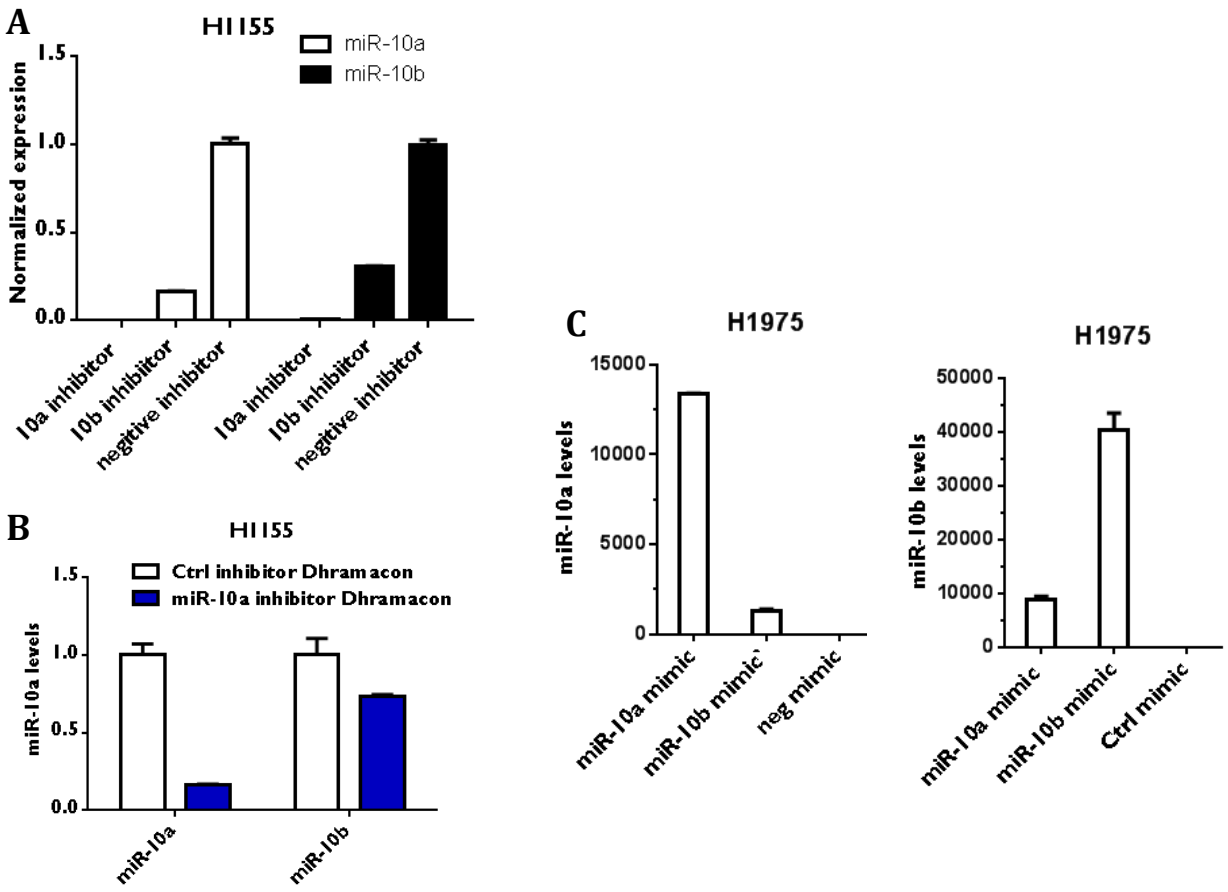

Figure 4.11 Cross Reaction of Taqman Probes and MiRNA Inhibitors on the miR-10 Family A. H1155 transfected with either miR-10a or10b inhibitor from Exiqon. miR-10a inhibitor leads to undetectable levels of both miR-10a and 10b while miR-10b inhibitor leads to ~ 80% reduction of both transcripts. **B.** Dharmacon inhibitor reduces miR-10a by ~90% and only inhibits miR-10b by ~13%. **C.** H1975 transfected with either miR-10a or 10b mimic. Taqman probes are able to detect both miRNA mimics. qPCR reads were first internally normalized to RNU-19 and then the control sample before fold change was calculated. All qPCR samples were an N=3.

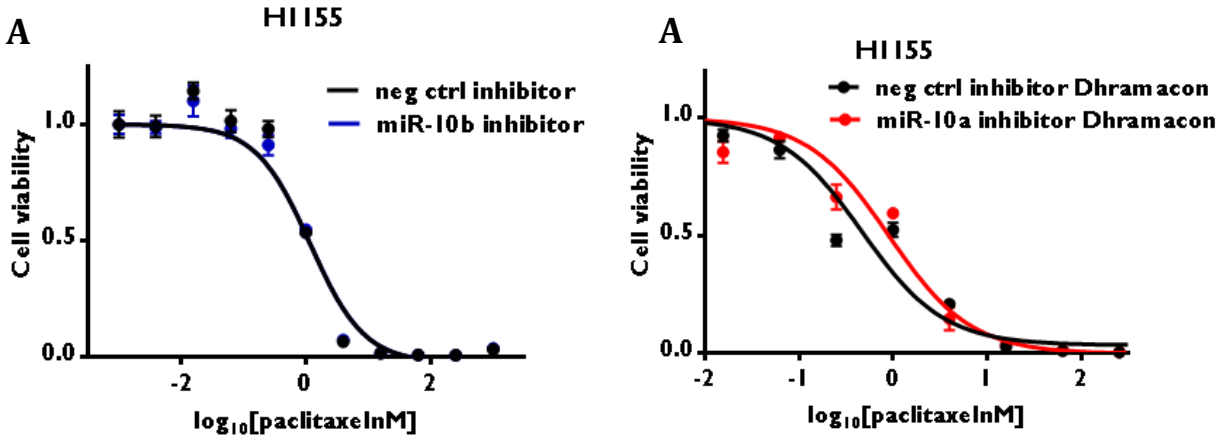

Figure 4.12 miR-10a not miR-10b is Responsible for Drug Response Observed in NSCLC. **A.** miR-10b inhibitor had no affect on cellular response to paclitaxel. **B.** H1155 cells pretreated with miR-10a inhibitor from Dharmacon led to a 2-fold desensitization of paclitaxel. EC_{50} shifted from 0.46nM for the negative control inhibitor to 0.90nM in cells treated with miR-10a inhibitor. N=4, p = 0.0192.

4.3 Discussion

Our genome-wide miRNA inhibitor screen uncovered 20 miRNAs that when lost decreased cellular viability in the presence of paclitaxel and 17 miRNA that increased viability. A large portion of miRNAs had no effect on cellular response to paclitaxel. This could be due several factors, such as loss of expression of the target miRNA during cancer progression or perhaps that many of the miRNA screened are not expressed in the lung. There was some discordance among the screen data and the validation; half a dozen screen hits changed arms following validation. This could be explained by many reasons, such as the confluence of the cells prior to transfection, condition of media such as subtle serum differences or amount of dissolved CO_2, which would affect pH. Additionally, plating of cells at the HTS core is done mechanically which could have impacted cell number per well. Finally, our screen data consisted of four replicates, while the validation was a triplicate of triplicates, which led to less variation, anyone of these or a combination of several could led to the observed change of a miRNA inhibitor from one arm to the other.

It is not surprising that in our inhibitor screen loss of miR-15a increased resistance to paclitaxel given its tumor suppressor phenotype documented in several other types of cancer. However, the target gene could not be Bcl-2 as paclitaxel induced apoptosis is depended on BCL-2 expression(Haldar, Chintapalli et al. 1996) . Additionally, we did not observe correlation of miR-15a and BCL2 expression in our NSCLC cell line panel. Looking through Targetscan.org we observed a significant number of genes involved in the MEK/ERK signaling pathway and following transfections with miR-15a mimic we observed loss of pERK. But this project was

ultimately terminated due to the inability to consistently reproduce results across our panel of cell lines and changes made to the inhibitor design by the company.

Our lead candidate miRNA, miR-10a, which not only was validated in several cells lines, the data was widely reproducible with small standard deviation. We serendipitously performed the screen in H1155, which has the second highest expression of miR-10a—second only to H2087 (Figure 4.7). The effect of miR-10a inhibition was the greatest in H1155, which became more than ten-fold more resistant to paclitaxel treatment. While the mimic's response was still significant, it only resulted in a six-fold change in paclitaxel response (Figure 4.5A&B). This response was not just specific to paclitaxel. The miR-10a mimic was able to sensitize H1155 to docetaxol as well, where only a 0.0039nM concentration reduced cell viability by almost 50% (Figure 4.6A&B). To confirm that the effect observed in H1155 was not idiosyncratic, we selected H460 which expression moderate levels of miR-10a allowing a larger experiment space (Figure 4.7). We observed a similar phenotypic effect of sensitization to paclitaxel in the presence of miR-10a mimic and desensitization when miR-10a was removed. Measuring the dynamic range we were able to achieve using both miR-10a mimic and inhibitor we observed that the range was in agreement with miRNA array data. H1155, which has higher endogenous levels, had a larger loss of miR-10a following transfection with the inhibitor then that of H460, which expressed miR-10a at a lower level (Figure 4.9A). Conversely, H460, which has lower endogenous expression, was able to obtain a larger increase of intracellular miR-10a following transfection with miR-10a mimic (Figure 4.9B). It is for this reasons we believe the miR-10a inhibitor had a larger effect in H1155 leading to over 10-fold desensitization while only a 3 fold

in H460. In contrast to miR-10a mimic had a larger effect in H460 then H1155. Illustrating that both cell lines were accustomed to specific endogenous levels of miR-10a and manipulation of miR-10a whether using he inhibitor or the mimic were buffered by endogenous miR-10a. This is best described in H1975, which expresses very low levels of miR-10a and when treated with miR-10a inhibitor no change in paclitaxel response was observed (Data not shown).

Upon closer interpretation of the raw data we made an interesting observation, when the dose response data were plotted as bar graphs loss of miR-10a increased cellular growth rate in H1155, while increasing miR-10a did not have any effect on cellular viability (Figure 4.5 B&D). This can be explained by high endogenous levels of miR-10a in H1155 which has acquired mutation that allow it to tolerate high miR-10a and only display a phenotype when stressed. This was experimentally proven as we observe sensitization to paclitaxel response when miR-10a levels were increased. This is further supported by H1155 treated with docetaxel. When docetaxel was not present miR-10a mimic had no effect on growth rate compared to the negative control mimic, as soon as we added a stress, in this case docetaxel, we observed a significant reduction in cellular viability (Figure 4.6B). It appears that there was a biphasic response to docetaxol in H1155 treated with miR-10a mimic. The first phase was when docetaxel was initially added and plateaued until 0.25nM as which point H1155 entered the second where any increase in docetaxol lead to a linear reduction in cellular viability (Figure 4.6B). At appears that 30% of H1155 cell population was primed for cell death prior to drug treatment.

The growth effects caused by miR-10a were also observed in H460, where similar manipulation in miR-10a effected growth. However, H460 which have lower levels of miR-10a

were much more sensitive to miR-10a mimic treatment (Figure 4.13A). This effect was specific to the mature miR-10a, as the star stand, which is typically not bioactive, did not affect cellular viability (Figure 4.13B). H460 treated with miR-10a mimic resulted in an 80% loss of cellular viability, only after seeding significantly more cells were we able to achieve dose curves (Figure 4.13A and 20A). This observation was confirmed in H1975; only the mature miR-10a had an effect on cellular viability (Figure 4.13 C&D). Collectively this data suggests that miR-10a is important in cellular viability.

Since miR-10a is one of two members of the miR-10 family, we had to parse if it was solely responsible for the phenotype or only partially contributed to the drug sensitizing phenotype. miR-10b is not widely expressed in our panel of cell lines and only two cells lines express miR-10b: H1155 and H1770, both of which are derived from tumors with neuroendocrine histological subtypes. Neuroendocrine histological subtypes confer poor prognosis in NSCLC and is similar to the more aggressive SCLC (Bhattacharjee, Richards et al. 2001). Additionally, we did not observe any correlation of expression between miR-10a and miR-10b (Figure 4.10C), suggesting that these miRNAs do not share similar regulatory mechanism. Deep sequencing of miRNAs across tissue types in humans support this finding, with miR-10a and miR-10b expression patterns differing widely (Landgraf, Rusu et al. 2007). miR-10a is most prevalent in the respiratory system while miR-10b is present in the nervous system and to lesser extent endocrine glands.

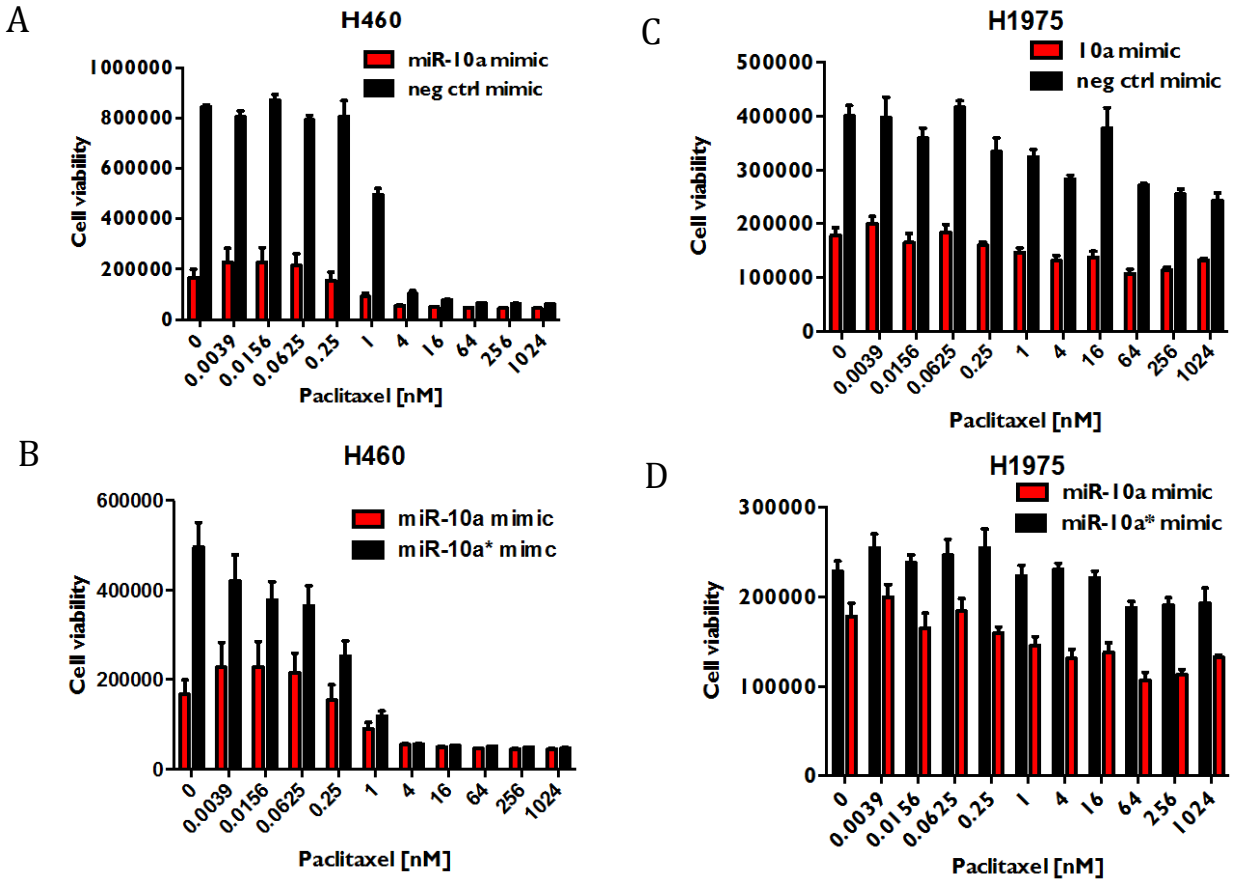

Figure 4.13 Growth Inhibitory Effect Observed in miR-10a Mimic Treated Cells. A. H460 cells treated with 20nM miR-10a mimic significantly inhibited growth. **B.** Growth inhibitory effect of miR-10a was specific to the miR-10a-5p and not miR-10a-3p or the * strand. **C.** 20nM of miR-10a mimic reduced growth in H1975 by over 50%. **D.** miR-10a star strand was not as effective as miR-10a at inhibiting growth rate in H1975.

Inhibiting miR-10b had no effect on cellular response to paclitaxel in H1155 (Figure 4.12A). While miR-10b inhibitor was not as effective in inhibiting expression levels as the miR-10a inhibitor, it still removed more than 80% of the endogenous mircoRNA (Figure 4.11A). Cross-reaction did raise concerns that miR-10a effect on cellular response to paclitaxel might be a result of loss of both family members. We addressed this in several ways: 1) H460 does not express miR-10b 2) Dharmacon inhibitors which showed greater specificity affected cellular response to paclitaxel 3) H1975 miR-10b mimic had no effect on viability (data not shown). The desensitization of paclitaxel using Dharmacon inhibitors was only 2-fold, not the 11-fold that was observed with the Exiqon inhibitor (Figure 4.12B Vs. 4.5A), illustrating that even small levels of miR-10a has the ability modulate paclitaxel response (Figure 4.9A&B). The use of two inhibitors also reduced the likelihood of an off-target effect. Finally, the similarity of miR-10a and miR-10b makes them difficult to distinguish using qPCR probes (Figure 4.10B). While we do observe larger increases in the target miRNA expression following mimic transfections, there is cross-reaction (Figure 4.10C). This could be due in large part to overload of the mature product and the Taqman primers unable to distinguish endogenous from exogenous miR-10 levels. This was confirmed in H460 as we were unable to detect endogenous miR-10b levels, similarly we could not detect miR-10a in H1770 (Data not shown). Collectively, this data suggest that miR-10a and not miR-10b is responsible for modulation of cellular response to paclitaxel.

Further confirming miR-10a's importance in lung cancer, parsing patient survival data we discovered that high miR-10a is predictive of recurrence free survival in white male smokers, increasing recurrence free survival by more than ten years (Figure 4.14A&B). However, overall this same group had the same percent survival, but it appears that between years 2 and 6 there could be a potential therapeutic window to intervene (Figure 4.14C). No correlation of patient survival was observed in similar groups when we look at miR-10b levels (Data not Shown).

4.4 Future Directions

We did not test the other class of microtubule destabilizers or DNA cross-linkers, nor did we test if miR-10a inhibitor would confer resistance to docetaxel, both questions that should be explored. Additionally, several miRNA inhibitors targeting the "star" strand were validated hits from the inhibitor screen. Only recently has the "star" strand biology been investigated (Yang, Phillips et al. 2011). Nonetheless this result is surprising and could be due to disruptions in the processing of the mature miRNA, which has not been reported and warrants further investigation. We also have several other miRNA inhibitors that are worth pursing, including miR-101, which regulates EZH2 and has been implicated in cancer stem cell maintenance and drug resistance (Sooryanarayana Varambally, Xiaosong Wang et al. 2007, Suva, Riggi et al. 2009). Other members in the lab are actively pursuing miRNA inhibitors that sensitize cells to paclitaxel and other microtubule-targeting agents.

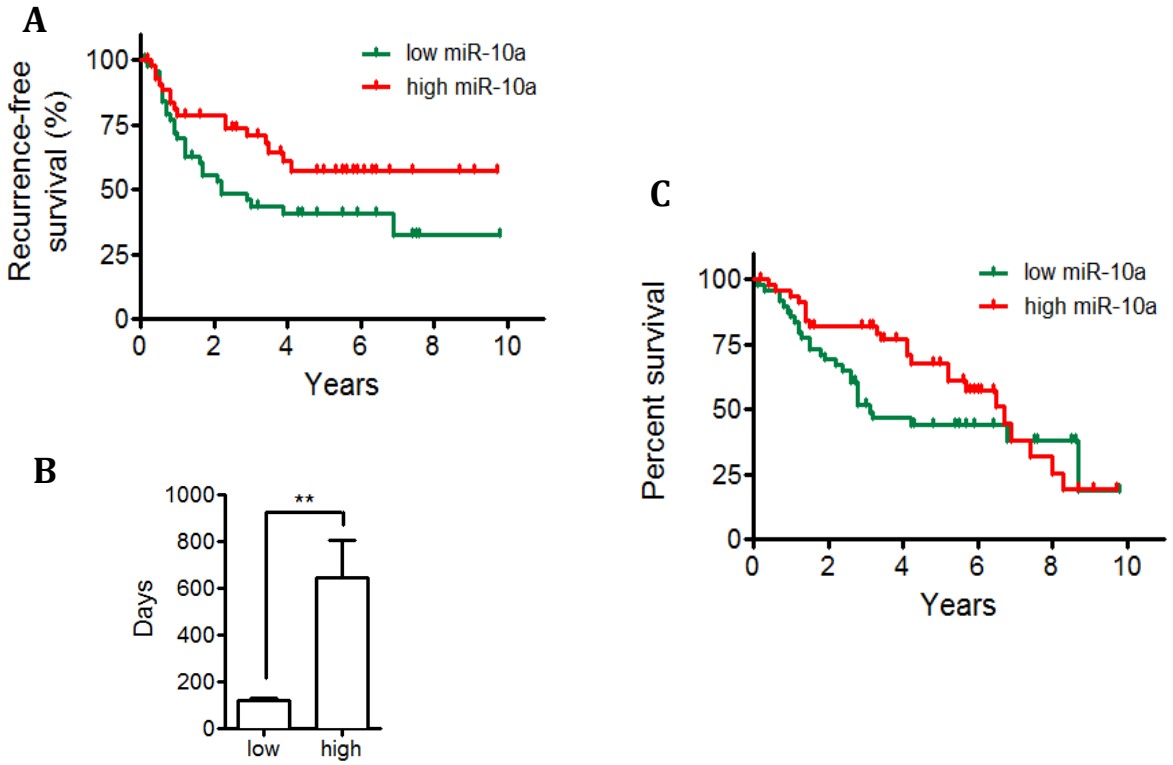

Figure 4.14 Tumor Levels of miR-10a are Associated with Patient Survival. (SPORE-Prospect Dataset) **A.** Expression levels were measured in 128 white male smokers by microarray. miR-10a expression for the lowest 50 (120.4 ±8.5) and the highest 50 (643.7 ±160.1); p=0.001 by two-sided t-test. **B.** RFS was longer in high miR-10a group (> 10 years) than in the low group (2.2 years); p=0.05 by the Gehan-Breslow-Wilcoxon test. **C.** In this same group overall survival was not changed

CHAPTER FIVE miR-10a Regulation of PI3K Signaling Through Direct and Indirect Mechanisms

5.1 Introduction

While the above findings suggest that miR-10a is a regulator of response to microtubule stabilizers in lung cancer, we do not know which miR-10a targets are responsible for mediating this effect. In parallel with the above studies, we were investigating miRNAs that regulate phosphatidylinositol 3-kinases (PI3K). It could be argued that PI3K is the linchpin not only in lung cancer, but also in many solid tumors. It lies directly downstream of both receptor tyrosine kinases (RTKs) such as EGFR and HER2/3, and KRAS. While mutations in PI3K are rare in lung cancer — comprising only about 10% of all mutations — when upstream signaling is taken into account, over 50% of lung cancer signals through PI3K (Larsen, Cascone et al. 2011). Currently, there are almost a dozen drugs targeting various components of the PI3K in clinical trials (Courtney, Corcoran et al. 2010).

PI3K is a heterodimer protein composed of a regulatory subunit, p85, encoded by the gene PIK3R1 and a catalytic subunit, p100α, encoded by the gene PI3KCA. The regulatory subunit directly interacts with RTKs, transducing extracellular signals to intracellular responses. The binding event relieves the inhibitory conformation of the catalytic subunit, which then acts on its substrate phosphatidylinositol 4,5-bisphosphate (PIP2), converting it to phosphatidylinositol 3,4,5-triphosphate (PIP3) (Zhao and Vogt 2008). The tumor suppressor

phosphatase and tensin homolog (PTEN) antagonizes the pathway by dephosphorylating PIP3 back to its inactive form PIP2. Additionally, KRAS can directly interact with the catalytic subunit to change it to the active form. Confirming PI3K involvement in KRAS-driven tumorigenesis was demonstrated using a mouse model of lung cancer that harbored a dominant negative form of PI3K-inhibited KRAS-induced lung cancer (Roy Katso1 2001).

PIP3 acts as a docking site for proteins that contain pleckstrin homology (PH) domains. Two widely studied PH domain-containing proteins are phosphoinositide-dependent kinases PDK1 and AKT. PDK1 phosphorylates AKT at threonine 308. Activated AKT then phosphorylates TSC2, inhibiting the GTPase activity of the TCS1/TCS2 dimer (Engelman 2009). This then relieves suppression of mTORC1 complex, in which the mammalian target of rapamycin, mTOR, lies at the catalytic center. The mTORC1 complex goes on to activate protein synthesis by phosphorylating eukaryotic initiation factor 4E (EIF4E) and the ribosomal subunit S6 proteins (Guertin and Sabatini 2007). Only recently was it discovered that activated ribosomal protein directly interacts with the mTORC2 complex, relieving its inhibition (Zinzalla, Stracka et al. 2011). Activation of mTORC2 allows for feed-forward signaling as it phosphorylates AKT at serine 473 allowing for full pathway activation (Figure 27A) (Courtney, Corcoran et al. 2010). Activation of the PI3K/AKT/mTOR pathway has been documented to regulate every one of the hallmarks of cancer and drug resistance (Engelman 2009).

Cancer constitutively activates the PI3K pathways through several somatic mutations in PIK3CA and inactivating mutations in PTEN. Mutations in PTEN are more frequently observed — typically deletions lead to a truncated, inactive protein (Song, Salmena et al. 2012). This inactivation causes accumulation of PIP3 and thus activation of the PI3K/AKT/mTOR signaling axis. As deep sequencing efforts have progressed over the years, several mutations in PIK3CA have been identified (Zhao and Vogt 2008). There are two hot-spot mutations, one in exon 9 and the other in exon 20. Exon 9 encodes the helical domain of the p110α protein, which directly interacts with the regulatory p85 subunit. The mutation changes the glutamic acid (E) at position 545 to a lysine (K) leading to a conformation change relieving the inhibitory effects of p85 subunit. This mutation is highly dependent on Ras-GTP activity (Zhao and Vogt 2008). The other hotspot mutation occurs in the catalytic site and changes the histidine (H) at position 1074 to an arginine (R), constitutively activating the protein. H1074R mutations are dependent on interaction with RTKs and are sufficient to induce lung adenocarcinomas (Engelman, Chen et al. 2008). The E545K and H1074R mutations are mutually exclusive, but *in vitro* experiments have found an additive effect, suggesting that such strong activation of the pathway inhibits tumor growth or progression (Zhao and Vogt 2008).

An immense amount of effort has been devoted to understanding the equilibrium that exists between PTEN and PI3K. Numerous reports have shown that subtle changes to PTEN are enough to allow for aberrant pathway activation (Carracedo, Alimonti et al. 2011), (Tay, Kats et al. 2011, Song, Salmena et al. 2012). It was first noted that primary non-metastatic prostate

tumors had one intact copy of PTEN while advanced metastatic tumors had complete inactivation. It was then experimentally shown that an 8% loss of PTEN resulted in a 28% increase in pAKT and that homozygous loss of PTEN was sufficient to cause invasive carcinomas (Trotman, Niki et al. 2003). Fitting with the observation that small decreases in PTEN predispose cells to oncogenic transformation, several groups discovered a handful of miRNAs that are over-expressed in cancer and repress PTEN. This was elegantly followed up by work in the Pandolfi lab that showed dysregulation of PTENP1, a pseudogene that is expressed, contains a 3'UTR that is highly homologous to that of PTEN and is selectively lost in human cancers (Poliseno, Salmena et al. 2010). PTENP1 over-expression increases PTEN protein levels by acting as a sponge for several miRNAs that would normally target PTEN. This concept has been expanded to integrate dozens of genes and miRNAs into a network of competing endogenous RNAs that act together to regulate PTEN protein levels (Figure 27B)(Salmena, Poliseno et al. 2011). Oddly, little effort has been paid to understanding whether the same degree of regulation exists for PI3K, in particular by miRNAs.

We discovered miR-10a as a regulator of PI3K levels that acts by directly interacting with the PIK3CA 3'UTR as well as through indirect mechanisms. We uncovered GATA6 as a transcription factor that activates PIK3CA expression and is also regulated by miR-10a. Finally, we identified miR-10a as a regulator of cellular growth in NSCLC.

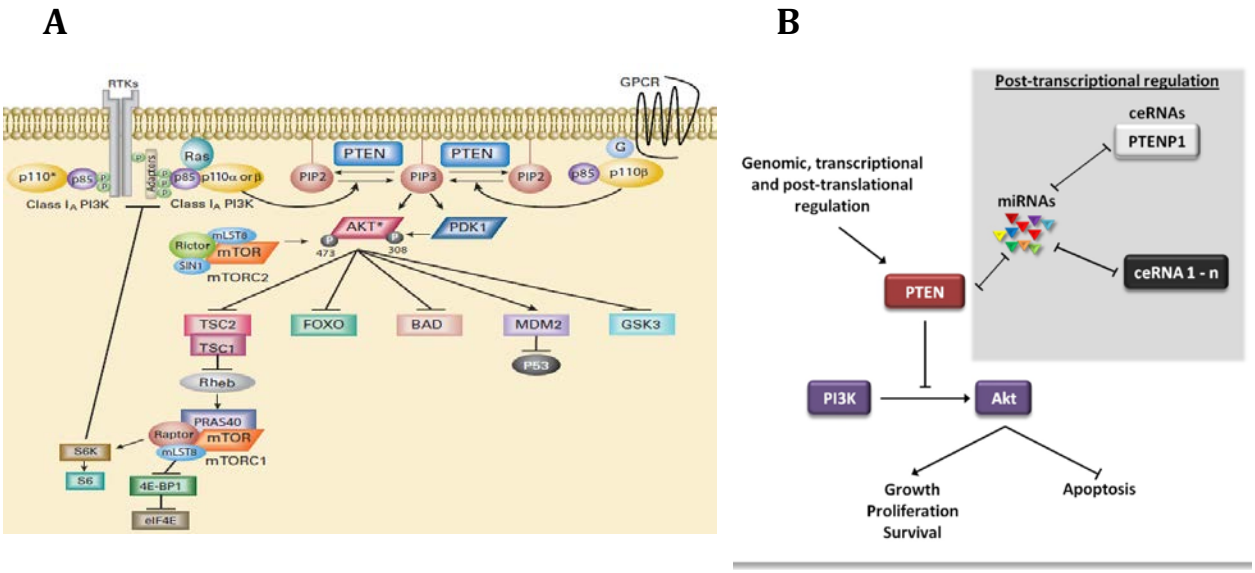

Figure 5.1 Overview of the PI3K/AKT/mTOR Pathway and Regulatory Pressure Placed on PTEN. A. PI3K receives signals from both RTKs and GPCRs leading to the accumulation of PIP3 and activation of the AKT, the main downstream effector. Activated AKT promotes cell cycle progression, induces cellular growth, promotes drug resistance and inhibits apoptosis. Antagonizing PI3K is PTEN, which dephosphorylates PIP3 back to PIP2. (Engelman J. Nature Reviews, 2009) **B.** Post transcriptional regulation placed on PTEN. Over half a dozen oncogenic miRNAs have been shown to regulate PTEN levels. Additionally, several competing endogenous mRNA and a pseudo gene act as sponges to allow for PTEN mRNA stability. (Song M, Salmena L, Pandolfi P. Nature Reviews, 2012).

5. 2 Results

5.2.1 miR-10a as a candidate for regulation of PIK3CA levels

To explore the influence that miRNAs potentially exert on PI3K, we investigated the PIK3CA 3'UTR which is highly conserved among mammals and at only 340bp, is half the length of the average 3'UTR (Figure 5.2A). Using several target prediction algorithms and seed sequence conservation we identified miR-10a as a potential regulator of PIK3CA (Figure 5.2 B, C&D Appendix D). As shown above, miR-10a expression is highly variable across our panel of NSCLC cell lines as determined by array and qPCR (Figure 4.7 and 5.3). However, no correlations between miR-10a expression and histological subtype, mutational status, or PIK3CA levels were observed (Figure 5.3). Although miR-10a expression was not down-regulated in lung tumor specimens relative to normal adjacent tissues, we did observe a significant reduction in breast and head and neck squamous cell carcinomas (HNSCC) tumors (Figure 4.4A-C). Given our previous findings of miR-10a regulation of paclitaxel response and its clinical markers, further exploration of miR-10a was warranted (Figure 4.5A&B and 4.14).

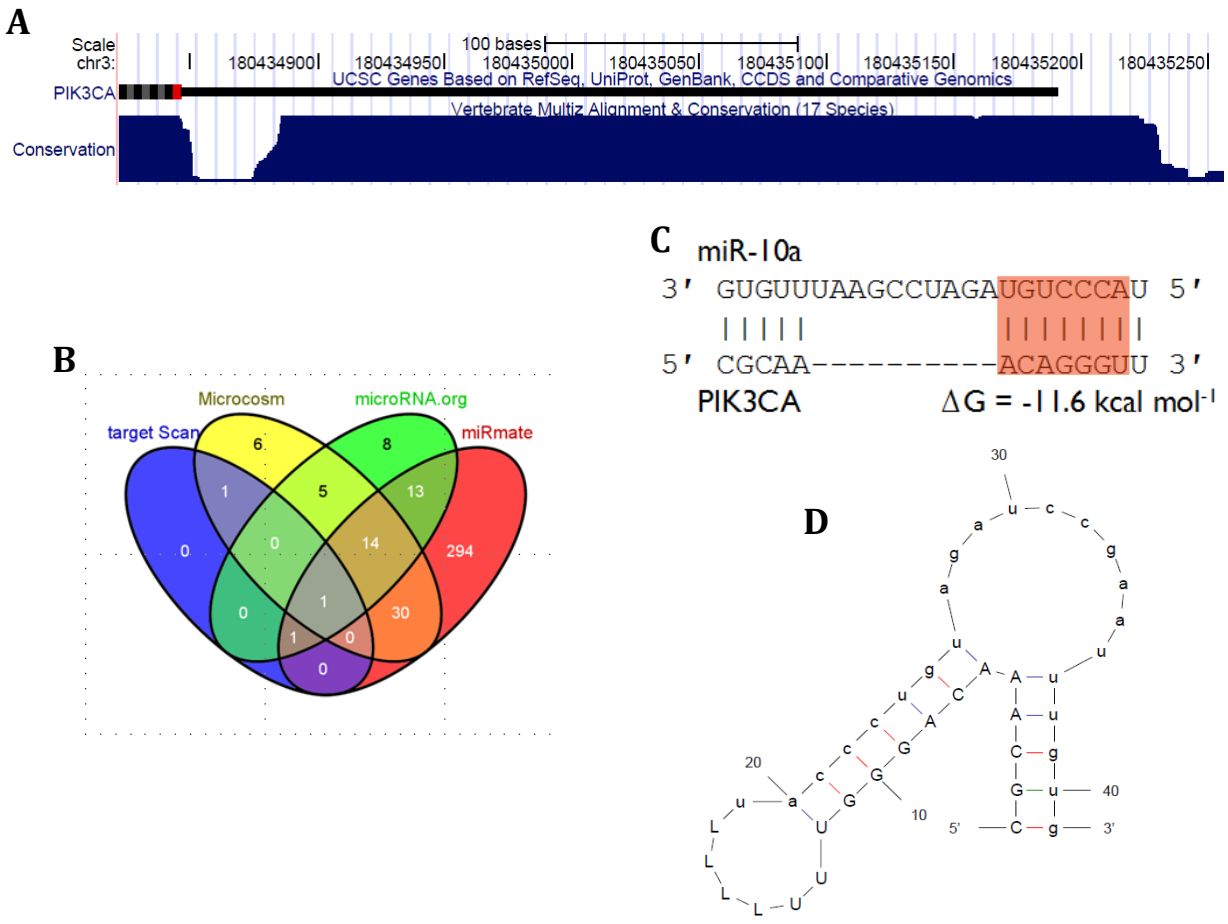

Figure 5.2 Identifying miR-10a as a Potential Regulator of PI3K.
A. The PIK3CA 3'UTR is highly conserved among vertebrates. UTR length and conservation determined by UCSC Genome Browser. **B.** Four target prediction methods were queried for miRNAs that potentially regulate PI3K; the methods agreed on only one candidate target. **C**. Interaction and energetics of the interaction between miR-10a and PIK3CA as determined by mFOLD. **D.** Structure of interaction between miR-10a (lower case) and PIK3CA (upper case). The single base difference between miR-10a and 10b is nucleotide 30. "LLLL" is a linker between the two sequences.

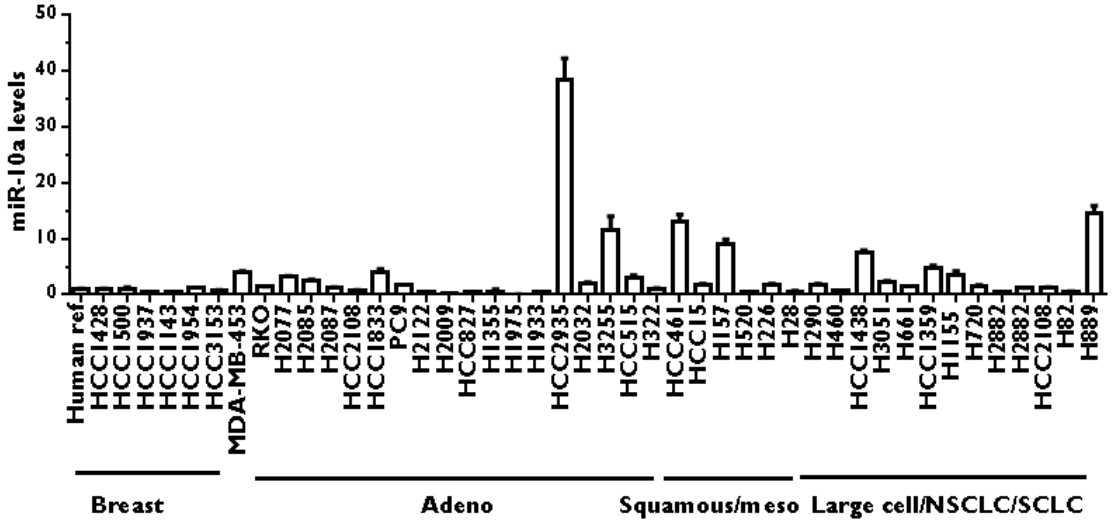

Figure 5.3 miR-10a Expression Does Not Correlate with Tissue or Histological Subtype. A. qRT-PCR data quantifying miR-10a levels across two tissue types and several histological subtypes. All qRT-PCR measurements were performed in triplicate and internally normalized to RNU19 and then normalized to human reference RNA (Sigma).

5.2.2 Direct Regulation of PIK3CA by miR-10a

To investigate the regulation of PIK3CA by miR-10a, we used H460 and H1155 as model cell lines, one harboring a canonical mutation in the PIK3CA kinase domain (E545K) and the other containing an inactivating mutation in PTEN, respectively. Exogenous expression of miR-10a in each cell line led to a 3,000-fold increase in miR-10a levels in H1155 cells and a 2,700 fold in H460 cells when compared to control treated cells (Figure 4.9B). In both cell lines we observed a 50% reduction in PIK3CA levels (Figure 5.4A). We then analyzed the robustness of the phenotype and transiently removed miR-10a from both H460 and H1155 cells using a LNA inhibitor specifically targeting miR-10a (Figure 4.9A). Removing miR-10a from H1155 and H460 cells resulted in three- and two-fold increases in PIK3CA levels, respectively (Figure 5.4B). To determine if in fact miR-10a was the only miRNA that regulated PIK3CA or was part of a network of miRNAs, we tested the effects of miR-10b and two other miRNAs, miR-124 and miR-203, which have conserved binding sites in the PIK3CA 3'UTR. Only when cells were transfected with miR-10a mimic did we observe a reduction in PIK3CA levels (Figure 5.4C). We then expanded this finding across a panel of cell lines containing various histological subtypes of lung cancer, three breast cancer lines and two colon cancer cell lines. In all cases miR-10a was able to reduce PIK3CA expression (Figure 5.4D). Since the observed changes at the mRNA level were relatively subtle, we were unsure if this reduction would have any effect on downstream signaling.

We looked at changes in PI3K and downstream phosphorylation sites of AKT. H460 cells transfected with miR-10a mimic exhibited only a 50% reduction of PI3K, yet we observed complete loss of phosphorylation of AKT at both Thr308 and Ser407 and the activation site of mTOR (Figure 5.5A). Treatment of both H1155 and H460 cells with miR-10 inhibitor resulted in significant up-regulation of PI3K levels and activation of Ser473 on AKT (Figure 5.5B). Finally, direct interaction was tested using a luciferase reporter construct, which upon miR-10a inhibition indicated a 4-fold increase in luciferase activity and upon miR-10a increase showed a 50% reduction in activity (Figure 5.6A&B). When three base pairs of the miR-10a target sequence were mutated in the PIK3CA 3'UTR, abrogating the interaction between miR-10a and the target site, miR-10a mimic had no effect on luciferase levels (Figure 5.6C). These results demonstrate a direct, specific and functional interaction between miR-10a and PIK3CA and are concordant with previous findings on the sensitivity of the PI3K/AKT/PTEN pathway to perturbation (Poliseno, Salmena et al. 2010).

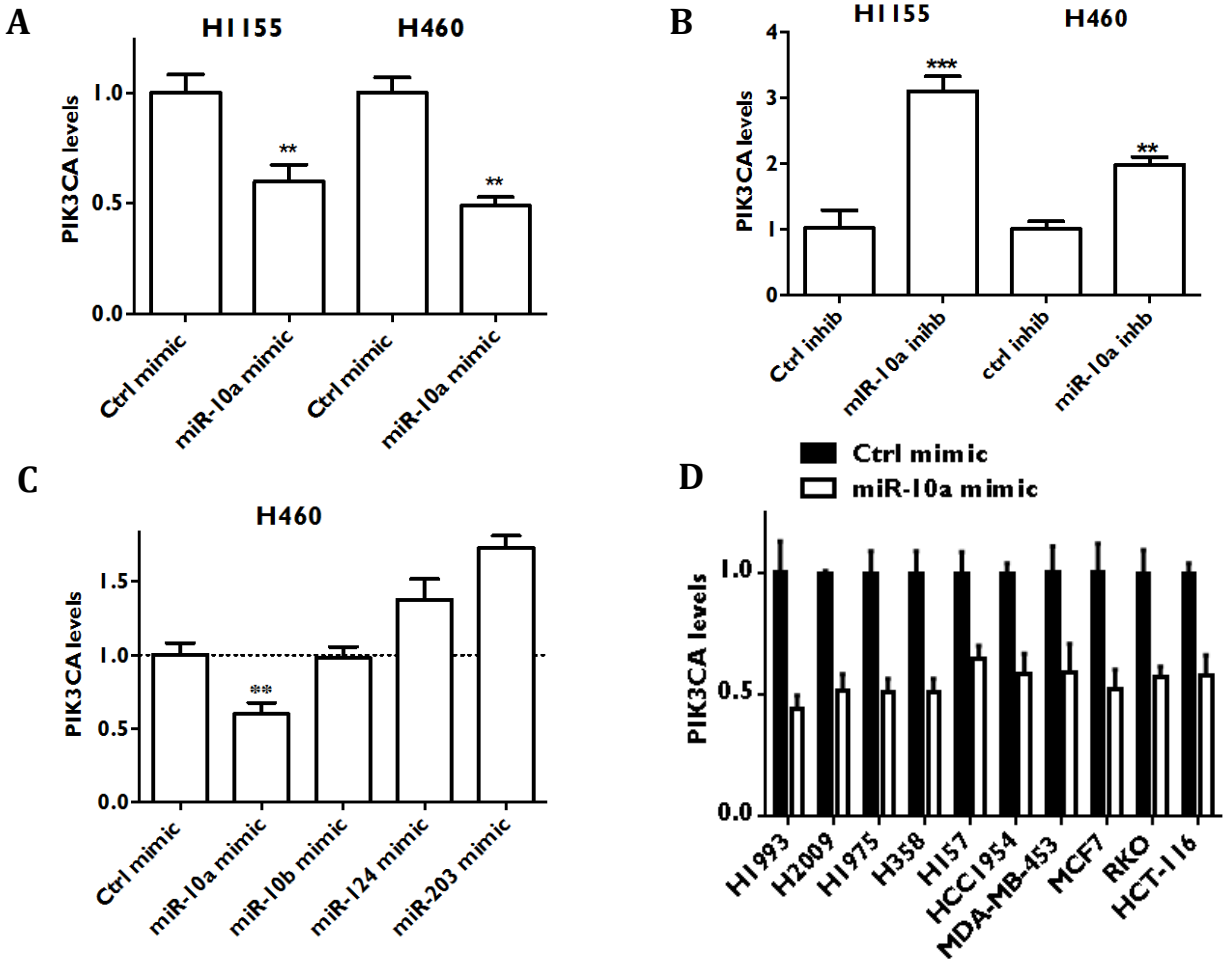

Figure 5.4 miR-10a Affects PIK3CA Expression. **A.** Transfection of H1155 and H460 cells with 20nM miR-10a mimic resulted in a ~50% reduction in PIK3CA levels. H1155: **, p = 0.0034; H460: **, p = 0.0017, by two-tailed unpaired t-test with n=3. **B.** Transfection of H1155 and H460 cells with 20nM miR-10a inhibitor (Exiqon) resulted in three- and two-fold increases in PIK3CA levels, respectively. H1155: ***, p = 0.0005; H460: **, p = 0.0029 by two-tailed unpaired t-test with n=3. **C.** Reverse transfection with 20nM of various miRNA mimics, **, p = 0.0034, by two-tailed unpaired t-test with n=3 **D.** Transfection of miR-10a mimic leads to reduction in PIK3CA across lung, breast (HCC1954, MDA-MB-453 and MCF7) and colon (RKO and HCT-116) cell lines.

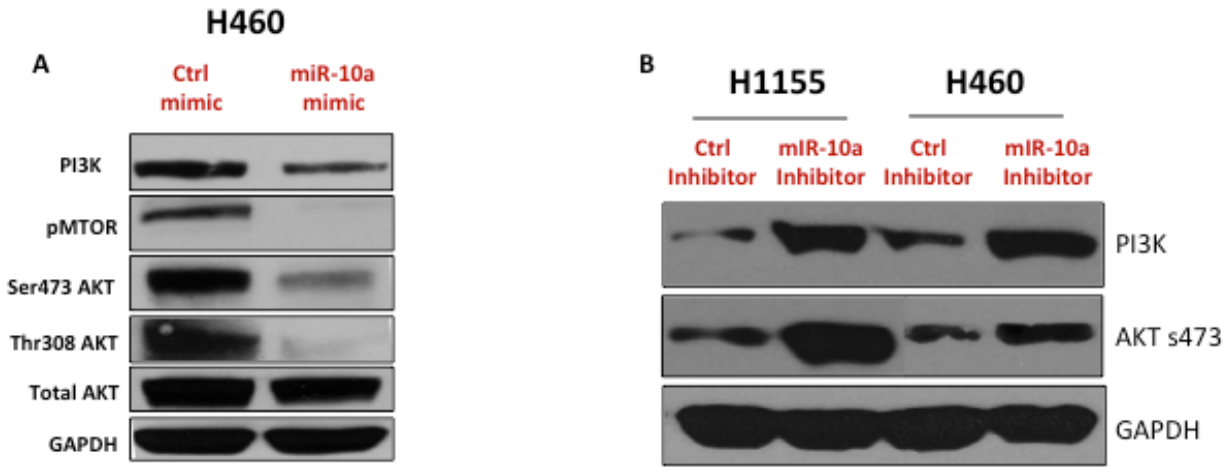

Figure 5.5 Effect of miR-10a on PIK3CA mRNA Levels Is Amplified at the Protein Level. **A.** miR-10a mimic was able to reduce PI3K levels by ~50%, leading to reduction of phosphorylation of AKT at Thr308 and Ser473 and complete inhibition of mTOR activation. **B.** miR-10a inhibitor was able to increase PI3K levels and phosphorylation of AKT at Ser473.

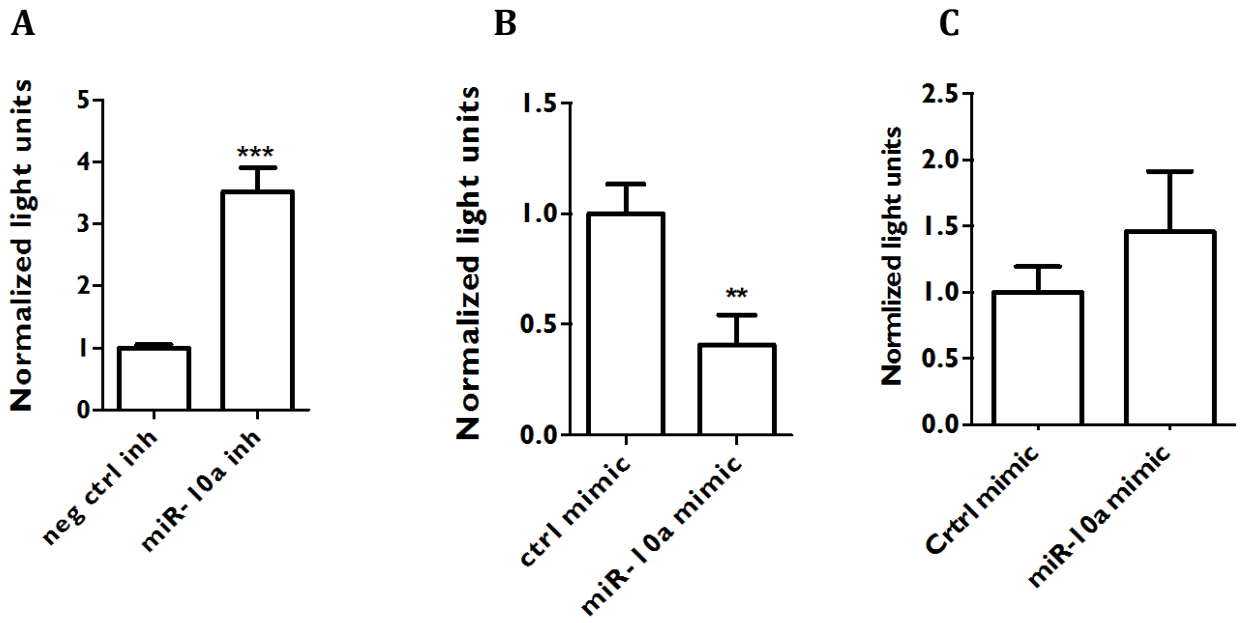

Figure 5.6 Direct Interaction of miR-10a and the PIK3CA 3'UTR. A. Inhibiting miR-10a expression in the presence of a luciferase reporter with the PIK3CA 3'UTR resulted in a 4-fold increase in luciferase activity, as measured in relative light units. ***, p = 0.0004, by two-tailed unpaired t-test with n=4. **B**. Co-treatment of miR-10a mimic and the reporter construct led to a 50% reduction in luciferase activity, as measured in relative light units. **, p = 0.0035 by two-tailed unpaired t-test with n-4. **C.** Ablating the miR-10a target site in the reporter construct led to no change in luciferase activity when cells were co-transfected with the miR-10a mimic.

5.2.3 Inhibiting PI3K Affects Cellular Response to Paclitaxel

Although our previous finding that miR-10a regulates paclitaxel response was robust, we did not know which target or targets of miR-10a were responsible for the phenotype. We have now uncovered that miR-10a regulates PI3K. Given the importance of the PI3K/AKT/mTOR pathway in both innate and acquired drug resistance (McCubrey, Steelman et al. 2006), we postulated that the changes in paclitaxel response we observed were due to changes in PI3K. To address this question, we took several approaches. First, we used both transient siRNA and stable shRNA transfection to knock down PIK3CA, both of which dramatically reduced PI3K levels (Figure 5.7A). In H460 cells, both the siRNA and shRNA targeting PI3K were able to sensitize cells to paclitaxel treatment. EC_{50}s for the ctrlSI and ctrlSH were 0.13 nM and 0.17 nM respectively, while for siPIK3CA and shPIK3CA they were 0.057 nM and 0.072 nM, respectively, with $p < 0.0001$ (Figure 5.7B-C). To confirm the effect was not cell type specific, we also used H1155 cells transiently transfected with siPIK3CA and observed similar results. siPIK3CA was able to shift the EC_{50} from 3.96 nM for the ctrlSI to 0.083 nM, a 50-fold decrease (Figure 5.7D).

Finally, we used BEZ-235, a small molecule inhibitor, to independently assess the synergy between inhibition of PI3K and paclitaxel. BEZ-235 is a dual inhibitor; it inhibits both PI3K and mTOR and has shown promise in clinical trials (Serra, Markman et al. 2008). We needed to select a concentration of BEZ-235 that only had minimal effect on cellular viability. From the dose-response curve (Figure 5.8A&B), 5 nM was selected as having only a minimal

effect on viability (Figure 5.8D). Following 72 h pre-treatment with 5 nM of BEZ-235, the EC_{50} for paclitaxel decreased from 3.06nM for DMSO to 0.933 nM (Figure 5.8C).

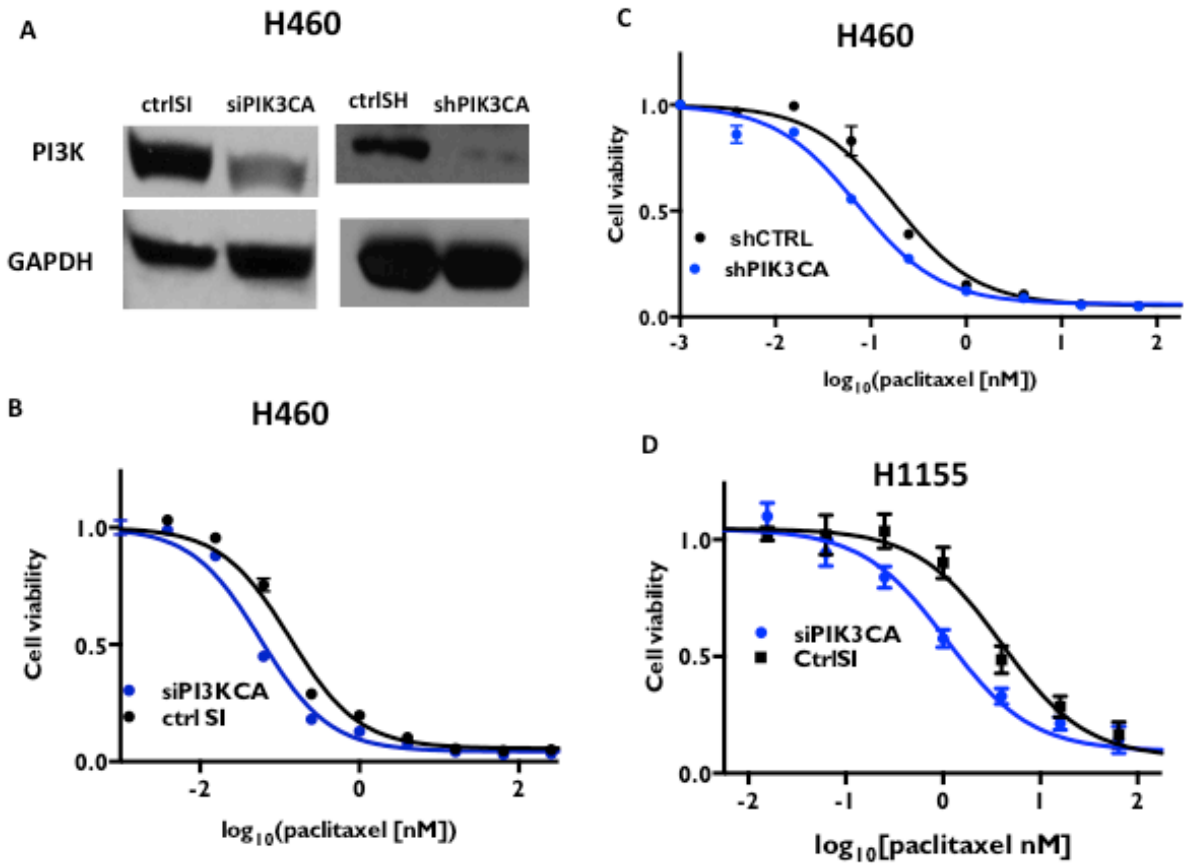

Figure 5.7 Loss of PI3K Sensitizes NSCLC Cells to Paclitaxel. A. Both siRNA and shRNA targeting PIK3CA were effective at removing PI3K. **B.** H460 cells pretreated with siPIK3CA for 72 h before incubation with paclitaxel resulted in a decrease of the EC_{50} from 0.1341nM for the ctrl siRNA to 0.05746 nM for the siRNA against PIK3CA. $p \leq 0.0001$, with n=3 for each data point. **C.** Stable loss of PIK3CA shifted the EC_{50} from 0.1787 nM for the control shRNA to 0.07224 nM for the shRNA against PIK3CA. $p \leq 0.0001$, with n=3 for each data point. **D.** Pre-treatment of H1155 cells with siPIK3CA for 72 h before incubation with paclitaxel resulted in a decrease of the EC_{50} of from 3.968 nM for the ctrl siRNA to 0.08335 nM for the siRNA against PIK3CA. $p \leq 0.0001$, with n=3 for each data point.

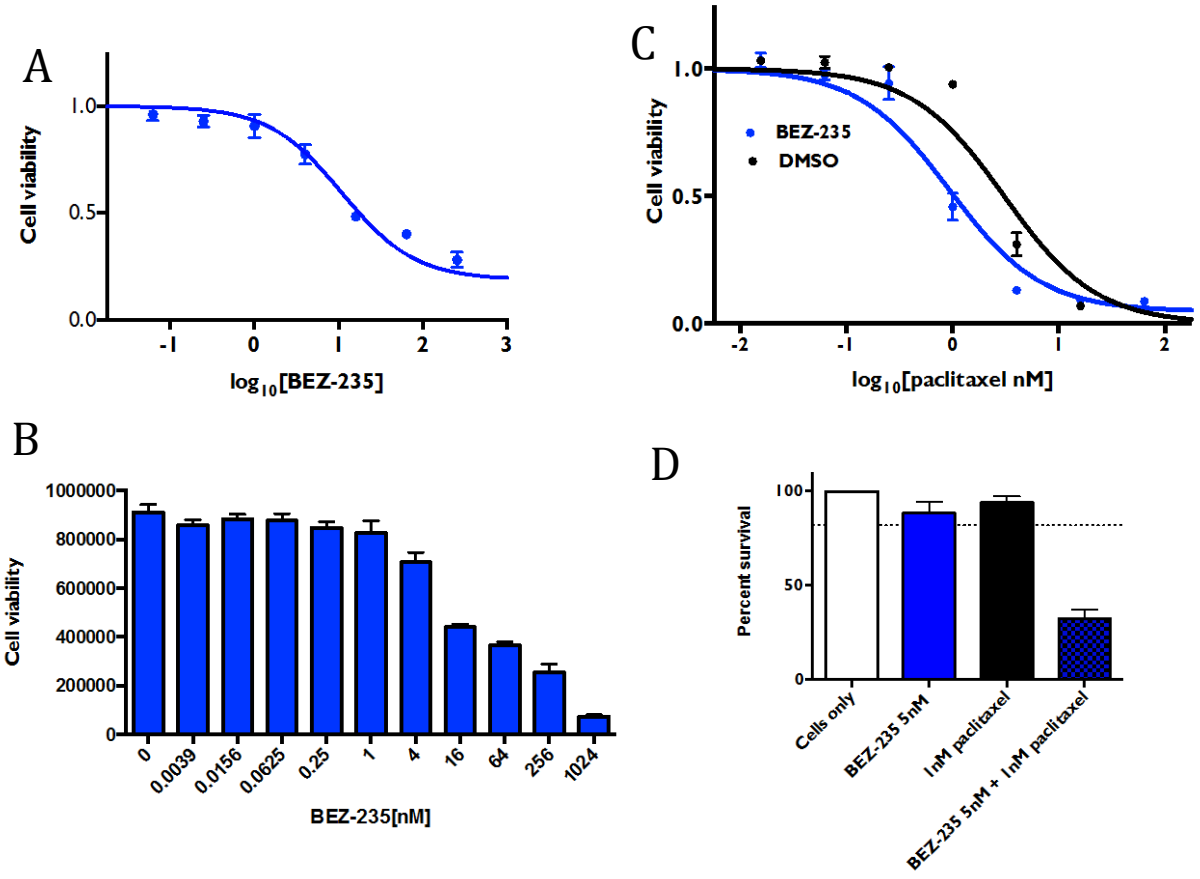

Figure 5.8 BEZ-235 Reduces H1155 Cell Viability in the Presence of Paclitaxel. A. Dose response curve for BEZ-235; concentrations ranged from 1024 nM to 0.0039 nM. EC_{50} = 12.53 nM, $p \leq 0.0001$, n=3 for each data point . **B.** Bar graph of raw dose response data. **C.** H1155 cells pretreated with 5 nM of BEZ-235 for 72 h before paclitaxel exposure. EC_{50} = 0.9337 nM when pre-treated with BEZ-235; carrier treated EC_{50} = 10.92 nM, $p \leq 0.0001$, n=3 for each data point.. **D.** Effect of 5 nM BEZ-235 on H1155 cell viability independent of paclitaxel treatment.

5.2.4 miR-10a Inhibits Growth and Induces Apoptosis

Previously, we observed that increasing intracellular levels of miR-10a mimic significantly inhibited cellular growth rates while decreasing miR-10a levels increased growth rates (Figure 4.13A-C and 4.5B). To test this further, we looked at growth rates using a kinetic assay with cell confluence measured every hour over the course of several days. We observed that manipulating miR-10a levels could move the growth curve in either direction (Figure 5.9A-B). Ectopic miR-10a completely inhibited growth of H460 cells while the control mimic had no significant effect on growth (Figure 5.9A). In stark contrast, the miR-10a inhibitor dramatically increased cellular growth (Figure 5.9B). To extend this measurement of growth promotion or inhibition over a longer time course, we looked at the ability of miR-10a to affect colony formation. Consistent with the effects on growth, increasing miR-10a inhibited colony formation while inhibiting miR-10a increased the number of colonies formed (Figure 5.9C). To control for possible off-target effects caused by miR-10a mimic, we employed stable over-expression that resulted in only a five-fold increase in miR-10a expression (Figure 5.9D). This relatively subtle increase was enough to inhibit colony formation significantly (Figure 5.9E).

Neither assay could explain how miR-10a was inhibiting growth; it could either be inducing apoptosis or having a cytostatic effect. We first looked at induction of apoptosis using DEVD-NucView from Essen BioScience (see Methods). Briefly, cells with activated caspase 3/7 will cleave DEVD-NucView to NucView, which will intercalate into the DNA and cause the cells to glow green. After 72 h of miR-10a mimic treatment nearly all the cells were green, indicating they were undergoing apoptosis compared to control mimic (Figure 5.10A-B). We

then independently confirmed this result by blotting for cleaved PARP; we observed an increase in cleaved PARP 48 h post transfection, indicating an activation of apoptosis (Figure 5.10C).

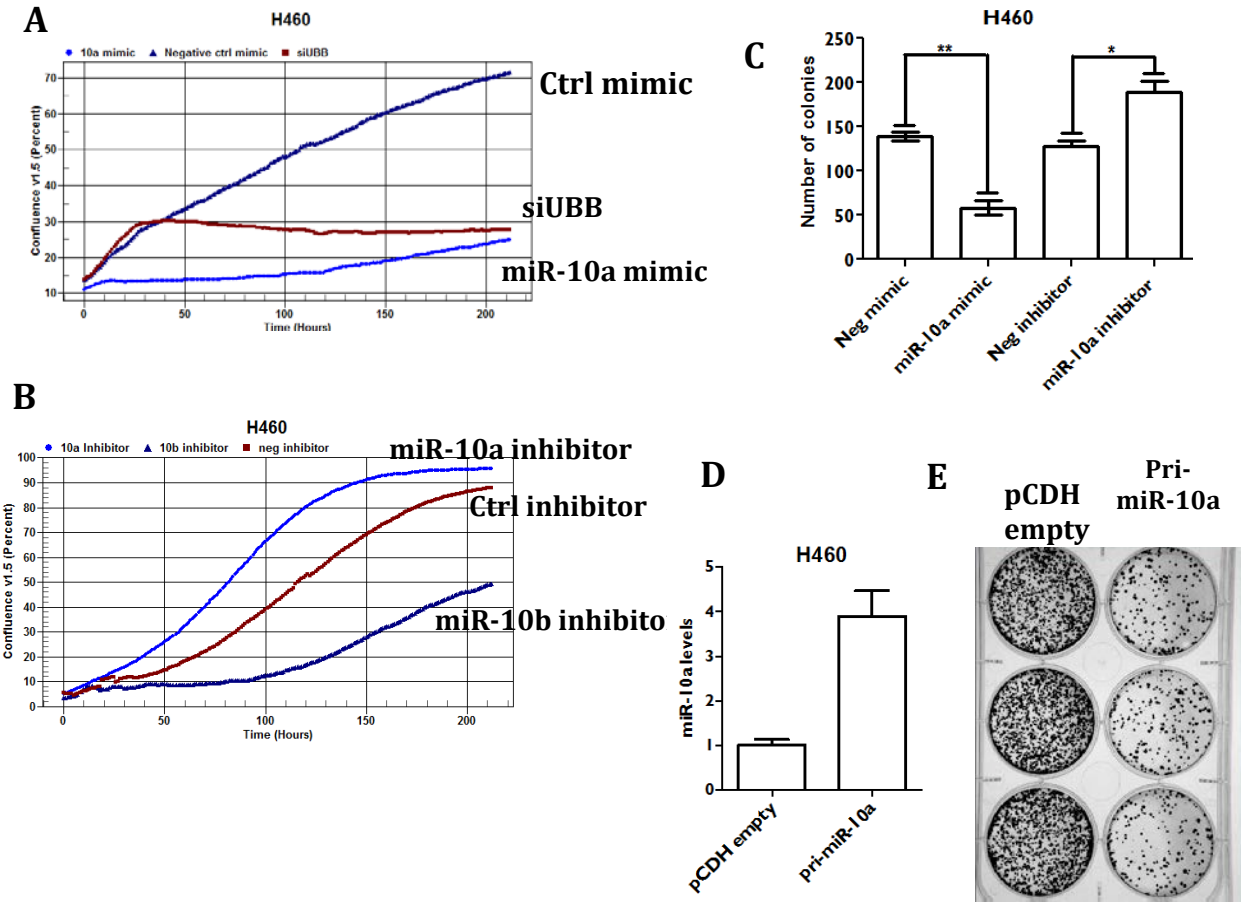

Figure 5.9 Changes in miR-10a levels Can Manipulate Growth Rate of NSCLC Cells. A. Kinetic assay for growth rate. Cell confluence measured every hour over 8 days shows that the miR-10a mimic is as effective at inhibiting cell growth as siUBB. **B.** H460 cells treated with miR-10a inhibitor show a decrease in doubling time from 40 hours to 30 hours. **C.** miR-10a levels affect the ability of H460 cells to form colonies, as shown by colony formation assay. Error bars indicate standard deviations; **, p = 0.011; *, p = 0.0284. **D.** Stable induction of miR-10a using a viral vector resulted in a 5-fold increase in expression. **E.** Colony formation in stably transduced H460 seeded at 1,000 cells per well. Over-expression of miR-10a resulted an 80% reduction in colony formation ability.

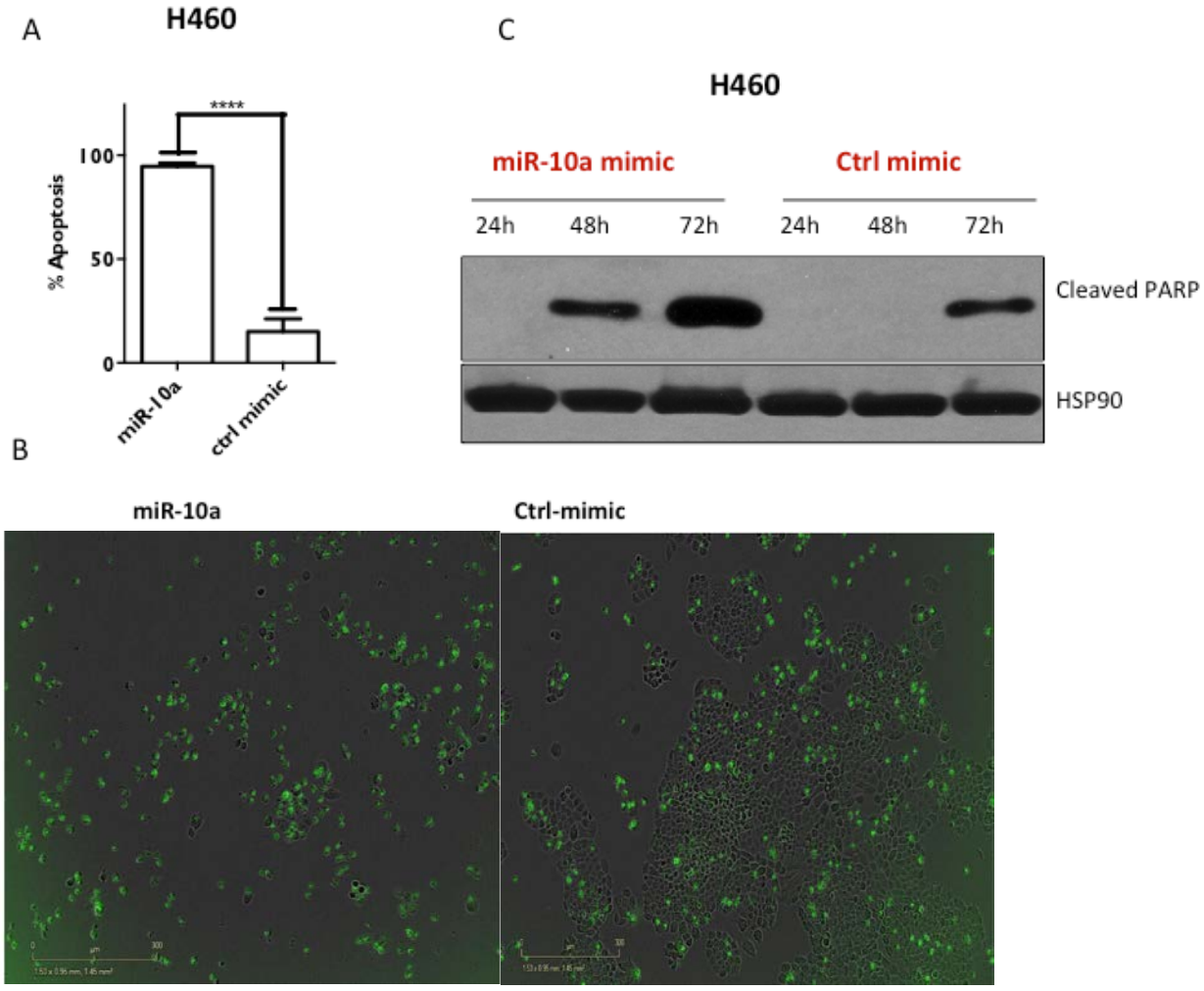

Figure 5.10 High miR-10a Levels Induce Apoptosis. A. H460 cells treated with 20nM of miR-10a mimic for 72 h resulted in a ~10-fold increase in apoptosis. **B. Image of H460 cells incubated with DEVD-NucView.** Green cells are actively undergoing apoptosis while unstained cells are not. **C.** Western blot for cleaved PARP at various time points post-transfection with 20 nM miR-10a mimic.

5.2.5 miR-10a Indirectly Regulates PIK3CA Through GATA6

miRNAs have relatively small effects on expression of individual genes (~40%), yet can exert profound phenotypic effects. The most likely explanation for this is that individual miRNAs target multiple genes in the same or related pathways or biological processes, as we and others have have previously shown (Du, Subauste et al. 2012). To explore this hypothesis in the context of miR-10a, we looked at both upstream and downstream components of the PI3K/AKT/mTOR pathway for potential miR-10a target sites. This search was unsuccessful. We then looked at the promoter of PIK3CA and found several hundred conserved transcription factor binding sites. We compared them to all putative miR-10a target genes listed in TargetScan 6.2 (Figure 5.11A) and uncovered two overlapping targets, GATA6 and HOXA3. We then investigated expression of each gene in our panel of cell lines and found that only GATA6 is expressed in our cell line panel with a positive correlation with PIK3CA expression (Figure 5.11B-C). To confirm that GATA6 regulates PIK3CA, we first used a siRNA targeting GATA6 (Figure 5.12A-B) and discovered that loss of GATA6 resulted in only a 50% reduction of PIK3CA, but complete loss of PI3K protein (Figure 5.12A-B). To confirm this was not an off-target effect, we generated a stable knockdown of GATA6 and PI3K and observed results similar to what was seen with the siRNA (Figure 5.12C). Interestingly, the shRNA targeting PI3K also resulted in loss of GATA6 expression, suggesting a feed-forward regulatory loop (Figure 5.12C). To confirm direct interaction, we have designed four sets of primers to encompass the GATA6 binding sites in the promoter of PI3KCA and are currently working on assay conditions.

Having confirmed GATA6 as a regulator of PIK3CA expression, we needed to test miR-10a regulation of GATA6 expression. Following transient transfection with miR-10a mimic, we observed a loss of GATA6 mRNA and protein (Figure 5.13A-B). To test the robustness of this phonotype, we depleted miR-10a levels using the miR-10a inhibitor and observed an increase in both GATA6 mRNA and protein (Figure 5.13A-B). To ensure that modulation of GATA6 levels was a direct result of miR-10a regulation, we cloned a large fragment of the GATA6 3'UTR containing the miR-10a target site downstream of a luciferase reporter construct. We were able to manipulate luciferase activity levels using both miR-10a mimic and inhibitor (Figure 5.13C) consistent with a direct and specific interaction. Following mutation of the miR-10a seed sequence, we were able to restore luciferase activity when cells were treated with miR-10a mimic (Figure 5.13D). Taken together, we have uncovered GATA6 as a regulator of PI3K, shown that PI3K and GATA6 are part of a feed-forward regulatory loop, and finally that miR-10a regulates GATA6.

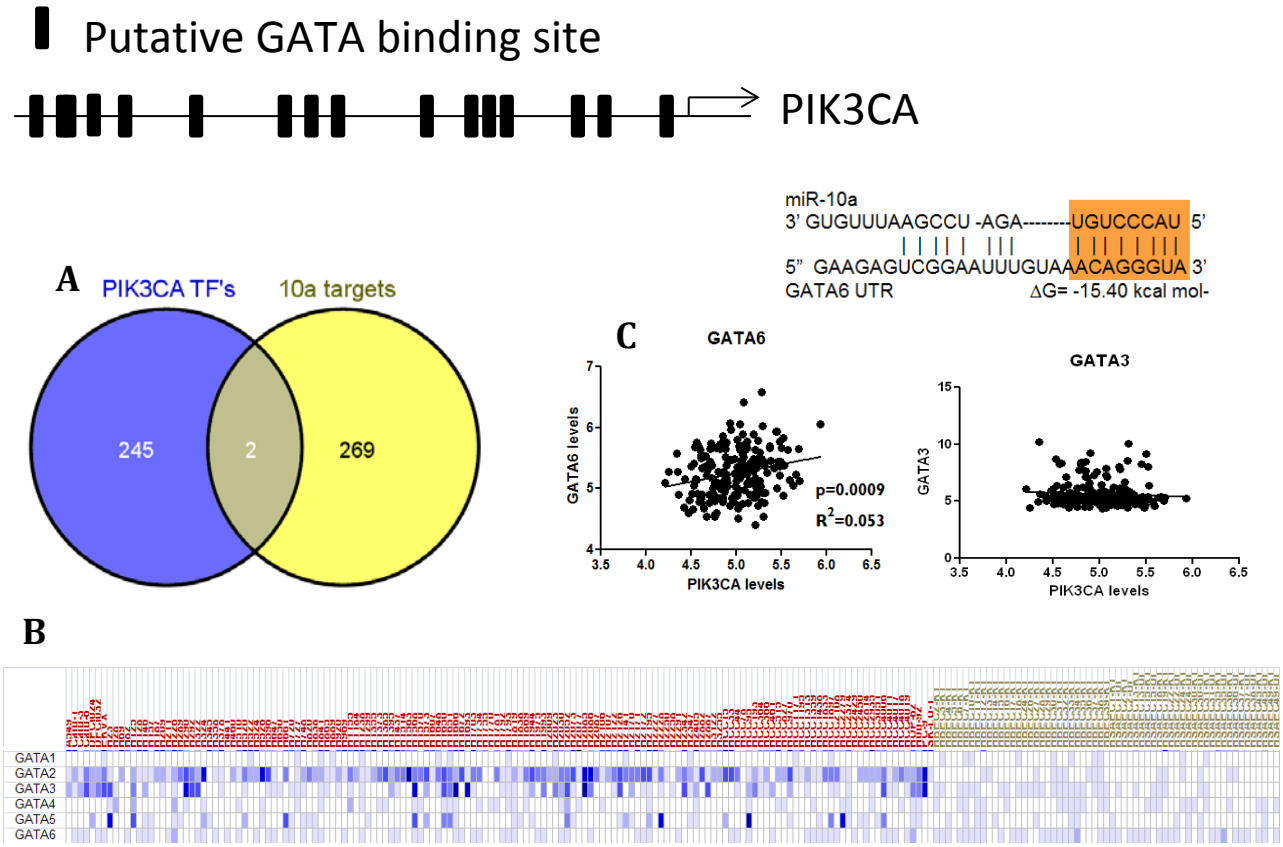

Figure 5.11 Potential Indirect Regulation of PI3K by miR-10a through GATA6.
A. Overlapping sets of miR-10a targets from Targetscan and conserved transcription factor-binding sites in the region +/- 3.5 KB from the TSS of PIK3CA. **B.** GATA family expression across our panel of NSCLC cell lines. C. The only GATA family member with a positive correlation with PIK3CA expression is GATA6; R = 0.23, p = 0.0009.

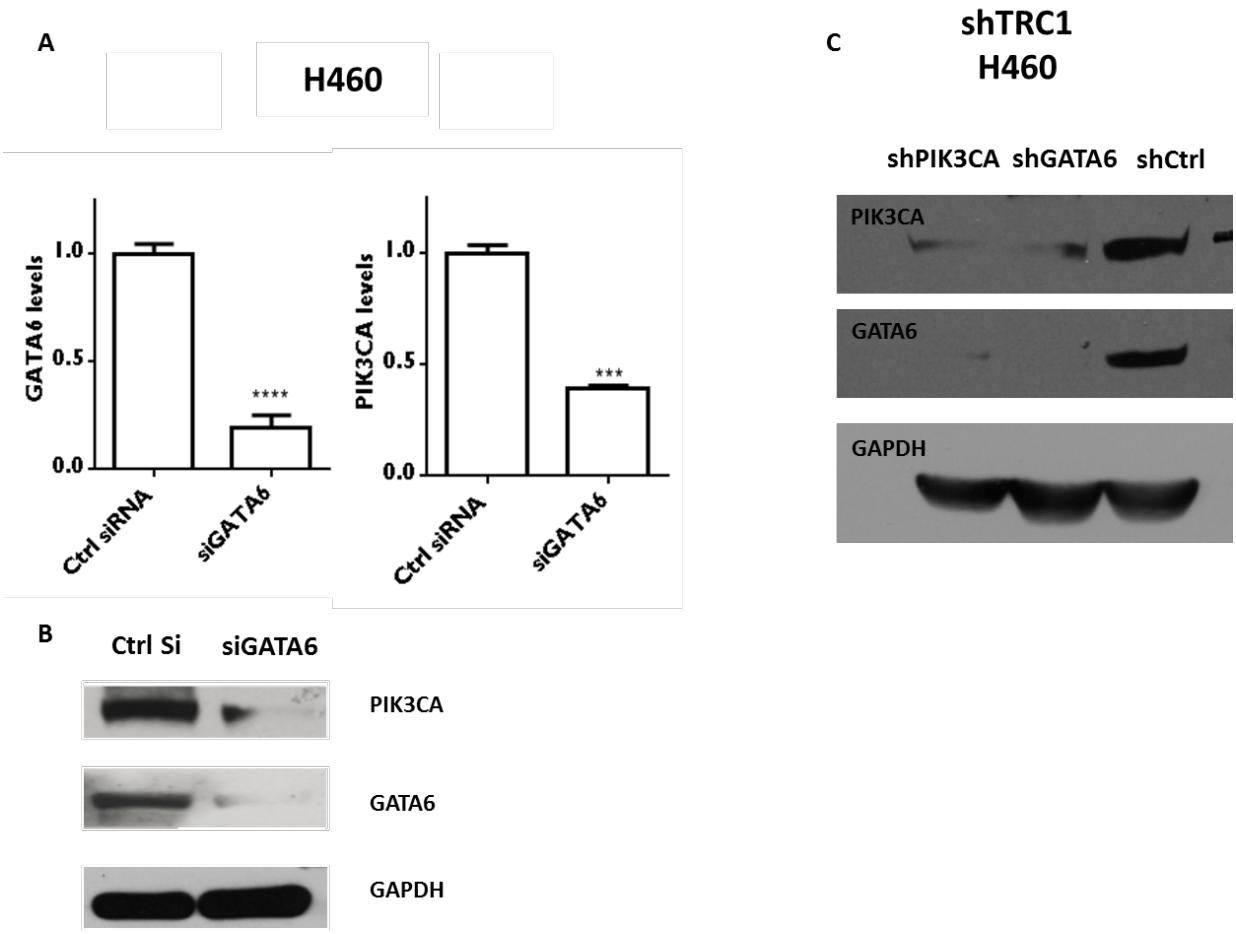

Figure 5.12 GATA6 Regulates PI3K. **A**. siRNA knock-down of GATA6 resulted in complete loss of GATA6 mRNA and resulted in ~50% decrease in PIK3CA mRNA. ***, p = 0.0001; ****, $p \leq 0.0001$ by unpaired two-tailed t-test with n=3. **B.** Transfection of the siRNA against GATA6 leads to complete loss of both GATA6 and PI3K after 72 h. **C.** Stable knock-down of GATA6 resulted in loss of PI3K expression; stable knock-down of PIK3CA resulted in loss of GATA6 expression.

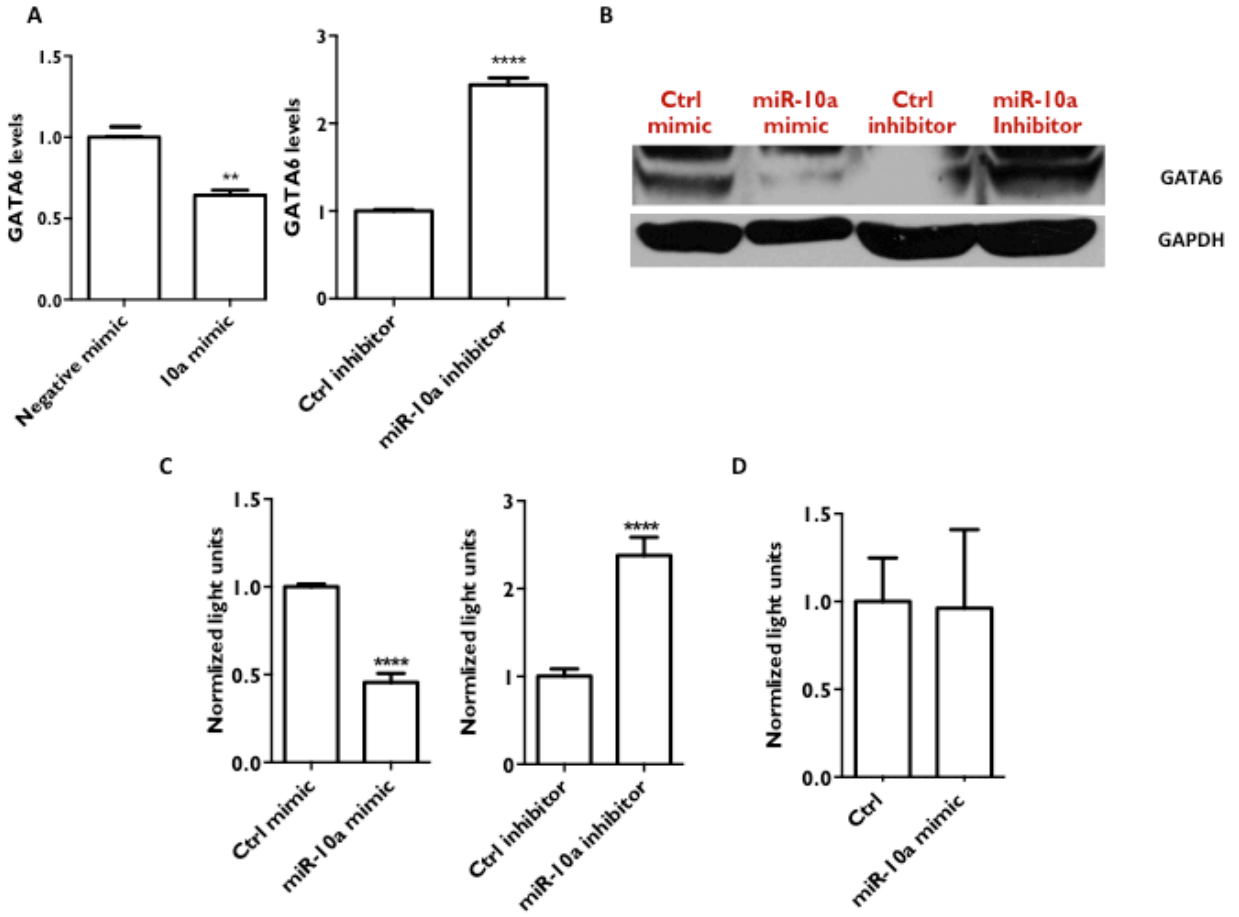

Figure 5.13 miR-10a Directly Regulates GATA6. A. Transfection of 20 nM of miR-10a mimic reduces GATA6 levels by ~40%, as measured by qRT-PCR. Transfection of 20nM of miR-10a inhibitor increases GATA6 levels by ~2.5-fold. **, $p = 0.039$; ****, $p \leq 0.0001$ by unpaired two-tailed t-test with n=3. **B.** miR-10a mimic leads to reduction in GATA6 protein levels while miR-10a inhibitor increases GATA6 protein levels**. C.** miR-10a interacts directly and specifically with the GATA6 3'UTR. miR-10a mimic results in ~50% reduction in luciferase activity, while miR-10a inhibitor leads to a ~2.5-fold increase in luciferase activity. ****, $p \leq 0.0001$ by unpaired two-tailed t-test with n = 4. **D.** Ablating the miR-10a target site in the reporter construct led to no change in luciferase activity following transfection of cells with miR-10a mimic.

5.2.6 Effects of Loss of GATA6 in NSCLC

Members of the GATA transcription factor family are zinc finger DNA binding proteins that control development by activating and inhibiting gene expression (Burch 2005). There are six members in the family: GATA1, GATA2 and GATA3 are expressed in the hematopoietic lineage, while GATA4, GATA5 and GATA6 are expressed in cells of the endoderm. Their role in cancer development and progression is just starting to come to light. Recently, it was shown that GATA2 is aberrantly expressed in NSCLC and required for KRAS driven lung cancer (Kumar, Hancock et al. 2012). GATA6 is over-expressed in esophageal adenocarcinoma (EAC) and is required for inhibition of p38α induction of apoptosis and for the regeneration of epithelial stem cells of the lung airways (Zhang, Goss et al. 2008, Lin, Bass et al. 2012). In addition to over-expression in EAC, GATA6 is over-expressed in pancreatic, colon and pancreatobiliary cancers (Shureiqi, Zuo et al. 2007, Fu, Luo et al. 2008, Kwei, Bashyam et al. 2008). The role of GATA6 in lung cancer, however, is largely unknown. To explore this question we used short-term loss of GATA6 using a siRNA, which resulted in modest growth inhibitory effects equivalent to that of siPIK3CA (Figure 5.15A). However, after several days cells were able to escape the inhibitory effects of GATA6 loss. To address this we turned to stably knocking-down GATA6 expression by shRNA in several cell lines of various histological subtypes and observed a loss in their ability to form colonies in vitro and inhibition of cellular growth rate (Figure 5.15B). Collectively, these results suggest that GATA6 is required for NSCLC cellular growth.

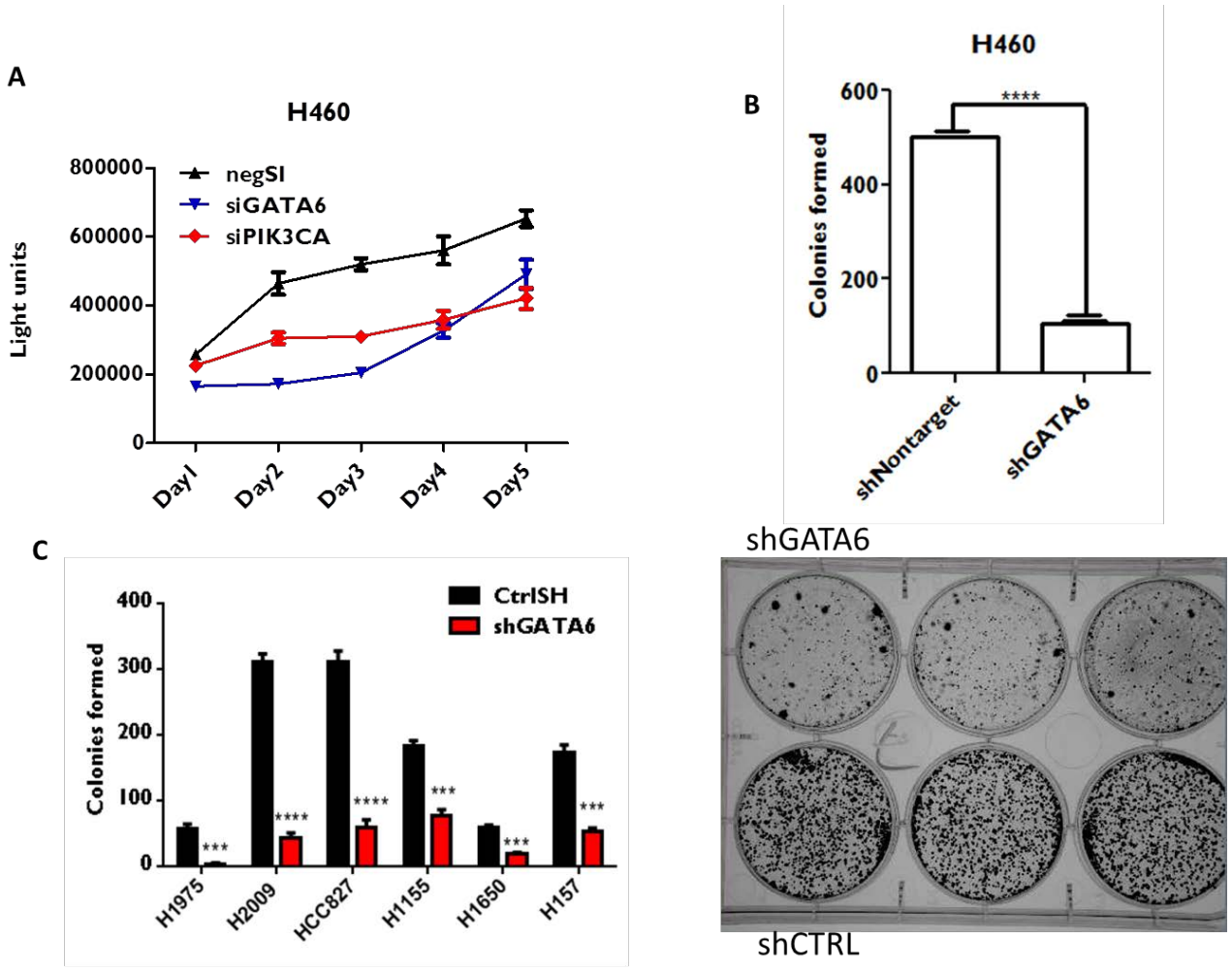

FIGURE 5.15 Loss of GATA6 Inhibits Growth and Colony Formation In NSCLC. A. siRNA-mediated silencing of GATA6 resulted in modest growth inhibition. **B.** Stable loss of GATA inhibited colony formation, leading to an 80% loss in H460 cells. ****, $p < 0.0001$ by unpaired two-tailed t-test. **C.** Loss of GATA6 across several histological subtypes. ****, $p < 0.0001$; ***, $p = 0.0003$ (H1975 cells), $p = 0.0001$ (H1155, H1650 and H157 cells).

5.4 Discussion

We have identified miR-10a as a novel regulator of the PI3K pathway both by directly interacting with the PIK3CA 3'UTR and indirectly via regulation of GATA6, a novel transcription factor that activates PIK3CA expression (Figure 5.16). The PIK3CA 3'UTR is highly conserved among mammals but extremely short, with only three conserved miRNA recognition sites. Following a bioinformatics approach, we identified miR-10a as a candidate regulator of PIK3CA. We have previously shown that miR-10a is a associated with recurrence-free survival in white male smokers. Unlike other miRNAs located in the HOX clusters, it is down-regulated in several types of cancer (Figure 4.14A-B, 4.4A-B and data not shown). In lung cancer patients, however, miR-10a does not appear to be down-regulated in tumors compared to NAT (Figure 4.4C) This could be due to the stage at which the samples were taken: In urothelial carcinomas, for example, miR-10a expression is high only during the early stages of development, specifically when the carcinoma is confined to the inner lining of the bladder wall. It is worth noting that a majority of these carcinomas exhibit activation of Fibroblast growth Factor Receptor 3 (FGFR3), which is directly upstream of the PI3K/AKT signaling axis, potentially indicating that the expression increase observed in miR-10a may be an attempt by the cell to inhibit the PI3K/AKT pathway (Veerla, Lindgren et al. 2009). We could be observing similar inhibitory or stimulatory effects of PI3K/GATA6 on miR-10a. Currently, investigating the potential regulation of miR-10a by GATA6 as the promoter of miR-10a does have several GATA binding elements.

To test our hypothesis that miR-10a regulates PI3K, we transfected H1155 and H460 cells with both miR-10a inhibitor and mimic and observed PIK3CA levels vary inversely with the perturbations. There are three other miRNAs to consider: the two other conserved predicted miRNA target sites in the PI3KCA 3'UTR and the other miR-10 family member, miR-10b, that could act as part of a PI3K regulatory network similar to what has been described with PTEN (Salmena, Poliseno et al. 2011). After testing all three miRNAs, only miR-10a was able to reduce PIK3CA levels. This finding was expanded to lung cancer cell lines of various histological subtypes and breast and colon cell lines most of which contained activating PIK3CA mutations. We consistently observed a 50% reduction in PIK3CA levels using miR-10a mimic and a two- to three-fold increase in PIK3CA when miR-10a levels were reduced. At the protein level, miR-10a mimic was able to reduce PI3K 50%, and this reduction was sufficient to completely inhibit downstream signaling. Phosphorylation of AKT atThr308, which is catalyzed by PDK1, was completely lost. This resulted in the loss of phosphorylation of mTOR at Ser2448, which is directly phosphorylated by AKT. Reduced activation of mTOR further inhibited signaling as loss of phosphorylation at AKT Ser473 was also observed. Our mRNA results demonstrated that loss of miR-10a would increase both PIK3CA and PI3K levels we observed a larger increase in PI3K then was observed with PIK3CA, this resulted in dramatic pathway activation determined by the increase in AKT Ser473 phosphorylation. To confirm that miR-10a was in fact directly regulating PI3K levels we cloned the entire 3'UTR of PIK3CA into the pMIR-Glo construct. Consistent with our previous findings miR-10a manipulations were able to change luciferase levels in the opposite direction and we were able to rescue this effect by

mutating several base pairs in the seed sequence. Collectively, these results demonstrate that miR-10a directly regulates PI3K levels and is sufficient to inhibit the PI3K/AKT/mTOR pathway.

Activation of the PI3K pathway has been implicated in resistance to targeted EGFR and HER2, radiation and chemotherapy (Mikhail Krasilnikov1 1999, West, Sianna Castillo et al. 2002). It is therefore unsurprising that upon inhibiting PI3K using a siRNA, shRNA, small molecule or miR-10a mimic we were able to sensitize NSCLC to paclitaxel treatment. While we did achieve sensitivity to paclitaxel treatment using various inhibitors of PI3K, we were never able to achieve an effect as large as that observed with over-expression of miR-10a, suggesting that co-reduction of other miR-10a target genes must be contributing to paclitaxel sensitivity.

We had previously observed that miR-10a was able to modulate growth levels in several cell lines that were being tested for changes in cellular response to paclitaxel. Following use of a kinetic assay for growth rate, we observed significant growth inhibitory effects when cells were treated with miR-10a mimic. miR-10a was as efficient as the toxic control at inhibiting NSCLC growth rates, while inhibiting miR-10a was able to accelerate growth rate. Interestingly, loss of miR-10b inhibited growth in H460 cells. miR-10b is expressed at very low levels, suggesting that low levels of miR-10b are selected for during tumorigenesis. Expanding on our short-term assay, we moved to the longer-term colony formation and again observed that miR-10a was able to influence growth in the opposite direction; high miR-10a inhibited colony formation and loss of miR-10a induced colony formation. We were able to confirm the growth inhibitory effects of

miR-10a using a stable expression vector. Only a five-fold increase in miR-10a was able to drastically affect colony formation; the observed growth inhibitory effect of miR-10a was a result of its ability to induce apoptosis. Collectively these finding suggest that miR-10a is an important mediator of growth rate in NCSCLC.

Finally, we were able to show that miR-10a also indirectly regulates PI3K through regulation of GATA6, and that GATA6 is important in NSCLC cellular survival. While GATA6 is expressed at relatively low levels across our panel of cell lines, it was the only GATA family member that showed a positive correlation with PIK3CA expression. Furthermore, it appears that GATA6 and PI3K act in a regulatory feedback loop. Additionally, we discovered that GATA6 expression is important in several cell lines among the NSCLC panel. We tested stable loss in H460, H2009, HCC827, H157, H1975, H1650 and H1155 cell lines; in each cell line following GATA6 loss there was a large reduction in cellular viability, as shown by the inability to form colonies *in vitro*. However, we did not observe any change in response to paclitaxel following GATA6 loss.

In contrast to our findings, a recent report indicated that GATA6 is a mediator of metastasis in adenocarcinoma (Cheung, Zhao et al. 2013, Cheung, Zhao et al. 2013). This would predict that … However, we were unable to reproduce these results and consistently found that loss of GATA6 inhibited colony formation and inhibited cellular growth. Additionally, GATA6 has been shown to activate vascular cell adhesion molecule-1, VCAM1. This interaction is inhibited by PTEN, in line with recent reports of PTEN nuclear function (Shen, Balajee et al. 2007, Tsoyi, Jang et al. 2010). Finally, VCAM1 is known to activate the PI3K/AKT pathway,

supporting our finding of PI3K regulation of GATA6 in a feed-forward system (Chen, Zhang et al. 2011) . Furthermore, our finding of GATA6 regulation of PI3K and the importance of PI3K in cellular metabolism was independently confirmed. The GATA6 expression signature was associated with mitochondrial activities connected to cellular oxidative phosphorylation (Kwei, Bashyam et al. 2008). Interestingly, GATA6 expression was positively correlated with that of ALDH1A1. ALDH+ cells are presumed to be lung cancer stem cells and show increased clonogenicity and tumorigenicity (Sullivan, Spinola et al. 2010). Collectively, these results demonstrate the importance of GATA6 in NSCLC. One potential explanation for the dramatic disagreement of phenotypes is that while GATA6 is important for the bulk of the population of cells, the subset that is able to survive GATA6 loss or do not express GATA6 is more metastatic. Additionally, the invasive and metastatic phenotype observed was dependent on both GATA6 and HOPX, as neither one alone had any significant effect(Cheung, Zhao et al. 2013) . However, further testing of this theory is needed.

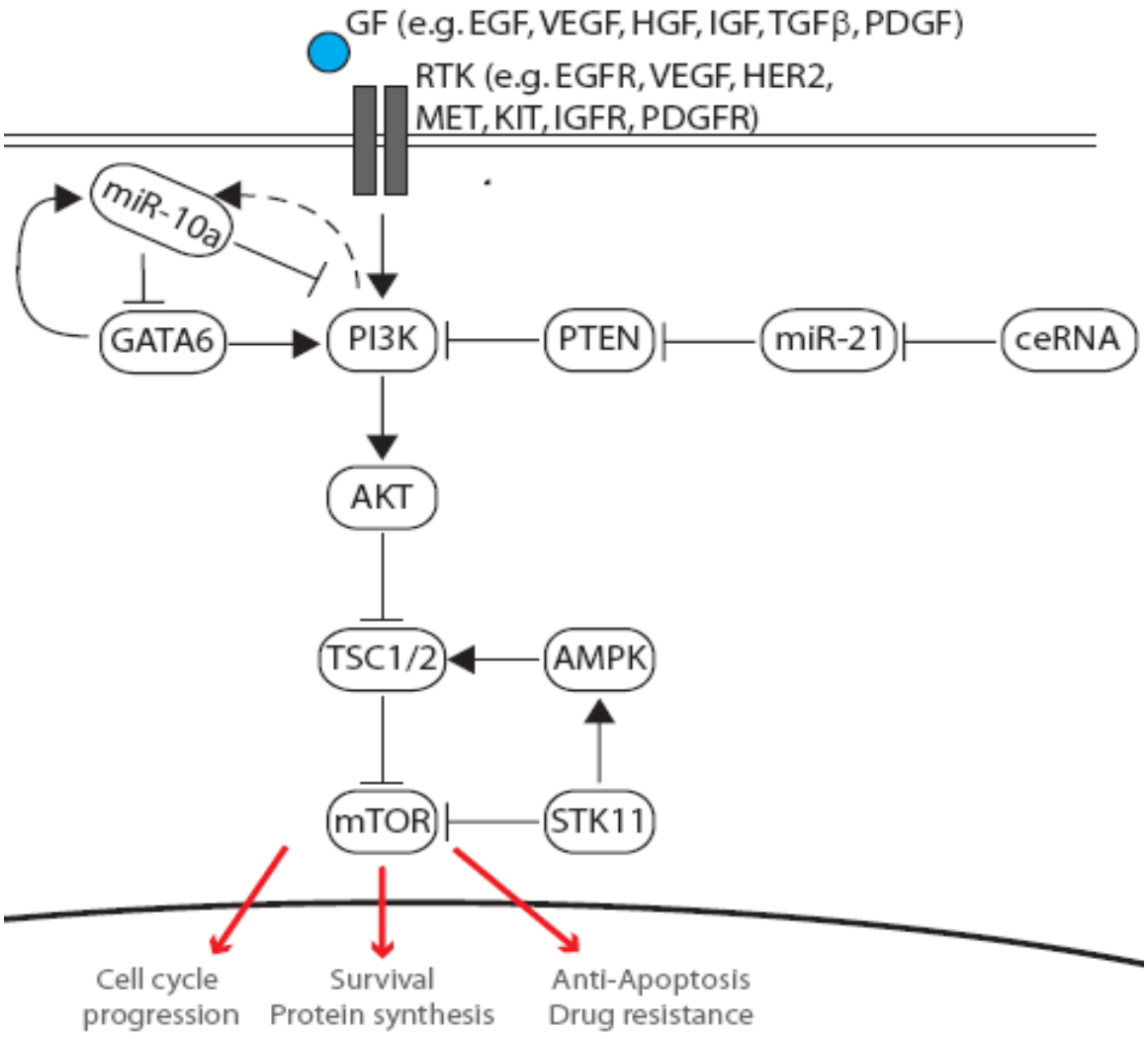

FIGURE 5.16 Summary of the PI3K/GATA6/miR-10a Pathway. miR-10a regulates both GATA6 and PI3K. GATA6, in turn, regulates PI3K expression. We have additional evidence to suggest that GATA6 regulates miR-10a levels.

CHAPTER SIX MIR-10A REGULATION OF NSCLC STEM CELLS THROUGH MODULATION OF THE WNT PATHWAY

6.1 Introduction

Lung cancer's high mortality rate is due to its remarkable ability to relapse despite complete disease regression. This suggests that there is a population of cells that is inherently resistant to treatment, phenotypically distinct from the bulk of the tumor mass, that gives rise to the heterogeneity observed in histological samples. This is the basis of the cancer stem cell model. Akin to organogenesis, cancer has a hierarchy, which consists of ultimately non-tumorgenic, terminally differentiated cells, and a minority population of progenitor "tumor-initiating" cells. This was first described over 30 years ago with only a small fraction of NSCLC patient tumor samples possessed the ability to form tumors in mice (Salk, Fox et al. 2010, Sullivan, Minna et al. 2010). Since their identification, the stem cell fraction can be enriched using basic flow cytometry based on the presence of cell surface markers or metabolic enzymes.

CD133 was used to identify the stem cell population of brain tumor samples and has since been expanded to include melanoma, breast, prostate and lung cancers (Sheila K. Singh 2003, Alamgeer, Peacock et al. 2013). The CD133+ fraction of cultured cells exhibit resistance to platinum-based therapies and is enriched for genes known to play a role in metastasis (Levina, Marrangoni et al. 2008). However, several reports have described that CD133- cells can give rise

to CD133+ cells and that both cell types can give rise to tumors and produce metastatic lesions (Wang, Sakariassen et al. 2008). Efforts devoted to exploring additional markers uncovered aldehyde dehydrogenase (ALDH) activity as a marker for stem cell populations. In NSCLC, the ALDH+ cell fraction demonstrates self-renewal, serial transplantation, resistance to therapy, and increased tumorigenicity (Liu, Yuan et al. 2006, Sullivan, Spinola et al. 2010).

The ALDH family is composed of 19 distinct isozymes that catalyze the oxidation of aldehydes generated from cellular metabolism or detoxification (Volinia, Calin et al. 2006) (Calin et al. 2006, Stark, Brennecke et al. 2005, Chin, Pomerantz et al. 1998, Kim, Yeo et al. 2012) to maintain a state of stemness. Cells that are enriched in ALDH activity have been shown to be more resistant to platinum treatment and exhibit gene expression profiles suggesting enhanced metastatic potential. Early work on ALDH enzymes in the hematopoietic system found that they maintain a state of undifferentiation through the oxidation of retinol to retinoic acid (Chute, Muramoto et al. 2006). Increased ALDH expression and activity have been found in stem cell populations of tumor of the brain, breast, and certain leukemia's (William Matsui 2003, Chute, Muramoto et al. 2006). Two isoforms, ALDH1A1 and ALDH3A1 were reported to be highly expressed in NSCLC cell lines, it was later discovered that ALDH protein was elevated in NSCLC patients samples with a history of smoking (Alamgeer, Peacock et al. 2013). Finally, the ALDH+ fraction of NSCLC cell lines is more clonogenic and tumorigenic then their ALDH- counterparts, and high ALDH1A1 levels are indicative of reduced overall patient survival (Sullivan, Spinola et al. 2010).

Differential gene expression analysis between ALDH+ and ALDH- cells revealed that ALDH1A3 is most highly expressed in ALDH+ cells and completely absent in ALDH- cells (Figures 6.1 & 6.2A). It was experimentally proven that ALDH1A3 is the predominant isoform among NSCLC cell lines as loss of expression of ALDH1A3 completely removed the ALDH+ cell population, e (Figure 6.2B). Finally, loss of ALDH1A3 expression inhibits growth both *in vitro* and *in vivo* (Figure 6.3A-B).

While improved understanding of the signaling pathways maintaining cancer stem cells has led to novel therapeutic approaches and improved clinical responses (Takebe, Harris et al. 2011), , the role of miRNAs in the regulation of cancer stem cells has not been explored. Our previous work on miR-10a as a modulator of paclitaxel response through its regulation of the PI3K pathway both directly and indirectly through interaction with GATA6 has demonstrated its importance in lung cancer.miR-10a is a miRNA located in the HOX cluster of genes, which is known to be important for the development of the body plane along the anterior-posterior axis active during embryogenesis (Yekta, Shih et al. 2004). Additionally, miR-10a is induced by all-trans-retinoic acid (ATRA), clinically used to induce differentiation in neuroblastoma and acute promyelocytic leukemia (Agirre, Jimenez-Velasco et al. 2008, Foley, Bray et al. 2011). Given miR-10a location in a developmental gene cluster and its induction by an inducer of differentiation we hypothesize that miR-10a may be critical for the differentiation of lung cancer stem cells into terminally differentiated, non-dividing cells.

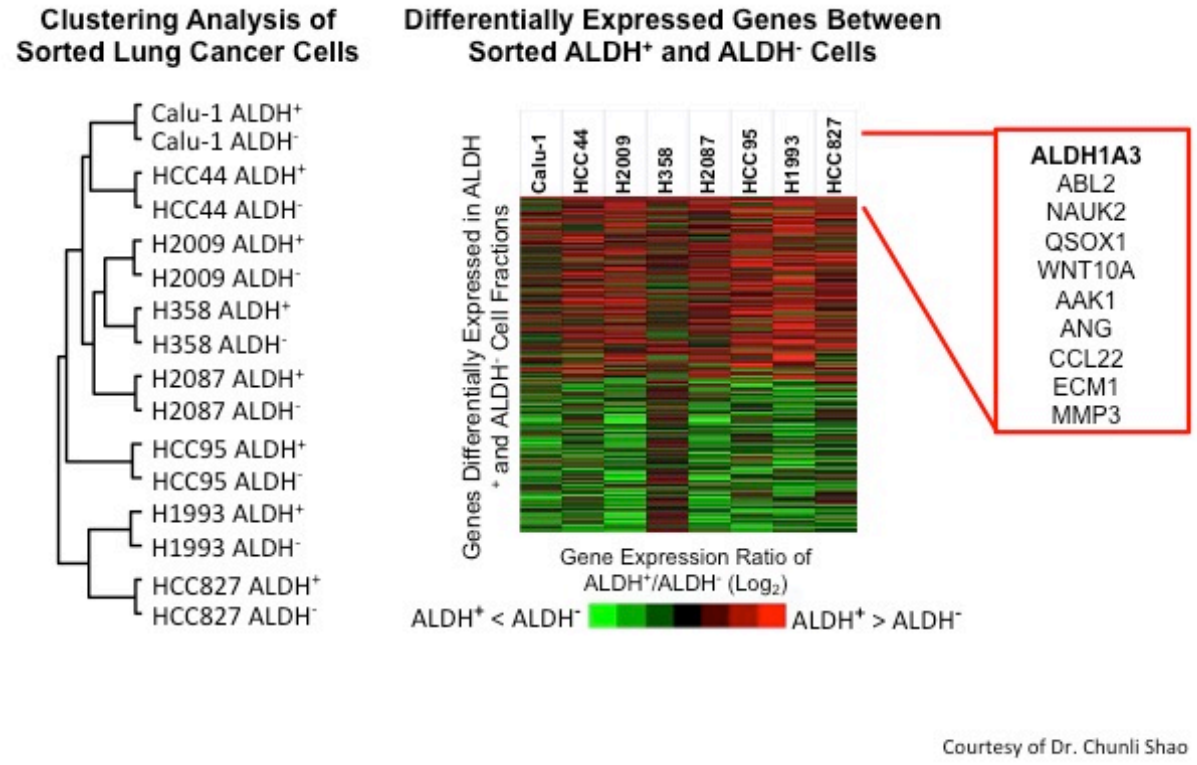

Courtesy of Dr. Chunli Shao

FIGURE 6.1 ALDH1A3 Is The Major Isozyme Responsible for Elevated ALDH Activity. Unsupervised clustering analysis of sorted cell gene expression profiles indicates limited common gene differences between sorted cell populations in different cell lines. ALDH1A3 was most commonly upregulated in $ALDH^+$ NSCLC cells.

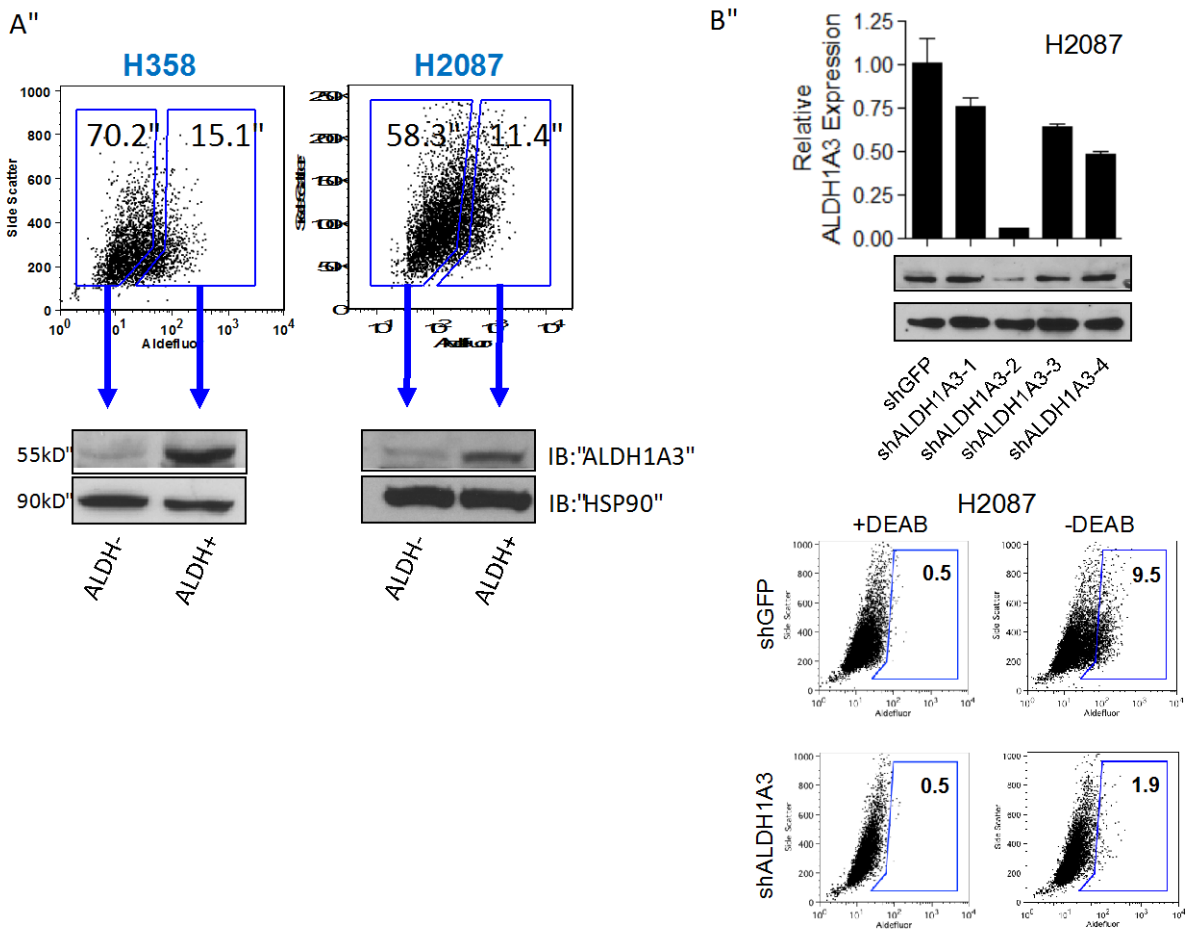

FIGURE 6.2 ALDH1A3 Protein is Enriched in ALDH+ Cells and is Responsible for the ALDH+ Population of Cells. A. ALDH1A3 protein is enriched in ALDH+ cell fraction. **B.** shRNA mediated loss of ALDH1A3 reduces the ALDH+ population. Courtesy of Dr. Chunli Shao.

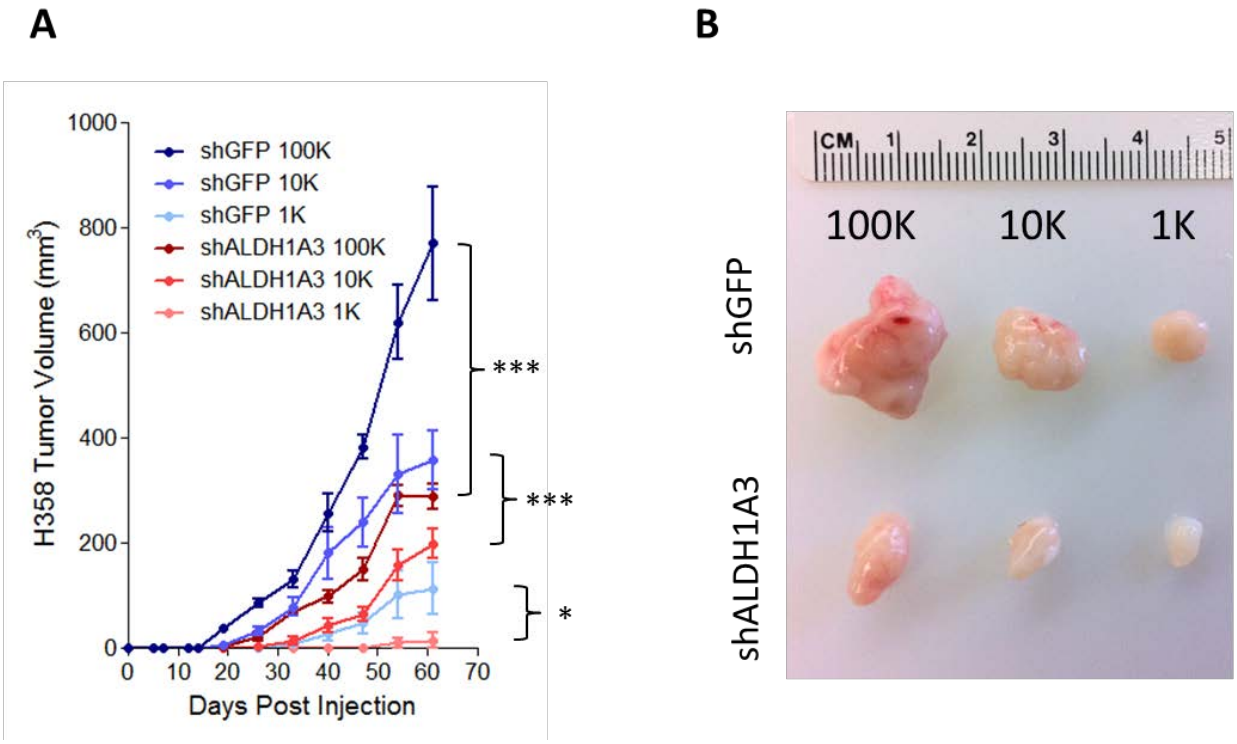

FIGURE 6.3 Loss of ALDH1A3 Inhibits Tumor Formation in Vivo. A&B Xenograft growth from limiting dilutions of stably transfected H358-shALDH1A3 cells. ***, p = 0.0001, n = 5. Courtesy of Dr. Chunli Shao.

6.2 Results

6.2.1Regulation of ALDH1A3 Levels and Activity by miR-10a

To discover novel pathways regulated by miR-10a in NSCLC, we performed expression profiling on H460 cells which had been transiently treated with miR-10a mimic. Among the most down-regulated genes was ALDH1A3 (Figure 6.4A), which is of particular interest given that loss of expression in NSCLC abolishes ALDH activity and inhibits tumor formation in mice. To confirm this finding, we validated the array results using taq-man probe for ALDH1A3 and expanded our finding across several cell lines (Figure 6.4B). However, H460 cells have a very small ALDH+ population (data not shown). Thus, to increase the signal space we used H2009 cells, which have a larger ALDH+ population and showed reduction of ALDH1A3 mRNA and protein upon miR-10a treatment (Figure 6.4B-D). To confirm that loss of ALDH1A3 mRNA and protein resulted in functional changes we employed the Aldefluor assay, which has been used to identify ALDH+ cells in various tumor types (Christophe Ginestier1, Julie Dutcher1 et al. , Ginestier, Hur et al. 2007, Huang, Hynes et al. 2009) and observed a significant reduction in ALDH+ cells treated with miR-10a mimic (Figure 6.4E). Taken together, these findings suggest that miR-10a regulates lung cancer stem cells (CSC) as defined by the ALDH+ sub-population.

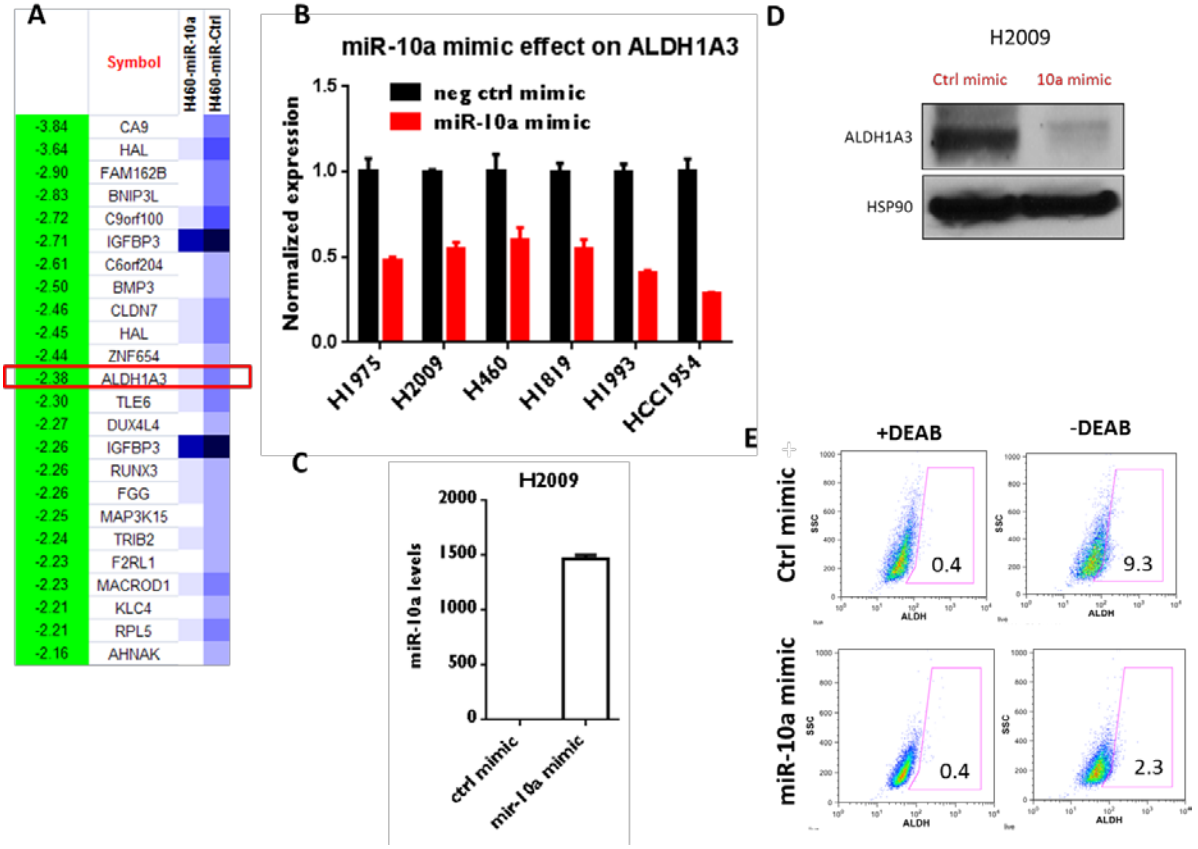

FIGURE 6.4 miR-10a Reduces ALDH1A3 Levels and Activity in NSCLC. A. Differential gene expression (log fold change) following 72 h transient transfection with 20 nM miR-10a mimic and control mimic, measured using Illumina HumanHT-V12 v4 arrays. **B.** ALDH1A3 levels in several cell lines treated with either miR-10a mimic or negative control mimic, measured by qRT-PCR. **C.** miR-10a levels in H2009 cells following transfection with miR-10a mimic. **D.** ALDH1A3 protein levels after miR-10a treatment as measured by western blot. **E.** Transfection of H2009 cells with 20 nM miR-10a mimic for 48 h resulted in a ~4-fold loss of ALDH activity, as measured byAldefluor assay. DEAB, an inhibitor of ALDH, is used for gating..

6.2.2 Inhibition of Cellular Growth Rate and Induction of Apoptosis by Increased miR-10a Levels

Although the above findings demonstrate that miR-10a down-regulates ALDH1A3 levels and therefore reduces the number of ALDH+ cells, it is unclear what effect miR-10a would have on growth rate *in vitro* and *in vivo*. We have previously shown that miR-10a does in fact inhibit growth in H460 and in H1155 cells. However, cell lines H460 and H1155 are both derived from large cell tumors and might not accurately represent all subtypes of NSCLC. To address this, we measured the growth rate of transiently transfected H2009 cells (derived from lung adenocarcinoma) over several days and observed a significant reduction in growth rate (Figure 6.5A-B). As expected, increasing miR-10a levels resulted in a significant decrease in growth rate. The mechanism, by which this decrease occurred, however, was unclear. To further explore the issue of growth rate inhibition, we looked at induction of apoptosis and observed an increase in apoptosis using both western blot for cleaved PARP and Caspase 3/7 activity as proxies for induction of apoptosis (Figure 6.5C and D).

To further validate miR-10a as an inhibitor of growth rate, we moved to the use of a stable overexpression construct. Although the construct was unable to achieve as high an intracellular level of miR-10a as transient transfection with a miR-10a mimic (Figure 6.4C & Figure 6.6A), we still observed reduction of ALDH1A3 mRNA and protein as measured by qRT-PCR and western blot, and inhibition of growth inhibition as measured by colony formation assay (Figure 6.6 B-D). To assess increased miR-10a levels *in vivo*, stably transfected cells were injected subcutaneously into NOD/SCID mice and a significant reduction in tumor growth was

observed (Figure 6.7). Collectively, these results indicated that miR-10a is a potent inhibitor of cancer cell growth both *in vitro* and *in vivo*.

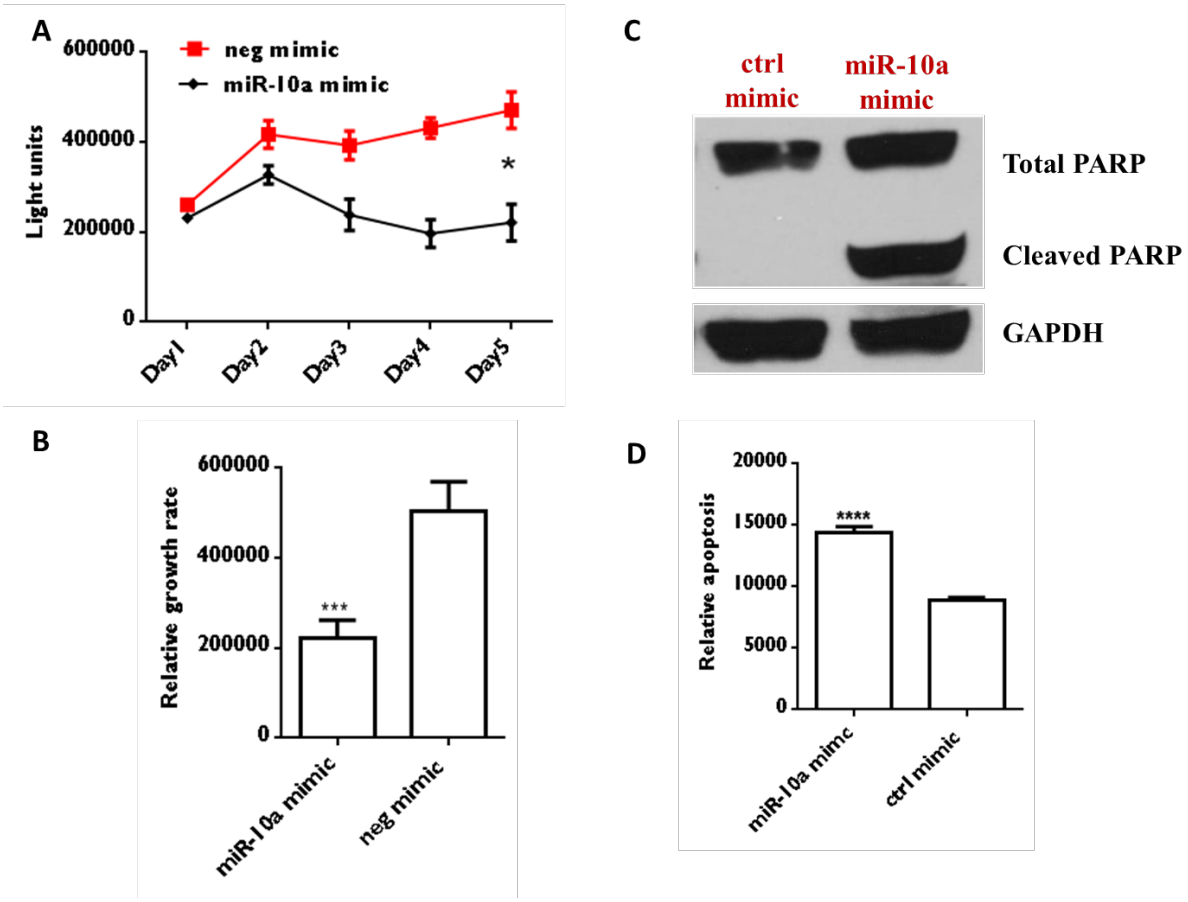

FIGURE 6.5 miR-10a Inhibits Growth and Induces Apoptosis. A. Growth rate for cells transfected with miR-10a mimic or negative control mimic, quantified using Promega Cell Titer Glo. *, p = 0.0225 by two-tailed t-test with n=3. **B.** Growth after five days for cells transfected with miR-10a mimic or negative control mimic. ***, p = 0.004 by two-tailed t-test with n=3. **C.** Increased apoptosis in cells treated with miR-10a mimic for 72 h as measured by western blot. **D.** Apoptosis 72 h after transfection of miR-10a mimic or negative control mimic, as measured by Capase3/7 Glo , ****, p < 0.0001 with n=4.

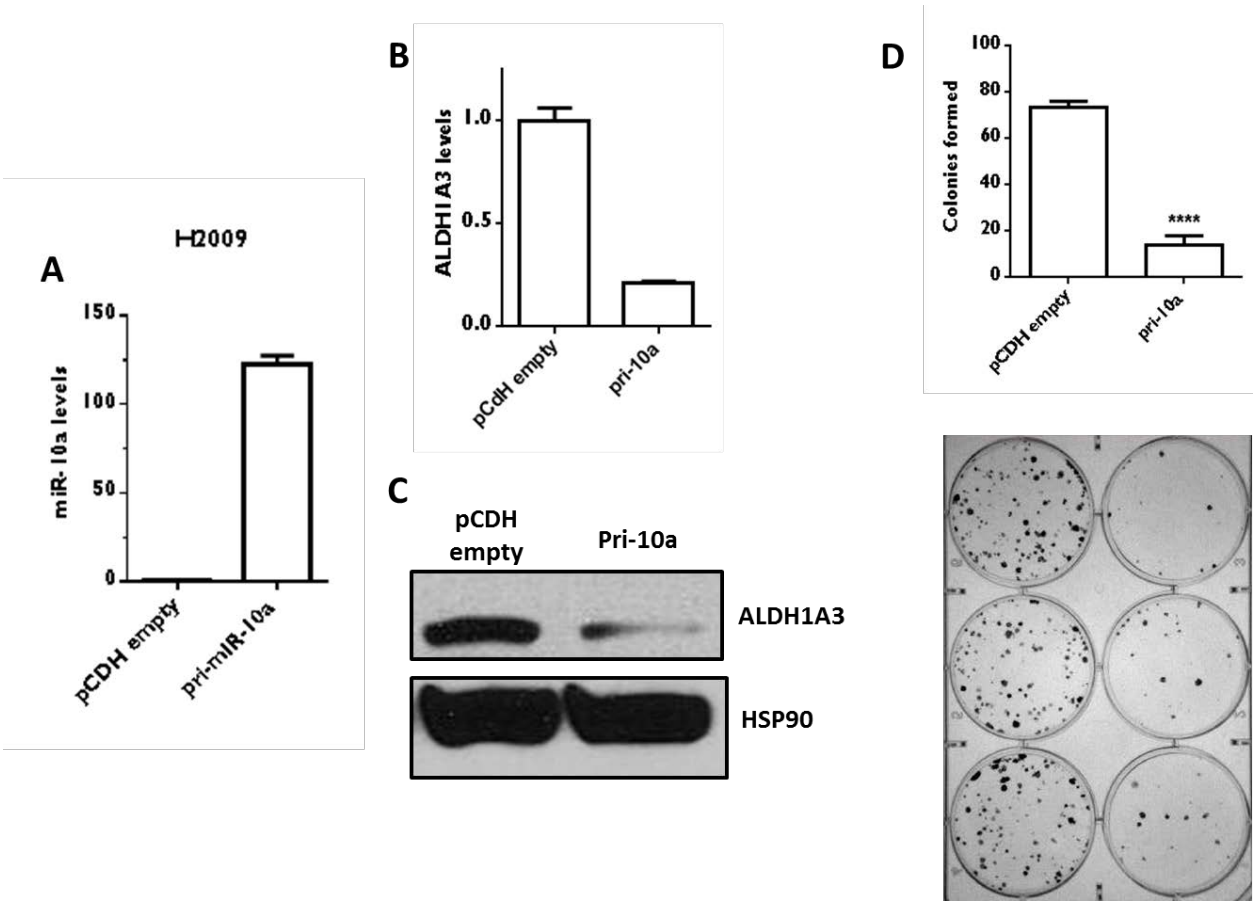

Figure 6.6 Stable Overexpression of miR-10a Reduces ALDH1A3 Protein and Inhibits Colony Formation. **A.** Stable overexpression of miR-10a led to a 130-fold increase in miR-10a levels. **B.** Reduction of ALDH1A3 mRNA in H2009 cells stably over-expressing miR-10a. **C.** Loss of ALDH1A3 protein in cells stably over-expressing miR-10a as assessed by western blot. **D.** Four-fold reduction in the ability of cells stably over-expressing miR-10a to form colonies. ****, $p < 0.0001$.

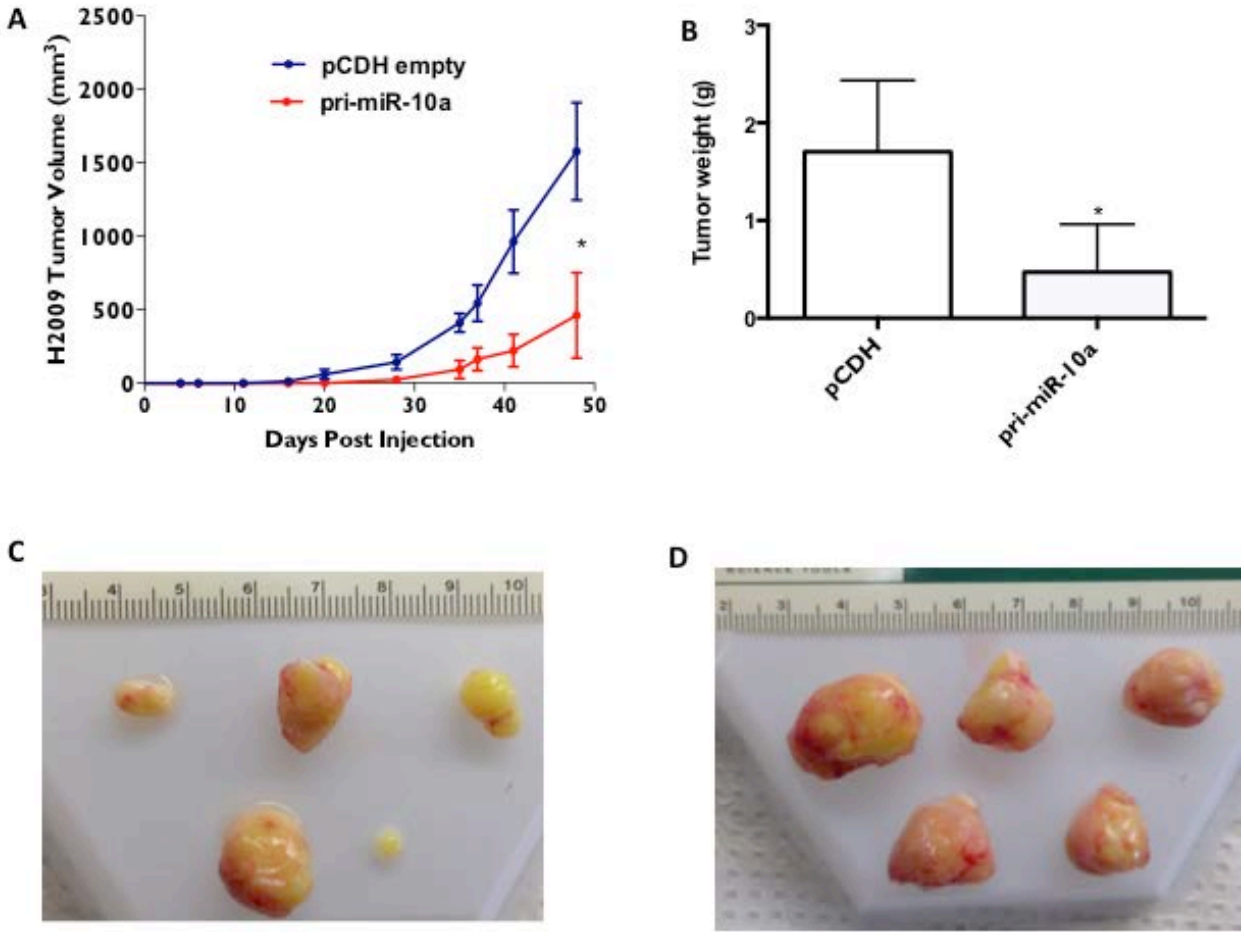

Figure 6.7 Stable Overexpression of miR-10a Inhibits in vivo Tumor Growth. A. Tumor volumes. Stable over-expression of miR-10a inhibited tumor growth in vivo. *, p = 0.0353, n=5. **B.** Tumor weights. Average weight for miR-10a over-expressing tumors was 0.4720 g ± 0.218 g; average weight for controls was 1.704 g ± 0.3278 g. *, p = 0.0141 as assessed by two-tailed t-test with n=5. **C.** pri-miR-10a tumors. **D.** pCDH control tumors. Ruler measurements are in cm.

6.2.3 miR-10a Inhibition of Growth Rate is Specific to Cancer Cells

To ensure that the observed induction of apoptosis and growth inhibition by miR-10a were specific to cancer cells, we used immortalized human bronchial epithelial cells (HBEC) to model normal lung cellular biology (Ramirez, Shelley Sheridan et al. 2004). We were able to obtain comparable induction of miR-10a, but did not observe a significant change in ALDH1A3 levels in HBEC3-KT cells (Figure 6.8A-C). Additionally, miR-10a had no effect on the colony forming ability of our normal model (Figure 6.8D). In total, these results suggest that miR-10a is selectively lethal in cancer cells.

6.2.4 miR-10a Regulates WNT and NOTCH Pathways by Targeting DVL3

We next explored how miR-10a is regulating ALDH+ cell population levels. Recent findings have shown that a large fraction of miRNA regulation is non-canonical; miR-10a has been shown to influence gene transcription in this manner (Orom, Nielsen et al. 2008, Helwak, Kudla et al. 2013). Comprehensive analysis of ALDH1A3 mature mRNA did not reveal any conserved miR-10a binding sites, indicating that miR-10a regulation of ALDH1A3 is through indirect interaction.

Stem cell self-renewal is a fundamental process that is tightly regulated and often involved in cancer initiation and progression. Three widely studied pathways central to self-renewal are Hedgehog, Notch, and WNT. The Hedgehog pathway is involved in regulation of

proliferation, migration and differentiation of progenitor cells and is not active in adult tissue (Merchant and Matsui 2010). Notch is frequently involved in cell fate determination of the proximal and distal epithelial cell fates of the normal lung (Pannuti, Foreman et al. 2010). WNT are a family of secreted glycoproteins that regulate proliferation, survival, migration and polarity, and self-renewal (Reya and Clevers 2005). Work in our lab and other labs has shown the importance of the NOTCH and WNT pathways on the maintenance of ALDH+ cells (Reya and Clevers 2005, Androutsellis-Theotokis, Leker et al. 2006, Sullivan, Spinola et al. 2010); however, little is known about Hedgehog signaling in maintaining the ALDH+ cell fraction in NSCLC.

To test our whether miR-10a regulated the NOTCH, WNT or Hedgehog pathway; we evaluated downstream signaling components of each pathway as representation of miR-10a regulation. We observed significant downregulation of NOTCH and WNT pathways following miR-10a transfections; however, no change in Hedgehog signaling was observed (Figure 6.10A). Surveying target predictions for conserved miR-10a targets in the WNT and NOTCH pathways, we uncovered potential pathway regulation through Dishevelled 3 (DVL3) (Figure 6.10B).

Once the WNT glycoprotein is secreted, it binds to the Frizzled (Fz) receptor. This interaction then recruits the intracellular Dishevelled (DVL3) family of proteins. DVL directly interacts with the Fz receptor propagating the WNT signal allowing for the stabilization of beta-catenin, which then translocates to the nucleus activating downstream components (Clevers and Nusse 2012). There are three DVL family members — DVL1, DVL2 and DVL3 — that are

expressed in both embryonic and adult tissues. DVL3 has been found to be overexpressed in 75% of NSCLC tumor specimens. Inhibition of its expression using a siRNA in H1703, a NSCLC cell line known to have activated beta catenin, resulted in growth inhibition (Uematsu, Kanazawa et al. 2003). The docking of DVL3 to Fz occurs through interaction of the PDZ domain of DVL and is currently being explored in the context of targeted therapy (Uematsu, Kanazawa et al. 2003, Grandy, Shan et al. 2009). Given the potential importance of DVL3, we compared its expression in ALDH+ relative to ALDH- cells and saw increased levels of both DVL3 mRNA and protein in ALDH+ cells, while no significant difference in miR-10a levels was observed (Figure 6.10 C-E). Further supporting increased WNT signaling in the ALDH+ cell fraction, our differential gene expression analysis showed that WNT10a is highly expressed in ALDH+ cells compared to ALDH- cells (Figure 6.1).

To test our hypothesis that miR-10a depletion of ALDH+ cell population is dependent on DVL3, we measured DVL3 mRNA and protein following transfection of miR-10a mimic. Both mRNA and protein were dramatically reduced following miR-10a treatment (Figure 6.11 A-B). To confirm a direct interaction, we cloned a large portion of the DVL3 3'UTR downstream of the luciferase CDS and observed a substantial reduction in luciferase activity in cells co-transfected with miR-10a, a reduction that we were able to rescue through mutagenesis of the seed sequence (Figure 6.11 C-D). Taken together, these results suggest that miR-10a directly regulates DVL3 expression.

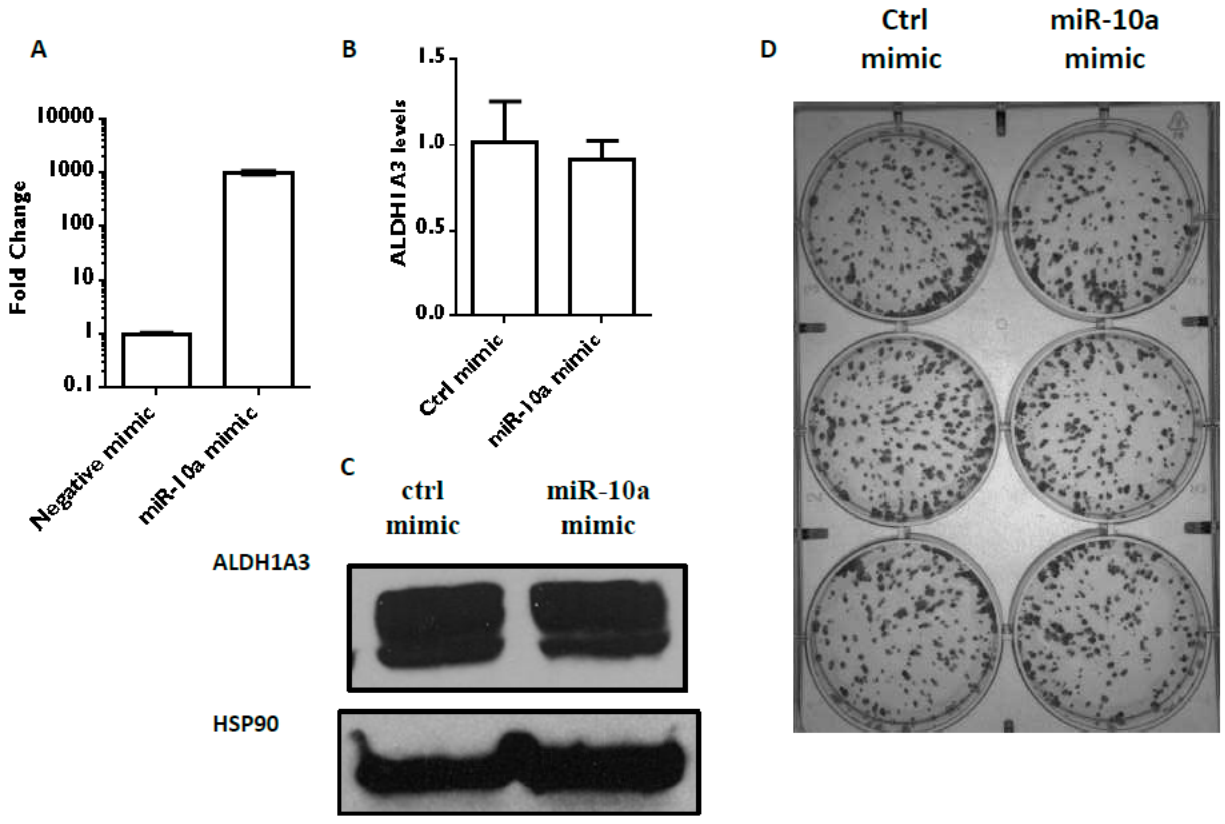

FIGURE 6.8 miR-10a Does Not Affect ALDH1A3 Levels or Colony Formation Ability in HBEC3-KT. A. Induction of miR-10a following transfection in H2009 cells. **B.** miR-10a had no effect on ALDH1A3 mRNA levels. **C.** miR-10a did not affect ALDH1A3 protein levels. **D.** Over expression of miR-10a had no effect on colony formation.

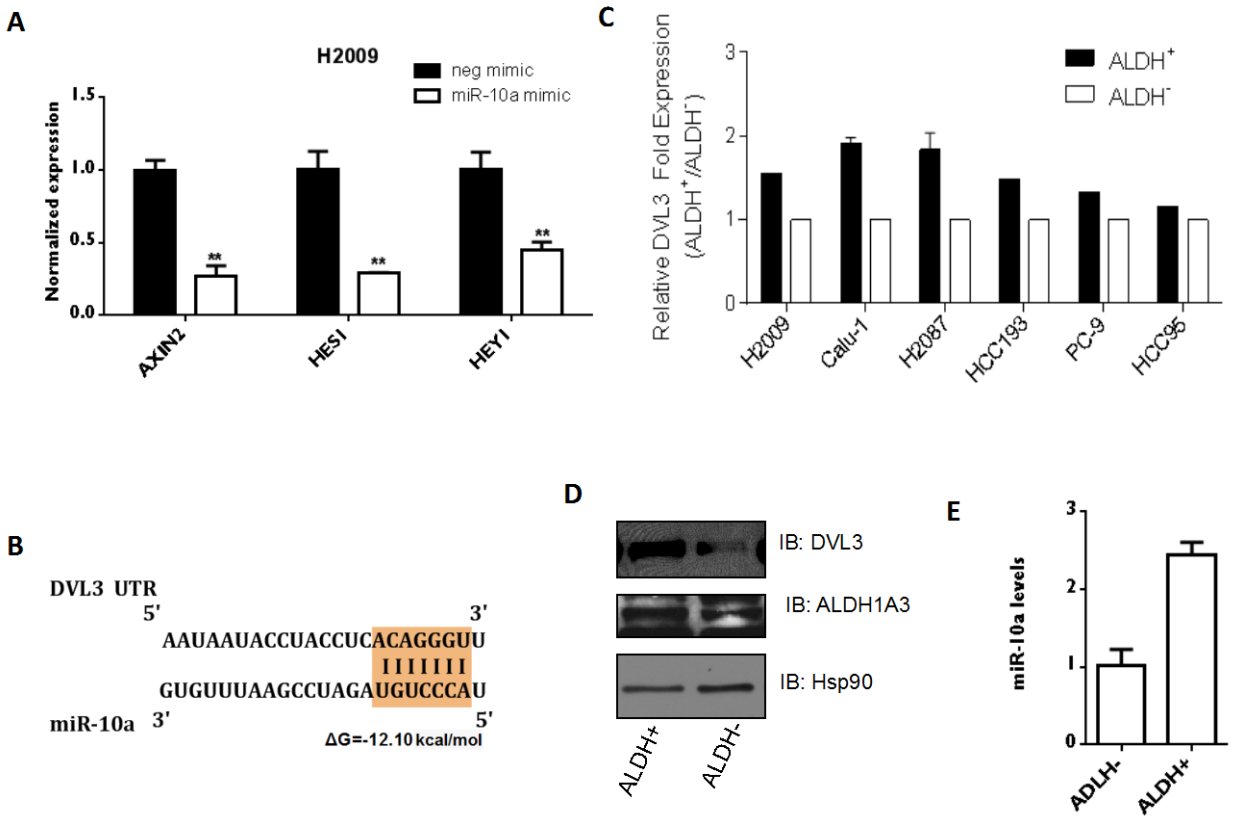

FIGURE 6.9 Induction of miR-10a Leads to a Reduction of WNT and NOTCH Signaling Through Potential Interaction with DVL3. A. Transfection of miR-10a mimic resulted in a ~75% reduction in AXIN2, an ~80% reduction in HES1, and a ~45% reduction in HEY1. Axin **, p = 0.0088; HES1 **, p = 0.0045; HEY1 **, p = 0.0019; by two- tailed t-test with n=3. **B.** Sequence alignment of miR-10a and the DVL3 3'UTR. The highlighted region is the seed sequence. Binding energy of the interaction is shown below the alignment. **C.** DVL3 levels in ALDH+ cells compared to ALDH- cells. **D.** DVL3 protein is enriched in ALDH+ cells relative to ALDH- cells, as measured by western blot. **E.** miR-10a levels are equivalent in both populations of cells.

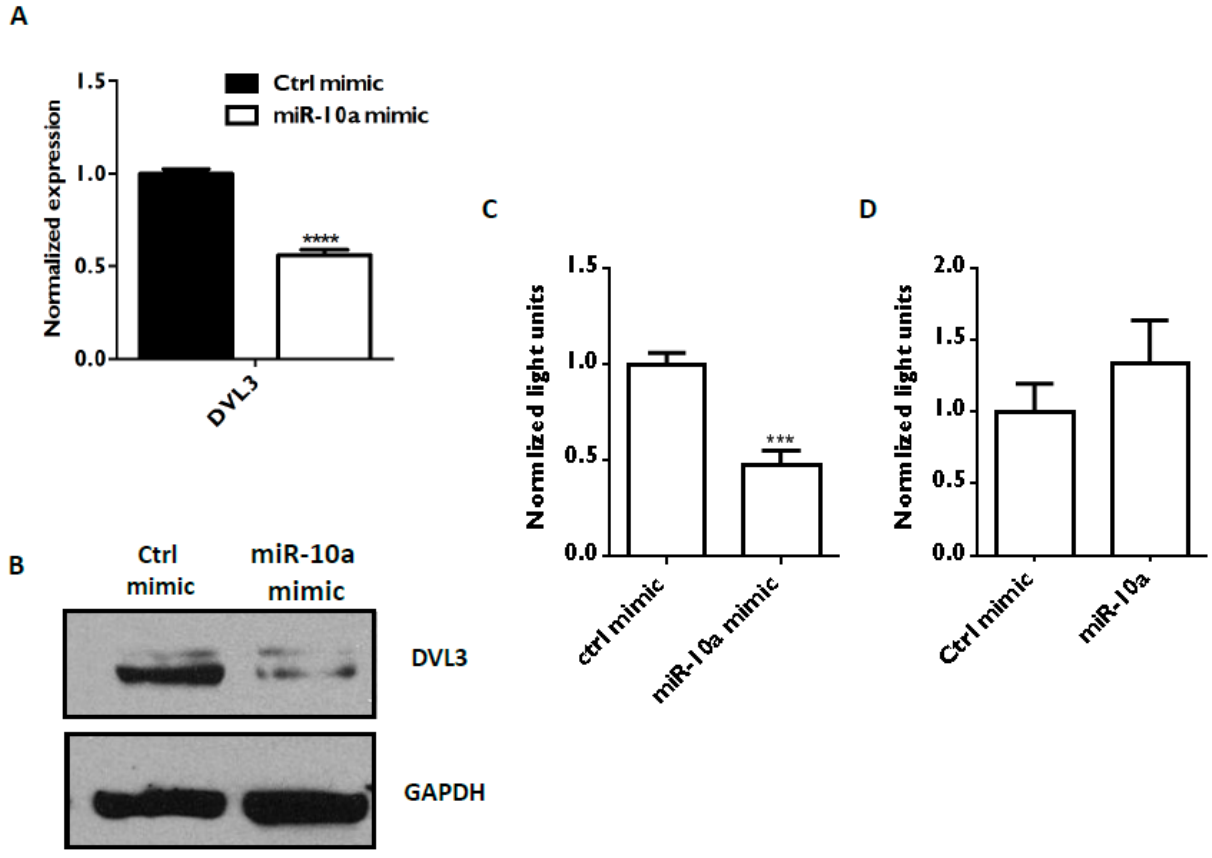

Figure 6.10 miR-10a Directly Regulates DVL3. A. DVL3 is reduced ~40% following miR-10a transfection.. $p < 0.0001$ by two-tailed t-test with n=3. **B.** Overexpression of miR-10a reduces DVL3 protein levels. **C.** miR-10a mimic interacts directly and specifically with the DVL3 3'UTR as shown by the decrease in luciferase activity.. ***, $p = 0.0003$, by unpaired two-tailed t-test with n=3. **D.** Ablating the miR-10a target site in the reporter construct abrogates the interaction between miR-10a and the DVL3 3'UTR.

6.2.5 DVL3 Regulates ALDH+ Cells

Although the above results describe miR-10a regulation of DVL3 and indicate that WNT signaling is more active in the ALDH+ cell fraction, we have not yet addressed the extent to which DVL3 and other miR-10a targets are important in the regulation of ALDH1A3 and ALDH+ cells. To do so, we examined several miR-10a targets — including DVL3, GATA6, PI3K, and NcoR2 — as regulators of ALDH1A3 levels using siRNAs. NCOR2 is a transcriptional co-repressor whose activity is enhanced following Notch and Sonic hedgehog activation and is enriched in CD133+ glioma stem cells. It has been shown that NCOR2is regulated by miR-10a and unpublished work in our lab has demonstrated NCOR2 importance in NSCLC cell growth (Ulasov, Nandi et al. 2011). Not only has GATA6 has been shown to bind the promoter of Fz-2 receptor and activate gene expression; it has also been shown to regulate WNT7b expression in the lung (Weidenfeld, Shu et al. 2002). Finally, PI3K activation inhibits glycogen synthase kinase 3 β (GSK3β), which stabilizes the beta-catenin destruction complex. We also evaluated the combination of all four miR-10a target genes, however only loss of DVL3 leads to a consistent reduction of ALDH+ cells (Figure 6.11 A-B). Further experimental refinement and optimization through manipulation of seeding number and culture time led to a 4-fold reduction in the ALDH+ cell fraction following siRNA-mediated loss of DVL3 expression (Figure 6.12A-B). To confirm that the loss of ALDH+ cells was not an off-target effect we used a stable shRNA targeting DVL3 and observed similar results (Figure 6.13 A-B). Finally, we confirmed that the reduction in ALDH+ cells was due to a loss of ALDH1A3, and that knockdown of DVL3 by both siRNA and shRNA resulted in a significant reduction in

ALDH1A3 protein levels (Figure 6.12B & Figure 6.13B). Collectively, these results demonstrate that loss of DLV3 expression reduces the ALDH+ cell fraction.

Condition	10/18/12	10/18/12	10/25/12	10/25/12
	DEAB	ALDH+	DEAB	ALDH+
Ctrl	0.45	4.73	0.46	4.66
siDVL3	0.43	1.88	0.4	3.13
siGATA6	0.43	11.3	0.47	6.35
siPIK3CA	0.47	4.73	0.44	18.9
siNCOR2	0.43	4.44	0.43	5.02
siCOMBO	0.46	5.31	0.41	7.25

Condition	% ALDH +	% ALDH +	Average	SD
Ctrl	**100**	**100**	**100.00**	
			49.44	
			196.99	
			1.49	**11.03**
siCOMBO	**113.32**	**162.86**	**138.09**	

Figure 6.11 Only Loss of DVL3 Affects the ALDH+ Cell Fraction. The top panel shows raw data collected at two separate time points. The bottom panel shows data normalized to a negative control oligo. ALDH activity was measured 72 h post transfection. DEAB was used for of gating,

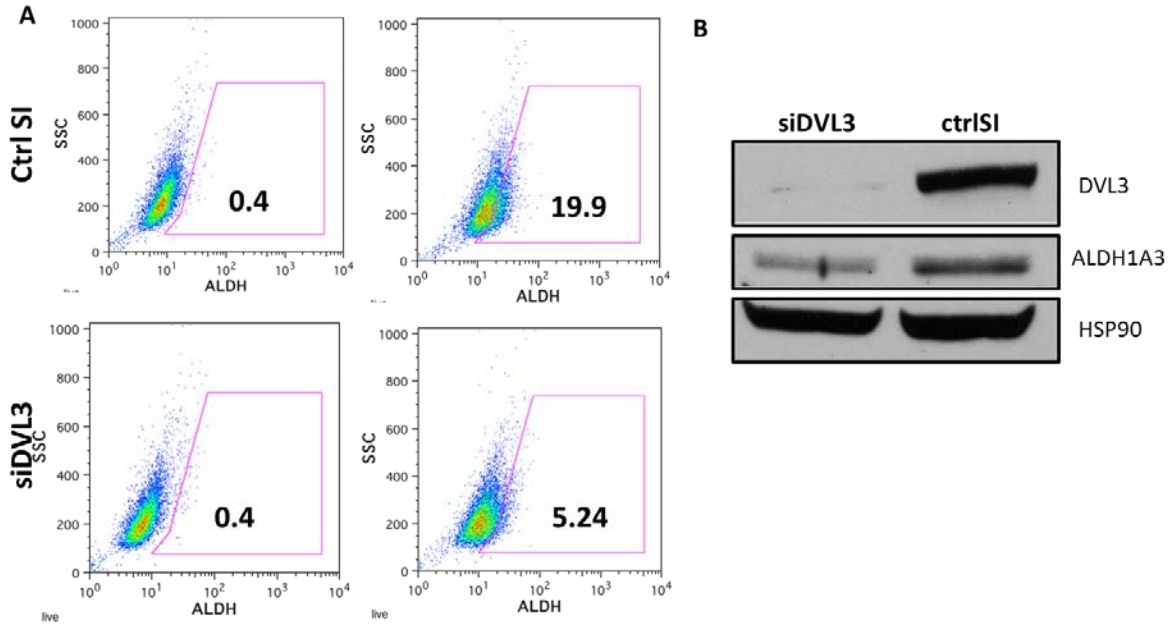

Figure 6.12 DVL3 Loss Reduces ALDH1A3 Protein Levels A. Loss of DVL3 expression leads to a four fold reduction of ALDH activity following. **B.** Loss of both DVL3 and ALDH1A3 protein following transfection with an siRNA against DVL3 relative to a negative control, confirmed by western blot.

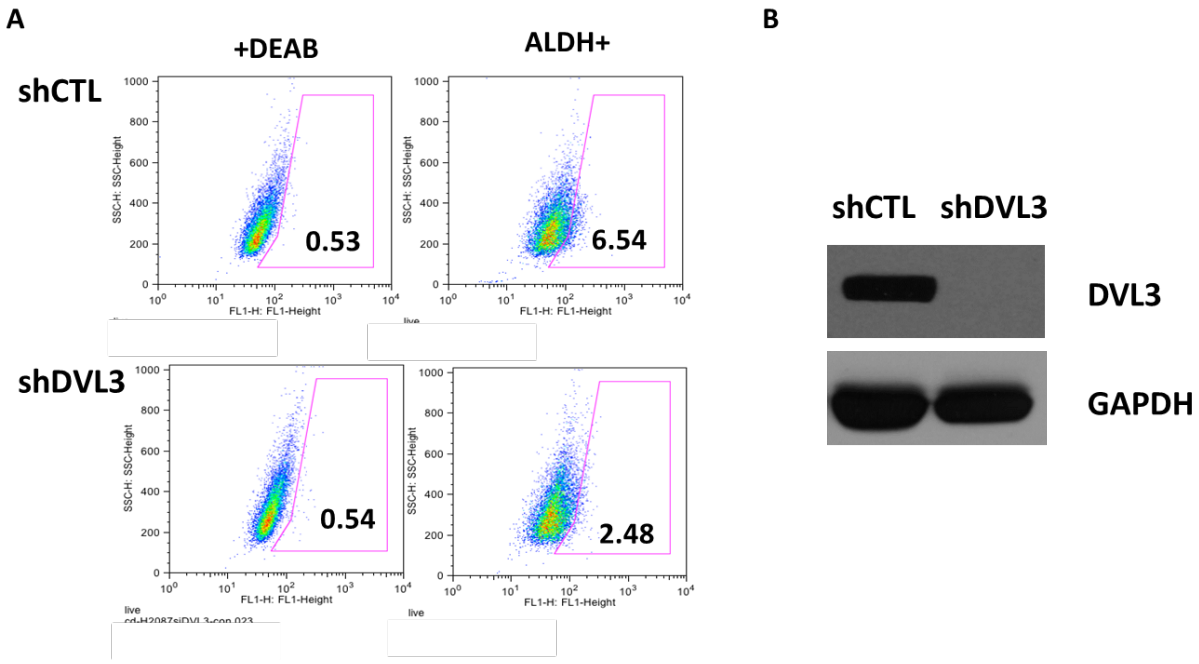

FIGURE 6.13 Stable Loss of DVL3 Reduces ALDH+ Cell Fraction A. Stable loss of DVL3 expression reduced ALDH+ cells by ~3-fold. **B.** Western blot confirmation of DVL3 loss.

6.2.6 DVL3 is Required for NSCLC Growth in Vitro and in Vivo.

Previous work in NSCLC has revealed growth inhibitory effects of DVL3 loss in H1703, a NSCLC cell line known to be dependent on WNT signaling. Previous work in our lab has shown that loss of ALDH1A3 inhibits tumor growth in vivo (Figure 6.3) and our above studies revealed DVL3 as a regulator of ALDH+ cells. However, it was unclear what phenotype loss of DVL3 would have both *in vitro* and *in vivo*. Transient loss of DVL3 led to only modest inhibition of growth (Figure 6.14A). However, a significant induction of apoptosis was observed 48 h post transfection (Figure 6.14B). Stable loss of DVL3 resulted in a significant reduction in colony formation ability (Figure 6.14C). While it appears that DVL3 is required for growth *in vitro*, it was unclear whether this was maintained *in vivo*. While control non-targeting shRNA cells led to robust tumor growth, DVL knockdown significantly inhibited tumor growth (Figure 6.14D). Loss of DVL3 in H2009 cells led to tumors being formed in only 3 out of 5 mice and at a much lower rate (Figure 6.13D). Collectively, these results indicate that DVL3 is crucial for maintaining the ALDH+ cell population and tumorigenesis.

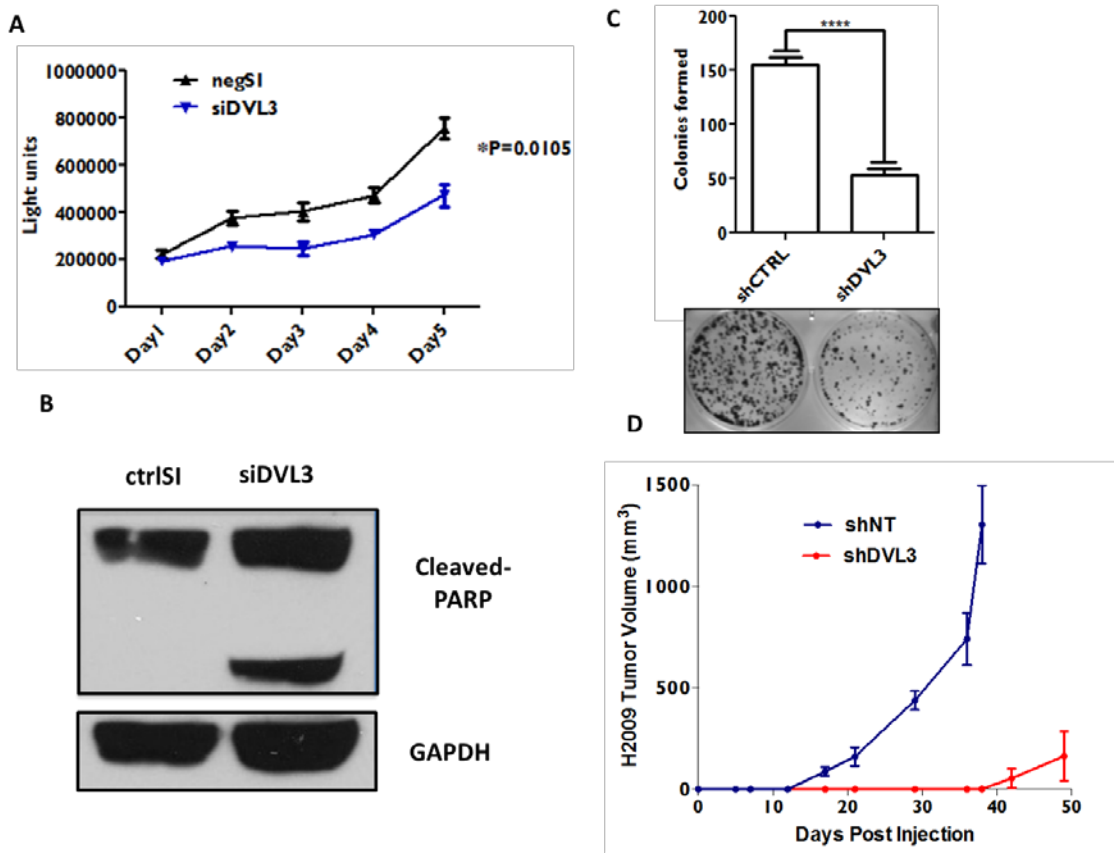

Figure 6.14 Loss of DVL3 Inhibits Growth Both In Vitro and In Vivo. **A.** Cells treated with 20 nM siDVL3 show growth reduction. *, $p = 0.0105$ by one-tailed t-test. **B.** H2009 cells transfected with siDVL3 for 72 h display an induction of apoptosis, shown by the presence of cleaved PARP by western blot. **C.** Stable loss of DVL3 leads to a 4-fold reduction in the ability to form colonies in vitro. ****, $p < 0.0001$. **D.** Loss of DVL3 inhibits tumor growth *in vivo*.

6.3 Discussion

Through gene expression analysis we discovered that miR-10a significantly reduced ALDH1A3 levels and the ALDH+ cell population, and that overexpression of miR-10a inhibited growth *in vitro* and *in vivo*. We showed that miR-10a mediated the depletion of lung cancer stem cells through its regulation of the NOTCH and WNT pathways via direct interaction with DVL3 (Figure 6.15). Finally, we observed that DVL3 not only regulates ALDH+ cell populations but is also vital for NSCLC tumor growth *in vivo*.

We expanded our finding across a panel of lung cancer cell lines representing various histological subtypes, demonstrating the robustness of the effect of miR-10a on ALDH1A3 levels. Not only did ectopic expression of miR-10a lead to the reduction of the ALDH+ cell population, but also significantly inhibited colony formation and induced apoptosis *in vitro*. Further supporting miR-10a as a critical modulator of cell growth, when H2009 cells were transiently transfected with miR-10a mimic and then injected the subcutaneously in mice (Figure 6.16B). Prior to injection we measured both DVL and ALDH1A3 levels and confirmed significant reduction in expression levels for each gene (Figure 6.16C). While there was a slight lag in tumor formation in miR-10a mimic treated cells, this difference was lost over time. Tumors were removed and miR-10a levels were quantified, it was found that miR-10a levels had returned to baseline levels (Figure 6.16 A-D). This finding suggests that either miR-10a cells underwent gradual apoptosis or that only cells with high expression propagated tumor formation. We believe the latter, as there was an initial lag in tumor formation and colony formation results

suggest that while miR-10a will not completely abolish colony formation it will significantly reduce it. To address this issue further we used stable over-expression of miR-10a. The over-expression construct led to more than a 100-fold increase in miR-10a, which was smaller than the increase achieved with transient transfections of the miR-10a mimic, but still enough to lead to a reduction in ALDH1A3 levels and inhibition of colony forming ability *in vitro*. When these stable cells were injected into mice, we observed a dramatic inhibition of tumor formation, implicating miR-10a as an important regulator of NSCLC growth both *in vitro* and *in vivo*. In our model "normal" lung system (immortalized bronchial epithelial cells) we saw that miR-10a affected DVL3 levels but had no effect on ALDH1A3 levels. This indicates that ALDH1A3 levels in HBEC3-KT are either maintained through alternative pathways or that parallel pathways still existed that are absent in H2009 or HCC827 cells. In support of our understanding of miRNAs as reactors to stress (Mendell and Olson 2012), miR-10a had no effect in normal HBEC cells but had profound effects on cancer cells, which are under a constant state of various stressors.

The reduction in ALDH1A3 levels was not a direct result of miR-10a, however, as the entire coding sequence did not contain any conserved miR-10a binding sites. Past and ongoing work in our lab has shown that the WNT pathway is important for NSCLC cellular growth. Gene expression analysis showed that WNT10a is enriched in the ALDH+ cell population (Figure 6.4A). Additionally, a mini siRNA screen, targeting genes implicated in stem cell maintenance, again revealed an enrichment of genes involved inn the WNT pathway are

important in cell survival (Figure 6.17). Interestingly, the WNT ligand, Frizzled receptor, and first down stream signaling component DVL3 are all top hits. Suggesting that inhibiting the WNT signaling upstream in the pathway is more effective then inhibiting downstream signaling components. Exploring genes in the WNT pathway, we validated DVL3 as a direct target of miR-10a regulation. Following siRNA loss of several known miR-10a target genes, only DVL3 was able to affect ADLH1A3 mRNA and protein and alter the ALDH+ cell fraction. Finally, when NSCLC cells were treated with an siRNA targeting DVL3, we observed a reduction in growth *in vitro* and an induction of apoptosis. Stable loss of DVL3 not only produced a more robust phenotype (a four-fold reduction in the ability to form colonies *in vitro* and delayed tumor onset by five weeks in NOD/SCID mice) but also reduced the likelihood of an off-target effect. Taken together, we have identified miR-10a as a regulator of ALDH+ cells through its direct interaction with DVL3, which is critical for NLCLC cellular viability.

6.5 Future Directions

While we have demonstrated that DVL3 expression is important for ALDH1A3 expression, we did not explore changes in phosphorylation of beta catenin or its subcellular localization. Thus we are uncertain if the reduction of ALDH+ due to loss of DVL3 is dependent on beta catenin or functions in a non-canonical manor to maintain ALDH1A3 levels. To address this issue we will use a fluorescence microscopy and stain for beta catenin localization in the ALDH+ population relative to the ALDH- population. Finally, we will profile expression

following DVL3 loss to determine the most significantly down regulated gene(s) to potentially uncover how DVL3 is regulating ALDH1A3 levels.

Several small molecules are available that inhibit WNT signaling. Two that we explored are tankyrase inhibitors, which stabilize the beta catenin destruction complex, and DVL3 inhibitors that prevent the docking of DVL3 with the Fz receptor. We only observed a reduction of ALDH+ cells with inhibitors targeting DVL3, supporting the results of our mini siRNA screen on the importance of inhibiting initiating WNT signaling events. We did not observe any effect on growth rate when cells were treated with DVL PDZ inhibitor; however, our previous work on miR-10a modulation of NSCLC cell response to paclitaxel leads us to believe that targeting DVL3 will sensitize cells to paclitaxel. This has been experimentally shown: depletion of stem cells in prostate cancer using drugs targeting the hedgehog pathway sensitized these cells to docetaxol (Domingo-Domenech, Vidal et al. 2012).

While others have reported WNT pathways activation in NSCLC, only two NSCLC cell lines have been identified with mutations in beta-catenin. It is conceivable that mutations could occur in DVL3, leading to aberrant pathway activation (Akiri, Cherian et al. 2009). Since direct inhibition of DVL3 is likely to be several years away from clinical application, we could use small molecules that either induce miR-10a expression or promote the degradation of DVL3 (Kwan, Chan et al. 2013). Given the increasing evidence supporting the targeting of cancer stem cells in clinical applications (Singh and Settleman 2010), our findings have uncovered a potential linchpin in tumor cell maintenance in NSCLC.

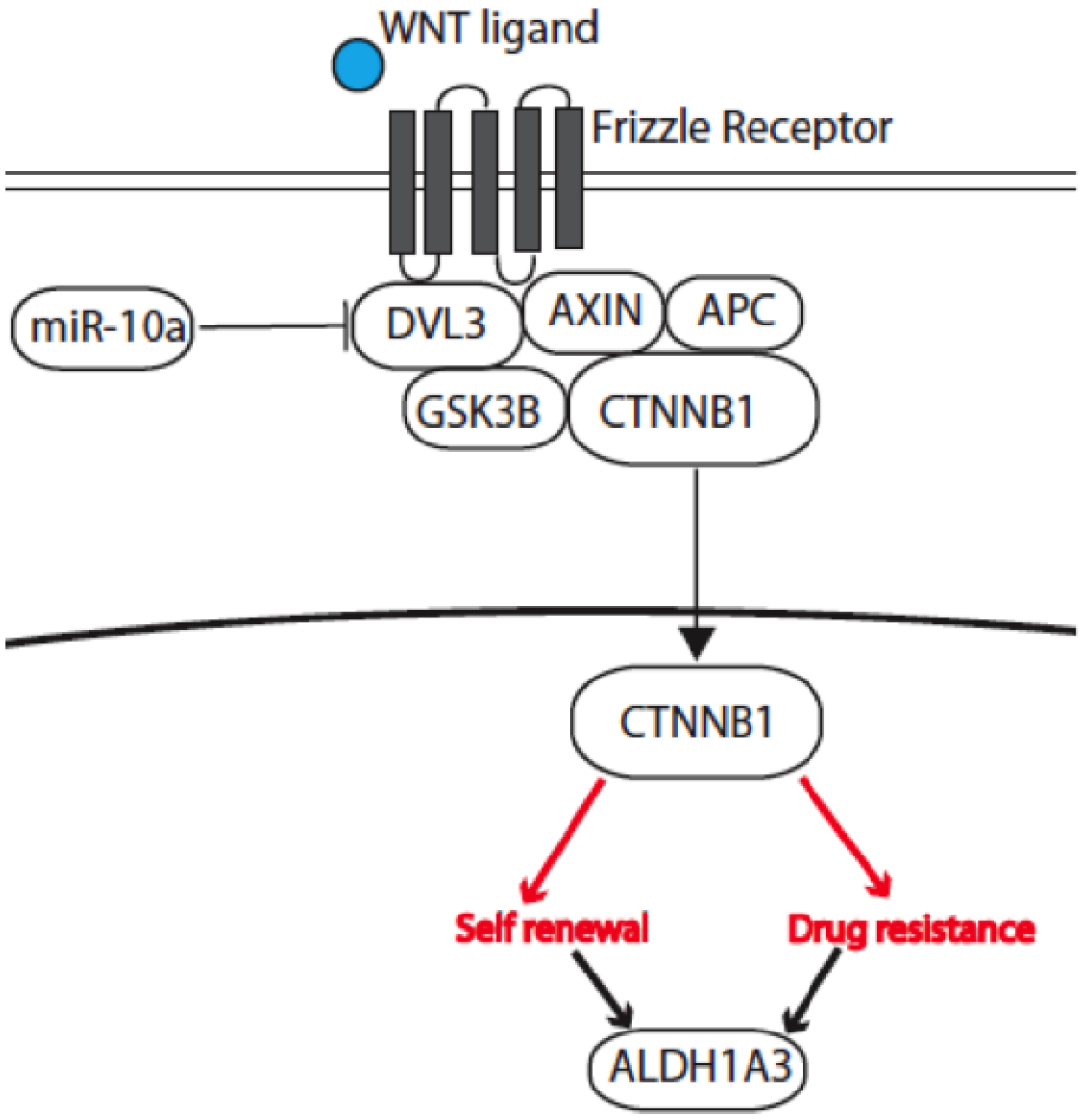

Figure 6.15 Summary: miR-10a Modulates ALDH1A3 Levels By Inhibiting DVL3

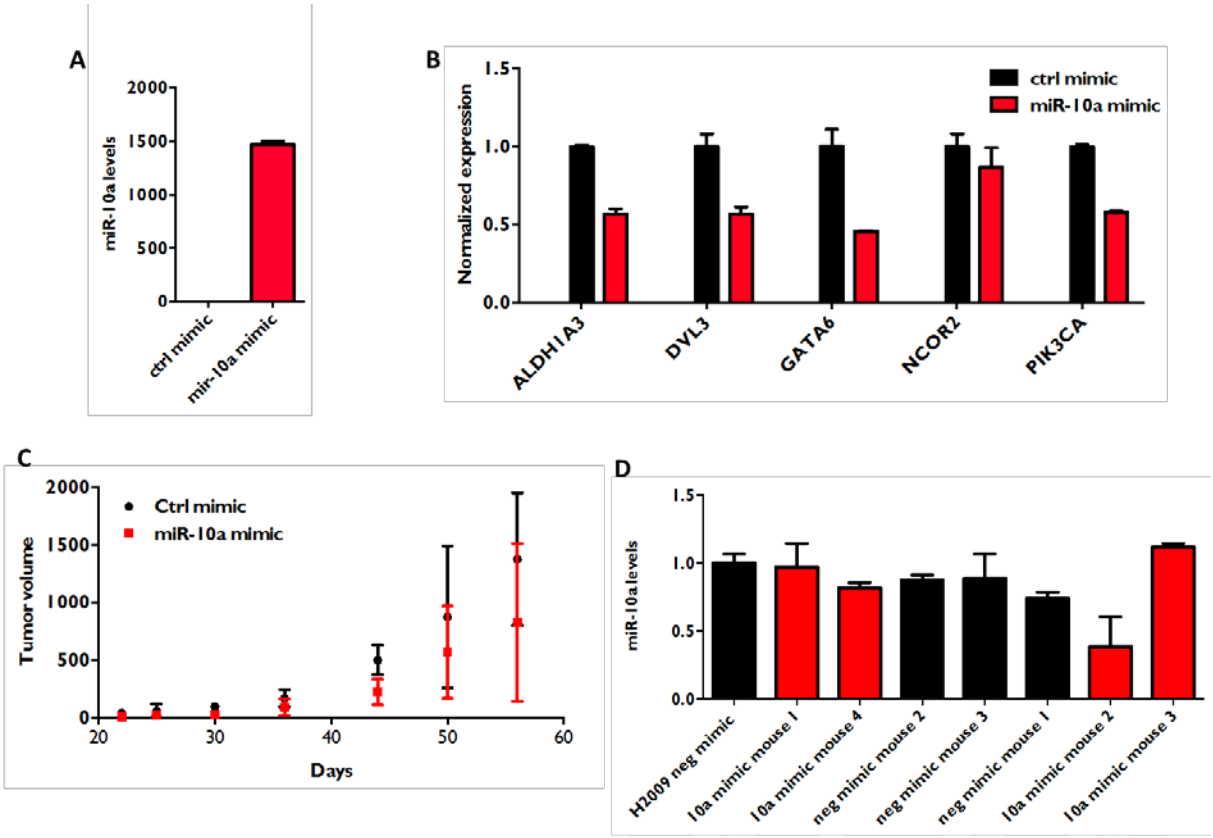

FIGURE 6.16 Transient Induction of miR-10a Does Not Inhibit Growth In Vivo
A. miR-10a levels prior to injection. **B.** Down-regulation of all miR-10a target genes prior to injection **C.** 1x10^5 cells injected into NOD/SCID mice; no change in tumor growth observed**. D.** miR-10a levels returned to baseline levels 7 weeks post-transfection.

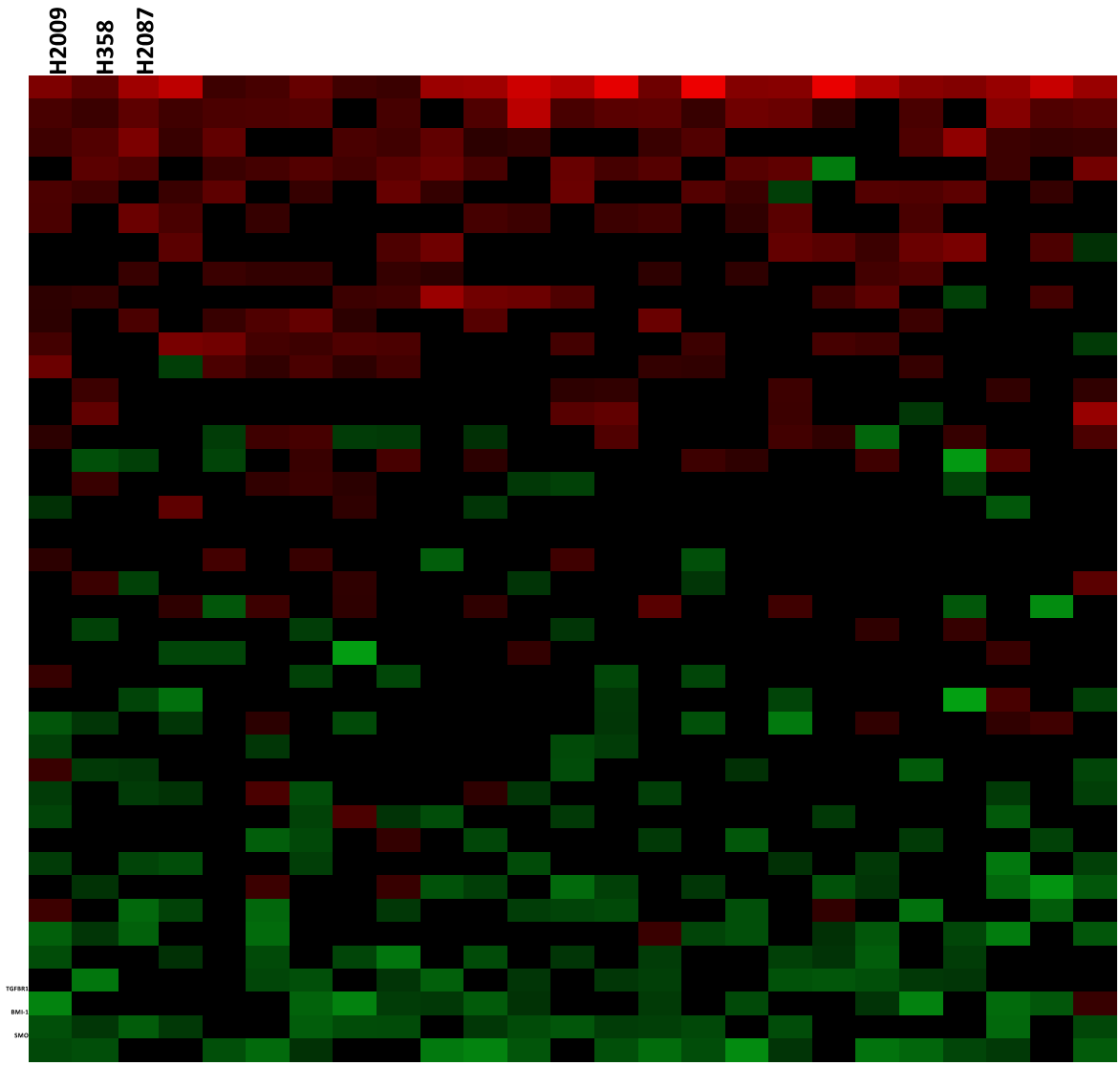

Figure 6.17 Mini siRNA Screen Targeting Genes Involved in Stem Cell Maintenance. Enrichment of genes involved in WNT pathway signaling are required for NSCLC growth. Endpoint was MTS assay 5-day post transfections; data plotted are triplicates of triplicates.

APPENDIX A
Bacterial Plasmid Stocks

BOX	Number	Backbone	conc (ng/uL)	BOX	Number	Backbone	conc (ng/uL)
1	**CD1**	dsRED Tre Tight	554	**1**	**CD32**	pCDH miR-10a	344
1	**CD2**	pTRE Tight	250	**1**	**CD33**	ctrl zip	318.8
1	**CD3**	GFP TRE Tight	746.6	**1**	**CD34**	miR-10a zip	486.2
1	**CD4**	pcDNA3.1	2863	**1**	**CD35**	Tet PLKO puro	
1	**CD5**	pGIPZ nontarget	220	**1**	**CD36**	pmIR glo	1714
1	**CD6**	pGIPZ empty	186.1	**1**	**CD37**	RAP1A SDm	2900.8
1	**CD7**	pTRIPZ	437.1	**1**	**CD38**	PIk3CA UTR	1907.7
1	**CD8**	pGIPZ shGATA6 B5	197.2	**1**	**CD39**	PIk3CA UTR	1460
1	**CD9**	pGIPZ shGATA6 B6	387.4	**1**	**CD40**	PIk3CA UTR SDM	203.1
1	**CD10**	pGIPZ shGATA6 A12	376.4	**1**	**CD41**	GATA6 UTR	257
1	**CD11**	pGIPZ shPIk3CA F6	433.2	**1**	**CD42**	GATA6 UTR	332.8
1	**CD12**	pGIPZ shPIk3CA E1	340	**1**	**CD43**	GATA6 UTR sdm	270
1	**CD13**	pGIPZ shPIK3CA G1	73.9	**1**	**CD44**	DVL3 UTR	170
1	**CD14**	pGIPZ shGATA2 F8	283.73	**1**	**CD45**	DVL3 UTR	146.1
1	**CD15**	pGIPZ shGATA2 C7	342.5	**1**	**CD46**	DVL3 UTR SDM	125.5
1	**CD16**	PCDNA3.1 GAPDH	3964	**1**	**CD47**	pGIpZ shDVL3 1	371
1	**CD17**	pCMV6 ALDH1A3	380	**1**	**CD48**	pGIpZ shDVL3 2	316
1	**CD18**	pSRH2	290	**1**	**CD49**	pGIpZ shDVL3 3	408
1	**CD19**	pSRH2 PTEN	190	**1**	**CD50**	shDVL3 TRC E3	144
1	**CD20**	pGL3 Basic	417.6	**1**	**CD51**	shGATA6 42 TRC	82.4
1	**CD21**	pGL3 Basic	140	**1**	**CD52**	shGATA6 55 TRC	130
1	**CD22**	pCMV6 Neo		**1**	**CD53**	shPIK3CA f4	280
1	**CD23**	pbabe puro PIk3CA	5821	**1**	**CD54**	shPIK3CA D6	70
1	**CD24**	pbabe puro E454K	4195	**1**	**CD55**	shPIK3CA C4	157.4
1	**CD25**	pbabe puro E454K	350	**1**	**CD56**	pCMV DeltaR8.91	185
1	**CD26**	pbabe puro H1047R	5770	**1**	**CD57**	pCMV DeltaR8.91	274
1	**CD27**	pbabe puro H1047R	5779	**1**	**CD58**	pv320	263.8
1	**CD28**	pbabe puro	222	**1**	**CD59**	pMD2 VSVG	185.7
1	**CD29**	pCDH-CMV EMPTY	500	**1**	**CD60**	pMD2 VSVG	240
1	**CD30**	pCDH-CMV EMPTY	254				
1	**CD31**	pCDH miR-10a	312.1				

APPENDIX B
Catalog of RNA preps

sample ID	Sample	Date	sample ID	Sample	Date
CDR1	H460-LUCIFERASE MIR-10A ZIP	6/27/2012	**CD32**	A549 DMSO	7/10/2012
CDR2	H460 MIR-10A ZIP	6/27/2012	**CD33**	A549 GDC0449 250nM	7/10/2012
CDR3	H1155-LUCIFERASE MIR-10A ZIP	6/27/2012	**CD34**	A358 DMSO	7/10/2012
CDR4	H1155-LUCIFERASE Scramble zip	6/27/2012	**CD35**	A358 GDC0449 250nM	7/10/2012
CDR5	H460 LUCIFERASE ZIP CTRL	6/29/2012	**CD36**	MCF-MIR-ZIP CTRL DMSO	7/10/2012
CDR6	H460-ZIP CTRL	6/29/2012	**CD37**	MCF-MIR-ZIP CTRL ATRA	7/10/2012
CDR7	MCF7-ZIP-CTRL	6/29/2012	**CD38**	MCF-MIR-ZIP-10A CTRL DMSO	7/10/2012
CDR8	MCF7-10A ZIP	6/29/2012	**CD39**	MCF-MIR-ZIP -10A CTRL ATRA	7/10/2012
CDR9	H460 LUC PRI-10A	6/29/2012	**CD40**	T47D R10 DMSO	7/12/2012
CDR10	H460 LUC pCDH-empty	6/29/2012	**CD41**	MCF7 R10 ATRA	7/12/2012
CDR11	H460 pri-10a	6/29/2012	**CD42**	T47D R10 ATRA	7/12/2012
CDR12	H460 pCDH-empty	6/29/2012	**CD43**	MCF7 R10 DMSO	7/12/2012
CDR13	H1155 luc pir-10a	6/29/2012	**CD44**	MCF7 R5 DMSO	7/12/2012
CDR14	H1155 luc pCDH-empty	6/29/2012	**CD45**	T47D R5 DMSO	7/12/2012
CDR15	H1155 piR-10a	7/2/2012	**CD46**	T47D R5 ATRA	7/12/2012
CDR16	H1155 pCDH empty	7/2/2012	**CD47**	MCF7 R5 ATRA	7/12/2012
CDR17	H358 piR-10a	7/2/2012	**CD48**	H1155 H1074R	11/2/2011
CDR18	H358 pCDH empty	7/2/2012	**CD49**	H1155 E545K	11/2/2011
CDR19	H1693 piR-10a	7/2/2012	**CD50**	H1155 WT	11/2/2011
CDR20	H1693 pCDH empty	7/2/2012	**CD51**	H1155 H1074R	2/19/2012
CDR21	H1975 piR-10a	7/2/2012	**CD52**	H1155 E545K	2/19/2012
CDR22	H1975 pCDH empty	7/2/2012	**CD53**	H1155 WT	2/19/2012
CDR23	H1819 piR-10a	7/2/2012	**CD54**	H1155 H1074R neg mimic	3/16/2012
CDR24	H1819 pCDH empty	7/2/2012	**CD55**	H1155 H1074R 10a mimic	3/16/2012
CD25	H1819 Ctrl zip	7/5/2012	**CD56**	H1155 E545K neg mimic	3/16/2012
CD26	H1819 miR-zip-10a	7/5/2012	**CD57**	H1155 E545K 10a mimic	3/16/2012
CD27	H1155 Ctrl zip	7/5/2012	**CD58**	H1155 WT neg mimic	3/16/2012
CD28	H1155 miR-zip 10a	7/5/2012	**CD59**	H1155 WT 10a mimic	3/16/2012
CD29	H460 LUC pCDH-empty sorted	7/10/2012	**CD60**	H1155 ctrl 10a mimic	5/3/2012
CD30	H460 luc pir-10a sorted	7/10/2012	**CD61**	H1155 ctrl 10a mimic	5/3/2012
CD31	H460 pri-10a sorted	7/10/2012	**CD62**	H1155 ctrl neg mimic	5/9/2012

sample ID	Sample	Date	sample ID	Sample	Date
CD63	H1155 ctrl 10a mimic	5/9/2012	**CD94**	H358 100nM 5aza 100k	3/1/2012
CD64	H1155 H1074R neg mimic	5/15/2012	**CD95**	H358 DMSO 200k	3/1/2012
CD65	H1155 H1074R 10a mimic	5/15/2012	**CD96**	H358 100nM 5aza 200k	3/1/2012
CD66	H1155 ctrl 10a mimic	5/15/2012	**CD97**	H358 500nM 5aza 200k	3/1/2012
CD67	H1155 ctrl 10a mimic	5/15/2012	**CD98**	H358 1000nM 5aza 200k	3/1/2012
CD68	HCC827 ctrl	5/29/2012	**CD99**	H358 100K DMSO	3/5/2012
CD69	HCC827 TGF	5/29/2012	**CD100**	H358 100K 100nM 5aza	3/5/2012
CD70	H2122 ctrl	5/29/2012	**CD101**	H358 200K DMSO	3/5/2012
CD71	H2122 TGF	5/29/2012	**CD102**	H358 100nM 5aza 200k	3/5/2012
CD72	HCC44 ctrl	5/29/2012	**CD103**	H358 500nM 5aza 200k	3/5/2012
CD73	HCC44 TGF	5/29/2012	**CD104**	H358 1000nM 5aza 200k	3/5/2012
CD74	H2087 ctrl	6/19/2012	**CD105**	H1975 DMSO 100K	3/5/2012
CD75	H2087 TGF	6/19/2012	**CD106**	H1975 1uM 5aza 100K	3/5/2012
CD76	H358 ctrl	6/19/2012	**CD107**	H358 DMSO	5/9/2012
CD77	H358 TGF	6/19/2012	**CD108**	H358 100nM 5aza	5/9/2012
CD78	HCC44 ctl	6/19/2012	**CD109**	H358 100nM 5aza + 10uM ATRA	5/9/2012
CD79	HCC44 TGF	6/19/2012	**CD110**	H1975 DMSO	5/9/2012
CD80	H1993 ctrl	6/19/2012	**CD111**	H1975 100nM 5aza	5/9/2012
CD81	H1993 TGF	6/19/2012	**CD112**	H1975 100nM 5aza + 10uM ATRA	5/9/2012
CD82	H2122 ctrl	6/19/2012	**CD113**	H1155 piR-10a sorted	7/18/2012
CD83	H2122 TGF	6/19/2012	**CD114**	MCF7 piR-10a sorted	7/18/2012
CD84	A549 ctrl	6/19/2012	**CD115**	H460 MIR-10A ZIP sorted	7/18/2012
CD85	A549 TGF	6/19/2012	**CD116**	RKO ETOH	3/18/2011
CD86	H358 100nM 5aza	10/28/2011	**CD117**	RKO 100nM ATRA	3/18/2011
CD87	H358 500nM 5aza	10/28/2011	**CD118**	RKO 500nM ATRA	3/18/2011
CD88	H358 1000nM 5aza	10/28/2011	**CD119**	RKO 1000nM ATRA	3/18/2011
CD89	H358 100nM 5aza +10uM ATRA	10/28/2011	**CD120**	H1155 etoh	3/24/2011
CD90	H358 DMSO	1/20/2012	**CD121**	H1155 100nM ATRA	3/24/2011
CD91	H358 100nM 5aza	1/20/2012	**CD122**	H1155 500nM ATRA	3/24/2011
CD92	H358 1uM 5aza	1/20/2012	**CD123**	H1155 100nM ATRA	3/24/2011
CD93	H358 DMSO 100k	3/1/2012	**CD124**	H460 etoh	3/24/2011

sample ID	Sample	Date	sample ID	Sample	Date
CD125	H460 500nM ATRA	3/24/2011	**CD156**	MCF7 48 hrs	8/11/2011
CD126	H460 1000nM ATRA	3/24/2011	**CD157**	MCF7 72 hrs	8/12/2011
CD127	H1155 etoh	3/25/2011	**CD158**	MCF7 neg inhibitor ATRA	9/30/2011
CD128	H1155 100nM ATRA	3/25/2011	**CD159**	MCF7 10a inhibitor ATRA	9/30/2011
CD129	H1155 500nM ATRA	3/25/2011	**CD160**	MCF7 DMSO Charcoal stripped	#######
CD130	H1155 1000nM ATRA	3/25/2011	**CD161**	MCF7 ATRA Charcoal stripped	#######
CD131	H460 etoh	3/25/2011	**CD162**	H358 DMSO	#######
CD132	H460 100nM ATRA	3/25/2011	**CD163**	H358 ATRA	#######
CD133	H460 500nM ATRA	3/25/2011	**CD164**	MCF7 DMSO	#######
CD134	H460 1000nM ATRA	3/25/2011	**CD165**	MCF7 ATRA	#######
CD135	H460 etoh	4/13/2011	**CD166**	MCF7 R10	12/5/2011
CD136	H460 1uM ATRA	4/13/2011	**CD167**	MCF7 R10 ATRA	12/5/2011
CD137	H460 5uM ATRA	4/13/2011	**CD168**	MCF7 R10 ATRA +BEZ	12/5/2011
CD138	H460 10uM ATRA	4/13/2011	**CD169**	MCF7 R10 +BEZ	12/5/2011
CD139	RKO etoh	4/13/2011	**CD170**	MCF7 Charcoal stripped DMSO	12/5/2011
CD140	RKO 1uM ATRA	4/13/2011	**CD171**	MCF7 Charcoal stripped ATRA	12/5/2011
CD141	RKO 5uM ATRA	4/13/2011	**CD172**	MCF7 DMSO	3/3/2012
CD142	RKO 10uM ATRA	4/13/2011	**CD173**	MCF7 ATRA 100nM	3/3/2012
CD143	RKO etoh	5/6/2011	**CD174**	MCF7 ATRA 500nM	3/3/2012
CD144	RKO ATRA	5/6/2011	**CD175**	MCF7 ATRA 1000nM	3/3/2012
CD145	H358 ATRA 24 hrs	5/18/2011	**CD176**	MCF7 ATRA 5000nM	3/3/2012
CD146	H358 ATRA 48 hrs	5/19/2011	**CD177**	MCF7 ATRA 10000nM	3/3/2012
CD147	H358 ATRA 72 hrs	5/20/2011	**CD178**	MDA-MB-453 DMSO	3/13/2012
CD148	MCF7 ATRA	6/17/2011	**CD179**	MDA-MB-453 5uM ATRA	3/13/2012
CD149	CCRL 2274 DMSO	6/24/2011	**CD180**	MDA-MB-453 10uM ATRA	3/13/2012
CD150	CCRL 2274 ATRA	6/24/2011	**CD181**	HCC1954 DMSO	3/13/2012
CD151	MCF7 DMSO	7/1/2011	**CD182**	HCC1954 5uM ATRA	3/13/2012
CD152	MCF7 ATRA	7/1/2011	**CD183**	HCC1954 10uM ATRA	3/13/2012
CD153	MCF7 DMSO	7/30/2011	**CD184**	T47D DMSO	5/5/2012
CD154	MCF7 ATRA	7/30/2011	**CD185**	T47D ATRA	5/5/2012
CD155	MCF7 24 hrs	8/10/2011	**CD186**	HCC1954 DMSO	5/5/2012

sample ID	Sample	Date	sample ID	Sample	Date
CD187	HCC1954 ATRA	5/5/2012	**CD218**	H596	10/18/2011
CD188	HCC1395 DMSO	7/21/2012	**CD219**	H1155	
CD189	HCC1395 ATRA	7/21/2012	**CD220**	H1299	11/7/2011
CD190	T47D DMSO	7/21/2012	**CD221**	H1299	
CD191	T47D ATRA	7/21/2012	**CD222**	H1355	
CD192	HCC1954	10/4/2011	**CD223**	H1693	
CD193	HCC1954	3/12/2012	**CD224**	H1975	
CD194	MCF7 Charcoal stripped	#######	**CD225**	H1819	10/18/2011
CD195	MCF7	2/19/2011	**CD226**	H1993	
CD196	MCF7	6/17/2011	**CD227**	H2009	
CD197	MDA-MB-268	2/9/2011	**CD228**	H2009	3/14/2012
CD198	MDA-MB-453	3/12/2012	**CD229**	H2122	3/12/2012
CD199	SK-BR-3	#######	**CD230**	H2882	
CD200	T47D	#######	**CD231**	H2935	
CD201	HBEC-2KT	3/12/2012	**CD232**	HCC44	
CD202	HBEC-3KT		**CD233**	HCC95	
CD203	HBEC-3KT	10/4/2011	**CD234**	HCC827	1/21/2011
CD204	HBEC-3KT	3/12/2012	**CD235**	HCC1171	
CD205	HBEC-4KT	3/12/2012	**CD236**	HCC2195	11/7/2011
CD206	HBEC-12KT	3/12/2012	**CD237**	HCC2450	10/18/2011
CD207	HBEC-30KT	10/4/2011	**CD238**	HCC4017	5/1/2011
CD208	HBEC-30KT	5/1/2011	**CD239**	HCC4017	5/16/2011
CD209	HBEC-30KT	5/16/2011	**CD240**	HCC4017 small RNA	5/16/2011
CD210	HBEC-30KT-Small fraction	5/16/2011	**CD241**	HCC4017	5/16/2011
CD211	A549	7/25/2011	**CD242**	H1299 ctrl	3/28/2012
CD212	H157		**CD243**	H1299 T15	3/28/2012
CD213	H157	3/12/2012	**CD244**	H1299 T18	3/28/2012
CD214	H226	3/14/2012	**CD245**	H1355 ctrl	3/28/2012
CD215	H358	5/20/2011	**CD246**	H1355 T16	3/28/2012
CD216	H358		**CD247**	PC9	3/12/2012
CD217	H460		**CD248**	RKO	2/19/2011

sample ID	Sample	Date	sample ID	Sample	Date
CD249	H1819 scramble	7/24/2012	**CD280**	h2087 neg mimic	1/29/2012
CD250	H1819 siNCOR2	7/24/2012	**CD281**	h2087 337 mimic	1/29/2012
CD251	MCF-7 miR-10a ZIP sorted	7/24/2012	**CD282**	h2087 neg mimic	2/24/2012
CD252	MCF-7 pCDH Sorted	7/24/2012	**CD283**	h2087 337 mimic	2/24/2012
CD253	H1155-LUC pCDH empty sorted	7/24/2012	**CD284**	H1299 empty pMIR glo	11/2/2011
CD254	H1155-LUC miR-10a ZIP sorted	7/24/2012	**CD285**	H1299 PIK3CA UTR in pMIR glo	11/2/2011
CD255	H460-LUC miR-10a ZIP sorted	7/24/2012	**CD286**	MCF7 negSI	2/28/2012
CD256	neg mimic H1155		**CD287**	MCF7 si PIK3CA	2/28/2012
CD257	H1155 101 mimic		**CD288**	MCF7 negSI	3/21/2011
CD258	H1155 101* mimic		**CD289**	MCF7 si PIK3CA	3/21/2011
CD259	H1155 15a mimic		**CD290**	H1819 negSI	2/28/2012
CD260	H1155 101 inhibitor		**CD291**	H1819 siPIK3CA	2/28/2012
CD261	H1155 15a inhibior		**CD292**	H1819 negSI	3/21/2011
CD262	H1155 NEG MIMIC	12/10/2010	**CD293**	H1819 siPIK3CA	3/21/2011
CD263	H1155 15a mimic	12/10/2010	**CD294**	H1819 negSI	7/27/2012
CD264	h1155 101 mimic	12/10/2010	**CD295**	H1819 siPIK3CA	7/27/2012
CD265	H1155 10a mimic	12/10/2010	**CD296**	HCT116 negSI	3/21/2011
CD266	H1155 neg mimic Dharmacon	1/17/2011	**CD297**	HCT116 siPIK3CA	3/21/2011
CD267	H1155 139-5p Dharmacon	1/17/2011	**CD298**	H1993 negSI	3/21/2011
CD268	H1155 139-3p Dharmacon	1/17/2011	**CD299**	H1993 siPIK3CA	3/21/2011
CD269	H1155 101* mimic	1/17/2011	**CD300**	H1299 negSI	11/7/2011
CD270	H1155 139-5p Dharmacon inhibitor	1/17/2011	**CD301**	H1299 siPIK3CA	11/7/2011
CD271	H1155 neg Dharmacon inhibitor	1/17/2011	**CD302**	H1975 negSI	1/17/2011
CD272	H1155 139-3p Dharmacon inhibitor	1/17/2011	**CD303**	H1975 siPIK3CA	1/17/2011
CD273	H1155 10a inhibitor Dharmacon	1/17/2011	**CD304**	H358 negSI	2/21/2011
CD274	H1155 MOCK	12/10/2010	**CD305**	H358 siKRAS	2/21/2011
CD275	H1155 15A Inhibitor	12/10/2010	**CD306**	H358 siPIk3CA+kras	2/21/2011
CD276	h1155 neg inhibitor	12/10/2010	**CD307**	H157 negSI	4/5/2012
CD277	H1155 101 inhibitor	12/10/2010	**CD308**	H157 siPIK3CA	4/5/2012
CD278	H1155 10A Inhibitor Exiqon	2/28/2011	**CD309**	H157 siGATA6	4/5/2012
CD279	H1155 neg Inhibitor Exiqon	2/28/2011	**CD310**	HCC1954 negSI	4/5/2012

sample ID	Sample	Date	sample ID	Sample	Date
CD311	HCC1954 siPIK3CA	4/5/2012	**CD342**	H460-luc siRXR	3/2/2012
CD312	HCC1954 siGATA6	4/5/2012	**CD343**	H460-luc siPIK3CA	3/2/2012
CD313	MDAMB453 negSI	4/5/2012	**CD344**	H460 negSI	1/17/2012
CD314	MDAMB453 siPIK3CA	4/5/2012	**CD345**	H460 siGATA6	1/17/2012
CD315	MDAMB453siGATA6	4/5/2012	**CD346**	RKO negSI 25nM	2/14/2011
CD316	H1155 negSI	2/28/2011	**CD347**	RKO siPIK3CA 25nM	2/14/2011
CD317	H1155 siPIK3CA	2/28/2011	**CD348**	RKO negSI	3/21/2011
CD318	H1155 negSI	1/14/2011	**CD349**	RKO siPIK3CA	3/21/2011
CD319	H1155 siPIK3CA	1/14/2011	**CD350**	RKO negSI 1.25nM	5/23/2011
CD320	H1155 negSI	1/17/2011	**CD351**	RKO negSI 2.5nM	5/23/2011
CD321	H1155 siGATA6	1/17/2011	**CD352**	RKO negSI 5nM	5/23/2011
CD322	H1155-luc negSI	2/13/2012	**CD353**	RKO negSI 10nM	5/23/2011
CD323	H1155-luc siGATA6	2/13/2012	**CD354**	RKO negSI 20nM	5/23/2011
CD324	H1155-luc siRXR	2/13/2012	**CD355**	RKO siPIK3CA .625nM	5/23/2011
CD325	H460 negSI 3.125nM	12/17/2010	**CD356**	RKO siPIK3CA 1.25nM	5/23/2011
CD326	H460 negSI 6.25nM	12/17/2010	**CD357**	RKO siPIK3CA 2.5nM	5/23/2011
CD327	H460 negSI 12.5nM	12/17/2010	**CD358**	RKO siPIK3CA 5nM	5/23/2011
CD328	H460 negSI 25nM	12/17/2010	**CD359**	RKO siPIK3CA 10nM	5/23/2011
CD329	H460 siPIK3CA 3.125nM	12/17/2010	**CD360**	RKO siPIK3CA 20nM	5/23/2011
CD330	H460 siPIK3CA 6.25nM	12/17/2010	**CD361**	H1975 neg Inhibitor	12/3/2010
CD331	H460 siPIK3CA 12.5nM	12/17/2010	**CD362**	H1975 10a inhibitor	12/3/2012
CD332	H460 siPIK3CA 25nM	12/17/2010	**CD363**	H1975 neg Inhibitor 25nM	1/17/2011
CD333	H460 negSI 25nM	1/14/2011	**CD364**	H1975 10B inhibitor 25nM	1/17/2011
CD334	H460 siPIK3CA 25nM	1/14/2011	**CD365**	H1299 neg inhibitor	11/7/2011
CD335	H460 negSI CFA	5/28/2011	**CD366**	H1299 10a inhibitor	11/7/2011
CD336	H460 siPIK3CA CFA	5/28/2011	**CD367**	H157 neg inhibitor	4/7/2012
CD337	H460-luc negSI	2/14/2012	**CD368**	H157 10a inhibitor	4/7/2012
CD338	H460-luc siRXR	2/14/2012	**CD369**	MDA-MB-453 neg inhibitor	4/7/2012
CD339	H460-luc siGATA6	2/14/2012	**CD370**	MDA-MB-453 10a inhibitor	4/7/2012
CD340	H460-luc negSI	3/2/2012	**CD371**	HCC1954 neg inhibitor	4/7/2012
CD341	H460-luc siGATA6	3/2/2012	**CD372**	HCC1954 10a inhibitor	4/7/2012

sample ID	Sample	Date	sample ID	Sample	Date
CD373	H460 neg inhibitor	12/3/2010	**CD404**	H1155 10A Inhibitor	4/29/2011
CD374	H460 10a inhibitor	12/3/2010	**CD405**	H1155 neg Inhibitor	5/9/2011
CD375	H460 neg inhibitor 50nM	2/18/2011	**CD406**	H1155 10A Inhibitor	5/9/2011
CD376	H460 10a inhibitor 50nM	2/18/2011	**CD407**	H1155 neg Inhibitor	5/31/2011
CD377	H460 neg inhibitor	2/25/2011	**CD408**	H1155 10A Inhibitor	5/31/2011
CD378	H460 10a inhibitor	2/25/2011	**CD409**	H1155 neg Inhibitor	6/24/2011
CD379	H460 neg inhibitor CFA	5/28/2011	**CD410**	H1155 10A Inhibitor	6/24/2011
CD380	H460 10a inhibitor CFA	5/28/2011	**CD411**	H1155 neg Inhibitor Exiqon	8/8/2011
CD381	H460 neg Dharmacon	8/8/2011	**CD412**	H1155 10A Inhibitor Exiqon	8/8/2011
CD382	H460 neg 10a Dharmacon	8/8/2011	**CD413**	H1155 neg Inhibitor Dharmacon	8/8/2011
CD383	H460 10a inhibitor	7/1/2011	**CD414**	H1155 10a inhibitor Dharmacon	8/8/2011
CD384	H460-Luc neg inhibitor	2/14/2012	**CD415**	H1155-luc neg Inhibitor	2/14/2012
CD385	H460-Luc 10a inhibitor	2/14/2012	**CD416**	H1155-luc 10A Inhibitor	2/14/2012
CD386	H460-Luc 10b inhibitor	2/14/2012	**CD417**	H1155 neg Inhibitor	3/19/2012
CD387	H460-Luc neg inhibitor	3/2/2012	**CD418**	H1155 10A Inhibitor	3/19/2012
CD388	H460-Luc 10a inhibitor	3/2/2012	**CD419**	H1155 neg Inhibitor	5/15/2012
CD389	H460-Luc neg inhibitor	3/16/2012	**CD420**	H1155 10A Inhibitor	5/15/2012
CD390	H460-Luc 10a inhibitor	3/16/2012	**CD421**	H358 neg mimic	8/5/2011
CD391	H460 neg inhibitor	5/15/2012	**CD422**	H358 203 mimic	8/5/2011
CD392	H460 10a inhibitor	5/15/2012	**CD423**	H157 neg mimic	3/16/2012
CD393	H460 neg inhibitor	7/1/2011	**CD424**	H157 10a mimic	3/16/2012
CD394	H1155 neg inhibitor 25nM	1/14/2011	**CD425**	HCC1954 neg mimic	3/16/2012
CD395	H1155 10b inhibitor 25nM	1/14/2011	**CD426**	HCC1954 10a mimic	3/16/2012
CD396	H1155 10a inhibitor 25nM	1/14/2011	**CD427**	MDA-MB-453 neg mimic	3/16/2012
CD397	H1155 neg inhibitor	1/17/2011	**CD428**	MDA-MB-453 10a mimic	3/16/2012
CD398	H1155 neg Inhibitor Exiqon	2/28/2011	**CD429**	H1299 neg mimic	11/7/2011
CD399	H1155 10A Inhibitor Exiqon	2/28/2011	**CD430**	H1299 10a mimic	11/7/2011
CD400	H1155 10B inhibitor Exiqon	2/28/2011	**CD431**	H1993 neg mimic	3/21/2011
CD401	H1155 neg Inhibitor Dharmacon	2/28/2011	**CD432**	H1993 10a mimic	3/21/2011
CD402	H1155 10a inhibitor Dharmacon	2/28/2011	**CD433**	HCT-116 neg mimic	2/28/2011
CD403	H1155 neg Inhibitor	4/29/2011	**CD434**	HCT-116 10a mimic	2/28/2011

sample ID	Sample	Date	sample ID	Sample	Date
CD435	HCT negSI really neg mimic	3/21/2011	**CD466**	H1155 10a mimic 25nM	1/14/2011
CD436	HCT-116 10a mimic	3/21/2011	**CD467**	H1155 neg mimic	2/28/2011
CD437	IMR-90 neg mimic	7/15/2011	**CD468**	H1155 10a mimic	2/28/2011
CD438	IMR-90 10a mimic	7/15/2011	**CD469**	H1155 neg mimic	4/29/2011
CD439	HBEC3KT neg mimic	8/1/2011	**CD470**	H1155 10a mimic	4/29/2011
CD440	HBEC3KT 10a mimic	8/1/2011	**CD471**	H1155 neg mimic	9/23/2011
CD441	MCF7 neg mimic 25nM	2/19/2011	**CD472**	H1155 10a mimic	9/23/2011
CD442	MCF7 10a mimic 25nM	2/19/2011	**CD473**	H1155 neg mimic	12/12/2011
CD443	MCF7 neg mimic	3/21/2011	**CD474**	H1155 10b mimic	12/12/2011
CD444	MCF7 10a mimic	3/21/2011	**CD475**	H1155 neg mimic	1/17/2012
CD445	H1819 neg mimic	2/28/2011	**CD476**	H1155 10a mimic	1/17/2012
CD446	H1819 10a mimic	2/28/2011	**CD477**	H1155-luc neg mimic	2/14/2012
CD447	H1819 neg mimic	3/21/2011	**CD478**	H1155-luc 10a mimic	2/14/2012
CD448	H1819 10a mimic	3/21/2011	**CD479**	H1155-luc 10b mimic	2/14/2012
CD449	H1975 neg mimic	12/3/2010	**CD480**	H1155-luc neg mimic	3/19/2012
CD450	H1975 10a mimic	12/3/2010	**CD481**	H1155-luc 10a mimic	3/19/2012
CD451	H1975 10a* mimic	12/3/2010	**CD482**	RKO neg mimic 25nM	2/19/2011
CD452	H1975 203 mimic	12/3/2010	**CD483**	RKO 10a mimic 25nM	2/19/2011
CD453	H1975 124 mimic		**CD484**	RKO neg mimic	3/21/2011
CD454	H1975 203 mimic		**CD485**	RKO 10a mimic	3/21/2011
CD455	H1975 neg mimic 25nM	1/17/2011	**CD486**	RKO neg mimic 72hrs	5/23/2011
CD456	H1975 10a mimic 25nM	1/17/2011	**CD487**	RKO neg mimic 96hrs	5/24/2011
CD457	H1975 neg mimic	5/15/2012	**CD488**	RKO neg mimic 120hrs	5/25/2011
CD458	H1975 10a mimic	5/15/2012	**CD489**	RKO neg mimic 144hrs	5/26/2011
CD459	H1975 10b mimic	5/15/2012	**CD490**	RKO neg mimic 220hrs	5/28/2011
CD460	H1975 neg mimic	8/5/2011	**CD491**	RKO 10a mimic 72hrs	5/23/2011
CD461	H1975 10a mimic	8/5/2011	**CD492**	RKO 10amimic 96hrs	5/24/2011
CD462	H1975 203 mimic	8/5/2011	**CD493**	RKO 10a mimic 120hrs	5/25/2011
CD463	H1975 neg mimic	3/2/2012	**CD494**	RKO 10a mimic 144hrs	5/26/2011
CD464	H1975 10a mimic	3/2/2012	**CD495**	RKO neg mimic 220hrs	5/28/2011
CD465	H1155 neg mimic 25nM	1/14/2011	**CD496**	RKO neg mimic .625nM	5/23/2011
sample ID	Sample	Date	**sample ID**	Sample	Date
CD497	RKO neg mimic 1.25nM	5/23/2011	**CD528**	H460 124 mimic 12.5	2/18/2011
CD498	RKO neg mimic 2.5nM	5/23/2011	**CD529**	H460 124 mimic 25nM	2/18/2011

CD499	RKO neg mimic 5nM	5/23/2011	**CD530**	H460 124mimic 50nM	2/18/2011
CD500	RKO neg mimic 10nM	5/23/2011	**CD531**	H460 203 mimic 12.5	2/18/2011
CD501	RKO neg mimic 20nM	5/23/2011	**CD532**	H460 203 mimic 25nM	2/18/2011
CD502	RKO 10a mimic .625nM	5/23/2011	**CD533**	H460 203 mimic 50nM	2/18/2011
CD503	RKO 10a mimic 1.25nM	5/23/2011	**CD534**	H460 neg mimic 25nM	2/25/2011
CD504	RKO 10a mimic 2.5nM	5/23/2011	**CD535**	H460 124 mimic 25nM	2/25/2011
CD505	RKO 10a mimic 5nM	5/23/2011	**CD536**	H460 203 mimic 25nM	2/25/2011
CD506	RKO 10a mimic 10nM	5/23/2011	**CD537**	H460 neg mimic CFA	5/28/2011
CD507	RKO 10a mimic 20nM	5/23/2011	**CD538**	H460 10a mimic CFA	5/28/2011
CD508	H460 neg mimic	12/3/2010	**CD539**	H460 neg mimic 24hrs	9/21/2011
CD509	H460 10a mimic	12/3/2010	**CD540**	H460 10a mimic 24hrs	9/21/2011
CD510	H460 10a* mimic	12/3/2010	**CD541**	H460 neg mimic 48hrs	9/22/2011
CD511	H460 124 mimic	12/3/2010	**CD542**	H460 10a mimic 48hrs	9/22/2011
CD512	H460 203 mimic	12/3/2010	**CD543**	H460 neg mimic 5nM	9/23/2011
CD513	H460 neg mimic 25nM	1/14/2011	**CD544**	H460 neg mimic 10nM	9/23/2011
CD514	H460 10a mimic 25nM	1/14/2011	**CD545**	H460 neg mimic 15nM	9/23/2011
CD515	H460 neg mimic	1/17/2011	**CD546**	H460 neg mimic 20nM	9/23/2011
CD516	H460 10a mimic	1/17/2011	**CD547**	H460 neg mimic 30nM	9/23/2011
CD517	H460 neg mimic 3.125		**CD548**	H460 10a mimic 5nM	9/23/2011
CD518	H460 neg mimic 6.25		**CD549**	H460 10a mimic 10nM	9/23/2011
CD519	H460 neg mimic 12.5		**CD550**	H460 10a mimic 15nM	9/23/2011
CD520	H460 neg mimic 25nM		**CD551**	H460 10a mimic 20nM	9/23/2011
CD521	H460 10a mimic 3.125		**CD552**	H460 10a mimic 30nM	9/23/2011
CD522	H460 10a mimic 6.25		**CD553**	H460 neg mimic	12/12/2011
CD523	H460 10a mimic 12.5		**CD554**	H460 10b mimic	12/12/2011
CD524	H460 10a mimic 25nM		**CD555**	H460-luc neg mimic	2/14/2012
CD525	H460 neg mimic 12.5	2/18/2011	**CD556**	H460-luc 10a mimic	2/14/2012
CD526	H460 neg mimic 25nM	2/18/2011	**CD557**	H460-luc 10b mimic	2/14/2012
CD527	H460 neg mimic 50nM	2/18/2011	**CD558**	H460-luc neg mimic	3/3/2012

sample ID	Sample	Date	sample ID	Sample	Date
CD559	H460-luc 10a mimic	3/3/2012	**CD590**	MCF7 DMSO	8/7/2012
CD560	H358 pCDH empty sorted	8/3/2012	**CD591**	MCF7 ATRA	8/7/2012
CD561	H358 pri10a sorted	8/3/2012	**CD592**	MDA-MB-175 DMSO	8/7/2012
CD562	H226 #772 TUMOR		**CD593**	MDA-MB-175 ATRA	8/7/2012
CD563	H226 #774 TUMOR		**CD594**	CD594 H358 1000-5aza +10uM ATRA	10/29/11.
CD564	H1155 #2 TUMOR		**CD595**	CD595 H358 500-5aza +10uM ATRA	10/29/11.
CD565	H1299 #4 TUMOR		**CD596**	CD596 H358 10uM ATRA	10/29/11.
CD566	H2009 #153 TUMOR		**CD597**	HBEC30KT shPTEN	Jill
CD567	H2882 #731 TUMOR		**CD598**	H358 10a mimic	8/5/2011
CD568	H2882 #735 TUMOR		**CD599**	H1819 neg inhibitor	8/10/2012
CD569	H2122 #770 TUMOR		**CD600**	H1819 10a inhibitor	8/10/2012
CD570	PC9 CTRL 756 TUMOR		**CD601**	H460-luc-miR-zip 10a clone 6	8/14/2012
CD571	PC #762 TUMOR		**CD602**	H460-luc-miR-zip 10a clone 12	8/14/2012
CD572	HBEC3K ui		**CD603**	H460-luc-miR-zip 10a clone 2	8/14/2012
CD573	H460 neg inhibitor Exiqon	8/8/2011	**CD604**	H460-luc-miR-zip 10a clone 8	8/14/2012
CD574	H460 10a inhibitor Exiqon	8/8/2011	**CD605**	H460-luc-miR-zip 10a clone 5	8/14/2012
CD575	T47D DMSO 96hrs	8/5/2012	**CD606**	H1975 10a mimic	8/21/2012
CD576	T47D ATRA 96hrs	8/5/2012	**CD607**	H1975 neg mimic	8/21/2012
CD577	MCF7 DMSO 96hrs	8/5/2012	**CD608**	T47D DMSO	8/21/2012
CD578	MCF7 ATRA 96hrs	8/5/2012	**CD609**	T47D ATRA	8/21/2012
CD579	H1975 si NCOR2	8/6/2012	**CD610**	MCF7 DMSO	8/21/2012
CD580	H1975 siGATA6	8/6/2012	**CD611**	MCF7 ATRA	8/21/2012
CD581	H1975 negSI	8/6/2012	**CD612**	MDA-MB-175 DMSO	8/21/2012
CD582	MCF7 ctrl zip DMSO	8/6/2012	**CD613**	MDA-MB-175 ATRA	8/21/2012
CD583	MCF ctrl zip ATRA	8/6/2012	**CD614**	HCC1500 DMSO	8/21/2012
CD584	MCF-zip 10a DMSO	8/6/2012	**CD615**	HCC1500 ATRA	8/21/2012
CD585	MCF7- zip 10a ATRA	8/6/2012	**CD616**	H1155-luc MIR-zip 10a CLONE 4	8/23/2012
CD586	BT483 DMSO	8/7/2012	**CD617**	H1155-luc MIR-zip 10a CLONE 5	8/23/2012
CD587	BT483 ATRA	8/7/2012	**CD618**	H1155luc MIR-zip 10a CLONE 8	8/23/2012
CD588	HCC1500 DMSO	8/7/2012	**CD619**	H1155-luc MIR-zip 10a CLONE 20	8/23/2012
CD589	HCC1500 ATRA	8/7/2012	**CD620**	H1155-luc MIR-zip 10a CLONE 21	8/23/2012

sample ID	Sample	Date	sample ID	Sample	Date
CD621	H1155-luc MIR-zip 10a CLONE 23	8/23/2012	**CD652**	H460 pri10a #11	9/18/2012
CD622	H1155-luc MIR-zip 10a CLONE 29	8/23/2012	**CD653**	H460 pri10a #4	9/18/2012
CD623	H358 pCDH empty sorted	8/28/2012	**CD654**	H460 pri10a #1	9/18/2012
CD624	H460-luc-pri-mir-10a clone 1	8/28/2012	**CD655**	MCF7 10aI unsorted	9/20/2012
CD625	H460-luc-pri-mir-10a clone 2	8/28/2012	**CD656**	MCF7 10aI sorted	9/20/2012
CD626	H460-luc-pri-mir-10a clone 3	8/28/2012	**CD657**	T47D ctrl I unsorted	9/20/2012
CD627	H460-luc-pri-mir-10a clone 4	8/28/2012	**CD658**	T47D ctrl I sorted	9/20/2012
CD628	H460-luc-pri-mir-10a clone 8	8/28/2012	**CD659**	T47d 10a I unsorted	9/20/2012
CD629	H460-luc-pri-mir-10a clone 10	8/28/2012	**CD660**	T47D 10a I sorted	9/20/2012
CD630	H460-luc-pri-mir-10a clone 11	8/28/2012	**CD661**	H2009 10A MIMIC	9/21/2012
CD631	MCF7-pri-10a clone 4	8/28/2012	**CD662**	H2009 neg mimic	9/21/2012
CD632	MCF7-pri-10a clone 11	8/28/2012	**CD663**	H2009 scramble	9/21/2012
CD633	MCF7-pri-10a clone 23	8/28/2012	**CD664**	H2009 siDVL3	9/21/2012
CD634	MCF7-pri-10a clone 24	8/28/2012	**CD665**	H2009 siGATA6	9/21/2012
CD635	H2009 neg mimic	8/29/2012	**CD666**	H2009 siNCOR2	9/21/2012
CD636	H2009 10a mimic	8/29/2012	**CD667**	H2009 siPIK3CA	9/21/2012
CD637	T47D 10A I DMSO	8/31/2012	**CD668**	H2009 siCOMBO	9/21/2012
CD638	T47D NEG I DMSO	8/31/2012	**CD669**	Human ref	9/26/2012
CD639	T47D 10A I ATRA	8/31/2012	**CD670**	MCF7 ZIP10A CLONE 3	10/8/2012
CD640	T47D NEG I ATRA	8/31/2012	**CD671**	MCF7 ZIP10A CLONE 6	10/8/2012
CD641	MCF7 10A I DMSO	8/31/2012	**CD672**	H358 pRi10a clone3	10/8/2012
CD642	MCF7 NEG I DMSO	8/31/2012	**CD673**	H358 pRi10a clone4	10/8/2012
CD643	MCF7 10A I ATRA	8/31/2012	**CD674**	H358 pRi10a clone6	10/8/2012
CD644	MCF7 NEG I ATRA	8/31/2012	**CD675**	H358 pRi10a clone7	10/8/2012
CD645	H2009 NEG mimic	9/5/2012	**CD676**	H460 IWR-1-ENDO 10um	10/10/2012
CD646	H2009 10a mimic	9/5/2012	**CD677**	H2009 IWR-1-ENDO 10um	10/10/2012
CD647	H1975 neg mimic	9/5/2012	**CD678**	H460 XAV939 1uM	10/10/2012
CD648	H1975 10a mimic	9/5/2012	**CD679**	H2009 XAV939 1uM	10/10/2012
CD649	skbr3 dmso	9/8/2012	**CD680**	H460 DMSO	10/10/2012
CD650	skbr3 atra	9/8/2012	**CD681**	H2009 DMSO	10/10/2012
CD651	H1155 pri10a #2	9/18/2012	**CD682**	skbr3 ATRA	10/10/2012

sample ID	Sample	Date	sample ID	Sample	Date
CD683	SKBR3 DMSO	10/10/2012	**CD714**	h2087 neg inhibitor	11/16/2012
CD684	MCF7 MIR10A-ZIP ATRA	10/10/2012	**CD715**	HCC44 ALDH +	11/27/2012
CD685	MC7 MIR-ZIP-10A DMSO	10/10/2012	**CD716**	HCC44 ALDH -	11/27/2012
CD686	H2009 scramble	10/18/2012	**CD717**	H2087 ALDH +	11/27/2012
CD687	H2009 siDVL3	10/18/2012	**CD718**	H2087 ALDH -	11/27/2012
CD688	H2009 siGATA6	10/18/2012	**CD719**	H2087 ALDH + II	11/27/2012
CD689	H2009 siNCOR2	10/18/2012	**CD720**	H2087 ALDH - II	11/27/2012
CD690	H2009 siPIK3CA	10/18/2012	**CD721**	H2087 shGFP	11/27/2012
CD691	H2009 siCOMBO	10/18/2012	**CD722**	H2087 shALDH1A3	11/27/2012
CD692	H2009 siDVL3	10/25/2012	**CD723**	H2087 XAV939 10uM	11/30/2012
CD693	H2009 siGATA6	10/25/2012	**CD724**	H2009 XAV939 10uM	11/30/2012
CD694	H2009 siNCOR2	10/25/2012	**CD725**	H1155 neg SI	11/30/2012
CD695	H2009 siPIK3CA	10/25/2012	**CD726**	H1155 siGATA6	11/30/2012
CD696	H2009 siCOMBO	10/25/2012	**CD727**	H1155 siPIK3CA	11/30/2012
CD697	H2009 scramble	10/25/2012	**CD728**	H2087 10a mimic	11/30/2012
CD698	H2009 neg mimic	10/25/2012	**CD729**	H2087 neg mimic	11/30/2012
CD699	H2009 10b mimic	10/25/2012	**CD730**	H2009 pCMV ALDH1A3	11/30/2012
CD700	H2009 10a mimic	10/25/2012	**CD731**	H2009 pCMV ctrl	11/30/2012
CD701	H358 neg mimic	10/25/2012	**CD732**	H2009 10a mimic mouse I	11/30/2012
CD702	H358 10b mimic	10/25/2012	**CD733**	H2009 10a mimic mouse IV	11/30/2012
CD703	H358 10a mimic	10/25/2012	**CD734**	H2009 neg mimic mouse II	11/30/2012
CD704	BT474 DMSO-I	11/2/2012	**CD735**	mouse sample A	11/30/2012
CD705	BT474 ATRA-I	11/2/2012	**CD736**	mouse sample X	11/30/2012
CD706	BT474 DMSO-II	11/2/2012	**CD737**	mouse sample Y	11/30/2012
CD707	BT474 ATRA-II	11/2/2012	**CD738**	mouse sample Z	11/30/2012
CD708	MCF7 MIR10A-ZIP DMSO	11/2/2012	**CD739**	H460 Neg si	12/3/2012
CD709	MCF7 MIR10A-ZIP ATRA	11/2/2012	**CD740**	H460 siPIk3ca	12/3/2012
CD710	h2087 10a mimic	11/8/2012	**CD741**	H460 siGATA6	12/3/2012
CD711	h2087 neg mimic	11/8/2012	**CD742**	BT474 DMSO	12/1/2012
CD712	h2087	11/8/2012	**CD743**	BT474 ATRA	12/1/2012
CD713	H2087 10a inhibitor	11/16/2012	**CD744**	BT474 ATRA	12/7/2012

sample ID	Sample	Date
CD745	H2009 NEG SI	12/7/2012
CD746	H2009 siDVL3	12/7/2012
CD747	H2087 10a inhibitor	12/11/2012
CD748	h2087 neg inhibitor	12/11/2012
CD749	H2087 10A MIMIC	12/11/2012
CD750	h2087 neg mimic	12/11/2012
CD751	BT474	12/11/2012
CD752	H2087 10a inhibitor	1/30/2013
CD753	h2087 neg inhibitor	1/30/2013
CD754	h358 siGATA6	1/30/2013
CD755	H358 negsSI	1/30/2013
CD756	H2009 siGATA6	1/30/2013
CD757	H2009 negSI	1/30/2013
CD758	H2087 siGATA6	1/30/2013
CD759	H2087 negSI	1/30/2013
CD760	H157 10a mimic-1	7/2/2013
CD761	H157 neg mimic-2	7/2/2013
CD762	H2009 10a mimic-1	7/2/2013
CD763	H2009-neg mimic-2	7/2/2013
CD764	HCC827 10a mimic - 1	7/2/2013
CD765	HCC827 neg mimic - 2	7/2/2013
CD766	H2009 piR-miR-10a	7/2/2013
CD767	H2009 PCDH	7/2/2013
CD768	H157 shctrl	7/19/2013
CD769	H157 shGATA6	7/19/2013
CD770	H1650 shCTRL	7/19/2013
CD771	H1650 shGATA6	7/19/2013
CD772	H460 zip 10a	7/19/2013
CD773	HCC827 shCTRL	7/19/2013
CD774	HCC827 shGATA6	7/19/2013
CD775	H1155 ctrl ZIP	7/19/2013
CD776	H2009 pri-mir-10a	7/19/2013
CD777	H460 shCTRL	7/22/2013
CD778	H460 shPIK3CA	7/22/2013
CD779	H460 shGATA6	7/22/2013
CD780	H1155 10a zip	8/2/2013
CD781	H2009 shDVL3	8/2/2013
CD782	HCC827 shDVL3	8/2/2013
CD783	H157 shPIK3CA	8/2/2013

APPENDIX C
Primer Sequences

Primer name	Sequence
TRC Validation F	GAAAGTATTTCGATTTCTTGGCTTTATATATCTTGTGG
TRC Validation R	TCTTTTAAAATTGTGGATGAATACTGCCATTTGTCTC
GATA6 binding site 1 F	GACATTTCACCTCCCGTCTT
GATA6 binding site 1 R	CGACTTCCCAGAGTGCTAGG
GATA6 binding site 2 F	TTATGTGCTGGATTGCGTGT
GATA6 binding site 2 R	TGTTATTTCCCCCATGATGC
GATA6 binding site 3 F	TTGGGACAAAATAAAACTTCATAGC
GATA6 binding site 3 R	GGGATACTGATTTGGGATGG
GATA6 binding site 4 F	AACTGAAAAATGGCTTCATGG
GATA6 binding site 4 R	GATTGTAAATACTTTCACTGGAGATG
PIK3CA SDM F	gaaataaaatactatataatttaaataatgtaaacgcaaacatttttgatagcacttaaactagttcatttcaaaattaagcttta
PIK3CA SDM R	ctttattttatgatatattaaatttattacatttgcgtttgtaaaaaactatcgtgaatttgatcaagtaaagttttaattcgaaat
GATA6 SDM F	5'-gatctgaagtcagtcggaatttgtaaacattttagcaaacaagatatttttcttccatgta
GATA6 SDM R	3'-ctagacttcagtcagccttaaacatttgtaaaatcgtttgttctataaaaagaaggtacat
DVL3 SDM F	5'-atgtaaaatgatgataataatacctacctcacatttttgttgtgaggatttaaattagatattgtacga-3'
DVL3 SDM R	3'-tacattttactactattattatggatggagtgtaaaaacaacactcctaaatttaatctataacatgct-5'
pmirGLO forward	CCTAAAGGACTGACCGGCAA
pmirGLO reverse	AGCGGCCGCCCCAAGGGGTT
pMIR-GLO sequence primer	ACACGGTAAAACCATGA
pMIR-GLO sequence primer	GTCCAAACTCATCAATGTA
DVL3UTR-3-R-XbaI	GCGGGCTCTAGAAGGAAGGAAGGGCAAGAAAG
DVL3UTR-4-F-SacI	GGGCCCGAGCTCTTCTCAACGATTGCTCATGC
PIK3CA-F-SacI	GCGCGGGAGCTC AAAGATAACTGAG
PIK3CA-R-XbaI	CCGGCCTCTAGACCTTCTCCTCTTT
GATA6-UTR-F	GCGCGGGAGCTCGCCACAGCCGCCAGG
GATA6-UTP-R	CCGGCCTCTAGACATTGTTCCCAAACAAAATGC

APPENDIX D
Potential MiRNA regulation of PI3KCA

Target Scan	Microcosm	miRNA.org	miRbase	miRbase	miRbase	miRbase	miRbase
miR-203	miR-202*	miR-590-3p	miR-1289	miR-517c	miR-454	miR-186*	miR-320b
miR-10	miR-143*	miR-203	miR-302d	miR-584	miR-491-3p	miR-450a	miR-450b-3p
miR-124/506	miR-302a	miR-520a-3p	miR-370	miR-1277	miR-548i	miR-574-5p	miR-629
	miR-525-5p	miR-520d-3p	miR-202*	miR-376a*	miR-24-1*	miR-548c-5p	miR-936
	miR-155	miR-302a	miR-302a	miR-519e	miR-451	miR-609	miR-1207-5p
	miR-302b	miR-302b	miR-302b	miR-103	miR-516a-5p	miR-621	miR-1254
	miR-302d	miR-302c	miR-1282	miR-1250	miR-1205	miR-1288	miR-214*
	miR-942	miR-302d	miR-525-5p	miR-384	miR-152	miR-1304	miR-519c-3p
	miR-373	miR-520b	miR-1206	miR-769-3p	miR-19b-2*	miR-139-5p	miR-542-5p
	miR-576-5p	miR-520c-3p	miR-573	miR-187	miR-30c	miR-196a	miR-553
	miR-512-3p	miR-520e	miR-32*	miR-19a	miR-449b	miR-198	miR-1201
	miR-370	miR-373	miR-302c	miR-19b	miR-517a	miR-23a*	miR-374b
	miR-27b*	miR-302e	miR-302e	miR-448	miR-518d-5p	miR-371-3p	miR-495
	miR-302c	miR-372	miR-543	let-7c*	miR-518e*	miR-450b-5p	miR-544
	miR-561	miR-155	miR-942	miR-1267	miR-519a*	miR-541*	miR-654-5p
	miR-520a-5p	miR-10b	miR-143*	miR-1308	miR-519b-5p	miR-548c-3p	miR-892a
	miR-9*	miR-10a	miR-302b*	miR-302d*	miR-519c-5p	miR-576-3p	miR-10a
	miR-148a	miR-370	miR-582-3p	miR-504	miR-520c-5p	miR-642	miR-1185
	miR-143	miR-384	miR-519b-3p	miR-590-3p	miR-522*	miR-129-5p	miR-124
	miR-372	miR-148a	miR-27b*	miR-1183	miR-523*	miR-208b	miR-1245
	miR-152	miR-148b	miR-890	miR-193a-5p	miR-526a	miR-635	miR-1252
	miR-193a-5p	miR-152	miR-143	miR-548a-5p	miR-1302	miR-135a*	miR-1322
	miR-376a*	miR-320a	miR-675	miR-620	miR-1303	miR-141*	miR-182
	miR-422a	miR-320b	miR-519a	miR-146b-3p	miR-299-5p	miR-142-3p	miR-196b
	miR-135b	miR-320c	miR-518f*	miR-30a	miR-637	miR-1827	miR-22
	miR-582-3p	miR-320d	miR-9*	miR-449a	let-7e	miR-183*	miR-

						518c*
miR-19a	miR-506	miR-548m	miR-576-5p	let-7g	miR-196a*	miR-570
miR-675	miR-124	miR-93	let-7d	miR-1253	miR-223*	miR-891b
miR-135a	miR-300	miR-1294	miR-296-3p	miR-148b	miR-497*	miR-23b*
miR-19b	miR-129-5p	miR-145	miR-325	miR-30b	miR-514	miR-320a
miR-101*	miR-21	miR-219-1-3p	miR-615-5p	miR-335*	miR-571	miR-338-3p
miR-93*	miR-381	miR-520a-5p	miR-921	miR-517b	miR-580	miR-618
miR-132	miR-590-5p	miR-409-3p	miR-135a	miR-369-3p	miR-649	miR-624
miR-518f*	miR-450a	miR-601	miR-135b	miR-212	miR-1265	miR-129*
miR-380	miR-876-5p	let-7i	miR-199b-5p	miR-335	miR-130a	miR-190b
miR-561	miR-212	miR-512-3p	miR-202	miR-382	miR-130b	miR-320d
miR-518e*	miR-132	miR-556-5p	miR-27a*	miR-422a	miR-548d-5p	miR-376c
miR-212	miR-339-5p	miR-30e	miR-507	miR-432	miR-548h	miR-548b-5p
miR-490-5p	miR-136	miR-1287	miR-1248	miR-509-3p	miR-592	miR-615-3p
miR-203	miR-219-5p	miR-126*	miR-186	miR-7	miR-200b*	miR-1259
miR-409-3p	miR-19a	miR-155	miR-18b	miR-1264	miR-32	miR-1283
miR-198	miR-19b	miR-708*	miR-605	miR-520e	miR-22*	miR-138
miR-520d-3p		let-7a	miR-708	miR-524-5p	miR-33a	miR-151-3p
miR-520b		miR-1226*	miR-15b	miR-549	miR-489	miR-190
miR-520e		miR-125b-2*	miR-184	miR-876-5p	miR-541	miR-25*
let-7c*		miR-16-1*	miR-1272	miR-92a-2*	miR-641	miR-365
miR-520a-3p		miR-337-3p	miR-128	miR-944	let-7f-1*	miR-367*
miR-10b		miR-376b	miR-1321	miR-98	miR-1182	miR-499-5p
miR-10a		miR-488	miR-154*	miR-1292	miR-1244	miR-513a-3p
miR-24-1*		miR-520d-3p	miR-181b	miR-320c	miR-340	miR-593
miR-518d-5p		miR-551b*	miR-185	miR-34c-5p	miR-96*	miR-600
miR-454		miR-557	miR-193a-3p	miR-409-5p	let-7b	miR-611
miR-491-3p		miR-122	miR-218	miR-484	miR-137	miR-651
miR-517c		miR-125a-5p	miR-24-2*	miR-518f	miR-145*	miR-9
miR-127-5p		miR-520g	miR-26b*	miR-548e	miR-147	miR-1257
miR-299-5p		miR-525-3p	miR-28-5p	miR-577	miR-148a	miR-367
miR-517b		miR-526b*	miR-302c*	let-7f	miR-1200	miR-1258

miR-517a

miR-548g	miR-328	miR-105*	miR-1255a	miR-126
miR-654-3p	miR-431*	miR-1273	miR-1293	miR-127-3p
miR-939	miR-513b	miR-1300	miR-140-5p	miR-1299
miR-1184	miR-548p	miR-205	miR-219-5p	miR-1324
miR-1269	miR-612	miR-299-3p	miR-28-3p	miR-1826
miR-153	miR-619	miR-29b	miR-363	miR-18a
miR-181d	miR-132	miR-302a*	miR-374a*	miR-19b-1*
miR-342-5p	miR-144	miR-31	miR-376a	miR-301b
miR-500	miR-181a*	miR-378	miR-421	miR-586
miR-593*	miR-183	miR-509-3-5p	miR-431	miR-106b*
miR-610	miR-34a	miR-510	miR-493*	miR-1290
miR-657	miR-34b*	miR-515-5p	miR-506	miR-135b*
miR-660	miR-374a	miR-559		miR-182*
miR-768-5p	miR-518d-3p	miR-582-5p		miR-208a

BIBLIOGRAPHY

Adams, J. M. and S. Cory (2007). "The Bcl-2 apoptotic switch in cancer development and therapy." Oncogene **26**(9): 1324-1337.

Agirre, X., A. Jimenez-Velasco, E. San Jose-Eneriz, L. Garate, E. Bandres, L. Cordeu, O. Aparicio, B. Saez, G. Navarro, A. Vilas-Zornoza, I. Perez-Roger, J. Garcia-Foncillas, A. Torres, A. Heiniger, M. J. Calasanz, P. Fortes, J. Roman-Gomez and F. Prosper (2008). "Down-regulation of hsa-miR-10a in chronic myeloid leukemia CD34+ cells increases USF2-mediated cell growth." Mol Cancer Res **6**(12): 1830-1840.

Ahmed, A. A., A. D. Mills, A. E. Ibrahim, J. Temple, C. Blenkiron, M. Vias, C. E. Massie, N. G. Iyer, A. McGeoch, R. Crawford, B. Nicke, J. Downward, C. Swanton, S. D. Bell, H. M. Earl, R. A. Laskey, C. Caldas and J. D. Brenton (2007). "The extracellular matrix protein TGFBI induces microtubule stabilization and sensitizes ovarian cancers to paclitaxel." Cancer Cell **12**(6): 514-527.

Akiri, G., M. M. Cherian, S. Vijayakumar, G. Liu, A. Bafico and S. A. Aaronson (2009). "Wnt pathway aberrations including autocrine Wnt activation occur at high frequency in human non-small-cell lung carcinoma." Oncogene **28**(21): 2163-2172.

Alamgeer, M., C. D. Peacock, W. Matsui, V. Ganju and D. N. Watkins (2013). "Cancer stem cells in lung cancer: Evidence and controversies." Respirology **18**(5): 757-764.

Androutsellis-Theotokis, A., R. R. Leker, F. Soldner, D. J. Hoeppner, R. Ravin, S. W. Poser, M. A. Rueger, S. K. Bae, R. Kittappa and R. D. McKay (2006). "Notch signalling regulates stem cell numbers in vitro and in vivo." Nature **442**(7104): 823-826.

Aqeilan, R. I., G. A. Calin and C. M. Croce (2010). "miR-15a and miR-16-1 in cancer: discovery, function and future perspectives." Cell Death Differ **17**(2): 215-220.

Artandi, S. E. and R. A. DePinho (2010). "Telomeres and telomerase in cancer." Carcinogenesis **31**(1): 9-18.

bai, R., G. Pettit and E. Hamel (1990). "Binding of dolastatin 10 to tubulin at a distinct site for peptide antimitotic agents near the exchangeable nucleotide and vinca alkaloid sites." J Biol Chem.

Bai, R., G. R. Pettit and E. Hamel (1990). "Binding of dolastatin 10 to tubulin at a distinct site for peptide antimitotic agents near the exchangeable nucleotide and vinca alkaloid sites." Journal of Biological Chemistry **265**(28): 17141-17149.

Bandi, N., S. Zbinden, M. Gugger, M. Arnold, V. Kocher, L. Hasan, A. Kappeler, T. Brunner and E. Vassella (2009). "miR-15a and miR-16 are implicated in cell cycle regulation in a Rb-dependent manner and are frequently deleted or down-regulated in non-small cell lung cancer." Cancer Res **69**(13): 5553-5559.

Bartel, D. P. (2009). "MicroRNAs: target recognition and regulatory functions." Cell **136**(2): 215-233.

Bernstein, E., S. Y. Kim, M. A. Carmell, E. P. Murchison, H. Alcorn, M. Z. Li, A. A. Mills, S. J. Elledge, K. V. Anderson and G. J. Hannon (2003). "Dicer is essential for mouse development." Nature Genetics **35**(3): 215-217.

Berx, G. and F. van Roy (2009). "Involvement of members of the cadherin superfamily in cancer." Cold Spring Harb Perspect Biol **1**(6): a003129.

Bhattacharjee, A., W. G. Richards, J. Staunton, C. Li, S. Monti, P. Vasa, C. Ladd, J. Beheshti, R. Bueno, M. Gillette, M. Loda, G. Weber, E. J. Mark, E. S. Lander, W. Wong, B. E. Johnson, T. R. Golub, D. J. Sugarbaker and M. Meyerson (2001). "Classification of human lung carcinomas by mRNA expression profiling reveals distinct adenocarcinoma subclasses." Proceedings of the National Academy of Sciences **98**(24): 13790-13795.

Bhattacharya, R., M. Nicoloso, R. Arvizo, E. Wang, A. Cortez, S. Rossi, G. A. Calin and P. Mukherjee (2009). "MiR-15a and MiR-16 control Bmi-1 expression in ovarian cancer." Cancer Res **69**(23): 9090-9095.

Bindra, R. S. and P. M. Glazer (2007). "Co-repression of mismatch repair gene expression by hypoxia in cancer cells: role of the Myc/Max network." Cancer Lett **252**(1): 93-103.

Bracken, C. P., P. A. Gregory, N. Kolesnikoff, A. G. Bert, J. Wang, M. F. Shannon and G. J. Goodall (2008). "A double-negative feedback loop between ZEB1-SIP1 and the microRNA-200 family regulates epithelial-mesenchymal transition." Cancer Res **68**(19): 7846-7854.

Brend, T. (2003). "Multiple levels of transcriptional and post-transcriptional regulation are required to define the domain of Hoxb4 expression." Development **130**(12): 2717-2728.

Brennecke, J., A. Stark, R. B. Russell and S. M. Cohen (2005). "Principles of microRNA-target recognition." PLoS Biol **3**(3): e85.

Brownson, R. C., M. C. Alavanja, N. Caporaso, E. J. Simoes and J. C. Chang (1998). "Epidemiology and prevention of lung cancer in nonsmokers." Epidemiologic reviews **20**(2): 218-236.

Burch, J. B. (2005). "Regulation of GATA gene expression during vertebrate development." Semin Cell Dev Biol **16**(1): 71-81.

Calin, G. A. (2004). "Human microRNA genes are frequently located at fragile sites and genomic regions involved in cancers." Proceedings of the National Academy of Sciences **101**(9): 2999-3004.

Calin, G. A., C. D. Dumitru, M. Shimizu, R. Bichi, S. Zupo, E. Noch, H. Aldler, S. Rattan, M. Keating, K. Rai, L. Rassenti, T. Kipps, M. Negrini, F. Bullrich and C. M. Croce (2002). "Frequent deletions and down-regulation of micro- RNA genes miR15 and miR16 at 13q14 in chronic lymphocytic leukemia." Proc Natl Acad Sci U S A **99**(24): 15524-15529.

Camps, C., F. M. Buffa, S. Colella, J. Moore, C. Sotiriou, H. Sheldon, A. L. Harris, J. M. Gleadle and J. Ragoussis (2008). "hsa-miR-210 Is induced by hypoxia and is an independent prognostic factor in breast cancer." Clin Cancer Res **14**(5): 1340-1348.

Carracedo, A., A. Alimonti and P. P. Pandolfi (2011). "PTEN level in tumor suppression: how much is too little?" Cancer Res **71**(3): 629-633.

Charles J Sherr1, F. M. (2002). "The RB and p53 pathways in cancer." cell.

Chen, Q., X. H. Zhang and J. Massague (2011). "Macrophage binding to receptor VCAM-1 transmits survival signals in breast cancer cells that invade the lungs." Cancer Cell **20**(4): 538-549.

Chen, X., Y. Ba, L. Ma, X. Cai, Y. Yin, K. Wang, J. Guo, Y. Zhang, J. Chen, X. Guo, Q. Li, X. Li, W. Wang, Y. Zhang, J. Wang, X. Jiang, Y. Xiang, C. Xu, P. Zheng, J. Zhang, R. Li, H. Zhang, X. Shang, T. Gong, G. Ning, J. Wang, K. Zen, J. Zhang and C. Y. Zhang (2008). "Characterization of microRNAs in serum: a novel class of biomarkers for diagnosis of cancer and other diseases." Cell Res **18**(10): 997-1006.

Chen, Y. and D. H. Gorski (2008). "Regulation of angiogenesis through a microRNA (miR-130a) that down-regulates antiangiogenic homeobox genes GAX and HOXA5." Blood **111**(3): 1217-1226.

Chendrimada, T. P., K. J. Finn, X. Ji, D. Baillat, R. I. Gregory, S. A. Liebhaber, A. E. Pasquinelli and R. Shiekhattar (2007). "MicroRNA silencing through RISC recruitment of eIF6." Nature **447**(7146): 823-828.

Cheung, W. K., M. Zhao, Z. Liu, L. E. Stevens, P. D. Cao, J. E. Fang, T. F. Westbrook and D. X. Nguyen (2013). "Control of alveolar differentiation by the lineage transcription factors GATA6 and HOPX inhibits lung adenocarcinoma metastasis." Cancer Cell **23**(6): 725-738.

Cheung, W. K., M. Zhao, Z. Liu, L. E. Stevens, P. D. Cao, J. E. Fang, T. F. Westbrook and D. X. Nguyen (2013). "Control of Alveolar Differentiation by the Lineage Transcription Factors GATA6 and HOPX Inhibits Lung Adenocarcinoma Metastasis." Cancer cell.

Christophe Ginestier1, M. H. H., Emmanuelle Charafe-Jauffret3, Florence Monville3,, M. B. Julie Dutcher1, Jocelyne Jacquemier3, Patrice Viens3, Celina Kleer1, Suling and A. S. Liu1, Dan Hayes1, Daniel Birnbaum3, Max S. Wicha1, and Gabriela Dontu1, "<ALDH1 is a marker of normal and malignant human mammary stem cells and a predictor of poor clinical outcome.pdf>."

Chute, J. P., G. G. Muramoto, J. Whitesides, M. Colvin, R. Safi, N. J. Chao and D. P. McDonnell (2006). "Inhibition of aldehyde dehydrogenase and retinoid signaling induces the expansion of human hematopoietic stem cells." Proc Natl Acad Sci U S A **103**(31): 11707-11712.

Cimmino, A., G. A. Calin, M. Fabbri, M. V. Iorio, M. Ferracin, M. Shimizu, S. E. Wojcik, R. I. Aqeilan, S. Zupo and M. Dono (2005). "miR-15 and miR-16 induce apoptosis by targeting BCL2." Proceedings of the National Academy of Sciences of the United States of America **102**(39): 13944-13949.

Clevers, H. and R. Nusse (2012). "Wnt/beta-catenin signaling and disease." Cell **149**(6): 1192-1205.

Cory, S. and J. M. Adams (2002). "The Bcl2 family: regulators of the cellular life-or-death switch." Nat Rev Cancer **2**(9): 647-656.

Costinean, S., S. K. Sandhu, I. M. Pedersen, E. Tili, R. Trotta, D. Perrotti, D. Ciarlariello, P. Neviani, J. Harb, L. R. Kauffman, A. Shidham and C. M. Croce (2009). "Src homology 2 domain-containing inositol-5-phosphatase and CCAAT enhancer-binding protein beta are targeted by miR-155 in B cells of Emicro-MiR-155 transgenic mice." Blood **114**(7): 1374-1382.

Courtney, K. D., R. B. Corcoran and J. A. Engelman (2010). "The PI3K pathway as drug target in human cancer." J Clin Oncol **28**(6): 1075-1083.

Crosby, M. E., R. Kulshreshtha, M. Ivan and P. M. Glazer (2009). "MicroRNA Regulation of DNA Repair Gene Expression in Hypoxic Stress." Cancer Research **69**(3): 1221-1229.

Dews, M., A. Homayouni, D. Yu, D. Murphy, C. Sevignani, E. Wentzel, E. E. Furth, W. M. Lee, G. H. Enders, J. T. Mendell and A. Thomas-Tikhonenko (2006). "Augmentation of tumor angiogenesis by a Myc-activated microRNA cluster." Nat Genet **38**(9): 1060-1065.

Di Cristofano, A. and P. P. Pandolfi (2000). "The Multiple Roles of PTEN in Tumor Suppression." Cell **100**(4): 387-390.

Ding, L. H., Y. Xie, S. Park, G. Xiao and M. D. Story (2008). "Enhanced identification and biological validation of differential gene expression via Illumina whole-genome expression arrays through the use of the model-based background correction methodology." Nucleic Acids Res **36**(10): e58.

Doench, J. G. and P. A. Sharp (2004). "Specificity of microRNA target selection in translational repression." Genes Dev **18**(5): 504-511.

Domingo-Domenech, J., S. J. Vidal, V. Rodriguez-Bravo, M. Castillo-Martin, S. A. Quinn, R. Rodriguez-Barrueco, D. M. Bonal, E. Charytonowicz, N. Gladoun, J. de la Iglesia-Vicente, D. P. Petrylak, M. C. Benson, J. M. Silva and C. Cordon-Cardo (2012). "Suppression of acquired docetaxel resistance in prostate cancer through depletion of notch- and hedgehog-dependent tumor-initiating cells." Cancer Cell **22**(3): 373-388.

Dong, J.-T. and H. Frierson (2001). "Loss of heterozygosity at 13q14 and 13q21 in high grade, high stage prostate cancer." The prostate.

Dong, J. T., J. C. Boyd and H. F. Frierson (2001). "Loss of heterozygosity at 13q14 and 13q21 in high grade, high stage prostate cancer." The Prostate **49**(3): 166-171.

Du, L., M. C. Subauste, C. DeSevo, Z. Zhao, M. Baker, R. Borkowski, J. J. Schageman, R. Greer, C. R. Yang, M. Suraokar, Wistuba, II, A. F. Gazdar, J. D. Minna and A. Pertsemlidis (2012). "miR-337-3p and its targets STAT3 and RAP1A modulate taxane sensitivity in non-small cell lung cancers." PLoS One **7**(6): e39167.

Eilers, M. and R. N. Eisenman (2008). "Myc's broad reach." Genes Dev **22**(20): 2755-2766.

Engelman, J. A. (2009). "Targeting PI3K signalling in cancer: opportunities, challenges and limitations." Nat Rev Cancer **9**(8): 550-562.

Engelman, J. A., L. Chen, X. Tan, K. Crosby, A. R. Guimaraes, R. Upadhyay, M. Maira, K. McNamara, S. A. Perera, Y. Song, L. R. Chirieac, R. Kaur, A. Lightbown, J. Simendinger, T. Li, R. F. Padera, C. Garcia-Echeverria, R. Weissleder, U. Mahmood, L. C. Cantley and K. K. Wong (2008). "Effective use of PI3K and MEK inhibitors to treat mutant Kras G12D and PIK3CA H1047R murine lung cancers." Nat Med **14**(12): 1351-1356.

Escobedo, L. G. and J. P. Peddicord (1996). "Smoking prevalence in US birth cohorts: the influence of gender and education." American Journal of Public Health **86**(2): 231-236.

Eulalio, A., E. Huntzinger and E. Izaurralde (2008). "Getting to the root of miRNA-mediated gene silencing." Cell **132**(1): 9-14.

Eulalio, A., J. Rehwinkel, M. Stricker, E. Huntzinger, S. F. Yang, T. Doerks, S. Dorner, P. Bork, M. Boutros and E. Izaurralde (2007). "Target-specific requirements for enhancers of decapping in miRNA-mediated gene silencing." Genes Dev **21**(20): 2558-2570.

Ferrara, N. (2010). "Pathways mediating VEGF-independent tumor angiogenesis." Cytokine Growth Factor Rev **21**(1): 21-26.

Foley, N. H., I. Bray, K. M. Watters, S. Das, K. Bryan, T. Bernas, J. H. Prehn and R. L. Stallings (2011). "MicroRNAs 10a and 10b are potent inducers of neuroblastoma cell differentiation through targeting of nuclear receptor corepressor 2." Cell Death Differ **18**(7): 1089-1098.

Friedman, R. C., K. K. Farh, C. B. Burge and D. P. Bartel (2009). "Most mammalian mRNAs are conserved targets of microRNAs." Genome Res **19**(1): 92-105.

Fu, B., M. Luo, S. Lakkur, R. Lucito and C. A. Iacobuzio-Donahue (2008). "Frequent genomic copy number gain and overexpression of GATA-6 in pancreatic carcinoma." Cancer biology & therapy **7**(10): 1593-1601.

Gadgeel, S. M., S. S. Ramalingam and G. P. Kalemkerian (2012). "Treatment of lung cancer." Radiol Clin North Am **50**(5): 961-974.

Gao, P., I. Tchernyshyov, T. C. Chang, Y. S. Lee, K. Kita, T. Ochi, K. I. Zeller, A. M. De Marzo, J. E. Van Eyk, J. T. Mendell and C. V. Dang (2009). "c-Myc suppression of miR-23a/b enhances mitochondrial glutaminase expression and glutamine metabolism." Nature **458**(7239): 762-765.

Garzon, R., G. A. Calin and C. M. Croce (2009). "MicroRNAs in Cancer." Annu Rev Med **60**: 167-179.

Gee, H. E., C. Camps, F. M. Buffa, S. Colella, H. Sheldon, J. M. Gleadle, J. Ragoussis and A. L. Harris (2008). "MicroRNA-10b and breast cancer metastasis." Nature **455**(7216): E8-E9.

Ginestier, C., M. H. Hur, E. Charafe-Jauffret, F. Monville, J. Dutcher, M. Brown, J. Jacquemier, P. Viens, C. G. Kleer and S. Liu (2007). "ALDH1 is a marker of normal and malignant human mammary stem cells and a predictor of poor clinical outcome." Cell stem cell **1**(5): 555-567.

Giraldez, A. J., Y. Mishima, J. Rihel, R. J. Grocock, S. Van Dongen, K. Inoue, A. J. Enright and A. F. Schier (2006). "Zebrafish MiR-430 promotes deadenylation and clearance of maternal mRNAs." Science **312**(5770): 75-79.

Göttlicher, M., S. Minucci, P. Zhu, O. H. Krämer, A. Schimpf, S. Giavara, J. P. Sleeman, F. L. Coco, C. Nervi and P. G. Pelicci (2001). "Valproic acid defines a novel class of HDAC inhibitors inducing differentiation of transformed cells." The EMBO journal **20**(24): 6969-6978.

Grandy, D., J. Shan, X. Zhang, S. Rao, S. Akunuru, H. Li, Y. Zhang, I. Alpatov, X. A. Zhang, R. A. Lang, D. L. Shi and J. J. Zheng (2009). "Discovery and characterization of a small molecule inhibitor of the PDZ domain of dishevelled." J Biol Chem **284**(24): 16256-16263.

Gregory, P. A., A. G. Bert, E. L. Paterson, S. C. Barry, A. Tsykin, G. Farshid, M. A. Vadas, Y. Khew-Goodall and G. J. Goodall (2008). "The miR-200 family and miR-205 regulate epithelial to mesenchymal transition by targeting ZEB1 and SIP1." Nat Cell Biol **10**(5): 593-601.

Grimson, A., K. K. Farh, W. K. Johnston, P. Garrett-Engele, L. P. Lim and D. P. Bartel (2007). "MicroRNA targeting specificity in mammals: determinants beyond seed pairing." Mol Cell **27**(1): 91-105.

Gritsko, T., A. Williams, J. Turkson, S. Kaneko, T. Bowman, M. Huang, S. Nam, I. Eweis, N. Diaz, D. Sullivan, S. Yoder, S. Enkemann, S. Eschrich, J. H. Lee, C. A. Beam, J. Cheng, S. Minton, C. A. Muro-Cacho and R. Jove (2006). "Persistent activation of stat3 signaling induces survivin gene expression and confers resistance to apoptosis in human breast cancer cells." Clin Cancer Res **12**(1): 11-19.

Grivennikov, S. I., F. R. Greten and M. Karin (2010). "Immunity, inflammation, and cancer." Cell **140**(6): 883-899.

Guertin, D. A. and D. M. Sabatini (2007). "Defining the role of mTOR in cancer." Cancer Cell **12**(1): 9-22.

Haldar, S., J. Chintapalli and C. M. Croce (1996). "Taxol induces bcl-2 phosphorylation and death of prostate cancer cells." Cancer research **56**(6): 1253-1255.

Hammond, J. W., D. Cai and K. J. Verhey (2008). "Tubulin modifications and their cellular functions." Curr Opin Cell Biol **20**(1): 71-76.

Hanahan, D. and R. A. Weinberg (2000). "The Hallmarks of Cancer." Cell **100**(1): 57-70.

Hanahan, D. and R. A. Weinberg (2011). "Hallmarks of cancer: the next generation." Cell **144**(5): 646-674.

He, L., X. He, L. P. Lim, E. de Stanchina, Z. Xuan, Y. Liang, W. Xue, L. Zender, J. Magnus, D. Ridzon, A. L. Jackson, P. S. Linsley, C. Chen, S. W. Lowe, M. A. Cleary and G. J. Hannon (2007). "A microRNA component of the p53 tumour suppressor network." Nature **447**(7148): 1130-1134.

Helwak, A., G. Kudla, T. Dudnakova and D. Tollervey (2013). "Mapping the human miRNA interactome by CLASH reveals frequent noncanonical binding." Cell **153**(3): 654-665.

Hermeking, H. (2010). "The miR-34 family in cancer and apoptosis." Cell Death Differ **17**(2): 193-199.

Hockenbery, D., G. Nuñez, C. Milliman, R. D. Schreiber and S. J. Korsmeyer (1990). "Bcl-2 is an inner mitochondrial membrane protein that blocks programmed cell death."

Huang, E. H., M. J. Hynes, T. Zhang, C. Ginestier, G. Dontu, H. Appelman, J. Z. Fields, M. S. Wicha and B. M. Boman (2009). "Aldehyde dehydrogenase 1 is a marker for normal and malignant human colonic stem cells (SC) and tracks SC overpopulation during colon tumorigenesis." Cancer Res **69**(8): 3382-3389.

Huang, H., C. Xie, X. Sun, R. P. Ritchie, J. Zhang and Y. E. Chen (2010). "miR-10a contributes to retinoid acid-induced smooth muscle cell differentiation." J Biol Chem **285**(13): 9383-9389.

Imielinski, M., A. H. Berger, P. S. Hammerman, B. Hernandez, T. J. Pugh, E. Hodis, J. Cho, J. Suh, M. Capelletti, A. Sivachenko, C. Sougnez, D. Auclair, M. S. Lawrence, P. Stojanov, K. Cibulskis, K. Choi, L. de Waal, T. Sharifnia, A. Brooks, H. Greulich, S. Banerji, T. Zander, D. Seidel, F. Leenders, S. Ansen, C. Ludwig, W. Engel-Riedel, E. Stoelben, J. Wolf, C. Goparju, K. Thompson, W. Winckler, D. Kwiatkowski, B. E. Johnson, P. A. Janne, V. A. Miller, W. Pao, W. D. Travis, H. I. Pass, S. B. Gabriel, E. S. Lander, R. K. Thomas, L. A. Garraway, G. Getz and M.

Meyerson (2012). "Mapping the hallmarks of lung adenocarcinoma with massively parallel sequencing." Cell **150**(6): 1107-1120.

Jackson, S. P. and J. Bartek (2009). "The DNA-damage response in human biology and disease." Nature **461**(7267): 1071-1078.

Jeong, H. W. and I. S. Kim (2004). "TGF-beta1 enhances betaig-h3-mediated keratinocyte cell migration through the alpha3beta1 integrin and PI3K." J Cell Biochem **92**(4): 770-780.

Jiang, S., H. W. Zhang, M. H. Lu, X. H. He, Y. Li, H. Gu, M. F. Liu and E. D. Wang (2010). "MicroRNA-155 functions as an OncomiR in breast cancer by targeting the suppressor of cytokine signaling 1 gene." Cancer Res **70**(8): 3119-3127.

Johnson, S. M., H. Grosshans, J. Shingara, M. Byrom, R. Jarvis, A. Cheng, E. Labourier, K. L. Reinert, D. Brown and F. J. Slack (2005). "RAS is regulated by the let-7 microRNA family." Cell **120**(5): 635-647.

Karube, Y., H. Tanaka, H. Osada, S. Tomida, Y. Tatematsu, K. Yanagisawa, Y. Yatabe, J. Takamizawa, S. Miyoshi, T. Mitsudomi and T. Takahashi (2005). "Reduced expression of Dicer associated with poor prognosis in lung cancer patients." Cancer Sci **96**(2): 111-115.

Kim, R., M. Emi and K. Tanabe (2007). "Cancer immunoediting from immune surveillance to immune escape." Immunology **121**(1): 1-14.

Kim, Y. K., J. Yeo, B. Kim, M. Ha and V. N. Kim (2012). "Short structured RNAs with low GC content are selectively lost during extraction from a small number of cells." Mol Cell **46**(6): 893-895.

Kinashi, T. and K. Katagiri (2004). "Regulation of lymphocyte adhesion and migration by the small GTPase Rap1 and its effector molecule, RAPL." Immunol Lett **93**(1): 1-5.

Klymkowsky, M. W. and P. Savagner (2009). "Epithelial-mesenchymal transition: a cancer researcher's conceptual friend and foe." Am J Pathol **174**(5): 1588-1593.

Korpal, M., E. S. Lee, G. Hu and Y. Kang (2008). "The miR-200 Family Inhibits Epithelial-Mesenchymal Transition and Cancer Cell Migration by Direct Targeting of E-cadherin Transcriptional Repressors ZEB1 and ZEB2." Journal of Biological Chemistry **283**(22): 14910-14914.

Korpal, M., E. S. Lee, G. Hu and Y. Kang (2008). "The miR-200 family inhibits epithelial-mesenchymal transition and cancer cell migration by direct targeting of E-cadherin transcriptional repressors ZEB1 and ZEB2." J Biol Chem **283**(22): 14910-14914.

Kosaka, T., Y. Yatabe, H. Endoh, K. Yoshida, T. Hida, M. Tsuboi, H. Tada, H. Kuwano and T. Mitsudomi (2006). "Analysis of epidermal growth factor receptor gene mutation in patients with non-small cell lung cancer and acquired resistance to gefitinib." Clin Cancer Res **12**(19): 5764-5769.

Kota, J., R. R. Chivukula, K. A. O'Donnell, E. A. Wentzel, C. L. Montgomery, H. W. Hwang, T. C. Chang, P. Vivekanandan, M. Torbenson, K. R. Clark, J. R. Mendell and J. T. Mendell (2009). "Therapeutic microRNA delivery suppresses tumorigenesis in a murine liver cancer model." Cell **137**(6): 1005-1017.

Krol, J., I. Loedige and W. Filipowicz (2010). "The widespread regulation of microRNA biogenesis, function and decay." Nat Rev Genet **11**(9): 597-610.

Kumar, M. S., D. C. Hancock, M. Molina-Arcas, M. Steckel, P. East, M. Diefenbacher, E. Armenteros-Monterroso, F. Lassailly, N. Matthews, E. Nye, G. Stamp, A. Behrens and J. Downward (2012). "The GATA2 transcriptional network is requisite for RAS oncogene-driven non-small cell lung cancer." Cell **149**(3): 642-655.

Kumar, M. S., J. Lu, K. L. Mercer, T. R. Golub and T. Jacks (2007). "Impaired microRNA processing enhances cellular transformation and tumorigenesis." Nat Genet **39**(5): 673-677.

Kwan, H., D. W. Chan, P. C. Cai, C. S. Mak, M. M. Yung, T. H. Leung, O. G. Wong, A. N. Cheung and H. Y. Ngan (2013). "AMPK Activators Suppress Cervical Cancer Cell Growth through Inhibition of DVL3 Mediated Wnt/β-Catenin Signaling Activity." PloS one **8**(1): e53597.

Kwei, K. A., M. D. Bashyam, J. Kao, R. Ratheesh, E. C. Reddy, Y. H. Kim, K. Montgomery, C. P. Giacomini, Y. L. Choi, S. Chatterjee, C. A. Karikari, K. Salari, P. Wang, T. Hernandez-Boussard, G. Swarnalata, M. van de Rijn, A. Maitra and J. R. Pollack (2008). "Genomic profiling identifies GATA6 as a candidate oncogene amplified in pancreatobiliary cancer." PLoS Genet **4**(5): e1000081.

Lagos-Quintana, M. (2003). "New microRNAs from mouse and human." Rna **9**(2): 175-179.

Lagos-Quintana, M., R. Rauhut, W. Lendeckel and T. Tuschl (2001). "Identification of novel genes coding for small expressed RNAs." Science **294**(5543): 853-858.

Landgraf, P., M. Rusu, R. Sheridan, A. Sewer, N. Iovino, A. Aravin, S. Pfeffer, A. Rice, A. O. Kamphorst, M. Landthaler, C. Lin, N. D. Socci, L. Hermida, V. Fulci, S. Chiaretti, R. Foa, J. Schliwka, U. Fuchs, A. Novosel, R. U. Muller, B. Schermer, U. Bissels, J. Inman, Q. Phan, M. Chien, D. B. Weir, R. Choksi, G. De Vita, D. Frezzetti, H. I. Trompeter, V. Hornung, G. Teng, G. Hartmann, M. Palkovits, R. Di Lauro, P. Wernet, G. Macino, C. E. Rogler, J. W. Nagle, J. Ju, F. N. Papavasiliou, T. Benzing, P. Lichter, W. Tam, M. J. Brownstein, A. Bosio, A. Borkhardt, J. J. Russo, C. Sander, M. Zavolan and T. Tuschl (2007). "A mammalian microRNA expression atlas based on small RNA library sequencing." Cell **129**(7): 1401-1414.

Larsen, J. E., T. Cascone, D. E. Gerber, J. V. Heymach and J. D. Minna (2011). "Targeted therapies for lung cancer: clinical experience and novel agents." Cancer J **17**(6): 512-527.

Larsen, J. E. and J. D. Minna (2011). "Molecular biology of lung cancer: clinical implications." Clin Chest Med **32**(4): 703-740.

Lau, N. C., L. P. Lim, E. G. Weinstein and D. P. Bartel (2001). "An abundant class of tiny RNAs with probable regulatory roles in Caenorhabditis elegans." Science **294**(5543): 858-862.

Lee, R., R. Feinbaum and V. Ambros (1993). "The C. elegans heterochronic gene lin-4 encodes small RNAs with antisense complementarity to lin-14." Cell.

Lee, R. C. (2001). "An Extensive Class of Small RNAs in Caenorhabditis elegans." Science **294**(5543): 862-864.

Lee, R. C. and V. Ambros (2001). "An extensive class of small RNAs in Caenorhabditis elegans." Science **294**(5543): 862-864.

Levina, V., A. M. Marrangoni, R. DeMarco, E. Gorelik and A. E. Lokshin (2008). "Drug-selected human lung cancer stem cells: cytokine network, tumorigenic and metastatic properties." PLoS One **3**(8): e3077.

Levine, A. J., W. Hu and Z. Feng (2006). "The P53 pathway: what questions remain to be explored?" Cell Death Differ **13**(6): 1027-1036.

Levine AJ, M. J., Finlay CA (1991). "The p53 tumour suppressor gene." Nature.

Lewis, B. P., C. B. Burge and D. P. Bartel (2005). "Conserved Seed Pairing, Often Flanked by Adenosines, Indicates that Thousands of Human Genes are MicroRNA Targets." Cell **120**(1): 15-20.

Lewis, B. P., I.-h. Shih, M. W. Jones-Rhoades, D. P. Bartel and C. B. Burge (2003). "Prediction of mammalian microRNA targets." Cell

Li, R., T. Moudgil, H. J. Ross and H. M. Hu (2005). "Apoptosis of non-small-cell lung cancer cell lines after paclitaxel treatment involves the BH3-only proapoptotic protein Bim." Cell Death Differ **12**(3): 292-303.

Li, Y., F. Wang, J. A. Lee and F. B. Gao (2006). "MicroRNA-9a ensures the precise specification of sensory organ precursors in Drosophila." Genes & Development **20**(20): 2793-2805.

Lin, L., A. J. Bass, W. W. Lockwood, Z. Wang, A. L. Silvers, D. G. Thomas, A. C. Chang, J. Lin, M. B. Orringer, W. Li, T. W. Glover, T. J. Giordano, W. L. Lam, M. Meyerson and D. G. Beer (2012). "Activation of GATA binding protein 6 (GATA6) sustains oncogenic lineage-survival in esophageal adenocarcinoma." Proc Natl Acad Sci U S A **109**(11): 4251-4256.

Lindsay, M. A. (2008). "microRNAs and the immune response." Trends Immunol **29**(7): 343-351.

Liu, G., X. Yuan, Z. Zeng, P. Tunici, H. Ng, I. R. Abdulkadir, L. Lu, D. Irvin, K. L. Black and J. S. Yu (2006). "Analysis of gene expression and chemoresistance of CD133+ cancer stem cells in glioblastoma." Mol Cancer **5**: 67.

Llave, C., Z. Xie, K. D. Kasschau and J. C. Carrington (2002). "Cleavage of Scarecrow-like mRNA targets directed by a class of Arabidopsis miRNA." Science **297**(5589): 2053-2056.

Lu, J., G. Getz, E. A. Miska, E. Alvarez-Saavedra, J. Lamb, D. Peck, A. Sweet-Cordero, B. L. Ebert, R. H. Mak, A. A. Ferrando, J. R. Downing, T. Jacks, H. R. Horvitz and T. R. Golub (2005). "MicroRNA expression profiles classify human cancers." Nature **435**(7043): 834-838.

Ma, L., F. Reinhardt, E. Pan, J. Soutschek, B. Bhat, E. G. Marcusson, J. Teruya-Feldstein, G. W. Bell and R. A. Weinberg (2010). "Therapeutic silencing of miR-10b inhibits metastasis in a mouse mammary tumor model." Nat Biotechnol **28**(4): 341-347.

Ma, L., J. Teruya-Feldstein and R. A. Weinberg (2007). "Tumour invasion and metastasis initiated by microRNA-10b in breast cancer." Nature **449**(7163): 682-688.

Mansfield, J. H., B. D. Harfe, R. Nissen, J. Obenauer, J. Srineel, A. Chaudhuri, R. Farzan-Kashani, M. Zuker, A. E. Pasquinelli, G. Ruvkun, P. A. Sharp, C. J. Tabin and M. T. McManus (2004). "MicroRNA-responsive 'sensor' transgenes uncover Hox-like and other developmentally regulated patterns of vertebrate microRNA expression." Nat Genet **36**(10): 1079-1083.

Marcato, P., C. A. Dean, D. Pan, R. Araslanova, M. Gillis, M. Joshi, L. Helyer, L. Pan, A. Leidal, S. Gujar, C. A. Giacomantonio and P. W. Lee (2011). "Aldehyde dehydrogenase activity of breast cancer stem cells is primarily due to isoform ALDH1A3 and its expression is predictive of metastasis." Stem Cells **29**(1): 32-45.

Mathers, C. D., D. M. Fat and J. Boerma (2008). The global burden of disease: 2004 update, World Health Organization.

Mayr, C. and D. P. Bartel (2009). "Widespread shortening of 3'UTRs by alternative cleavage and polyadenylation activates oncogenes in cancer cells." Cell **138**(4): 673-684.

Mayr, C., M. T. Hemann and D. P. Bartel (2007). "Disrupting the pairing between let-7 and Hmga2 enhances oncogenic transformation." Science **315**(5818): 1576-1579.

McCubrey, J. A., L. S. Steelman, S. L. Abrams, J. T. Lee, F. Chang, F. E. Bertrand, P. M. Navolanic, D. M. Terrian, R. A. Franklin, A. B. D'Assoro, J. L. Salisbury, M. C. Mazzarino, F. Stivala and M. Libra (2006). "Roles of the RAF/MEK/ERK and PI3K/PTEN/AKT pathways in malignant transformation and drug resistance." Adv Enzyme Regul **46**: 249-279.

Mendell, J. T. (2008). "miRiad roles for the miR-17-92 cluster in development and disease." Cell **133**(2): 217-222.

Mendell, J. T. and E. N. Olson (2012). "MicroRNAs in stress signaling and human disease." Cell **148**(6): 1172-1187.

Merchant, A. A. and W. Matsui (2010). "Targeting Hedgehog--a cancer stem cell pathway." Clin Cancer Res **16**(12): 3130-3140.

Mikhail Krasilnikov1, V. A., Serge Y. Fuchs2, Zheng Dong2, Adriana Haimovitz-Friedman3, Meenhard Herlyn4, Ze'ev Ronai2,* (1999). "Contribution of phosphatidylinositol 3-kinase to radiation resistance in human melanoma cells." Molecular carinogenesis.

Nagy, J. A., S. H. Chang, S. C. Shih, A. M. Dvorak and H. F. Dvorak (2010). "Heterogeneity of the tumor vasculature." Semin Thromb Hemost **36**(3): 321-331.

Ng, D. C. H., B. H. Lin, C. P. Lim, G. Huang, T. Zhang, V. Poli and X. Cao (2006). "Stat3 regulates microtubules by antagonizing the depolymerization activity of stathmin." The Journal of cell biology **172**(2): 245-257.

Olivier, M., M. Hollstein and P. Hainaut (2010). "TP53 mutations in human cancers: origins, consequences, and clinical use." Cold Spring Harb Perspect Biol **2**(1): a001008.

Orom, U. A., S. Kauppinen and A. H. Lund (2006). "LNA-modified oligonucleotides mediate specific inhibition of microRNA function." Gene **372**: 137-141.

Orom, U. A., F. C. Nielsen and A. H. Lund (2008). "MicroRNA-10a binds the 5'UTR of ribosomal protein mRNAs and enhances their translation." Mol Cell **30**(4): 460-471.

Pannuti, A., K. Foreman, P. Rizzo, C. Osipo, T. Golde, B. Osborne and L. Miele (2010). "Targeting Notch to target cancer stem cells." Clin Cancer Res **16**(12): 3141-3152.

Pao, W. and K. E. Hutchinson (2012). "Chipping away at the lung cancer genome." Nat Med **18**(3): 349-351.

Pasquinelli, A. E. (2012). "MicroRNAs and their targets: recognition, regulation and an emerging reciprocal relationship." Nat Rev Genet **13**(4): 271-282.

Petersen, C. P., M. E. Bordeleau, J. Pelletier and P. A. Sharp (2006). "Short RNAs repress translation after initiation in mammalian cells." Mol Cell **21**(4): 533-542.

Pleasance, E. D., R. K. Cheetham, P. J. Stephens, D. J. McBride, S. J. Humphray, C. D. Greenman, I. Varela, M. L. Lin, G. R. Ordonez, G. R. Bignell, K. Ye, J. Alipaz, M. J. Bauer, D. Beare, A. Butler, R. J. Carter, L. Chen, A. J. Cox, S. Edkins, P. I. Kokko-Gonzales, N. A. Gormley, R. J. Grocock, C. D. Haudenschild, M. M. Hims, T. James, M. Jia, Z. Kingsbury, C. Leroy, J. Marshall, A. Menzies, L. J. Mudie, Z. Ning, T. Royce, O. B. Schulz-Trieglaff, A. Spiridou, L. A. Stebbings, L. Szajkowski, J. Teague, D. Williamson, L. Chin, M. T. Ross, P. J. Campbell, D. R. Bentley, P. A. Futreal and M. R. Stratton (2010). "A comprehensive catalogue of somatic mutations from a human cancer genome." Nature **463**(7278): 191-196.

Poliseno, L., L. Salmena, J. Zhang, B. Carver, W. J. Haveman and P. P. Pandolfi (2010). "A coding-independent function of gene and pseudogene mRNAs regulates tumour biology." Nature **465**(7301): 1033-1038.

Poliseno, L., L. Salmena, J. Zhang, B. Carver, W. J. Haveman and P. P. Pandolfi (2010). "A coding-independent function of gene and pseudogene mRNAs regulates tumour biology." Nature **465**(7301): 1033-1038.

Polyak, K. and R. A. Weinberg (2009). "Transitions between epithelial and mesenchymal states: acquisition of malignant and stem cell traits." Nat Rev Cancer **9**(4): 265-273.

Porkka, K. P., M. J. Pfeiffer, K. K. Waltering, R. L. Vessella, T. L. Tammela and T. Visakorpi (2007). "MicroRNA expression profiling in prostate cancer." Cancer Res **67**(13): 6130-6135.

Quintana, E., M. Shackleton, M. S. Sabel, D. R. Fullen, T. M. Johnson and S. J. Morrison (2008). "Efficient tumour formation by single human melanoma cells." Nature **456**(7222): 593-598.

Raica, M., A. M. Cimpean and D. Ribatti (2009). "Angiogenesis in pre-malignant conditions." Eur J Cancer **45**(11): 1924-1934.

Ramirez, R. D., Shelley Sheridan, Luc Girard, Mitsuo Sato, Young Kim, Jon Pollack, Michael Peyton, Ying Zou, Jonathan M. Kurie, J. Michael DiMaio, Sara Milchgrub, Alice L. Smith, Rhonda F. Souza, Laura Gilbey, Xi Zhang, Kenia Gandia, Melville B. Vaughan, Woodring E. Wright, Adi F. Gazdar, 4, Jerry W. Shay and and John D. Minna1 (2004). "Immortalization of Human Bronchial Epithelial Cells in the Absence of viral oncoproteins." Cancer Res

Raposo, G. and H. Geuze (1996). "B lymphocytes secrete antigen-presenting vesicles."

Ravi, A., A. M. Gurtan, M. S. Kumar, A. Bhutkar, C. Chin, V. Lu, J. A. Lees, T. Jacks and P. A. Sharp (2012). "Proliferation and tumorigenesis of a murine sarcoma cell line in the absence of DICER1." Cancer Cell **21**(6): 848-855.

Raz, D. J. M. G., David V. PhD†; Odisho, Anobel Y. BA‡; Jablons, David M. MD* (20007). "Clinical Characteristics and Survival of Patients with Surgically Resected, Incidentally Detected Lung Cancer." Journal of Thoracic Oncology

Reinhart, B. J., F. J. Slack, M. Basson, A. E. Pasquinelli, J. C. Bettinger, A. E. Rougvie, H. R. Horvitz and G. Ruvkun (2000). "The 21-nucleotide let-7 RNA regulates developmental timing in Caenorhabditis elegans." Nature **403**(6772): 901-906.

Reya, T. and H. Clevers (2005). "Wnt signalling in stem cells and cancer." Nature **434**(14).

Riondel, J., M. Jacrot, F. Picot, H. Beriel, C. Mouriquand and P. Potier (1986). "Therapeutic response to taxol of six human tumors xenografted into nude mice." Cancer chemotherapy and pharmacology **17**(2): 137-142.

Robert Jan Lebbink, Maggie Lowe, Theresa Chan, Htet Khine, Xiaoyin Wang and M. T. McManus (2011). "Polymerase II Promoter Strength Determines Efficacy of microRNA Adapted shRNAs." PLoS Biol

Roy Katso1, K. O., Khatereh Ahmadi1, Sarah White1, John Timms1, and Michael D. Waterfield1,2 (2001). "Cellular function of phosphoinositide 3-kinases Implications for development, homeostasis, and cancer." Annual Review of Cell and Developmental Biology **17**.

Rudin, C. M., E. Avila-Tang, C. C. Harris, J. G. Herman, F. R. Hirsch, W. Pao, A. G. Schwartz, K. H. Vahakangas and J. M. Samet (2009). "Lung cancer in never smokers: molecular profiles and therapeutic implications." Clin Cancer Res **15**(18): 5646-5661.

Salk, J. J., E. J. Fox and L. A. Loeb (2010). "Mutational heterogeneity in human cancers: origin and consequences." Annu Rev Pathol **5**: 51-75.

Salmena, L., L. Poliseno, Y. Tay, L. Kats and P. P. Pandolfi (2011). "A ceRNA hypothesis: the Rosetta Stone of a hidden RNA language?" Cell **146**(3): 353-358.

Sara Pensa, Gabriella Regis, Daniela Boselli, F. Novelli and V. Poli (200). "STAT1 and STAT3 in Tumorigenesis: Two Sides of the Same Coin?" cell biology.

Sarkar, F. H., Y. Li, Z. Wang, D. Kong and S. Ali (2010). "Implication of microRNAs in drug resistance for designing novel cancer therapy." Drug Resist Updat **13**(3): 57-66.

Scott W. Lowe1, E. C. G. E. (2004). "Intrinsic tumour suppression." Nature

Serra, V., B. Markman, M. Scaltriti, P. J. Eichhorn, V. Valero, M. Guzman, M. L. Botero, E. Llonch, F. Atzori, S. Di Cosimo, M. Maira, C. Garcia-Echeverria, J. L. Parra, J. Arribas and J. Baselga (2008). "NVP-BEZ235, a dual PI3K/mTOR inhibitor, prevents PI3K signaling and inhibits the growth of cancer cells with activating PI3K mutations." Cancer Res **68**(19): 8022-8030.

Sharma, S. V., D. W. Bell, J. Settleman and D. A. Haber (2007). "Epidermal growth factor receptor mutations in lung cancer." Nat Rev Cancer **7**(3): 169-181.

Sheila K. Singh, I. D. C., Mizuhiko Terasaki, Victoria E. Bonn, Cynthia Hawkins, Jeremy Squire, and Peter B. Dirks (2003). "Identification of a Cancer Stem Cell in Human Brain Tumors." Cancer Res

Shen, B., M. K. Delaney and X. Du (2012). "Inside-out, outside-in, and inside-outside-in: G protein signaling in integrin-mediated cell adhesion, spreading, and retraction." Curr Opin Cell Biol **24**(5): 600-606.

Shen, W. H., A. S. Balajee, J. Wang, H. Wu, C. Eng, P. P. Pandolfi and Y. Yin (2007). "Essential role for nuclear PTEN in maintaining chromosomal integrity." Cell **128**(1): 157-170.

Sherr, C. J. and F. McCormick (2002). "The RB and p53 pathways in cancer." Cancer cell **2**(2): 103-112.

Shureiqi, I., X. Zuo, R. Broaddus, Y. Wu, B. Guan, J. S. Morris and S. M. Lippman (2007). "The transcription factor GATA-6 is overexpressed in vivo and contributes to silencing 15-LOX-1 in vitro in human colon cancer." FASEB J **21**(3): 743-753.

Siddik, Z. H. and K. Mehta (2009).

Siegel, R., D. Naishadham and A. Jemal (2013). "Cancer statistics, 2013." CA: a cancer journal for clinicians **63**(1): 11-30.

Singh, A. and J. Settleman (2010). "EMT, cancer stem cells and drug resistance: an emerging axis of evil in the war on cancer." Oncogene **29**(34): 4741-4751.

Song, M. S., L. Salmena and P. P. Pandolfi (2012). "The functions and regulation of the PTEN tumour suppressor." Nat Rev Mol Cell Biol **13**(5): 283-296.

Sooryanarayana Varambally, 2,3* Qi Cao,1,2* Ram-Shankar Mani,1,2 Sunita Shankar,1,2, Xiaosong Wang, 2 Bushra Ateeq,1,2 Bharathi Laxman,1,2 Xuhong Cao,1,4 Xiaojun Jing,1,2, Kalpana Ramnarayanan, J. Chad Brenner, 2,6 Jindan Yu,1,2 Jung H. Kim,1,3 Bo Han,1,2, Patrick Tan, 7 Chandan Kumar-Sinha,1,2 Robert J. Lonigro,1,3 Nallasivam Palanisamy,1,2,5 and Christopher A. Maher, 2 Arul M. Chinnaiyan1,2,3,4,6, (2007). "Genomic Loss of microRNA-101 Leads to Overexpression of Histone Methyltransferase EZH2 in Cancer." Science.

Stark, A., J. Brennecke, N. Bushati, R. B. Russell and S. M. Cohen (2005). "Animal MicroRNAs confer robustness to gene expression and have a significant impact on 3'UTR evolution." Cell **123**(6): 1133-1146.

Stephan Gasser, D. H. R. (2006). "Activation and self-tolerance of natural killer cells." Immunological reviews.

Stern-Ginossar, N., N. Elefant, A. Zimmermann, D. G. Wolf, N. Saleh, M. Biton, E. Horwitz, Z. Prokocimer, M. Prichard, G. Hahn, D. Goldman-Wohl, C. Greenfield, S. Yagel, H. Hengel, Y. Altuvia, H. Margalit and O. Mandelboim (2007). "Host immune system gene targeting by a viral miRNA." Science **317**(5836): 376-381.

Stern-Ginossar, N., C. Gur, M. Biton, E. Horwitz, M. Elboim, N. Stanietsky, M. Mandelboim and O. Mandelboim (2008). "Human microRNAs regulate stress-induced immune responses mediated by the receptor NKG2D." Nat Immunol **9**(9): 1065-1073.

Storer, C. M. and E. D. Salmon (1997). "Microtubule dynamics treadmilling comes around again." Current biology

Suarez, Y., C. Fernandez-Hernando, J. Yu, S. A. Gerber, K. D. Harrison, J. S. Pober, M. L. Iruela-Arispe, M. Merkenschlager and W. C. Sessa (2008). "Dicer-dependent endothelial microRNAs are necessary for postnatal angiogenesis." Proc Natl Acad Sci U S A **105**(37): 14082-14087.

Sullivan, J. P., J. D. Minna and J. W. Shay (2010). "Evidence for self-renewing lung cancer stem cells and their implications in tumor initiation, progression, and targeted therapy." Cancer Metastasis Rev **29**(1): 61-72.

Sullivan, J. P., M. Spinola, M. Dodge, M. G. Raso, C. Behrens, B. Gao, K. Schuster, C. Shao, J. E. Larsen, L. A. Sullivan, S. Honorio, Y. Xie, P. P. Scaglioni, J. M. DiMaio, A. F. Gazdar, J. W. Shay, Wistuba, II and J. D. Minna (2010). "Aldehyde dehydrogenase activity selects for lung adenocarcinoma stem cells dependent on notch signaling." Cancer Res **70**(23): 9937-9948.

Suva, M. L., N. Riggi, M. Janiszewska, I. Radovanovic, P. Provero, J. C. Stehle, K. Baumer, M. A. Le Bitoux, D. Marino, L. Cironi, V. E. Marquez, V. Clement and I. Stamenkovic (2009). "EZH2 is essential for glioblastoma cancer stem cell maintenance." Cancer Res **69**(24): 9211-9218.

Takamizawa, J., H. Konishi, K. Yanagisawa, S. Tomida, H. Osada, H. Endoh, T. Harano, Y. Yatabe, M. Nagino and Y. Nimura (2004). "Reduced expression of the let-7 microRNAs in human lung cancers in association with shortened postoperative survival." Cancer research **64**(11): 3753-3756.

Takebe, N., P. J. Harris, R. Q. Warren and S. P. Ivy (2011). "Targeting cancer stem cells by inhibiting Wnt, Notch, and Hedgehog pathways." Nat Rev Clin Oncol **8**(2): 97-106.

Tay, Y., L. Kats, L. Salmena, D. Weiss, S. M. Tan, U. Ala, F. Karreth, L. Poliseno, P. Provero, F. Di Cunto, J. Lieberman, I. Rigoutsos and P. P. Pandolfi (2011). "Coding-independent regulation of the tumor suppressor PTEN by competing endogenous mRNAs." Cell **147**(2): 344-357.

Tiburi, M. and H. h. andrade (2002). "Comparative genotoxic effect of vincristine, vinblastine, and vinorelbine in somatic cells of Drosophila melanogaster." Mutational Reserach

Trotman, L. C., M. Niki, Z. A. Dotan, J. A. Koutcher, A. Di Cristofano, A. Xiao, A. S. Khoo, P. Roy-Burman, N. M. Greenberg, T. Van Dyke, C. Cordon-Cardo and P. P. Pandolfi (2003). "Pten dose dictates cancer progression in the prostate." PLoS Biol **1**(3): E59.

Trowsdale, R. A. E. J. (2007). "Promiscuity and the single receptor NKG2D." Nature reviews immunology.

Tsoyi, K., H. J. Jang, I. T. Nizamutdinova, K. Park, Y. M. Kim, H. J. Kim, H. G. Seo, J. H. Lee and K. C. Chang (2010). "PTEN differentially regulates expressions of ICAM-1 and VCAM-1 through PI3K/Akt/GSK-3beta/GATA-6 signaling pathways in TNF-alpha-activated human endothelial cells." Atherosclerosis **213**(1): 115-121.

Uematsu, K., S. Kanazawa, L. You, B. He, Z. Xu, K. Li, B. M. Peterlin, F. McCormick and D. M. Jablons (2003). "Wnt Pathway Activation in Mesothelioma evidacne of Dishvelled overexpression and transcriptional activity of beta cat." Cancer Res **63**: 4547-4551.

Ulasov, I. V., S. Nandi, M. Dey, A. M. Sonabend and M. S. Lesniak (2011). "Inhibition of Sonic hedgehog and Notch pathways enhances sensitivity of CD133(+) glioma stem cells to temozolomide therapy." Mol Med **17**(1-2): 103-112.

Vajdic, C. M. and M. T. van Leeuwen (2009). "Cancer incidence and risk factors after solid organ transplantation." Int J Cancer **125**(8): 1747-1754.

Valadi, H., K. Ekstrom, A. Bossios, M. Sjostrand, J. J. Lee and J. O. Lotvall (2007). "Exosome-mediated transfer of mRNAs and microRNAs is a novel mechanism of genetic exchange between cells." Nat Cell Biol **9**(6): 654-659.

Vandewalle, C. (2005). "SIP1/ZEB2 induces EMT by repressing genes of different epithelial cell-cell junctions." Nucleic Acids Research **33**(20): 6566-6578.

Veerla, S., D. Lindgren, A. Kvist, A. Frigyesi, J. Staaf, H. Persson, F. Liedberg, G. Chebil, S. Gudjonsson, A. Borg, W. Mansson, C. Rovira and M. Hoglund (2009). "MiRNA expression in

urothelial carcinomas: important roles of miR-10a, miR-222, miR-125b, miR-7 and miR-452 for tumor stage and metastasis, and frequent homozygous losses of miR-31." Int J Cancer **124**(9): 2236-2242.

Verzi, M. P., H. Shin, H. H. He, R. Sulahian, C. A. Meyer, R. K. Montgomery, J. C. Fleet, M. Brown, X. S. Liu and R. A. Shivdasani (2010). "Differentiation-specific histone modifications reveal dynamic chromatin interactions and partners for the intestinal transcription factor CDX2." Dev Cell **19**(5): 713-726.

Vogler, M., D. Dinsdale, M. J. S. Dyer and G. M. Cohen (2008). "Bcl-2 inhibitors: small molecules with a big impact on cancer therapy." Cell Death and Differentiation **16**(3): 360-367.

Volinia, S., G. A. Calin, C. G. Liu, S. Ambs, A. Cimmino, F. Petrocca, R. Visone, M. Iorio, C. Roldo, M. Ferracin, R. L. Prueitt, N. Yanaihara, G. Lanza, A. Scarpa, A. Vecchione, M. Negrini, C. C. Harris and C. M. Croce (2006). "A microRNA expression signature of human solid tumors defines cancer gene targets." Proc Natl Acad Sci U S A **103**(7): 2257-2261.

Wang, J., P. O. Sakariassen, O. Tsinkalovsky, H. Immervoll, S. O. Boe, A. Svendsen, L. Prestegarden, G. Rosland, F. Thorsen, L. Stuhr, A. Molven, R. Bjerkvig and P. O. Enger (2008). "CD133 negative glioma cells form tumors in nude rats and give rise to CD133 positive cells." Int J Cancer **122**(4): 761-768.

Warburg, O. (1956). "<On the origins of a cancer cell.pdf>." Science.

Weidenfeld, J., W. Shu, L. Zhang, S. E. Millar and E. E. Morrisey (2002). "The WNT7b promoter is regulated by TTF-1, GATA6, and Foxa2 in lung epithelium." J Biol Chem **277**(23): 21061-21070.

Weiss, G. J., L. T. Bemis, E. Nakajima, M. Sugita, D. K. Birks, W. A. Robinson, M. Varella-Garcia, P. A. Bunn, Jr., J. Haney, B. A. Helfrich, H. Kato, F. R. Hirsch and W. A. Franklin

(2008). "EGFR regulation by microRNA in lung cancer: correlation with clinical response and survival to gefitinib and EGFR expression in cell lines." Ann Oncol **19**(6): 1053-1059.

West, K. A., S. Sianna Castillo and P. A. Dennis (2002). "Activation of the PI3K/Akt pathway and chemotherapeutic resistance." Drug resistance updates **5**(6): 234-248.

Whitehurst, A. W., B. O. Bodemann, J. Cardenas, D. Ferguson, L. Girard, M. Peyton, J. D. Minna, C. Michnoff, W. Hao, M. G. Roth, X. J. Xie and M. A. White (2007). "Synthetic lethal screen identification of chemosensitizer loci in cancer cells." Nature **446**(7137): 815-819.

Wightman, B., I. Ha and G. Ruvkun (1993). "Posttranscriptional regulation of the heterochronic gene lin-14 by lin-4 mediates temporal pattern formation in C. elegans." cell.

William Matsui, C. A. H., Qiuju Wang, Matthew T. Malehorn, James Barber, Yvette Tanhehco, B. Douglas Smith, Curt I. Civin, and Richard J. Jones (2003). "Characterization of clonogenic multiple myeloma cells." Blood.

Wright1, J. W. S. W. E. (2000). "Hayflick, his limit, and cellular ageing." Nature Reveiws

Yachida, S., S. Jones, I. Bozic, T. Antal, R. Leary, B. Fu, M. Kamiyama, R. H. Hruban, J. R. Eshleman, M. A. Nowak, V. E. Velculescu, K. W. Kinzler, B. Vogelstein and C. A. Iacobuzio-Donahue (2010). "Distant metastasis occurs late during the genetic evolution of pancreatic cancer." Nature **467**(7319): 1114-1117.

Yang, J. S., M. D. Phillips, D. Betel, P. Mu, A. Ventura, A. C. Siepel, K. C. Chen and E. C. Lai (2011). "Widespread regulatory activity of vertebrate microRNA* species." RNA **17**(2): 312-326.

Yang, W. J., D. D. Yang, S. Na, G. E. Sandusky, Q. Zhang and G. Zhao (2005). "Dicer is required for embryonic angiogenesis during mouse development." J Biol Chem **280**(10): 9330-9335.

Yardena Samuels1, Z. W., Alberto Bardelli1, Natalie Silliman1, Janine Ptak1, Steve Szabo1, Hai Yan2, Adi Gazdar3, Steven M. Powell4, Gregory J. Riggins1, James K. V. Willson5, Sanford Markowitz5, Kenneth W. Kinzler1, Bert Vogelstein1, Victor E. Velculescu (2004). "High Frequency of Mutations of the PIK3CA Gene in Human Cancers." Science.

Yekta, S., I. H. Shih and D. P. Bartel (2004). "MicroRNA-directed cleavage of HOXB8 mRNA." Science **304**(5670): 594-596.

Yuneva, M., N. Zamboni, P. Oefner, R. Sachidanandam and Y. Lazebnik (2007). "Deficiency in glutamine but not glucose induces MYC-dependent apoptosis in human cells." The Journal of Cell Biology **178**(1): 93-105.

Zamore, P. D., T. Tuschl, P. A. Sharp and D. P. Bartel (2000). "RNAi." Cell **101**(1): 25-33.

Zhang, B., H. Chen, L. Zhang, O. Dakhova, Y. Zhang, M. T. Lewis, C. J. Creighton, M. M. Ittmann and L. Xin (2013). "A dosage-dependent pleiotropic role of Dicer in prostate cancer growth and metastasis." Oncogene.

Zhang, L., D. Hou, X. Chen, D. Li, L. Zhu, Y. Zhang, J. Li, Z. Bian, X. Liang, X. Cai, Y. Yin, C. Wang, T. Zhang, D. Zhu, D. Zhang, J. Xu, Q. Chen, Y. Ba, J. Liu, Q. Wang, J. Chen, J. Wang, M. Wang, Q. Zhang, J. Zhang, K. Zen and C. Y. Zhang (2012). "Exogenous plant MIR168a specifically targets mammalian LDLRAP1: evidence of cross-kingdom regulation by microRNA." Cell Res **22**(1): 107-126.

Zhang, Y., A. M. Goss, E. D. Cohen, R. Kadzik, J. J. Lepore, K. Muthukumaraswamy, J. Yang, F. J. DeMayo, J. A. Whitsett, M. S. Parmacek and E. E. Morrisey (2008). "A Gata6-Wnt pathway required for epithelial stem cell development and airway regeneration." Nat Genet **40**(7): 862-870.

Zhao, L. and P. K. Vogt (2008). "Class I PI3K in oncogenic cellular transformation." Oncogene **27**(41): 5486-5496.

Zheng, T., J. Wang, X. Chen and L. Liu (2010). "Role of microRNA in anticancer drug resistance." Int J Cancer **126**(1): 2-10.

Zinzalla, V., D. Stracka, W. Oppliger and M. N. Hall (2011). "Activation of mTORC2 by association with the ribosome." Cell **144**(5): 757-768.